Calmodulin regulation of calcium channels and neurotransmitter release in bovine adrenal chromaffin cells.

Robert C.E. Wykes.
Department of Cell Physiology and Pharmacology

A dissertation submitted for the degree of Doctor of Philosophy at the University of Leicester, 2004.

UMI Number: U186303

UMI U186303

Calmodulin regulation of calcium channels and neurotransmitter release in bovine adrenal chromaffin cells.

Robert C.E. Wykes BSc (Hons).

Abstract

Calmodulin is a molecule implicated in regulating voltage-gated calcium channels (VGCC's) and the exocytotic machinery to fine tune neurotransmitter release. I have investigated the role this molecule plays in stimulus-secretion coupling in bovine adrenal chromaffin cells by over-expressing either wild type (CaM_{wt}), or a mutated calmodulin (CaM_{1234}), rendered incapable of binding calcium by adenoviral infection. Stimulus-evoked secretion was monitored by combined measurements of membrane capacitance (ΔC_m) and voltage-clamp recording of calcium currents in single cells. Cells were clamped in either the perforated patch or whole-cell configuration and calcium-dependent exocytosis evoked by single depolarizing voltage steps or trains of depolarisations. I show that the exocytotic efficiency, derived by dividing ΔC_m by the integral of the calcium current, is reduced for N-type channels compared to P/Q-type channels. Cation substitution experiments revealed that pharmacologically isolated N-type channels displayed the most profound sensitivity to calcium-dependent inactivation. Studies aimed at eluding the molecular mechanisms underlying calcium-dependent inactivation show that inhibiting calcinuerin by 20 mins preincubation with $1\mu M$ cyclosporine A or by introducing $30\mu M$ calmodulin inhibitory peptides through the patch pipette did not significantly reduce the level of whole cell calcium-dependent inactivation. In contrast, adenoviral mediated expression of a mutant calmodulin deficient in calcium binding resulted in a highly significant reduction in N-type, but not P/Q-type channel inactivation. This is the first time that calmodulin has been shown to regulate endogenously expressed N-type calcium channels. These results are consistent with calmodulin acting directly to control N-type channel inactivation and therefore limit this channels ability to couple to exocytosis during prolonged stimulation. Ca^{2+}/calmodulin was also found to interact with the secretory machinery. Expression of CaM_{1234} significantly reduced the exocytotic efficiency of brief depolarisations ($\leq 100ms$), however the exocytotic efficiency to longer depolarisations ($\geq 200ms$) was not significantly different between cells expressing CaM_{1234} and CaM_{wt}. This suggests that Ca^{2+}-Calmodulin is required for filling and/or release from a rapidly releasable pool of vesicles which is easily depleted, but not from the slowly releasable pool which dominates exocytotic responses measured with prolonged responses. Over-expression of CaM_{1234} also selectively inhibited clathrin-mediated endocytosis, leaving other endocytotic pathways unaltered. Taken together, these results place calmodulin as a central molecule that controls calcium entry (calcium channels) and the exocytotic machinery to regulate stimulus-coupled secretion.

DECLARATION

The majority of the results presented in this dissertation were carried out in the Department of Cell Physiology and Pharmacology, University of Leicester, between October 2000 and September 2003 and are my own work. A few experiments were conducted at the University of Sheffield due to the movement of my supervisor. No part of this dissertation has already been or is being concurrently submitted for any other degree, diploma or other qualification at this or any other University.

Robert C.E. Wykes

Acknowledgments.

I am indebted to my supervisor, Dr Liz Seward, for her mentoring and direction. Her enthusiasm and passion for science has inspired me.
Many thanks Liz.

I would like to thank all the members of the laboratory, past and present, who have aided my research by helping with cell culture preparations and other communal laboratory tasks, scientific discussion of data and most importantly good banter.

I would like to thank the numerous abattoirs which have provided the bovine adrenal glands for the last four years and the slaughter men for making the process of gland collection an 'interesting' experience.

I would like to thank all members from the departments of Cell Physiology and Pharmacology at the University of Leicester and the Institute of Molecular Physiology at the University of Sheffield for practical help and theoretical discussion of science.

I would also like to thank the Biotechnology and Biological Sciences Research Council, (BBSRC) for sponsoring my PhD and financial support.

Finally I would like to thank my friends and family, who have supported and encouraged me.

Dedicated with love and thanks to my parents,
for all their help and support.

TABLE OF CONTENTS

BIBLIOGRAPHY   **285**

List of Abbreviations.

Ach – Acetylcholine
AID – α-interacting domain
AP's – Action potentials
ATP – Adenosine tri-phosphate
Ba^{2+} - Barium
BAPTA –[1,2-bis(o-Aminophenoxy)ethane-N,N,N',N'-tetraacetic acid, tetrasodium salt
BHK – Baby hamster kidney
BID – B-interacting domain
BK – Large conductance calcium-activated potassium channel
BoNtC1 – Botulinum C
Ca^{2+} - Calcium
cAMP – Cyclic adenosine mono-phosphate
CaBP's – Calcium binding proteins
CaCl$_2$ – Calcium chloride
CdK5 – Cyclin-dependent kinase 5
CaM – Calmodulin
CaMKII – Calmodulin kinase II
CBD – Calmodulin binding domain
CdCl$_2$ – Cadmium chloride
CICR – Calcium-induced-calcium-release
C$_m$ - Capacitance
Cp – Pipette capacitance
CREB – Cyclic AMP-response element binding protein
CsOH – Cesium hydroxide
CSP – Cysteine-string protein
ΔC$_m$ – Change in capacitance
DAG - Diacyglycerol
DHPs - Dihydropyridines
DIDS - 4,4'- diisothiocyanatostilbene-2,2'-disulphonate
DMEM – Dulbecco's Modified Eagle's Medium
DMSO – Dimethylsulfoxide Methyl sulfoxide
DNA – Deoxyribose nucleic acid
DRG – Dorsal root ganglia
EDF – Electrochemical driving force
EGFP – Enhanced green fluorescent protein
EGTA – Ethylenediaminetetraacetic acid
EPSC's – Excitatory post-synaptic potentials
E$_{Rev}$ – Reversal potential
GABA – Gamma-aminobutryic acid
GFP – Green fluorescent protein
GPCR – G-protein coupled receptor
HCSP – Highly calcium sensitive pool

i

HEK – Human embryonic kidney
HEPES – (n-[2-Hydoxyethyl] piperazine-N'-[2-ethanesulfonic acid])
HVA – High voltage activated
IK - Intermediate conductance calcium-activated potassium channel
IP$_3$ – Inositol- 1,4,5, tri-phosphate
IRES – Internal ribosome entry segment
IRP – Immediately releasable pool
I/V – Current-voltage relationship
LDCV – Large dense core vesicle
LVA – Low voltage activated
MAGUKs – Membrane-associated guanylate kinases
MARKS – Myrisolyated, alanine-rich, protein kinase C substrate
MAPK – Mitogen-activated protein kinase
MgCl$_2$ – Magnesium chloride
MLCK – Myosin light chain kinase
mRNA – Messenger Ribonucleic acid
NaCl – Sodium chloride
NaHCO$_3$ – Sodium bicarbonate
NaOH – Sodium hydroxide
NCS-1 – Neuronal calcium sensor – 1
NMR – Nuclear magnetic resonance
NMDA – N-Methyl D Aspartate
NPY – Neuropeptide Y
K$_2$HPO$_4$ – Potassium phosphate (dibasic)
KH$_2$PO$_4$ – Potassium phosphate (monobasic)
KCl – Potassium chloride
PBS - Phospho-buffered saline
P$_O$ – Open probability
PIP$_2$ - Phosphatidyl-4,5-inositol-biphosphate
PKA – Protein kinase A
PKC – Protein kinase C
PLC – Phospholipase C
PSD – Post-stimulus drift
RE – Rapid endocytosis
RE's – Restriction enzymes
RRP – Readily releasable pool
R$_s$ – Series resistance
ΣCa^{2+} - Sum of calcium entry
SCG – Superior cervical ganglia
SFV – Semliki Forest virus
SK - Small conductance calcium-activated potassium channel
SNAREs – Soluble NSF attachment protein receptors
SRP – Slowly releasable pool
Synprint – *Syn*aptic *pro*tein *in*teraction
TEA-Cl – Tetraethyl-ammonium chloride
TeTX – Tetanus toxin

TIRF – Total internal reflection microscopy
TRP – Transient receptor potential
TTX – Tetrodotoxin
VGCC's – Voltage-gated calcium channels
V$_{Command}$ – Voltage command
V$_m$ – Voltage potential
ω-Aga-IVA – omega-Agatoxin IVA
ω-CTX MVIIC – omega-conotoxin MVIIC
ω-CTX GTX-GVIA – omega-conotoxin GVIA
WT – Wild type

Chapter 1 Introduction.

Calcium channel subtypes are of functional importance in neurones. Calcium entry through different voltage-gated calcium channels (VGCC's) delivers calcium ions to specific intracellular compartments in a highly regulated manner. These discrete calcium signals are responsible for many physiological processes in the nervous system including neurotransmitter release. Excess calcium entry, which would be detrimental to the cell, is prevented primarily through the inactivation of VGCC's, but also through other mechanisms such as calcium uptake into the mitochondria or other organelles, and active extrusion of calcium from the cell. Release of neurotransmitter is the primary form of communication in the nervous system and is highly controlled. The mechanism of stimulus-coupled exocytosis is not confined to neurones and the same basic machinery is also used to regulate release of neurotransmitters, hormones and peptides from a variety of neuroendocrine and exocrine cells.

1.1 Chromaffin cells as a model to study the molecular mechanisms of neurotransmitter release.

Chromaffin cells are a useful model to study the cellular and molecular mechanisms involved in neurotransmitter release. They are embryonically derived from the neural crest, the same precursor of sympathetic neurons (Unsicker et al. 1997). The majority of fusion proteins implicated in neuronal calcium-dependent exocytosis are also expressed in chromaffin cells (Morgan and Burgoyne 1997), although the expression levels and isoforms of some exocytotic proteins can differ. Chromaffin cells also express the high voltage activated (HVA), calcium channels found in neurones (Artalejo et al. 1994). Many mammalian nerve terminals are small and inaccessible making direct investigations of stimulus-coupled exocytosis difficult. Due to the large spherical size of chromaffin cells and their release of an oxidisable neurotransmitter (catecholamine) it is possible to apply high time resolution techniques like membrane capacitance measurements and amperometry (Neher

1

1998), which have enabled an estimation of the kinetics of neurosecretion (Chow et al. 1992; Chow et al. 1996). However care should be taken when interpreting results from chromaffin cells, as several aspects of the secretory response are distinct from those of neurones, including the rate of transmitter release (Martin 2003).

1.1.1 Images of chromaffin cells from a bovine cell culture and a rat slice.
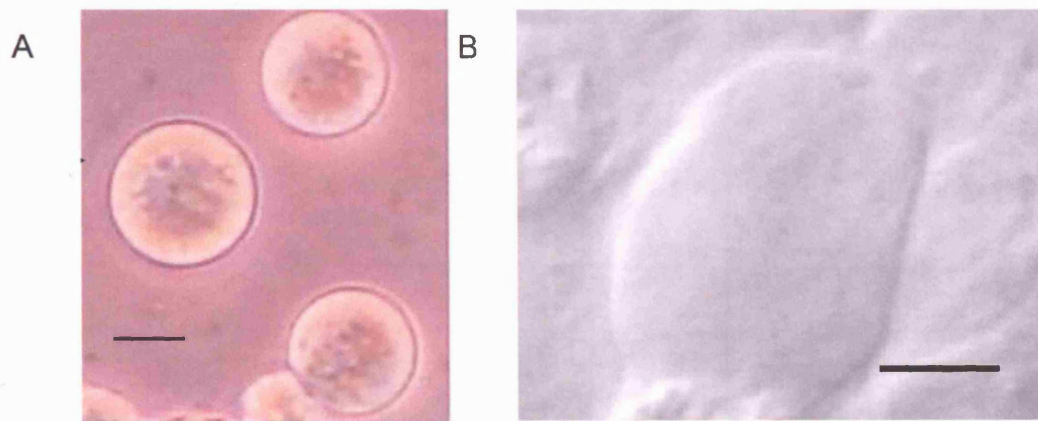
Images of individual chromaffin cells, scale bar represents 10μm in each picture.
A. Image of bovine chromaffin captured 72 hrs after culture.
B. Image of an individual chromaffin cell on the surface of a rat adrenal slice, the image was taken 4 hrs post sacrifice.

1.2 Nomenclature of calcium channels

Over the years several different terms have been used to describe the same type of calcium channel, table 1.2.1 is a summary of the most common nomenclature. Since I distinguish between different channel types on the basis of their sensitivity to specific pharmacological inhibitors (dihydropyridines, ω-conotoxin GVIA and ω-agatoxin IVA), I refer in this thesis to channel subtypes primarily as L-type, N-type or P/Q-type channels.

2

1.2.1 Nomenclature and function of different calcium channels.

Calcium Channel	Calcium current type	Primary localizations	Previous name of α_1 subunit	Specific blocker	Functions
Ca$_v$1.1	L	Skeletal muscle	α_{1S}	Dihydropyridines (DHPs).	Excitation-contraction coupling, calcium homeostatis, gene regulation.
Ca$_v$1.2	L	Cardiac muscle, endocrine cells, neurones	α_{1C}	DHPs	Excitation-contraction coupling, hormone secretion, gene regulation.
Ca$_v$1.3	L	Endocrine cells, neurones	α_{1D}	DHPs	Hormone secretion, gene regulation.
Ca$_v$1.4	L	Retina	α_{1F}	DHPs	Tonic neurotransmitter release.
Ca$_v$2.1	P/Q	Nerve terminals, dendrites	α_{1A}	ω-Agatoxin-IVA	Neurotransmitter release, dendritic calcium transients.
Ca$_v$2.2	N	Nerve terminals, dendrites	α_{1B}	ω-Conotoxin-GVIA	Neurotransmitter release, dendritic calcium transients
Ca$_v$2.3	R	Cell bodies, dendrites, nerve terminals	α_{1E}	SNX-482 (inhibits some Ca$_v$2.3 channels with selectivity over other channel subtypes).	Calcium dependent action potentials, neurotransmitter release.
Ca$_v$3.1	T	Cardiac muscle, skeletal muscle, neurones	α_{1G}	None	Repetitive ring.
Ca$_v$3.2	T	Cardiac muscle, neurones	α_{1H}	None	Repetitive ring.
Ca$_v$3.3	T	Neurones	α_{1I}	None	Repetitive ring.

Reproduced from (Catterall 2000) & (Stotz et al. 2004) .

1.3 Subunit composition of calcium channels

At the molecular level, high voltage activated calcium channels are composed of four subunits, the pore-forming α_1 subunit and the auxiliary $\alpha_2\delta$, and β subunits and in some cases a transmembrane γ subunit (Arikkath and Campbell 2003). All cloned α_1 subunits share the same overall structural features of four highly conserved hydrophobic homologous transmembrane domains (Catterall 1999), (figure 1.3.1). However the cytoplasmic loops (1-4) linking these domains are highly divergent. Mutagenesis studies suggest that these intracellular linkers and the N and C terminus domains are the sites for the differential modulation of calcium channels leading to a variety of biophysical responses including inactivation kinetics. The auxiliary subunits modulate trafficking and the biophysical properties of the α_1 subunit. Ten α_1 subunits, four $\alpha_2\delta$ complexes, four β subunits and eight γ subunits are known so far (Stotz et al. 2004) thereby allowing a plethora of biophysical properties to arise from the pairing up of different subunits. In addition most of these subunits can alternatively splice leading to an even greater variety in the biophysical properties of functional channels. In addition to the classical auxiliary subunits mentioned above, it has been argued that some intracellular proteins like calmodulin, syntaxin or the $\beta\gamma$ subunits of G-proteins could also be described as calcium channel subunits (Jones 2003). The case is strongest for calmodulin, as it is constitutively associated with the α_1 subunits and interacts directly to modulate the biophysical properties of the channel.

1.3.1 Schematic representation of the α_1 pore forming subunit and ancillary subunits.

A.

B.
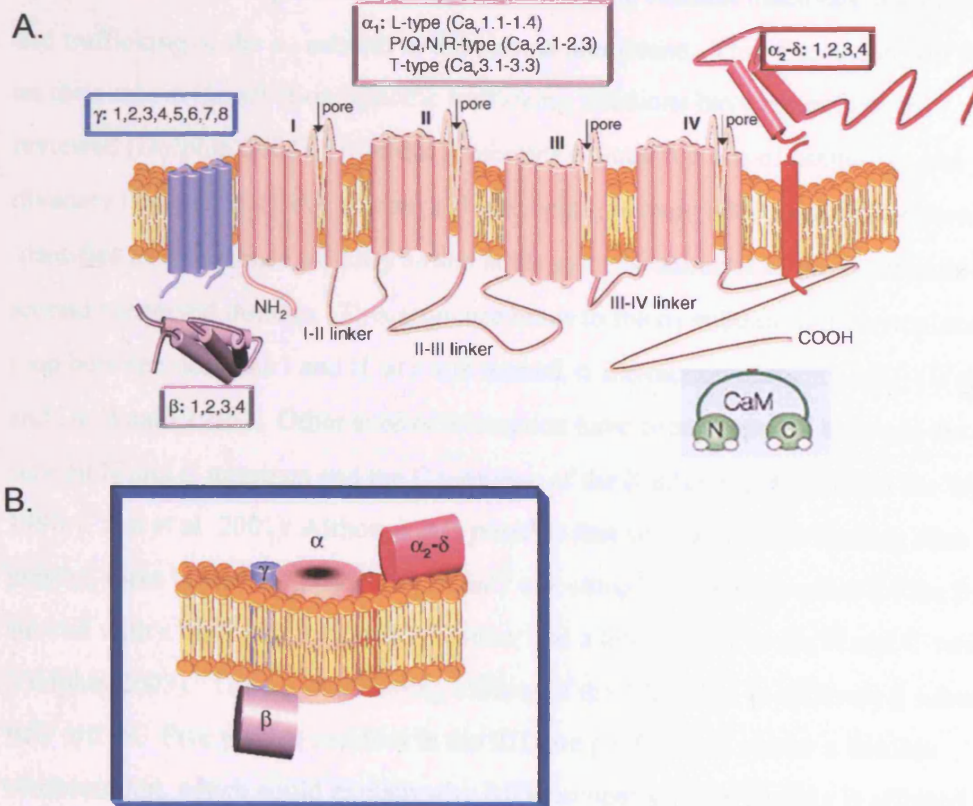
A. There are 10 known α_1 subunits divided into three families based on their sequence identity Ca$_v$ 1-3. An α_1 subunit consists of four domains (I-IV), each containing six transmembrane segments (S1-S6). The p-loops between S5 and S6 in each domain come together to form the ion-selective pore. The β-subunits (1-4) are cytoplasmic proteins that associate with the domain I-II linker region of the α_1 subunit. The α_2-δ subunits (1-4) are derived from a single gene, but are cleaved post-translationally into α_2 (extracellular) and δ (membrane spanning) subunits that are linked via disulphide bonds. The γ subunits (1-8) consist of four membrane-spanning regions. There may be a case to include calmodulin which is constitutively associated with the C-terminal tail of the α_1 subunit as a bonafide calcium channel auxiliary subunit.
B. Representation of an *in vivo* channel containing a α_1 subunit and a single member of each of the 'classical' accessory subunits.
Taken and adapted from (Stotz et al. 2004).

1.4 The β-subunits.

The β subunits are important in terms of determining channel inactivation kinetics and trafficking of the α_1 subunit to the plasma membrane. This discussion will focus on their role in inactivation, specific trafficking functions have recently been reviewed (Dolphin 2003). Different β subunits contain regions of homology and diversity (figure 1.4.1). All contain a β-interacting domain (BID) which has been identified as a sequence of thirty amino acids at the N terminus of the β-subunits second conserved domain. This sequence binds to the α_1 subunit in the cytoplasmic loop between domains I and II, at a site termed, α interaction domain (AID) (Walker and De Waard 1998). Other sites of interaction have been proposed between the α_1 subunit N and C terminus and the C terminus of the β subunit (Walker and De Waard 1998; Canti et al. 2001). Although it is possible that several distinct binding sites are present, there is also the possibility of only one complex binding pocket for the β subunit with a high affinity to the I-II linker and a low affinity to the N and C-termini (Dolphin 2003). The *in vitro* binding affinity of the I-II linker to different β subunits BID differs. Five proline residues in the BID are predicted to confer a flexible conformation, which could explain why BIDs competence for binding is affected by surrounding sequences (Walker and De Waard 1998).

1.4.1 Functional map of the β subunit.

% identity						
2%	1st conserved domain 65%	11%	2nd conserved domain 78%		3%	

BID (Voltage dependence of activation, current increase).

0   58   165   215   418   597

Inactivation kinetics

Kinetics and voltage dependence of inactivation
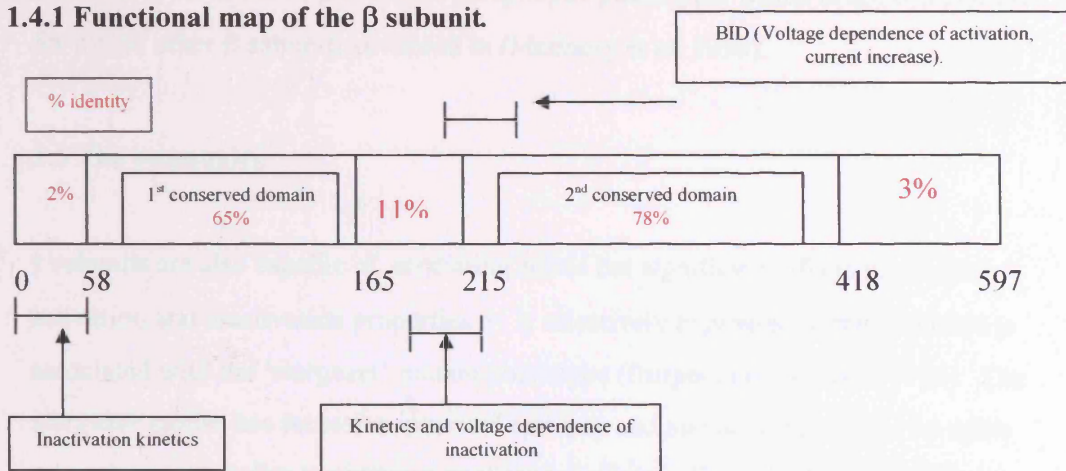
Comparison of the β-subunits sequences has revealed two highly conserved regions. Alternative splicing occurs, particularly within the three variable regions. The BID site and regions implicated in modulating inactivation are highlighted. Reproduced from (Walker and De Waard 1998).

Each of the four β subunit genes can alternatively splice yielding several isoforms with distinct patterns of tissue expression (Davila 1999; Catterall 2000). β_{1b} and β_3 can substantially increase the speed of inactivation, whereas β_{2a} can substantially slow inactivation (Stotz and Zamponi 2001). The β_2 subunit contains two cysteine residues, which can be palmitoylated. Palmitoylation could restrict mobility of the L_{1-2} linker as a result of the palmitoylated N terminus of the β subunit being anchored to the plasma membrane. Studies favour dynamic palmitoylation as a form of regulating calcium channels containing the β_2 subunit, as prevention of palmitoylation using tunimycin reduces the ability of β_{2a} to slow channel inactivation (Hurley et al. 2000). A link between an N-terminal membrane anchoring site (MAS) of the β_{2a} subunit and the BID causing immobilisation of the channel inactivation gate has also been described (Restituito et al. 2000). This suggests that the subunit acts as an anchor for the calcium channel I-II loop preventing its movement and reducing inactivation. β subunits also contain a Src homology 3 domain (SH3), which may mediate specific protein-protein interactions involved in signal transduction and/or specific targeting (Davila 1999; Dolphin 2003). Although some aspects of β subunit function are likely to be conserved others clearly are not. For

7

example a knock out of β4 leads to an epileptic phenotype, which is not compensated for by the other β subunits reviewed in (McEnery et al. 1998).

1.5 The γ-subunits.

γ subunits are also capable of mediating subtle but significant effects in channel activation and inactivation properties. γ2 is selectively expressed in the brain and is associated with the 'stargazer' mutant phenotype (Burgess and Noebels 1999). The *stargazer* mouse has recessive inherited epilepsy and ataxia characterised by spike wave seizures, similar to *petit mal* or absence epilepsy (Chen et al. 1999). The functional roles of γ2, γ3 and γ4, have been examined by expression with the P/Q type channel and different β subunit combinations in *Xenopus* oocytes (Rousset et al. 2001). They found that in the absence of β subunits, γ2 and γ3 subunits hyperpolarised channel activation and increased inactivation. However these effects were differentially affected upon co-expression with the various types of β subunits. The results imply that the effects of the γ subunits on channel properties are sensitive to the α and β subunits present. The loss of the γ subunit function could explain some pathological conditions, as calcium channels could inactivate more slowly and at more depolarised potentials leading to an increase in calcium influx, neurotransmitter release and neuronal excitability (Rousset et al. 2001).

1.6 Mechanisms and molecular determinants of calcium channel inactivation

There are three different conformational changes in which calcium channels can inactivate: a fast, and slow voltage-dependent inactivation process and calcium-dependent inactivation (Hering et al. 2000). The intrinsic properties of the α_1 pore determines many aspects of the calcium current kinetics, but interactions with other subunits and synaptic proteins are also believed to strongly influence current kinetics especially inactivation (Walker and De Waard 1998; Catterall 2000; Hering et al. 2000). The molecular mechanisms of calcium channel inactivation are not as well

understood as some potassium or sodium channels. Evidence regarding the molecular mechanisms of calcium channel inactivation has come from recombinant and mutagenesis studies of the α_1 subunit, studying gain-of-function chimeras, channel splice variants and studies investigating regulation by other calcium channel subunits, such as the β subunit and intracellular proteins like syntaxin or calmodulin. Heterologous experiments are useful in identifying components of inactivation but care should be taken when interpreting the results as the native phenotype is dependent on a complete intracellular environment, which may be missing in these expression systems. Cell specific posttranslational modifications, the complement of different subunit isoforms present, the calcium buffering capabilities of the cell, or the expression of G-protein-coupled receptors (GPCR's) on the cell surface and their ability to release G protein subunits which can interact with the calcium channel can all affect inactivation rates. Many experiments use barium as the charge carrier to maximize current amplitudes, an important point to take into consideration when interpreting these results is that calcium dependent inactivation will be masked.

1.7 Mechanisms of fast voltage dependent inactivation.

In response to prolonged membrane depolarisation calcium channels enter a non-conducting inactivated state. When expressed in the absence of auxiliary subunits it is observed that barium currents through various HVA calcium channels display pronounced voltage-dependent inactivation, suggesting that structural determinants on the α_1 subunit itself can mediate voltage-dependent inactivation. Experiments performed using chimeras, mutatgenesis, over-expression of peptide fragments resembling parts of the channels and analysis of naturally occurring splice variants concluded that two regions on the α_1 pore were vitally important in this process (reviewed in Stolz et al 2003). These were the S6 segments from all four domains and the cytoplasmic domain I-II linker. Other regions including the domain III-IV linker and the C and N terminus have also been implicated in regulating this process. By combining the information provided by structure-function studies the following model has been proposed to account for fast voltage-dependent inactivation of HVA

calcium channels. In response to membrane depolarisation, the S6 segments undergo a conformational change allowing the domain I-II linker to physically occlude the pore by docking to the cytoplasmic end of the S6 segments. β-subunits can differentially modulate inactivation kinetics by binding to and regulating mobility of the I-II linker. The C and N-termini and the domain III-IV linker regions of the channel can modulate inactivation rates through interactions with the I-II linker region either directly or indirectly through interactions with β subunits (Stotz et al. 2004).

1.7.1 Regions implicated in mediating fast voltage-dependent inactivation.
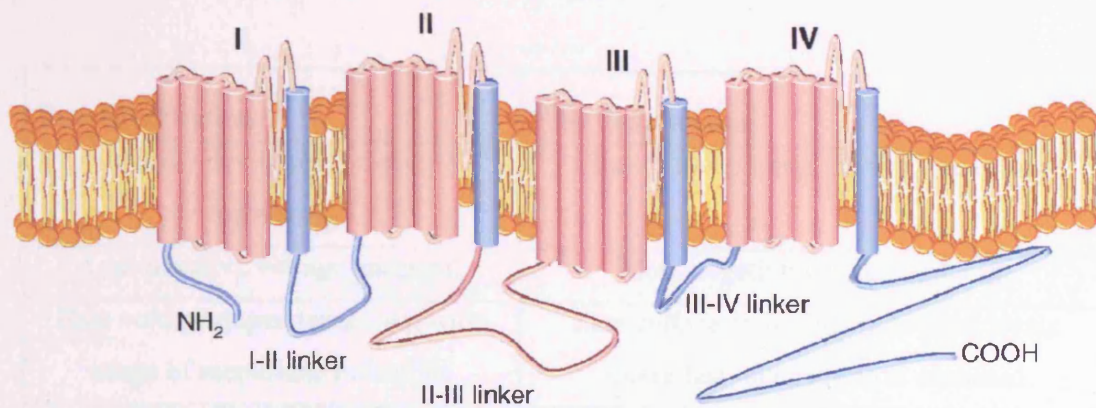
The regions of the α_1 subunit that have been implicated in fast voltage-dependent inactivation are shown in blue. Taken from (Stotz et al. 2004).

1.8 Slow voltage-dependent inactivation.

Calcium channels are thought to undergo more than one conformational change during inactivation. Experiments which exclude calcium-dependent inactivation by substituting extracellular calcium with barium commonly observe a biexponential decay of currents, (Hering et al. 2000). This biexponential timecourse has been interpreted as resulting from two mechanisms of inactivation, fast and slow. Fast inactivation occurs over several tens to hundreds of milliseconds, whereas slow

10

inactivation requires much more prolonged membrane depolarisation (seconds to minutes), (Stotz et al. 2004). The mechanisms underlying slow inactivation remain a poorly understood process. Hering and co-workers suggest that P/Q type channels can proceed to the slow inactivated state from the fast inactivated state as well as directly from the open state (Hering et al. 2000). However the channels enter the slow inactivation state more willingly from the open than from the fast inactivated state and the expression of different β isoforms can indirectly affect the rate of inactivation (Sokolov et al. 2000). Fast and slow inactivation has also been reported for N type channels, below in table 1.5.1 are some of the published findings.

1.8.1 Contrasting properties of fast and slow inactivation of N type calcium channels.

Fast Inactivation	Slow inactivation
Rapidly developing, rapidly recovering	Slowly developing, slowly recovering
Less negative voltage midpoint	More negative voltage midpoint
Rate voltage-dependence over wide range of membrane potentials	Rate voltage-independent beyond levels where fast inactivation is saturated
Temperature-dependent	Onset not intrinsically temperature-dependent; recovery strongly temperature-dependent
Onset accelerated by repetitive pulsing	Onset accelerated by repetitive pulsing
Unaffected by syntaxin.	Strongly promoted by syntaxin.

Reproduced from (Degtiar et al. 2000).

1.9 Calcium-dependent inactivation.

Several criteria are commonly used to describe calcium dependent inactivation. Inactivation is faster when the charge carrier is calcium *vs* barium or any other cation. High extracellular calcium concentrations speed the rate of inactivation and the

voltage dependence of inactivation is U shaped and parallels calcium entry by decreasing at strongly depolarised voltages (Jones 1999). Buffering of intracellular calcium can also reduce inactivation and is sometimes used as evidence for calcium dependent inactivation but is highly dependent on the preparation and concentration/type of buffer used and will be discussed in more detail latter. It was first proposed that calcium channel inactivation results from calcium entry through the open channels in the late 1970's (Brehm and Erkert 1978). A number of different groups using a variety of preparations reported similar observations. For a review on this early work see (Eckert and Chad 1984). However the molecular mechanism of this calcium-dependent inactivation could not be thoroughly investigated until the advent of patch clamp, gene cloning and other recombinant-based molecular techniques. L type calcium channels are generally accepted as inactivating primarily by a calcium-dependent process, consequently the molecular mechanisms underlying this process have been mostly studied in L-type channels. Several groups suggested that calmodulin was the calcium sensor for inactivation of L type channels (Peterson et al. 1999; Zuhlke et al. 1999).

1.9.1 Molecular determinants of calcium-dependent inactivation of L-type channels.

Inspection of the C-terminal tail of the channel revealed two sites potentially important in mediating calcium-dependent inactivation. An IQ motif (small structural domain that mediates interactions with calmodulin), and an EF hand (a calcium-binding domain), (Budde et al. 2002). Initial studies investigating the role of calmodulin in mediating calcium-dependent inactivation of L-type (α_{1C}) channels determined that, the IQ motif in the C terminus of the channel acts as a Ca^{2+}/calmodulin effector site (Peterson et al. 1999; Zuhlke et al. 1999), with the C terminal channel EF hand site contributing to the downstream signal transduction (Peterson et al. 2000). These studies employed mutants of calmodulin incapable of binding calcium as a dominant negative mutant to determine a role for Ca^{2+}/calmodulin and showed that mutated calmodulin was capable of binding to the

12

channel, which implies that L-type channels harbour an apoCalmodulin (ie calcium-independent) binding site. A variety of biochemical (Pate et al. 2000; Romanin et al. 2000; Mouton et al. 2001 and Pitt et al. 2001) and imaging (Erickson et al. 2003) techniques have determined a region of ~ 110 amino acids between the EF and IQ regions as the apoCalmodulin interaction site although the exact region remains controversial. Two models of how Ca^{2+}/calmodulin can mediate channel inactivation have recently been proposed and are now discussed. It is believed that the signal transduction mechanisms underlying both calcium and voltage-dependent inactivation converge to utilize the same molecular machinery to actually induce inactivation (Cens et al. 1999). The first model proposed by (Kim et al. 2004) predicts that the EF hand sits between the calmodulin binding domain and the I-II loop and prevents the I-II loop, either directly or indirectly from blocking the channel. This interaction is stabilized by hydrophobic contacts formed by I_{1654} (the I in the IQ motif) (figure 1.9.1.1). In the absence of calcium, membrane depolarisation induces a conformational change in the transmembrane segments which is translated to the EF hand, allowing the I-II loop to slowly move and initiate inactivation. Calcium accelerates this process by inducing a Ca^{2+}/calmodulin conformational change which removes inhibition of the I-II loop movement by I_{1654} and allows the calcium sensing apparatus to interact directly with the I-II loop to facilitate pore block (figure 1.9.1.1).

1.9.1.1 Model 1 for voltage and calcium-dependent inactivation of L-type channels.
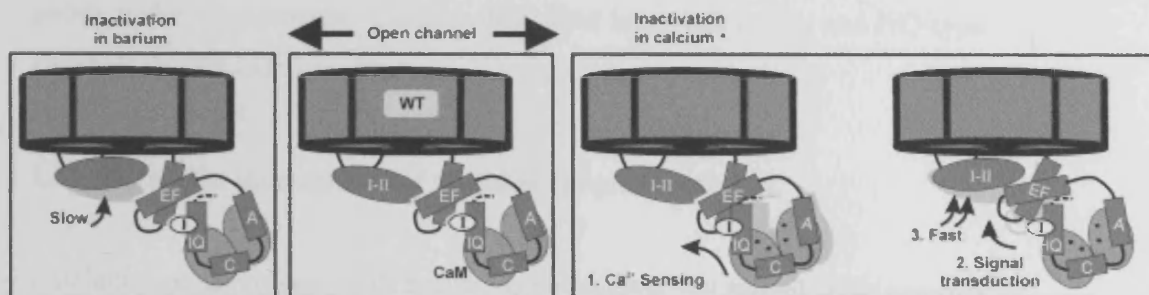
Model depicted for a normal (WT) channel. The open channel is shown in the middle box. In the absence of calcium, voltage induces a slow conformational change that allows the I-II loop to interact with the pore (left). Calcium influx induces a Ca^{2+}/calmodulin-induced conformational change that relieves EF-mediated inhibition of the I-II loop, allowing an accelerated interaction of the I-II loop with the pore (right). Taken from (Kim et al. 2004). The A and C domains are regions on the channel C-terminus thought to harbour apoCalmodulin binding. The highlighted I represents I_{1654} in the IQ motif which is thought to stabilize the EF-mediated inhibition of loop I-II movement.

The second model proposed by Nikolai Soldatov suggests that Ca^{2+}/calmodulin mediated calcium-dependent inactivation is also connected to the mechanism which induces voltage-dependent inactivation, however the process is fundamentally different. In this model, voltage-dependent inactivation is proposed to arise primarily from a constriction of the pore by movement of the S6 segments and does not account for pore block by movement of the I-II loop. In this model apoCalmodulin is bound to the C-terminus which is folded back so that calmodulin sits within the channel pore. The presence of calmodulin therefore prevents full pore constriction after membrane depolarisation keeping the channel open. By binding calcium, calmodulin is able to leave its resting binding site and bind to the IQ motif (outside the pore), thereby no longer preventing full pore block and allowing inactivation to proceed (Soldatov 2003). Both models are working hypothesis which require further rigorous testing, however at present I favour the first model as it accounts for a role of the I-II loop in mediating inactivation, which supports previous studies investigating voltage-dependent inactivation (section 1.4). Further information to take into account when modelling calcium-dependent inactivation of L-type channels should include the basal phosphorylation state of the channel. PKA phosphorylation of the channel is

14

believed to enhance calcium-dependent inactivation whereas dephosphorylation is believed to result in purely voltage-dependent inactivation (Findlay 2004). When I started this project calcium-dependent inactivation of non-L-type channels was a poorly understood process. Calcium-dependent inactivation of N and P/Q-type channels are discussed in chapter 6.

1.10. Molecular mechanisms of stimulus-coupled secretion.

Calcium-dependent exocytosis occurs via a regulated, but modulatable complex pathway of multiple protein-protein interactions. Using a combination of genetic, biochemical and biophysical techniques the role(s) and importance of individual proteins in this pathway can be investigated. A considerable amount of knowledge, particularly in the last decade has been obtained, and while a thorough understanding of this process is far from complete the molecular mechanisms underlying distinct stages in this pathway have been described and comprehensively reviewed (recent reviews include; Bennett 1997; Zheng and Bobich 1998; Turner et al. 1999; Bajjalieh 1999; Benfenati et al. 1999; von Gersdorff and Matthews 1999; Brunger 2000; Klenchin and Martin 2000; Cousin 2000; Lin and Scheller 2000; Valtorta et al. 2001; Richmond and Broadie 2002; Gundelfinger et al. 2003; Rosenmund et al. 2003; Gerst 1999; Li and Chin 2003, Sudhof 2004 and Sorensen, 2004).

1.11 Overview of the vesicle exo/endocytosis cycle.

Synaptic transmission is initiated when an action potential triggers calcium influx, fusion of synaptic vesicles and release of neurotransmitter from a presynaptic nerve terminal (Katz 1969). There are numerous types of vesicle found within cells, some are important in intracellular trafficking, some in constitutive exocytosis, some in receptor-mediated endocytosis and others in protein sorting. In this thesis I use the term vesicle to describe solely vesicles involved in calcium-dependent exocytosis of neurotransmitters, peptides or hormones. Several sequential stages in the secretory vesicle cycle have been described. Firstly neurotransmitter is loaded into synaptic vesicles in neurones or into dense core vesicles in neuroendocrine cells, then vesicles

15

translocate from an intracellular reserve pool and dock at the plasma membrane. They then undergo maturation or priming to obtain a fusion competent state. Upon membrane depolarisation and calcium entry through voltage-gated calcium channels, primed vesicles fuse with the membrane and release their contents. After fusion pore dilation and neurotransmitter release, vesicles are endocytosed via one of three alternative endocytotic pathways. The first is colloquially termed 'kiss and stay', where vesicles stay at the site of release, reacidify and refill neurotransmitter without undocking from the plasma membrane. The second pathway termed 'kiss and run', is similar to 'kiss and stay' except that vesicles undock and recycle locally to be refilled with neurotransmitter. The third pathway involves endocytosis through clathin coated pits, with reacidification and refilling occurring either directly or through an endosomal intermediate (Sudhof 2004). Fast vesicle recycling (kiss and stay or kiss and run) will probably involve a transient fusion pore without complete trans-bilayer mixing, whereas slow recycling (clathrin-dependent) is likely to occur after the full collapse of the vesicle into the plasma membrane.

1.11.1 The synaptic vesicle cycle.
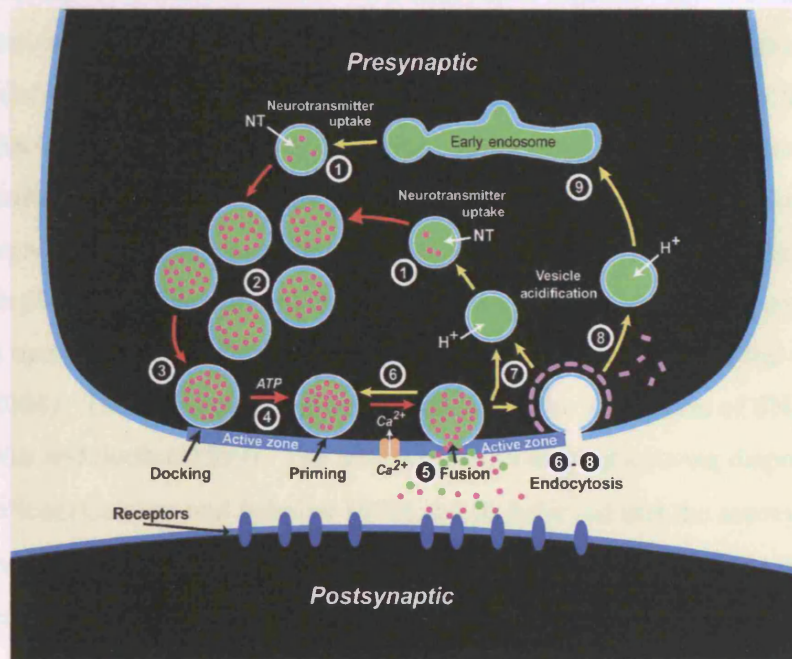
Vesicles are filled with neurotransmitter (step 1), and then translocate from a reserve pool (step 2) to the plasma membrane and dock (step 3). After docking they undergo priming reactions (step 4) to make them fusion-competent requiring only a rise in calcium to trigger exocytosis (step 5). After fusion pore closure vesicles undergo endocytosis via one of several pathways. Either local reuse (step 6), fast recycling without an endosomal intermediate (step 7), or clathrin-mediated endocytosis (step 8) with recycling via an endosome (step 9). Steps in exocytosis are shown by red arrows and steps in endocytosis and recycling are shown by yellow arrows. Taken from (Sudhof 2004). Although this picture illustrates synaptic vesicle cycling in neurones, the same processes shown are believed to occur in neuroendocrine cells such as chromaffin cells.

1.12 The SNARE hypothesis.

Three small membrane proteins are believed to play a central role in exocytosis, synaptobrevin, syntaxin and SNAP-25, commonly called SNARE proteins (acronym for soluble NSF attachment protein receptors), (Rothman and Warren 1994). The use of clostridial and botulinum neurotoxins, which specifically cleave these proteins have shown SNAREs to be essential for exocytosis (Schiavo et al. 1992; Blasi et al. 1993; Lawrence et al. 1994; Graham et al. 2000). According to the SNARE hypothesis, synaptobrevin on vesicles acts as a v-SNARE and SNAP-25 and syntaxin

17

on the presynaptic plasma membrane serve as t-SNARES (Jahn and Sudhof 1999). The vesicle and target membranes interact when these proteins form a trans-SNARE 'core' complex. Originally SNAREs were believed to mediate vesicle docking to release sites on the plasma membrane (Sollner et al. 1993). However experimental evidence does not support this hypothesis. Firstly proteolytic cleavage of SNARE proteins does not prevent vesicle docking (O'Connor et al. 1996), and secondly genetic studies in drosphophila have shown normal numbers of vesicles docked to the plasma membrane in syntaxin-deficient mutants (Broadie et al. 1995). The current hypothesis places the formation of the SNARE core complex as a direct precursor of the fusion event, requiring just a rise in intracellular calcium to trigger full fusion (Sudhof 2004). These proteins bind to each other via the interaction of SNARE motifs (Jahn and Sudhof 1999). The SNARE motifs display a strong disposition to form α-helices (Calakos and Scheller 1996) and its believed that the association of these domains functions in a manner similar to leucine zippers. Analysis of the crystal structure of the core complex (Sutton et al. 1998), suggests that the α-helices wrap around each other to form a coiled-coil structure which zippers up and pulls the vesicle membrane towards the plasma membrane, allowing partial fusion (hemifusion) of the two membranes (figure 1.12.1)

1.12.1 Formation of a trans-SNARE core complex
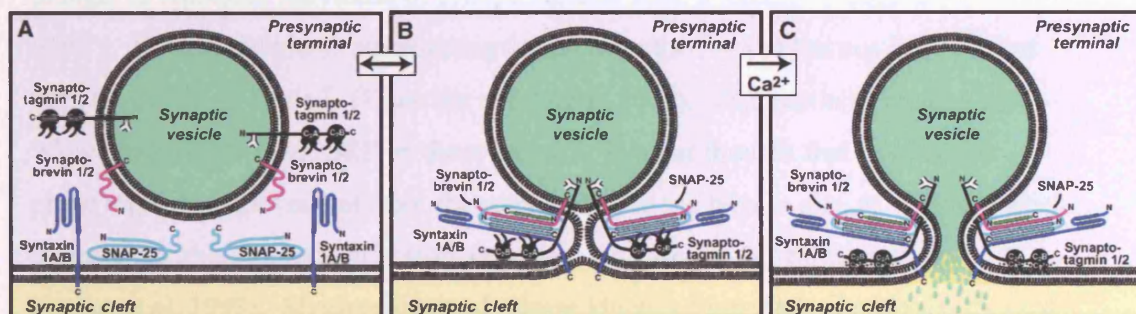
This scheme represents the minimal fusion machinery required for exocytosis. A. The vesicle is docked to the plasma membrane but SNAREs are not engaged. B Synaptobrevin on the vesicle interacts with syntaxin and SNAP-25 in the plasma membrane. The formation of the core SNARE complex pulls the vesicle and plasma membranes close together and may induce hemifusion. C Activation of calcium channels and subsequent calcium binding to synaptotagmin triggers fusion. Taken from (Sudhof 2004).

1.13 Definition of different functional pools of vesicles.

Morphological and fluorescent microscopy studies on bovine chromaffin cells suggest that around 450-1000 dense core vesicles are located near the plasma membrane, (Vitale et al. 1995; Steyer et al. 1997; Oheim et al. 1998), however electrophysiological measurements show that upon stimulation only a small fraction of these vesicles are rapidly released (Neher and Zucker 1993). This suggests that docked vesicles undergo maturation or priming to become fusion competent. The priming of vesicles is ATP-dependent and many factors including the synthesis of phoshoinositides, NSF-mediated priming of SNARE complexes and protein kinase-mediated protein phosphorylations have been suggested as being important for priming in neuroendocrine cells, (Klenchin and Martin 2000). Other proteins like munc-13 (discussed section 1.15) have also been shown to be essential for vesicle priming in neurones (Brose et al. 2000). Priming of docked vesicles is believed to be the rate-limiting step in regulated exocytosis in neurones and neuroendocrine cells. Membrane capacitance measurements of regulated exocytosis have revealed several distinct kinetic phases of vesicle fusion. This has been interpreted as populations of vesicles in different fusion competent stages. The first phase, (the exocytotic burst in flash photolysis of caged calcium experiments), occurs within milliseconds, and is thought to represent the fusion of primed vesicles from a readily releasable pool (RRP). The second phase representing fusion from the docked but not fully primed vesicles occurs in seconds (Klenchin and Martin 2000). This has been termed the 'slowly releasable pool' SRP by some authors. It is not thought that this second phase represents movement from the reserve pool to the release site, as optical studies indicate that this is a relatively slow process taking around 6-7 minutes to occur (Steyer et al. 1997). Measurements of release kinetics from flash photolysis of caged calcium experiments has revealed that release from the RRP has a time constant of 20-40ms at 20μM calcium and release from the SRP has a time constant of ~ 200ms at 20μM calcium (Heinemann et al. 1994; Xu et al. 1999; Voets et al. 1999; Voets 2000). A picture has emerged in which it is envisaged that once a vesicle docks a series of biochemical modifications occur to prime the vesicle for fusion competence.

19

The scheme suggests that as the RRP depletes the SRP matures and becomes readily releasable. In chromaffin cells the transition from the RRP to the SRP takes around 4 seconds and has been inferred as the conversion between a loose and tight state of the trans-SNARE complex (Voets 2000). Although it can be considered that the RRP and SRP are molecularly distinct pools of vesicles and the RRP may not be refilled from vesicles in the SRP, but by direct maturation of other docked vesicles. Within the RRP there is a subset of vesicles located in the immediate proximity of the calcium channels. This group of vesicles referred to as the 'immediately releasable pool' IRP respond the quickest to voltage stimulation (figure 1.13.1). In chromaffin cells the IRP is believed to represent ~25% of the RRP size (Voets et al 1999). Recently flash photolysis experiments have defined a small pool of vesicles with even faster release kinetics at low $[Ca^{2+}]_i$ than the rest of the RRP, termed the highly calcium sensitive pool (HCSP), (Yang et al. 2002). The size of this pool can be greatly increased by PKC (more so than the RRP) and has the highest release rates during small global increases in $[Ca^{2+}]_i$, which are likely to occur after release of calcium from intracellular stores. Therefore this pool has a large potential for physiological regulation. This small pool has only been defined by flash photolysis experiments at a controlled and low $[Ca^{2+}]_i$, and at present the relationship between the HCSP and other pools of vesicles (IRP/RRP/SRP) is not known. With this in mind I have limited the interpretation and discussion of my results regarding different vesicle pools to the well defined IRP, RRP and SRP.

1.13.1 Different pools of vesicles exist, with distinct release kinetics.
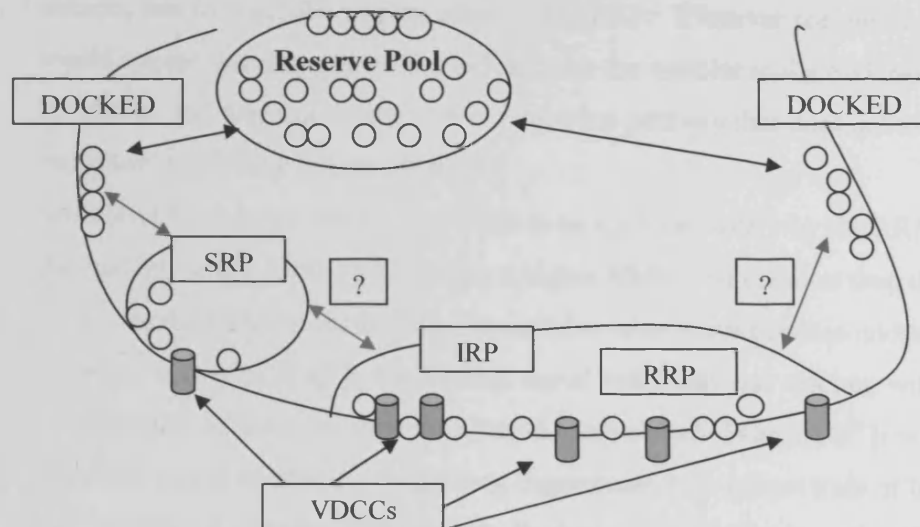
Several defined pools of vesicles exist. The majority of vesicles are kept away from the plasma membrane (the reserve pool). Translocation of vesicles from the reserve pool to the membrane results in docked vesicles incapable of fusion. A series of maturation or priming reactions converts these vesicles into a slowly fusible state (the SRP). To obtain the kinetics of fast stimulus-coupled release, further priming steps are required to create highly fusion-competent vesicles, awaiting only a rise in calcium to trigger fusion. Such a pool or vesicles is called the RRP (a subset of vesicles from this pool, the IRP are located immediately next to the source of calcium entry and are the first to fuse). It has been proposed that additional maturation converts a SRP vesicle into a RRP vesicle however it is feasible that the two pools contain molecularly distinct vesicles and a separate pool of docked vesicles are primed directly into the RRP. Blue arrows represent reversible priming reactions.

The RRP is believed to be in dynamic equilibrium with less fusion-competent intermediates. Various proteins (ie complexin) and signaling molecules are believed to influence the forward and backward priming rates (Sudhof 2004). For fast calcium-triggered exocytosis the overall forward and backward priming rates are required to be adjusted so that a RRP of significant size can form in the absence of release. It also requires that the fusion rate is very low at basal $[Ca^{2+}]i$ and very high at stimulated $[Ca^{2+}]i$. This necessitates that the fusion rate has a steep dependence on calcium (Sorensen 2004). As the kinetics of fusion are different between the two releasable pools at a defined concentration of calcium, this indicates that the calcium sensor(s) in the RRP has a different binding affinity than the calcium sensor(s) in the SRP, (Seward et al. 1996; Voets 2000). This may reflect different isoforms of the calcium sensor(s), different protein folding/interactions or phosphorylation states

21

between the two pools. Alternatively there could be two molecularly distinct calcium sensors, one for the SRP and the other for the RRP. Whatever the mechanism it would appear that during a prolonged stimulus the vesicles in the SRP become fusion competent and fuse (albeit at a slower rate) via a pathway that does not involve the transition to the RRP (Voets 2000).

With brief stimulation release is thought to be mediated solely by the RRP, despite the calcium sensor for the SRP having a higher affinity for calcium than the calcium sensor for the RRP (Voets 2000). This is believed to occur because under conditions of rapidly changing $[Ca^{2+}]i$, the calcium signal will decay and calcium will dissociate from the SRP calcium sensor before fusion can proceed. When $[Ca^{2+}]i$ is raised for a sustained period of time, (ie with a long depolarisation or robust train of brief depolarisations), then the RRP will rapidly deplete and fusion from the SRP will ensue.

1.14. Synaptotagmin I as a calcium sensor for fast calcium-dependent exocytosis.

Synaptotamin is an abundant vesicle associated protein that is capable of binding calcium ions. This protein contains a short intravesicular N-terminus, a transmembrane region, followed by a short linker sequence and two cytoplasmic C_2 domains (C_2A and C_2B), (Perin 1996). The intrinsic calcium affinities of the C_2 domains are very low (0.5-5mM) as the coordination of the binding site is incomplete. However the apparent calcium affinity of the C_2 domains increases dramatically (1000-fold) when the C_2 domains bind phospholipids, which provides additional coordination sites for bound calcium (Fernandez-Chacon et al. 2001). This protein has received considerable attention and there is now good evidence to support synaptotagmin I as the calcium sensor for fast calcium-dependent exocytosis. I discuss here a few of the salient experiments which have led to this conclusion. For more detailed reviews of this protein see (Yoshihara et al. 2003; Koh and Bellen 2003; Bai and Chapman 2004; Sudhof 2004). Defects in neurotransmitter release are observed in worms, flies and mice after knockout of synaptotagmin I. In mice this is lethal with studies in hippocampal neurones (Geppert et al. 1994) and chromaffin

22

cells (Voets et al. 2001) reporting a selective loss of fast, but not slow calcium-dependent exocytosis. A concern with genetic experiments is the ability of the organism to compensate or adapt, masking the true function of a protein *in vivo*. In a beautiful study an inducible deletion of synaptotagmin I was investigated. Graeme Davis's laboratory constructed a C-terminal-tagged synaptotagmin I which can be inactivated by fluorophore-assisted light inactivation (Marek and Davis 2002). The tetracysteine-tagged synaptotagmin I (Syt 14C), was able to rescue drosphophila null mutants, demonstrating that it is functionally equivalent to wild type protein. After a 10 second photo-inactivation which cleaves the protein the calcium cooperativity of exocytosis was reduced from a pre-inactivation value n = 3.4 to n = 0.9. This elegant study supports the knockout data that synaptotagmin I is critically involved in calcium sensing and fusion. Further studies determined that a point mutation in the C_2A domain which alters the overall apparent calcium affinity of synaptotagmin I induced an identical shift in the calcium cooperativity of exocytosis (Fernandez-Chacon et al. 2001). Experiments in chromaffin cells using flash photolysis show that this mutant shifts the apparent calcium affinity of fast (but not slow) exocytosis in exactly the same manner (Sorenson et al 2003). Amperometric studies in PC12 cells show that over-expression of synaptotagmin I extends the transition between fusion-pore opening and dilation (Wang and Zucker 1998). The current hypothesis is that oligomerization of synaptotagmin I and the SNARE complex temporally stabilizes the fusion pore and possibly drives the fusion of the vesicle into the plasma membrane. Recent studies have determined that the length of the linker between to the two C_2 domains is critical in controlling the stability of the fusion pore (Bai and Chapman 2004). Synaptotagmin I is not only thought to trigger fast calcium-dependent exocytosis, but is also a critical protein required for a compensatory endocytosis pathway (Jorgensen et al. 1995; Poskanzer et al. 2003). Therefore it plays a crucial and central role in the secretory vesicle cycle.

1.15 Regulators of trans-SNARE complex formation.

During the process of targeting, docking, and priming vesicles, numerous proteins interact. These interactions often involve binding of relatively large domains of protein partners (Benfenati et al. 1999), multiple partners often compete for the same binding site and the formation of multimeric protein complexes may uncover new binding sites for other protein partners (Benfenati et al. 1999). In this way protein interactions can be directed along the pathway leading to exocytosis. More than a thousand proteins function in the presynaptic nerve terminal, and hundreds are thought to participate in exocytosis (Sudhof 2004). In this section I will introduce four key proteins implicated in either vesicle docking to the plasma membrane, facilitation, stabilization or inhibition of SNARE complex assembly, and thereby determine the number of fusion competent vesicles and the size of the RRP and SRP. There are several published reviews, which comprehensively discuss the roles of other SNARE protein regulators (Jahn and Sudhof 1999; Jahn et al. 2003; Sudhof 2004).

1.15.1 Munc-18

Genetic studies in mice have identified an essential role for munc-18-1 (Verhage et al. 2000; Voets et al. 2001) in mammals and its homologues (unc-18 and Rop) for synaptic transmission in worms and flies (Weimer et al. 2003; Harrison et al. 1994). Munc-18 has been suggested to assist in the formation of SNARE complexes, and the roles of other important exocytotic proteins are primarily thought to revolve around their interactions with SNAREs and/or munc-18 (Rizo and Sudhof 2002). Initially it was believed that munc-18's main function was to prevent SNARE complex formation, by binding to syntaxin (Fujita et al. 1996; Haynes et al. 1999). Syntaxin can adopt two formations, an open conformation amenable to binding other SNARE proteins and a closed formation incapable of interactions with SNARE proteins (Dulubova et al. 1999). Munc-18 is proposed to bind to the closed conformation, preventing transition to the open conformation. Indeed the crystal structure of the

24

munc-18-1-synatxin-1 complex shows that munc-18-1 wraps around syntaxin in its closed conformation (Misura et al. 2000). This suggests that munc-18 is a negative regulator of SNARE complex formation and exocytosis. Biochemical *in vitro* studies have determined that the phosphorylation state of munc-18 can influence its binding to syntaxin, perhaps explaining a component of either PKC (de Vries et al. 2000) or cdk5 (Fletcher et al. 1999), facilitation of neurotransmitter release. It is thought that other proteins binding to munc-18 may interrupt its binding to syntaxin and therefore facilitate exocytosis. Proteins such as Doc2 (Duncan et al. 2000), Mints (Okamoto and Sudhof 1997), Tomosyn (Fujita et al. 1998) and munc-13 (Garner et al. 2000) have been implicated in this way. Although the interaction between syntaxin and munc-18 is thought to be stronger than the interaction of these other proteins, the equilibrium may be shifted in favour of say the Doc2-munc-18 interaction by other vesicle and core complex proteins modulating the affinity of the syntaxin-munc-18 interaction (Verhage et al. 1997). As munc-18 can interact with many proteins it is ideally suited to play a role in regulating the superstructure required for fusion (Jahn 2000). However these proposals do not reconcile with functional studies from knockouts, which indicate that secretion is dramatically inhibited, and over-expression of munc-18 can facilitate exocytosis by increasing both the size of releasable pools and the priming rate (Voets et al. 2001). This observation therefore is inconsistent with a role of munc-18 as a negative regulator of exocytosis and suggests that munc-18 is in involved directly in vesicle priming or indirectly by increasing the number of docked vesicles. The increase in the size of the RRP and SRP after over-expression of munc-18 could occur indirectly of a specific priming role. A larger pool of docked, but un-primed vesicles, will in a reversible priming reaction scheme (section 1.13), result in an increase in the size of the RRP and SRP. In fact a recent and thorough examination of unc-18 knockouts in *C.elegans* concludes that although unc-18 may play a secondary role in SNARE complex formation, the primary and essential role of unc-18 is in vesicle docking (Weimer et al. 2003).

1.15.2 Munc-13

Munc-13 is a homologue of the *C. elegans* unc-13 and is a target of the diacylglycerol second messenger pathway that acts in parallel with PKC to regulate neurotransmission (Betz et al. 1998). Munc-13 was identified as a priming protein originally based on the observation that synaptic exocytosis in knock-out mice is inhibited without impairment of vesicle docking (Augustin et al. 1999). Therefore all docked vesicles are in an unprimed state. Syntaxin is thought to be the molecular target of munc-13 mediated priming (Brose et al. 2000). The hypothesis follows that munc-13 binding to syntaxin results in a conformational change in syntaxin from the closed to open state, where its SNARE motif becomes accessible for binding to other SNARES and the subsequent formation of the core complex. This hypothesis was elegantly investigated in *C. elegans* where inhibition of exocytosis induced by knock-out of unc-13 was abolished in a strain that carried a permanently open mutant syntaxin (Richmond et al. 2001). Over-expression of munc-13 in chromaffin cells causes a greater than three-fold increase in the size of the releasable pools without changing the time constant for fusion, suggesting that munc-13 accelerates the vesicle transfer of docked, but unprimed vesicles to a release-competent primed state (Ashery et al. 2000). Knockout mice have provided evidence to suggest that munc-13 is an essential protein for vesicle maturation in some neurones (Augustin et al. 1999), as have studies looking at unc-13 mutants in *C.elegans* (Betz et al. 1997). However secretion from chromaffin cells was found to be normal in munc-13 knockout mice (Voets 2000). The expression levels of munc-13-1 and munc-13-3 in bovine chromaffin cells are very low, but in bovine brain synaptosomes the levels are much higher, at least ten times higher than those found in chromaffin cells (Ashery et al. 2000). Others isoforms however may be important in chromaffin cells, but these have so far not been directly tested. In hippocampal glutamatergic neurones munc-13 has been shown to be an essential priming protein (Augustin et al. 1999). Further studies in hippocampal neurones indicate that the facilitation of neurotransmitter release observed after application of phorbol esters is mediated solely by the C1 domain of munc-13 and not by PKC (Rhee et al. 2002). This is different from the

effect observed in chromaffin cells, where phorbel ester induced potentiation can be blocked by inhibitors of PKC (Vitale et al. 1995; Gillis et al. 1996). It is probable that although munc-13 can enhance secretion in chromaffin cells in over-expression studies, it is not a required priming protein in this cell type.

1.15.3 Complexin

Pulling synaptic and plasma membranes together will create an unstable intermediate and vesicles may regress via less fusion competent states to a docked state which does not engage plasma membrane SNAREs. Indeed this is believed to happen as pools of vesicles in different fusion-competent states are in equilibrium with each other. To maintain a pool of highly fusion-competent vesicles, nature has evolved proteins which can stabilize the SNARE complex once it has formed. One such protein is complexin, which has been shown to bind to assembled SNARE complexes including synaptotagmin (McMahon et al. 1995). Complexin binds to the synaptobrevin-syntaxin groove of the SNARE complex in an anti-parallel fashion, which is thought to help overcome the strong repulsive forces between vesicle and plasma membranes (Chen et al. 2002; Pabst et al. 2002), (figure 1.15.3.1). This is believed to stabilize the assembled SNARE complex in the fully primed, or 'tight' state, maintaining a highly fusion-competent pool of vesicles. Evidence for a post-priming role for complexin comes from studies on knock-out mice which display a reduction in the calcium-sensitivity of release, but have a normal sized pool of primed vesicles (Reim et al. 2001).

1.15.3.1 Model of complexin function.
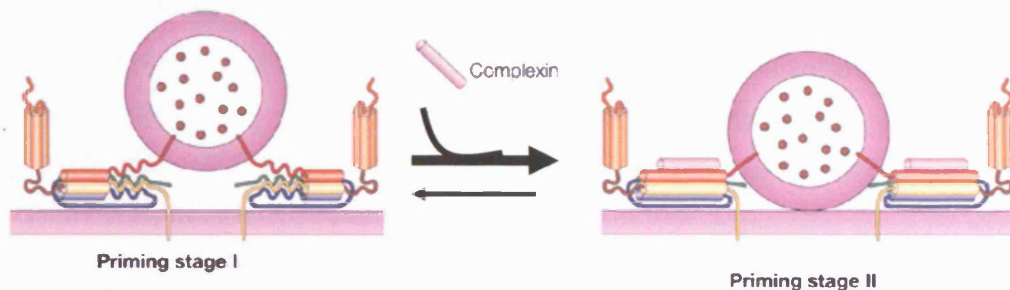
Complexins are thought to bind after trans-SNARE formation to maintain the stability of the RRP. Picture adapted from (Rizo and Sudhof 2002).

1.15.4 Tomosyn

So far I have described proteins essential for the formation or stabilization of the RRP. There are also proteins which regulate exocytosis in an inhibitory manner. Tomosyn is a protein thought to regulate SNARE complex formation via a C-terminal SNARE motif that can substitute for synaptobrevin in the SNARE complex (Fujita et al. 1998). Tomosyn is able to displace Munc-18 from syntaxin, and its affinity for syntaxin binding is increased after phosphorylation by Rho-associated serine/threonine kinase (ROCK), (Sakisaka et al. 2004). Syntaxin phosphorylated by ROCK forms a stable tomosyn complex reducing the availability of syntaxin for the formation of the SNARE complex, and subsequently inhibiting exocytosis. Extension of neurites requires the SNARE-dependent fusion of plasmalemmal precursor vesicles with the plasma membrane in growth cones. Regulation of the subcellular localization of tomosyn is used by the neurone as a mechanism to determine neurite extension and retraction (Sakisaka et al. 2004). In chromaffin cells over-expression of tomosyn decreased release probability and reduced the number of fusion-competent vesicles (mainly those residing in the RRP) by 50% (Yizhar et al. 2004). The number of docked vesicles and the fusion kinetics of vesicles were not altered suggesting that tomosyn inhibits a priming step. This inhibition was relieved at elevated calcium concentrations and calcium ramp experiments conclude that inhibition results from a shift in the calcium-dependence of secretion (Yizhar et al.

28

2004). The mechanisms underlying this calcium-dependency are not known, tomosyn does not possess a calcium-binding motif, but does interact with proteins known to be regulated by calcium (synaptotagmin, SNAP-25, syntaxin). Expression and localization of tomosyn would appear to be a cellular mechanism to down-regulate exocytosis. In this respect it is interesting to note that another protein, amysin also contains a C-terminal SNARE motif that can substitute for synaptobrevin in the synaptic SNARE complex and has been shown to inhibit exocytosis (Scales et al. 2002).

Therefore, there are numerous proteins which facilitate, stabilize or inhibit the formation of the trans-SNARE complex. The expression levels, subcellular localization and regulation by signalling pathways of these proteins will determine the size of the releasable pools and subsequently the exocytotic response. Activation of signalling pathways via membrane receptors has evolved as an additional mechanism to modulate the secretory machinery.

1.16 Interactions of calcium channels with SNARE proteins.

The cytoplasmic loop between domains II and III of N and P/Q type channels (L_{2-3}) can bind to SNARE proteins. This 'synprint' site, (*syn*aptic *pr*otein *int*eraction) is found between residues 718-963 and can bind syntaxin 1A and SNAP-25 as well as synaptotagmin (reviewed in Sheng, Westenbroek et al. 1998; Catterall 1998). Targeting of the exocytotic machinery to calcium channels is a mechanism to increase the efficiency of synaptic transmission. Experiments disrupting the physical link between N type channels and SNARE proteins can displace vesicles from the channels and shift the calcium dependence of neurotransmitter release to higher levels (Catterall 1999). As synaptic protein interactions with the synprint site are competitive, they may occur in series and represent steps in the pathway of docking and release (Walker and De Waard 1998). A hypothesis put forward by Proffesor William Catterall proposes that at resting calcium concentrations N type channels can bind to syntaxin and SNAP-25. Calcium influx can greatly increase the affinity of

this coupling, and may therefore contribute to early priming steps of the fusion process. As calcium levels rise and reach threshold for release (20-50 μM), this binding affinity is reduced and syntaxin and SNAP-25 are displaced and allow synaptotagmin to bind in order for membrane fusion to proceed (Sheng et al. 1996). An isoform of the α_{1A} channel, rbA is unable to bind to syntaxin, rbA and a different syntaxin-binding isoform B1, share an overall sequence identity of >98%, but share only 78% identity in the L_{2-3} region indicating that the synprint region is capable of alternative splicing (Catterall 1998). If syntaxin binding to the calcium channel is required for efficient coupling of calcium influx with vesicle fusion, then regulation of the expression of the different isoforms could modulate the efficacy of synaptic transmission in a particular neurone. These two isoforms are found differentially distributed in synapses of rat brain consistent with this idea (Sakurai et al. 1995). A recent study has shown that the synprint site is necessary for the proper localization of channels to the presynaptic terminal (Mochida et al. 2003). Deletion of the synprint site in P/Q-type channels reduced the efficiency of synaptic transmission and prevented correct localization of the channel in the presynaptic terminal. In addition, substitution of the P/Q-or N-type synprint site into L-type channels localized this chimera channel to the presynaptic terminal and was sufficient to allow this channel to contribute to synaptic transmission. A physical and functional interaction between syntaxin and specific voltage-gated potassium channels has also been shown (Fili et al. 2001). In this study syntaxin is able to bind the potassium channels and modulate their inactivation kinetics. The physical interaction occurs when syntaxin is in a molecular complex with SNAP-25 and synaptotagmin and can be altered by stimulation that induces neurotransmitter release (Fili et al. 2001). It is tempting to speculate that syntaxin may regulate both calcium and potassium signals to finely tune neurotransmission. Other modular adaptor proteins can bind to calcium channels and help to localise calcium channels to appropriate presynaptic sites for neurotransmitter release. For example the modular adaptor proteins Mint1 and CASK have been found to bind to the cytosolic carboxyl terminus of N type channels (Maximov et al. 1999). The carboxyl terminal of N–type channels can bind to the first PDZ domain of Mint1, and a proline rich sequence just upstream of this binds to

30

the SH3 domain of CASK (Maximov et al. 1999). Neurexins link the pre- and postsynaptic compartments of synapses by binding extracellularly to postsynaptic cell adhesion molecules and intracellularly to presynaptic PDZ domain proteins. Using triple-knockout mice, Suhof and co-workers have shown that α-neurexins are not required for synapse formation, but are essential for calcium triggered neurotransmitter release. Neurotransmitter release is impaired because synaptic calcium channel function is markedly reduced, although the number of cell-surface calcium channels appears normal. This study suggests that α-neurexins organize presynaptic terminals by functionally coupling calcium channels to the presynaptic machinery (Missler et al. 2003).

1.17 Regulation of calcium channel inactivation via interactions between G-proteins and SNARE proteins.

N, P/Q and L type channels differ in their ability to undergo voltage-dependent inhibition. This type of inhibition is slowest in the L type channel, and in chromaffin cells N type current inhibition sensitive to voltage is two times greater than that observed in the P/Q type current (Currie and Fox 1997). Voltage-dependent inhibition involves the activation of G-protein coupled receptors. This type of modulation has several typical characteristics; a slowed rate of activation, a positively shifted voltage-dependence of activation, and relief of inhibition by a strong depolarising prepulse, reviewed in (Dolphin et al. 1999). The role of G-proteins in the inhibition of calcium currents by GPCR activation was first demonstrated in the mid 1980's (Holz et al. 1986; Scott and Dolphin 1986). The role of G-protein subunits in mediating this process was suggested from experiments in which the response to an agonist could be mimicked by application of GTPγS (Dolphin et al. 1987), or by photoactivation of a caged GTP analogue (Dolphin et al. 1988) and agonist induced inhibition could be prevented by application of a GDP analog (Holz et al. 1986; Dolphin et al. 1987). Several groups identified the G$\beta\gamma$ subunit and not the Gα subunit as the mediator of this modulation (Herlitze et al. 1996; Ikeda 1996; DeWaard et al. 1997), and showed that G$\beta\gamma$ can directly bind to the α_1 subunit of the

calcium channel. The Gβγ subunit was originally proposed to bind to the loop

between domain I and II (L$_{1-2}$) of the α subunit (DeWaard et al. 1997). The sequence

motif QXXER is proposed to be involved in the interaction between Gβγ subunits

and target proteins, and this sequence is present in L$_{1-2}$ of N and P/Q type calcium

channels but not in L type channel (Herlitze et al. 1997). A single mutation, R to E in

the fifth position of this sequence has been shown to have a large effect on voltage-

dependent inactivation (Herlitze et al. 1997). This mutation in P/Q type channels

slows the rate of inactivation and shifts the voltage-dependence to a more positive

membrane potential (Herlitze et al. 1997). This creates a channel with the same type

of inactivation properties observed in L type channels. It is of interest to note that

this L$_{1-2}$ region is the same site that β subunits interact with and the Gβγ binding

sequence overlaps this BID (Walker and De Waard 1998). This suggests a possible

mechanism of allosteric hindrance and antagonism between Gβγ and β subunits.

However the role of the I-II linker Gβγ binding site in the process of G protein

modulation is controversial (see Dolphin 2003 for a critical analysis of early

experiments). Other studies have indicated that there may be other sites on the α$_1$

subunit for both Gβγ and β subunit binding. Dolphin and co-workers have identified

an eleven amino acid stretch in the N terminus N–type channel 45-55

(YKQSIAQRART) as essential for the G protein modulation of this channel (Page et

al. 1998; Canti et al. 1999). Likewise C terminus sequences have been implicated in

mediating aspects of G protein modulation and inactivation (Furukawa et al. 1998;

Furukawa et al. 1998), although other groups imply that this is not a generalized or

important interaction site (Stephens et al. 1998). This implies that either several Gβγ

subunits can bind to an α$_1$ subunit, or that 1 Gβγ subunit binds and other regions in

the α$_1$ subunit contribute to mediate the functional consequences of binding.

Evidence for the latter scenario comes from Zamponi and co-workers whose results

in a recombinant system suggest that prepulse facilatition involves the complete

dissociation of a single Gβγ molecule from the channel and that rebinding occurs via

a bimolecular interaction between the channel and a single Gβγ (Zamponi and Snutch

32

1998). It is unlikely that all three regions (L_{1-2}, N or C terminus) contribute equally to G protein inhibition of different neuronal calcium channels.

As well as mediating the formation of SNARE complexes in the immediate vicinity of calcium channels, syntaxin has been implicated in regulating calcium channel function by causing a hyperpolarising shift in the steady-state inactivation and by mediating a tonic inhibition of the channels by $G\beta\gamma$ subunits (Jarvis and Zamponi 2001). It has been proposed that syntaxin 1A can simultaneously bind to both $G\beta\gamma$ subunits and the synprint motif in L_{2-3} of N type channels (Jarvis et al. 2000). Tonic inhibition of the channels by $G\beta\gamma$ is dramatically reversed upon application of botulinum toxin C, indicating that syntaxin 1A is involved in mediating the effects of $G\beta\gamma$ (Jarvis et al. 2000). However exogenous application of $G\beta\gamma$ subunits or activation of G protein receptors rescued their effect suggesting that syntaxin 1A optimises $G\beta\gamma$ inhibition rather than being essential for it. They suggest a mechanism by which syntaxin 1A induces a more efficient G protein coupling by mediating the co-localisation of $G\beta\gamma$ subunits and the N type channels. The importance of syntaxin 1A in mediating the effects of $G\beta\gamma$ were shown in experiments in chick dorsal root ganglia (Lu et al. 2001). These neurones do not express syntaxin 1A and addition of purified $G\beta\gamma$ is not able to produce voltage-dependent inhibition of the N type currents in these cells (Lu et al. 2001). Likewise syntaxin 1B which retains the ability to induce a negative shift in half-inactivation potential is unable to transduce the $G\beta\gamma$ inhibition signal to N type channels (Jarvis and Zamponi 2001). It is interesting to note that P/Q type channels can mediate calcium-dependent gene transcription of syntaxin 1A (Sutton et al 1999), therefore one type of calcium channel is capable of regulating the function of a different calcium channel. Syntaxin binding to the synprint region of N type channels can cause a −15-20mV negative shift in the half-inactivation potential (Bezprozvanny et al 1995, Jarvis et al. 2000), as well as an enhanced slow inactivation (Degtiar et al. 2000), again botulinum toxin C can sharply attenuate these observations on channel gating. Co-expression of either SNAP-25 or munc-18 can antagonise the ability of syntaxin 1A to inactivate calcium channels, whereas the ability of syntaxin 1A to enhance G protein inhibition is retained in the presence of SNAP-25 or munc-18 (Wiser et al. 1996, Jarvis and

Zamponi 2001). This suggests that the molecular mechanisms determining inactivation and G protein inhibition are separate. An interesting finding was that munc-18 on its own could enhance G-protein inhibition of the channel (Jarvis and Zamponi 2001). The authors tentatively suggest that munc-18 may act by creating a $G\alpha$ 'sink' allowing endogenous $G\beta\gamma$ to modulate the channel, rather than munc-18 itself mediating the co-localisation of channels and $G\beta\gamma$, but more biochemical work is required to substantiate this hypothesis.

To flip the earlier argument around, as well as the calcium channels acting as anchors for the successive protein-protein interactions in the pathway for fusion, these proteins can determine the temporal amount of calcium entry through these channels by their differential effects on channel gating and inhibition. For example in the presence of only syntaxin 1A, vesicles are not docked close to the channel and this channel is unlikely to participate in neurotransmitter release. Tonic G protein inhibition and a negative shift in inactivation would prevent unnecessary calcium entry through this channel (Jarvis and Zamponi 2001). Upon binding of SNAP-25 and the creation of the SNARE complex leading to fusion competence the level of G protein inhibition and inactivation will reduce allowing the calcium channel to become maximally responsive. Cysteine string proteins (CSPs), found on vesicles have also been proposed to play a role in G protein modulation of N-type calcium channels (Seagar et al. 1999; Magga et al. 2000). Deletion of the CSP gene in *Drosophila* severely impairs presynaptic neuromuscular transmission indicating that CSP's function is critical for neurotransmission (Zinsmaier et al. 1994). Other studies have suggested that the default involves an inability for calcium to trigger exocytosis or a deficit in calcium entry (Umbach and Gundersen 1997). Recent studies by Zamponi's group show that CSP can physically interact with both the N type L_{2-3} region and $G\beta\gamma$ proteins (Magga et al. 2000). They hypothesize that CSP may chaperone interactions between the synprint site of presynaptic calcium channels and SNARE proteins regulating the sequential protein-protein interactions necessary for fusion. CSP can bind $G\beta\gamma$ proteins and by also binding to the N type calcium channel may therefore help target $G\beta\gamma$ to its site of action at the calcium channel, the L_{1-2} region. By interacting with synprint binding proteins and $G\beta\gamma$ proteins, CSP's

34

are in a position to regulate the steady state inactivation and level of G protein inhibition of presynapic calcium channels. A dynamic series of protein-protein interactions may not only help in the formation of the exocytotic machinery, but could also optimise calcium influx for each step of the cycle. As both N and P/Q-type calcium channels mediate neurotransmitter release, their differential modulation by G proteins suggests that these channels can be selected to fine tune neurotransmission. The patchwork distribution of calcium channel subtypes might enable terminal specific modulation of transmitter release, enhancing the power of synaptic processing (Zamponi and Snutch 1998).

1.18 Calmodulin regulation of exocytosis.

Previous studies (mainly biochemical assays), have shown an inhibition of calcium-dependent exocytosis after addition of calmodulin inhibitors (Burgoyne and Geisow 1982; Ganguly et al. 1992), anti-calmodulin antibodies (Steinhardt and Alderton 1981; Kenigsberg and Trifaro 1985; Brailoiu et al. 2002), or calmodulin inhibitory peptides (Birch et al. 1992; Matsumura et al. 1999). However other studies suggest that calmodulin-binding peptides and anti-calmodulin antibodies do not affect exocytosis directly, concluding that calmodulin is only involved in the regulation of endocytosis (Artalejo et al. 1996). A role for calmodulin enhancing exocytosis is also implied from studies on permeablised (cracked) cell assays of PC12 or adrenal chromaffin cells (Okabe et al. 1992; Chamberlain et al. 1995; Chen et al. 1999), based on the stimulatory effect of added calmodulin. Since docking of new vesicles is unlikely to happen during infusion experiments of cracked cells (Martin and Kowalchyk 1997), the calmodulin affect is likely to act at either priming or calcium-dependent fusion. Stage-specific assays reveal that calmodulin stimulates exocytosis when added at the calcium triggering step but not before MgATP-dependent priming (Chamberlain et al. 1995; Chen et al. 1999). In addition, experiments in which a mutated calmodulin (incapable of binding calcium) was added, show that Ca^{2+}/calmodulin is required (Chen et al. 2001). These studies indicate that calmodulin interacts with membrane associated proteins (that are not washed out during

permeabilasation) and regulates a late stage in exocytosis. However studies conducted in cracked cells cannot determine whether the RRP is specifically affected. When secretion is assayed by slow techniques, fusion from the SRP is likely to dominate the exocytotic response. Some of these studies were conducted in PC12 cells which have fusion rates considerably slower than chromaffin cells or neurones thereby limiting interpretation. Even when temporal resolution is improved by the use of fast rotating-disc-electrode voltammetry to detect catecholamine release, secretion is still detected on a timescale of seconds (Earles et al. 2001), suggesting that the equivalent of a chromaffin cell RRP (or even an SRP) is not found in PC12 cells (Sorensen 2004). To evaluate a role for calmodulin in mediating release from specific pools of vesicles a faster measurement of exocytosis is required. By measuring quantal release rates at the Calyx of Held a role for calmodulin was described in mediating refilling of vesicle pools as introduction of calmodulin inhibitory peptides reduces vesicle pool refilling (Sakaba and Neher 2001). Monitoring cell membrane capacitance in combination with the patch clamp technique also offers good temporal resolution. Basic capacitance experiments have shown that calmodulin application via the patch pipette can increase the initial rate of exocytosis (Kibble and Burgoyne 1996). In this study cells were dialysed for ten minutes with internal solution with or without 250μg/ml of purified calmodulin. After 10 minutes a 1 second depolarisation was evoked and changes in capacitance monitored. The size of the capacitance jump was not significantly different, but the initial rate was increased after application of calmodulin, suggesting that calmodulin could promote the kinetics of release.

1.19 Calmodulin diversity in target recognition.

Ca^{2+}/calmodulin can activate a multitude of different target systems, including, protein kinases and phosphatases, nitric oxide synthases and calcium-extruding pumps (Vogel 1994). I have presented evidence suggesting that calmodulin can regulate both calcium channels and the secretory machinery. An intriguing question to structural biologists and biochemists is how calmodulin, a small (16.7 kDa) protein is able to form complexes with so many different proteins and lead to target activation in response to elevations in cytoplasmic calcium. Raising intracellular calcium can regulate calmodulin in several ways. It can target calmodulin to specific subcellular regions, promote different modes of association with target proteins and mediate different conformational states, allowing target specific activation (Chin and Means 2000). Activation of Ca^{2+}/calmodulin kinases, generates an additional mode and specificity to target activation. A high content of methionine residues (9 out of 148 residues) in calmodulin are believed to be responsible for its ability to bind numerous target proteins. Indeed, 8 of the 9 methionines are directly involved in binding to all target peptides studied so far by x-ray and NMR. Calcium-dependent interactions occur after calcium binding to calmodulin induces a conformational change that exposes binding sites for both hydrophobic and basic amino acids. Investigations into calmodulin interactions with calmodulin-dependent kinases revealed that calmodulin can assume at least three different conformations by virtue of a flexible linker connecting the N and C lobes, (reviewed in Chin and Means 2000). From these studies putative calmodulin recruitment motifs were derived and fall into three classes, 1-10, 1-14 and 1-16. 1-14 was the first family described (Rhoads and Friedberg 1997), the main feature of this family is the spacing between two bulky hydrophobic residues. Ideally, two bulky hydrophobic residues are spaced by 12 amino acid residues in an amphipathic helice. Some have additional anchoring residues in the middle. It is not known whether binding affinities vary with having more bulky hydrophobic residues in the middle. These sequences primarily bind calmodulin in the presence of calcium. Another calmodulin binding motif is the 'IQ' motif, which corresponds to an IQxxxRGxxxR consensus sequence and is known to

37

bind numerous proteins in a predominantly calcium-independent manner, as such this motif is thought to be responsible primarily for constitutative binding of calmodulin to target proteins, however it can also be important in mediating specific Ca^{2+}/calmodulin affects (Hoeflich and Ikura 2002). Additionally calmodulin has been shown to induce dimerization of membrane proteins and in the case of small conductance potassium channels this is responsible for their gating (Schumacher et al. 2001). In this case, the C lobe EF hands mediate tethering to the channel and the N-lobe EF hands are responsible for calcium-induced dimerisation, leading to channel gating. A working hypothesis is that various calmodulin binding partners can control the 3D structure of calmodulin by changing the orientation of the N and C lobes (Hoeflich and Ikura 2002). Indeed recent crystallographic studies indicate significant rearrangement of EF-hand helices within each calmodulin lobe to adjust its conformation for optimal binding with target proteins (Kurokawa et al. 2001). A comprehensive calmodulin target recognition data base is available on the internet at http://calcium.uhnres.utoronto.ca.

1.20 Modulation of neurotransmitter release via activation of GPCRs

The process of calcium-regulated exocytosis can be modulated by a variety of mechanisms. Modulation to the exocytotic pathway is important for numerous neural functions, such as spinal reflexes, learning and memory. Modulating mechanisms have also been implicated in several mental illnesses and in acquired diseases like drug addiction (Zheng and Bobich 1998; MacDermott et al. 1999). A thorough understanding of the mechanisms controlling and modulating neurotransmitter release will have wide-ranging and important pharmacological implications. G protein-coupled receptors are capable of modulating neurotransmitter release and hence synaptic strength. Their mode of action can be either inhibitory or facilatory. The inhibitory pathway, usually resulting from Gi/o receptor activation, leads to an inhibition of calcium currents either directly, or indirectly by altering the function of potassium channels (Majewski et al. 1997). However presynaptic inhibition can also be mediated via effects on the secretory machinery. A facilatory pathway can result

38

in a cascade of second messenger-mediated changes in the activity of the proteins controlling exocytosis (Teschemacher and Seward 2000) or have an effect on membrane excitability (ie phosphorylation of ion channels). Gq receptors typically stimulate phospholipase C (PLC) activity. PLC can cleave PIP_2 into IP_3 which releases calcium from internal stores and diacylglycerol (DAG) which can recruit PKC to the plasma membrane. DAG production has additional neuromodulatory functions such as translocating munc-13 to neurotransmitter release sites at the plasma membrane (Brose et al 2000). This pathway of G protein-mediated production of IP_3 and DAG has been observed in response to several different secretogogues like Angiotensin 2 (Teschemacher and Seward 2000) and histamine (Trifaro et al. 2000). Some substrate receptors such as Ang2 type1 receptors can couple to several types of G protein (Teschemacher and Seward 2000). This means that a single neuromodulator acting through one receptor can either inhibit or facilitate exocytosis. The resulting effect may depend on the concentration of agonist used, the rate of desensitisation of the receptor or the cellular compartmentalisation of the receptors (Teschemacher and Seward 2000). Alternatively different secretagogues such as Ach and 5-HT acting on the same cell can oppose each other at the second messenger level (Brose et al. 2000). Some types of muscarinic receptors are positively coupled to PLC via Gq receptors and activation leads to the production of DAG. 5-HT receptors couple to Go receptors and can activate diacyglycerol kinase (DGK-1), or inhibit Gq receptors (Lackner et al. 1999). Therefore competing pathways can simultaneously modulate neurotransmitter release (figure 1.20.1).

1.20.1. GPCRs can enhance or inhibit neurotransmitter release.
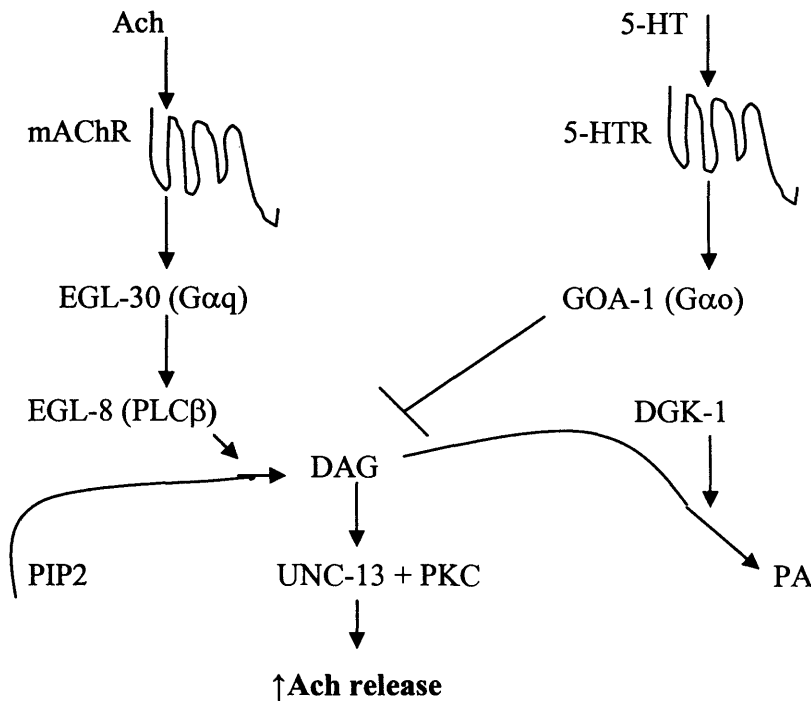
At this synapse DAG is proposed to be a critical second messenger. Presynaptic DAG can recruit unc-13 to the neurotransmitter release sites and may facilitate neurotransmission through the activation and translocation of PKC.
The levels of activated DAG are under the control of two opposing neuromodulators. Ach and 5-HT.

A model for the modulation of the C.elegans neuromuscular junction, reproduced from (Lackner et al. 1999)

Phosphorylation of the proteins involved in exocytosis is a probable cause of presynaptic plasticity. The SNARE proteins syntaxin, SNAP-25 and VAMP as well as calcium sensing proteins and SNARE complex regulating proteins like munc-18 have all shown to be *in vitro* substrates for protein kinases, reviewed in (Klenchin and Martin 2000, Lin and Scheller 2000). Various protein kinases can antagonize inhibitory effects on the calcium channels. Both the α_1 and β subunits are substrates for phosphorylation, suggesting that kinase activation is another route in which to dynamically regulate channel function. The $\alpha 1$ L_{1-2} region appears to mediate 'crosstalk' between protein kinase C (PKC) and $G\beta\gamma$ proteins (Zamponi et al. 1997). The attenuation of the $G\beta\gamma$ response is mediated by the PKC-dependent phosphorylation of residues covered in N–type (410-428) and P/Q-type (416-434) channels (Zamponi et al. 1997). In N-type channels, phosphorylation of threonine 422 appears to play a central role in this antagonistic effect on $G\beta\gamma$ channel inhibition

(Cooper et al. 2000). Studies showed that the degree of PKC antagonism varied depending on which GPCR had been activated to produce the $G\beta\gamma$ mediated channel inhibition (Cooper et al. 2000). Investigation of threonine 422 phosphorylation in the presence of different $G\beta\gamma$ isoforms, found that channel inhibition by $G\beta\gamma 1$ was antagonised by PKC, but was not inhibited by $G\beta\gamma 2$, $G\beta\gamma 3$, $G\beta\gamma 4$ (Cooper et al. 2000). Therefore neuromodulators which activate receptors exclusively coupled to $G\beta\gamma 1$ are susceptible to cross-modulation by PKC signals, whereas those which couple to the other isoforms are not, and those which couple to $G\beta\gamma 1$ and to the others isoforms will show an intermediate response to PKC. *In Vitro* biochemical studies show PKC and CaMKII to phosphorylate the synprint region, and by doing so inhibit the binding of recombinant syntaxin and SNAP-25, providing yet another avenue for modulating channel steady-state kinetics (Catterall, 1999; Degtiar et al. 2000). In addition it would appear that alternatively spliced isoforms of N and P/Q-type channels have different sensitivities to phosphorylation, again adding specificity to intracellular signals and to the tuning of transmitter release (Davila 1999). Activation of CaMKII is important in determining calcium-dependent facilitation of L-type channels (Dzhura et al. 2000). Cdk5 phosphoryation of P/Q-type channels has also been reported (Tomizawa et al. 2002). In this study Cdk5 phosphorylation of the II-III linker region reduced calcium influx and prevented interactions with SNAP-25 and synaptotagmin, the physiological outcome of which was to reduce neurotransmitter release.

1.21 Summary

It is clear that there are many structural determinants of the α_1 subunits that are essential for inactivation of calcium channels. Temporal, compartmental and tissue specific expression of different isoforms and splice variants create channels with unique biophysical properties. Other channel subunits, G proteins, calmodulin, SNARE proteins, protein kinases and other modifiers of channel function interact to specify gating kinetics. Divergent second messenger signals can converge at the

level of the calcium channel to highly regulate calcium entry, thereby fine tuning neurotransmitter release (figure 1.21.1).

1.21.1 Sites of regulation of Ca_v2 channels.
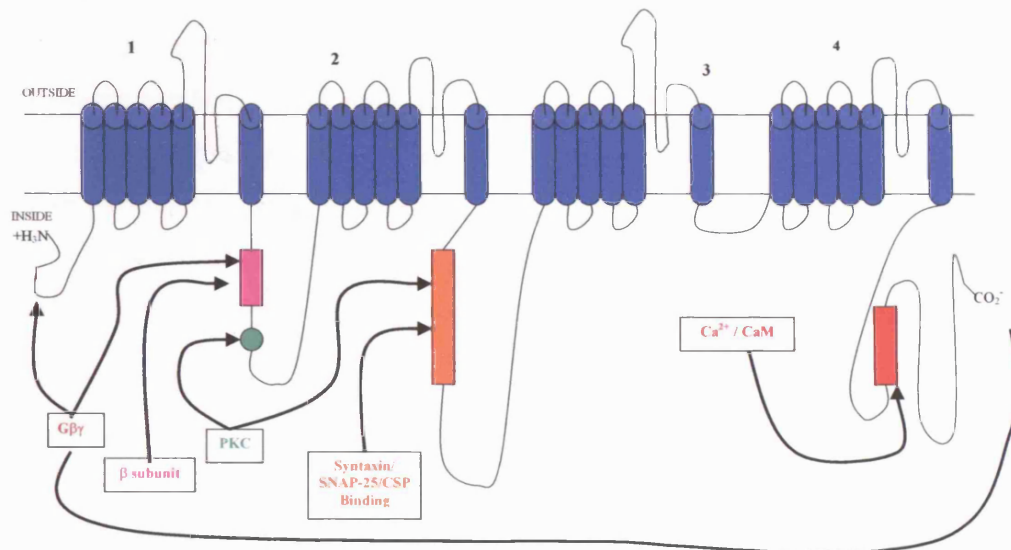
Schematic representation of the proposed binding sites on the α_1 subunit of Ca_v2 family calcium channels for regulators of inactivation.

In addition to the regulation of calcium entry, the release site of the presynaptic nerve terminal is a highly organised specialised macromolecular complex, and there is reasonable evidence to suggest that neuroendocrine cells also contain discrete exocytotic sites (Robinson et al. 1995; Salaun et al. 2004). Proper localisation of synaptic compartments is maintained via a complex network of protein-protein interactions, usually mediated by modular adaptor proteins to ensure a highly efficient temporal and spatial control of neurotransmitter release. At every stage of the vesicle cycle there are numerous protein targets for the modulation of neurotransmitter release. A detailed understanding of the function and modulatory effects of these proteins is a challenge for the future.

42

1.22 Aims of thesis.

An interesting question to physiologists is why neurones and specialised secretory cells, like chromaffin cells possess several types of high voltage calcium channels? The physiological relevance appears to be that specific calcium-dependent processes can be preferentially coupled to individual subtypes. The initial aim of my thesis was to determine whether exocytosis was preferentially coupled to a particular channel subtype in chromaffin cells. The second aim was to investigate the molecular basis for differential regulation of calcium channel inactivation between endogenously expressed channels. The third aim of my thesis was to examine the stage(s) in the secretory vesicle cycle which are controlled by Ca^{2+}/calmodulin and define whether specific pools of vesicles are targeted for regulation by this molecule.

Chapter 2: Materials and Methods

2.1 Preparation and maintenance of chromaffin cells.

At a local abattoir, adult bovine adrenal glands were cut out of the animal's carcass immediately after slaughter. Excess fat was removed and the glands placed in ice cold Locke's buffer containing (in mM), NaCl 154; KCl 2.6; K_2HPO_4 2.2; KH_2PO_4 0.85; glucose 1; HEPES 0.5; phenol red 1. Saturated with CO_2/O_2 (5%/95%), pH adjusted to 7.2 with NaOH with 0.2 mg/ml penicillin, 0.05mg/ml streptomycin and 0.05mg/ml gentamycin. In the laboratory the adrenal vein was canulated and the gland was superfused with the same buffer. The outer capsule and cortex were dissected from the gland taking care not to puncture the medulla. The gland was then perfused $\sim$ 10ml/min with 35ml of Locke's buffer with reduced antibiotic concentration (0.1mg/ml penicillin and streptomycin, 0.05 mg/ml gentamycin) and, supplemented with 10mg of collagenase (type II, Worthington Biochmical corporation) and 0.5 mg of DNAse I (Sigma) at $37^{\circ}C$ for $\sim$ 30 minutes. Residual cortex was scraped off using a scalpel blade and the medulla minced and placed in a trypsinisation jar containing 25ml of the perfusion buffer (plus enzymes) and stirred for 25-30 minutes at $37^{\circ}C$. This suspension of cells was filtered through a 40μm nylon mesh and diluted 2x with enzyme free Locke's buffer. The cells were pelleted by centrifugion at 600g for 5 minutes at room temperature. A further 25 mls of enzyme free Locke's buffer was used to gently resuspend the cells. A sample was taken for counting and the solution accordingly diluted to $2x10^5$ cells/ml. Cells were then plated onto 13 or 16mm collagen-coated coverslips in 24 or 12 well plates at either 100,000 or 200,000 cells/well and covered with 1 or 2 mls of feeding media (10% foetal calf serum, 90% DMEM supplemented with 44mM $NaHCO_3$, 15mM HEPES, 0.1 mg/ml penicillin/streptomycin solution, gentamycin 0.05 mg/ml, 5'-fluorodeoxyuridine 2.5 mg/ml, cytosine-β–γ-Arabino-Furanoside 0.5mg/ml and 1% glutamine). Cells were kept in a humidified incubator (5% CO_2 at $37^{\circ}C$). 24 hrs post preparation $\sim$ 70-80% of the feeding media was exchanged with fresh media. Cells

were typically used 48 – 120hrs post preparation. Adenoviral infection of cells was performed 24 hrs after plating by adding 3μl of the concentrated viral stock per well directly onto the cells after the feeding media was exchanged. Infected cells were used 24-72hrs later.

2.1.1 Collagen coating of coverslips

A 10mg vial of rat tail collagen, type VII (Sigma) was dissolved in 2ml of 0.1% acetic acid and mixed at room temperature for 1hr. 0.2ml aliquots were placed in 15 ml tubes and kept at -20°C until required. On the day of cell preparation an aliquot was diluted with 8mls of 60% ethanol and 100μl added to a 13mm coverslip or 150μl added to a 16mm coverslip. Coverslips were allowed to dry under sterile conditions before use. Diluted aliquots were kept at 4°C for up to 2 weeks.

2.1.2 Rat/Mouse chromaffin cell slice preparation

9-14 day-old rats/mice were decapitated and the chest cavity opened to reveal the kidneys. With fine forceps the adrenal glands were teased away and placed in external solution. Under a dissecting microscope the outer capsule and fat were removed leaving behind a small ball of cortical and medulla cells. The bolus was then placed in liquid agar (2.5% made with PBS without calcium) at 37°C and the agar encouraged to set quickly by placing on ice. A square section of agar containing the gland was fixed to a DSK microslicer (DSK 1000) and 150μm slices cut into a solution of ice cold PBS without calcium. Slices were then quickly transferred to external solution (see section 2.1.4 for composition) and bubbled at room temp with 95% O_2/5% CO_2. The slices were given 1-2 hrs to recover and experiments were performed for the next 4-8 hrs.

2.1.3 Solutions for cultured bovine adrenal chromaffin cells

External: (in mM); NaCl 150; KCl 2; NaHCO₃ 5; MgCl₂ 1; CaCl₂ 2.5; glucose 10; HEPES 10; pH adjusted to 7.3 with NaOH; osmolarity ~ 300 mOsm. After voltage clamp was obtained the external solution was exchanged for one in which the [NaCl] was reduced by 10mM and replaced with 10mM TEA-Cl. This was necessary to prevent activation of a calcium-dependent outward current which could contaminate calcium current traces during long depolarisations (see appendix 1). This solution was only exchanged after establishing voltage clamp as we did not want the cell to depolarize (due to block of potassium channels by TEA-Cl) and secrete before applying our voltage protocols. Tetrodotoxin ($1\mu M$) was added to the external solution in initial experiments to determine the degree of sodium current contamination of calcium current recordings. After this information was obtained, (chapter 3, section 3.1) tetrodotoxin was omitted from the external solution as it slows sodium channel gating 10 fold resulting in non-exocytotic changes in C_m measurements (Horrigan and Bookman 1994). Measurements of calcium currents in TTX-free solutions were determined 3ms after the start of the depolarization to avoid contamination by sodium currents.

Internal: (in mM); Cs- D-glutamate 145; HEPES 10; NaCl 8.5; BAPTA 0.3-10, adjusted to pH 7.3 with CsOH; osmolarity ~290-300 mOsm. The internal solution was made fresh every 1-2 weeks and kept at 4°C. Mg-ATP was added at a concentration of 2mM on the day of recording, solution pH was readjusted using CsOH and internal solution was kept on ice for the duration of the experiment. In perforated patch experiments gramicidin D (Sigma) at a final concentration of ~50µg/ml was added. Gramacidin D was made up as a 1mg/ml stock in DMSO on the day of use, vortexed for ~ 30 seconds, and 2.5 µl added to 0.5mls of internal. The electrode tip was dipped for a few seconds into gramicidin free internal and then backfilled with internal containing gramicidin. Internal solution was briefly vortexed before pipette filling. Osmolarity of solutions was measured using a Vapro osmometer (model # 5520).

2.1.4 Solutions for rat/mouse chromaffin slice preparation.

External: (in mM); NaCl 125; KCl 2.5; glucose 10; NaH_2PO_4 1.25; Na Pyruvate 2; myo-inositol 3; ascorbic acid 0.5; $NaHCO_3$ 0.5; saturated with CO_2/O_2 (5%/95%) before addition of $CaCl_2$ 2; $MgCl_2$ 1; osmolarity ~290 mOsm.

Internal: (in mM); Cs- D-glutamate 145; NaCl 8; $MgCl_2$ 1; Mg-ATP 2; Cs-HEPES 10; BAPTA 0.1-3; adjusted to pH to 7.4 ; osmolarity ~280 mOsm.

2.2 Electrophysiology apparatus.

2.2.1 Fabrication of patch pipettes.

Custom made capillary borosilicate glass microelectrodes with external and internal diameters of 1.65 and 1.3 mm respectively (Drummond Scientific Company) were pulled on a Narashige 2-stage vertical puller (model # PP-83). The heat of the second pull was altered according to recording configuration with electrodes after fire polishing producing resistances of 1.5-2.2 mΩ for perforated patch or 2-4 mΩ for whole cell recordings.

2.2.2 Reducing stray capacitance.

It is essential when making capacitance recordings that there are minimal stray capacitance changes associated with the pipette. Most stray capacitance arises across the pipette wall between the pipette and bath (Ogden and Stanfield 1994). Pipette capacitance can be reduced using the pipette capacitance cancellation circuitry on the patch clamp amplifier. It is possible (and necessary) to reduce stray capacitance further by using a small perfusion chamber, keeping the depth of the bathing solution to a minimum and only filling the electrode with enough internal solution so as to make contact with the silver wire (Ag/AgCl$_2$). Stray capacitance was attenuated further by coating the shank of the pipette up to the tip with a hydrophobic substance to prevent liquid from 'climbing' up and wetting the pipette due to surface tension. To achieve this we coat our electrodes with Sylguard (Dow Corning), which also has

the advantage of thickening the wall of the pipette reducing capacitive coupling between the bath and pipette solutions.

2.2.3 Sylguard

Sylguard was prepared by mixing nine parts resin to one part catalyst oil. This mixture was then aliquoted into 200μl tubes or placed into a 1ml syringe, which were stored at -20°C until needed. Sylguard was applied around the shank of the electrode up to the tip using a 200μl Gilson tip pipette dipped into an aliquot. Alternatively a needle was attached to the 1ml syringe and a small amount of Sylguard was 'painted' around the shank up to the tip of the pipette. The sylguard was cured quickly by placing the electrode between the coils of a fine wire heater for ~30 seconds.

2.2.4 Fire Polishing

Fire polishing removes any contaminants and smoothes the edges of the pipette to aid 'giga seal' formation with the membrane. A Narishige microforge (MF-83), was used to fire polish the electrodes, with a platinum filament lightly coated with melted electrode glass providing the heat source. A reduction in pipette tip diameter and a faint darkening of the tip indicated that polishing had occurred.

2.2.5 Pipette Filling

Pipette tips were dipped into filtered internal solution for a few seconds to induce uptake by capillary action, they were then backfilled using a MicroFil™ non-metallic syringe needle. Gentle shaking and flicking of the pipette removed any air bubbles. In perforated patch recordings, the same procedure was applied although the tips were dipped in gramicidin-free internal for roughly 10 seconds prior to backfilling with internal containing gramicidin.

2.2.6 Microscopes

Isolated bovine adrenal chromaffin cells plated on collagen-coated coverslips were transferred to a superfusion chamber (Warner instruments, model P3/P4), placed on the stage on an inverted microscope (axivert-25, Zeiss) and viewed under phase contrast optics at 320 or 400x magnification. For experiments in which cells had been loaded with fura-2, cells were viewed at 600x magnification (60 x oil immersion lens with a numerical aperture of 1.3 (Zeiss) and 10 x eye piece) and alternatively illuminated at 340 and 380 nm using a monochromator (TILL Photonics), controlled by the C_m data acquisition software. Emission > 430nm was collected with a photomultiple tube (TILL Photonics) and sampled every 12 ms. For identification of GFP positive cells, a 50W mercury arc lamp (Zeiss) was used to excite the fluorophore at 488nm, green emission was viewed at > 540 nm. Rat/mouse slices were viewed with an upright microscope (Axioskop, Ziess) at 400x magnification. Slices embedded in agar were transferred to a superfusion chamber and held in place using a platinum harp (U-shaped piece of platinum with very fine strands of nylon glued across). By placing this harp over the slice the cells stay in the same position and the slice does not move upon fluid superfusion.

2.2.7 Superfusion

Cells were continually superfused (~1-2ml/min) with external solution to remove effects of released endogenous modulators (Carabelli et al. 1998). All solutions were kept at room temperature which varied from 19-26°C. Superfusion was obtained by use of gravity flow from a 1litre reservoir bottle. Solutions containing drugs or altered external composition were stored in 10, or 50ml syringes connected in series with the main reservoir bottle. The solutions could be changed by switching a three way tap connected to the bottom of the syringes. The height of the syringes was adjusted so that the flow rate from them would match the rate from the reservoir bottle. Additionally stoppers containing a fixed length of plastic tubing were placed into the syringes to insure a constant flow rate (figure 2.2.7.1). The outflow was

controlled by a peristaltic pump (Gilson, minipuls 3). A narrow bore metal tube, bent at 45 degrees and beveled at one end was attached to the outflow tubing. This metal tube was placed in the superfusion chamber and held in place by either a small magnet or a piece of blue-tac^{TM}. The tip of this metal tube was placed just below the meniscus of the desired bath volume. The outflow tube contained a small piece of silver wire and was passed through a bubble trap to reduce noise. A steady rate (inflow matching outflow) was achieved by optimizing the diameter of tubing flowing in and out of the system.

2.2.7.1 The perfusion system.

1 litre resevoir bottle

Drug Bottles

3-way tap

Perfusion chamber

Inflow

Peristaltic pump

Microscope staging

Microscope objective
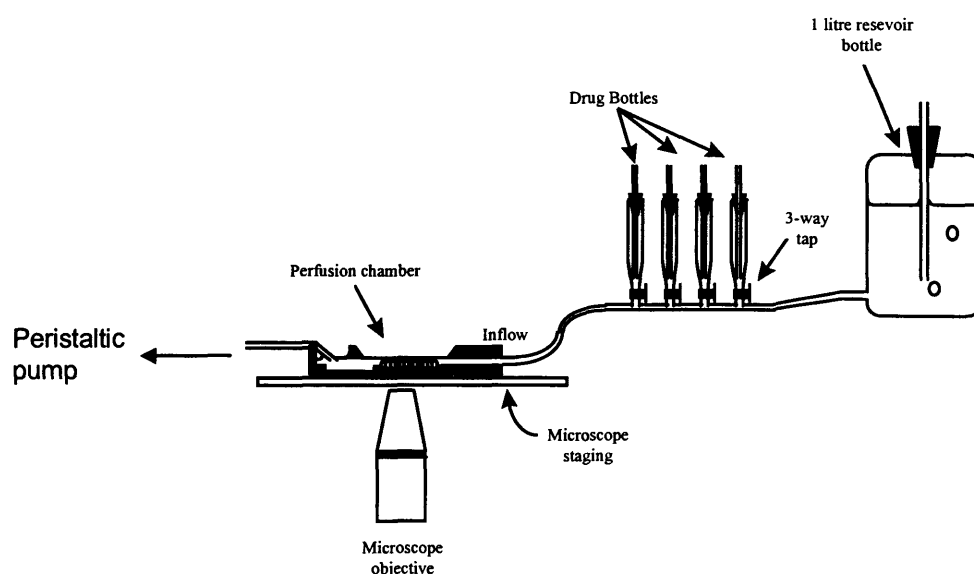
A schematic representation of the perfusion system used, taken and adapted from (Powell 2000).

After drug application (or the ionic composition of the external changed ie to ones containing barium or TEA-Cl) the inflow/outflow tubes were washed with copious amounts of external solution or distilled water before subsequent experiments were performed.

2.2.8 Amplifier, filter and acquisition equipment.

Whole cell and perforated patch recordings were performed using an Axopatch 200B patch clamp amplifier (Axon Instruments). Voltage protocol generation and data acquisition were performed using custom data acquisition software (written by Dr AP Fox, University of Chicago and updated by Dr EP Seward, University of Sheffield) running on a Pentium computer equipped with a Digidata 1200 acquisition board (Axon Instruments). Occasionally, when capacitance information was not required voltage protocol generation and data acquisition were performed using pClamp (Clampex version 6.0 program). Current traces were low pass filtered at 5 kHZ using the four-pole Bessel filter supplied with the amplifier and digitized at 10kHz. Currents were not corrected for leak. The typical linear leakage current at the holding potential of -80mV was <10pA. Capacitance measurements were recorded using a software based phase tracking technique (Joshi and Fernandez 1988; Filder and Fernandez 1989) this method is described in detail in section 2.4.2.6. Data was stored on the computer hard drive and analysed off-line using self-written analysis software (Axobasic, Axon Intruments), or Clampfit. Analysed files were exported and analysed further using Origin version 6 (Microcal).

2.3 The voltage clamp technique

Much of what is known about the properties of ion channels in cell membranes has come from experiments using voltage clamp. This technique allows ion flow across a cell membrane to be measured as electrical current, whilst the membrane voltage is held under experimental control with a feedback amplifier (Halliwell et al. 1994).

2.3.1 Forming a 'giga'seal.

The filled pipette was attached to the headstage of the amplifier and lowered into the bath solution with positive pressure applied to prevent the tip being clogged before it reached the cell membrane. Much less positive pressure was applied in perforated

patch experiments as the aim is to achieve giga seal formation before the perforant (gramacicidin D) reaches the tip and perforation commences. Junction potential differences were cancelled using the pipette offset dial after the pipette entered the bath solution. The pipette was manipulated until its shadow could be seen under high magnification and then placed directly above a target cell. The pipette was slowly lowered onto the cell using the fine control on the micromanipulator (Burleigh PLS-P560). Before going whole cell, or obtaining electrical assess with the perforated patch method it is necessary to obtain a giga seal (a seal whose electrical resistance is > 1GΩ) between the electrode tip and cell. Once achieved this is called the cell attached configuration. A seal test was applied using the patch amplifier. This consists of sending a 5-10mV test pulse of 5ms duration run continuously at 10Hz. The amplitude and duration of the resultant current can be seen on the computer screen or oscilloscope. With the dissociated cells a 50% decrease in the seal test amplitude was normally observed as the pipette touched the cell membrane, at this point negative pressure was applied by sucking on a tube connected to the back of the pipette to encourage an increase in seal resistance. With the slice cells the pipette was lowered until a 'bleb' appeared on the surface of the cell, at this point the positive pressure was released and negative pressure applied. After the pipette touched the cell the holding potential was dropped from 0mV to -80mV, as this aided in giga seal formation and was the potential at which the cells were experimentally held. A giga seal was usually obtained within seconds of touching a cell. The only differences between obtaining a giga seal from the two preparations were that more positive pressure was applied in the slice preparation before the pipette reached the cell membrane, this was to try and blow away debris that was on the cell surface. Secondly the pipette was lowered further with the positive pressure applied so that when it was released a seal immediately formed with gentle suction without the need to go down further with the micromanipulator.

SPECIAL NOTE

TEXT SKEWED.

IS AS ORIGINAL.

2.3.2 Whole cell recordings

After the resistance reached a giga seal, further gentle suction leads to a sudden increase in capacitive transients, indicative of a disruption of the membrane patch spanning the pipette and entering the whole-cell configuration of recording. This increase in current reflects the addition of the whole cell membrane to the pipette input capacitance. These transients at the start and end of a pulse can be zeroed by use of the patch amplifier correction circuitry and allows whole cell capacitance and series resistance values to be measured. Typically whole cell capacitance is $\sim$ 6pF (mean = 5.8 pF $\pm$ 0.1 n = 248), and series resistance <10mΩ (mean = 8.2 mΩ $\pm$ 0.2 n = 248). Occasionally the series resistance could increase during the course of an experiment; this was usually rectified by briefly applying more negative pressure.

2.3.3 Series resistance compensation.

In the whole cell configuration there is a resistance in series with the membrane and the pipette. When a current (I) flows across the membrane, series resistance will cause a difference between the measured membrane potential, and the actual potential difference across the membrane. Remembering Ohm's law, V=IR, the size of this error will be proportional to the size of the current. The larger the current, the greater the error will be. Series resistance also poses another problem in whole cell recordings. In an ideal situation the time resolution for measuring membrane currents and changing the membrane voltage would be limited to the speed of the electronics (μs). Unfortunately series resistance results in rounding the voltage clamp ($\tau=R_sC$), such that the membrane voltage potential (V_m) lags behind the voltage command ($V_{Command}$). This delay could cause problems if the change in membrane potential is not sufficiently rapid for capacity current transients to be completed by the time that fast ionic currents are measured. The problem can be reduced by use of the series resistance compensation circuitry on the patch clamp amplifier. This essentially works by increasing the $V_{Command}$ proportionally to the measured current output. This

53

increased command potential compensates in part for the potential drop across the pipette caused by the access resistance of the cell. Therefore the membrane charges faster and the voltage drop is decreased (due to the apparent reduced R_s). There are a couple of limitations however to the amount of compensation achievable. The electronic circuit can saturate at high compensation levels, and the current feedback is positive, which means that the stability of the circuit can be degraded by the feedback at high compensation levels leading to circuit oscillations (Ogden and Stanfield 1994). Typically series compensation was set between 65-75% in my experiments. Additionally it is possible to minimize the size and time error in voltage due to series resistance by keeping R_s as small as possible by using low resistance pipettes.

2.3.4 Perforated Patch Configuration

In whole cell recordings reproducible measurements of calcium currents and exocytosis are not feasible over long periods due to dialysis of cytoplasmic factors up the patch pipette which lead to 'rundown'. Exocytotic efficiency has been reported to decline with a time constant of 23 minutes in the whole cell configuration (Seward and Nowycky 1996). The problem can be overcome by using the perforated patch configuration of the whole cell technique. This method allows the intracellular milieu of proteins to remain intact whilst allowing electrical access to the cell. This results in reproducible recordings of calcium currents and exocytosis for durations of several hours assuming proper voltage clamp is retained (personal record is 4hrs 43 minutes). The technique works by selectively perforating a patch of the membrane beneath the pipette tip by including a channel forming antibiotic in the pipette solution. Electrical access is possible as the channels formed are permeable to monovalent ions, allowing quick exchange of intracellular ions with those in the electrode. These channels are very selective and therefore retain intracellular proteins maintaining the cytoplasmic milieu. Several substances have been used to induce membrane perforation including the polyene antibiotics nystatin (Horn and Marty 1988) and amphotericin B (Rae et al. 1991; Engisch and Nowycky 1998). The channels formed by these antibiotics permeate monovalent anions and cations. An

alternative antibiotic gramicidin D is also commonly used. The pore formed by this channel is only permeable to monovalent cations and in contrast to the nystatin or amphotericin B will not pass anions. The channel formed by gramicidin D has been extensively investigated and is well characterized (for review see Busath 1993). Of particular advantage to electrophysiologists is the fact that the association and subsequent dissociation rates of the gramicidin peptide into the cell membrane is voltage and agonist independent. Gramacidin D is easier to prepare and keep compared to nystatin or amphotericin as it does not require rounds of sonication or to be shielded from light to prevent degradation. In my perforated patch studies I used gramicidin D. The method of perforated patch is essentially the same as whole cell, however after obtaining a giga seal further negative pressure is not applied to rupture the cell membrane and gain electrical access. Instead, over time gramicidin peptides insert into the cell membrane creating channels. As this happens the pipette conductance slowly increases. This process can be monitored by applying a seal test and observing the increase in capacitance transients at the beginning and end of voltage steps as the cell perforates. With my recording configurations it usually took around 30 mins for the access resistance and membrane capacitance of the cell to stabilise. Membrane capacitance and series resistance are cancelled in an identical manner to whole cell recordings. With this technique it was possible to achieve series resistance values comparable to those observed in the whole cell configuration $\sim10m\Omega$ (whole cell mean = 8.2 mΩ ± 0.2 n = 248, perforated mean = 11.4 mΩ ± 0.3 n = 108), series resistance was restricted to a maximum value of 17mΩ by the limitations imposed in our ability to measure capacitance (section 2.4.2.9). There are several disadvantages to the perforated technique. Firstly, it is more difficult to obtain the initial cell-attached configuration due to using larger resistance pipettes (necessary for adequate diffusion of gramicidin D down the pipette) and antibiotic and/or DMSO in the solution. Secondly it takes a considerable time to obtain low resistance access to the cells (typically ~30 minutes). Thirdly, it is not possible to introduce peptides or antibodies to the cell via the patch pipette in the manner well exploited in the whole cell configuration. Finally, the success of gramicidin D to perforate the cell membranes did appear to vary from culture to culture, suggesting

that slight differences in membrane composition between cultures could affect the ability of the antibiotic to enter the membrane.

2.3.5 Liquid Junction Potentials

In patch clamp recordings, when the bath and the patch pipette contain solutions of different ionic composition then a liquid junction potential will exist at the pipette tip. This is because ions present in each solution have different ionic mobility and therefore diffuse at different rates. For example, in a simplified situation, if the bath contains 150mM NaCl and the pipette contains 150mM KCl then the pipette would become negatively charged in relation to the bath. This is because Cl^- has a higher ionic mobility than Na^+ and therefore diffuses into the patch pipette more rapidly than Na+, this produces a net negative charge on the pipette. K^+ and Cl^- have similar ionic mobility and therefore diffuse from the pipette at similar rates producing no net charge. Therefore the liquid junction potential calculated in this case is +4.3mV, bath solution with respect to pipette (Barry and Lynch 1991). The error in membrane voltage measurement will arise because the liquid junction potential of the pipette tip is zeroed before making a seal by dialling the pipette offset knob on the patch clamp amplifier. This results in the amplifier applying a voltage of equal size to the liquid junction potential but in the opposite direction. Once a seal is formed, the liquid junction potential disappears because there is now a barrier between the pipette and bath solutions. This leaves the pipette potential displaced from true zero by the amount equal to the initial pipette-bath potential difference, opposite in polarity to the junction potential and therefore contributing to the measured membrane potential of the patch (Ogden and Stanfield 1994). In whole cell recordings, a new, transient liquid junction potential will arise between the pipette and cytosol until the cell is dialysed with the pipette solution, leaving just the original pipette-bath potential added to the holding current. Due to the channel forming properties of gramicidin A whether the same situation is true for perforated patch recordings is unclear. The voltage error induced by liquid junction potentials is fairly easy to measure. With the patch clamp amplifier set to current clamp, a pipette containing internal solution is

56

placed into the bath, which also contains internal solution. Any tip potential should then be zeroed before exchanging the bath solution for external solution. A liquid junction potential between internal and external will be displayed on the amplifier, which can be noted. This potential difference can be applied to the voltage command when performing experiments or corrected for when analysing results if desired. In my experiments the liquid junction potential between standard internal and external solutions was ~ +15mV (bath solution with respect to pipette solution). When the bath solution is changed for one with a different ionic composition, a further liquid junction will develop between the new bath solution and the reference (ground) electrode. In this case an agar or salt bridge is usually employed to keep the reference electrode zero. This was not necessary in the course of my experiments as changes in external solution were subtle (ie replacement of 2.5mM $CaCl_2$ with eqimolar $BaCl_2$). These subtle ionic substitutions did not change the liquid junction potential. Data presented in my thesis has not been corrected for liquid junction potentials.

2.4 Measuring Secretion

The ability to measure secretion has been an important advancement in our understanding of the mechanisms underlying stimulus-coupled exocytosis. Biochemical methods, like spectrophotometric detection (a chemical reaction between the released product and an extracellularly applied molecule leading to formation of a coloured or fluorescent signal), or radiochemical detection (radio labelling of the released product) have been useful but offer poor time resolution and report secretion from a population of cells. Biophysical methods like amperometry, (electrochemical detection), or membrane capacitance measurements have much higher temporal resolution. These techniques allow the kinetics of release to be studied in detail at the single cell level.

2.4.1 Commonly used techniques to measure exocytosis.

2.4.1.1 Amperometry

The principle of this technique relies on the electrochemical detection of the secreted chemical. This technique can be used to measure transmitters which can readily be oxidized or reduced, making it ideal for studying catecholamine release from chromaffin cells. A carbon fibre electrode is placed very close to, or just touching the cell and a voltage applied across this electrode. The voltage is related to the redox potential for the transmitter under investigation and is usually set to exceed this potential to favour rapid conversion of all the molecules (Chow 1995). Oxidation of a transmitter, ie adrenaline, results in an amperometric current. The temporal resolution of amperometry is superior to capacitance, allowing fusion pore kinetics to be studied (Chow et al. 1992). Although usually combined with voltage clamp electrophysiology experiments, patch clamping is not an intrinsic part of the methodology and amperometric currents can be stimulated by simple depolarising solutions or specific secretatogues. The three main advantages of amperometry over capacitance is that it directly measures exocytosis (the secreted transmitter) without contamination from endocytosis, there is no restriction on the cell morphology to apply this technique (as voltage clamp is not required) and the greater time resolution allows studies of fusion pore kinetics. However the technique is limited to studies on easily oxidisable transmitters, which precludes this technique from studies on glutamate or GABA release. It only records secretion from part of the cell (the part directly next to the electrode) and there appears at present to be inconsistency in the way amperometric currents are analysed, resulting in conflicting results appearing in the literature.

2.4.1.2 Optical – fluorescent imaging.

Optical imaging is a fairly recent but rapidly expanding method to study exocytosis and endocytosis. It is possible to image secretory dynamics using lipophilic styryl dyes, like FM1-43 (Cochilla et al. 1999). These dyes reversibly stain membranes, are

58

membrane impermeable and most importantly their fluorescent intensity increases several hundred fold when they are partitioned in membranes. The technique works by stimulating cells with the dye in the extracellular solution, this leads to vesicles taking up the dye as the membrane is subsequently endocytosed. Wash out of dye, leaves the dye only inside vesicles, allowing following rounds of exocytosis to be studied. This technique has been well exploited to monitor synaptic vesicle dynamics in a wide number of preparations. Other optical techniques employ the use of acidtropic dyes, like acridine orange, which selectively partition into intravesicle compartments. A loss of fluorescence after stimulation is used as an indication of exocytosis (Oheim et al. 1999). More recently this technique has been extended using a molecular strategy to over-express vesicle associated proteins tagged with a pH sensitive GFP to monitor vesicle cycling (Sankaranarayanan et al. 2000). In addition to the advancement in the dyes and molecular tools, the microscopy side of imaging has also improved dramatically. Optical imaging of exocytosis is now usually viewed using 'total internal reflection microscopy' (TIRF). This technique restricts illumination to within a few hundred nanometers of the plasma membrane (Oheim 2001a; Oheim 2001b), allowing the resolution of the moment of individual vesicles. This technique has also been used to study vesicle selection in response to different stimuli (Duncan et al. 2003). Imaging approaches offer many advantages over capacitance and amperometry, particularly in regard to spatial resolution, but at present lack the temporal resolution.

2.4.1.3 Recording postsynaptic potentials

This is one of the oldest techniques used to monitor neurotransmitter release and is still being used today. Many neuronal presynaptic synapses are presently too small to adequately patch, although there are some 'giant' synapses, (Forsythe et al. 1998). However it is sometimes possible to patch the post-synaptic cell. Therefore stimulation of the presynaptic cell, will lead to neurotransmitter release, diffusion across the synaptic cleft and stimulation of the post-synaptic cell resulting in a post-synaptic current. This offers good time resolution but lacks the advantage of being

able to manipulate stimulus-coupled exocytosis by introduction of peptides or antibodies etc via a pre-synaptic patch pipette. With the advancement of molecular and genetic tools, these problems are being overcome (Richmond et al. 1999).

2.4.2 Secretion from single cells can be quantified by measuring membrane capacitance changes.

Exocytosis involves the fusion of a secretory vesicle (a membrane enclosed packet of neurotransmitter) with the cell plasma membrane, to release its contents to the outside. The mixing of vesicle and cell membranes leads to an increase in the surface area of the plasma membrane. This increase in cell surface area can be measured by determining the cell membrane capacitance C_m, since the value of a capacitor is directly proportional to its surface area.

The specific membrane capacitance of almost all biological membranes can be calculated (and experimentally measured using a modified Wheatstone bridge current balance) to be roughly $1\,\mu F/cm^2$ (Cole, 1968).

$$C_m = (\varepsilon\varepsilon_0/d)A$$

(ε = dielectric constant, ε_0 = polarizability of free space, d = membrane thickness, A = area)

Therefore a cell of $13\,\mu m$ diameter will have a C_m of about 5.0pF (Gillis 1995).

If the size of the vesicle can be calculated and a change in capacitance is measured then it is possible to determine how many vesicles have fused in response to a given stimulus.

2.4.2.1 Membrane capacitance techniques in combination with whole-cell patch clamp.

These techniques essentially apply a voltage and separate a capacitative current from a resistive current

The current that flows across a capacitor is given by:

$$I_C = C*dV/dt$$

Thus, if the voltage does not change there is no capacitative current.

60

Membranes also have resistive properties and the current that flows across a resistor is given by Ohm's law:

$$I_R = V/R$$

Several distinct techniques have been developed for detecting C_m changes resulting from vesicle fusion.

1. Time domain based techniques
2. Pseudorandom binary sequence (PRBS) techniques
3. Sine wave voltage based techniques.

2.4.2.2 Time domain based techniques

This technique involves applying square voltage pulses (at hyperpolarized voltages that will not activate non-linear membrane conductances). The capacitive transients that charge the membrane capacitance are then cancelled. Subsequent voltage steps to depolarized potentials evoke a non-linear ionic current of interest. This current declines with an exponential time course. Fitting this exponential can be used to evaluate ΔC_m. A problem associated with this technique is that it relies on an instantaneous voltage step, which experimentally is difficult to achieve (pipette resistance can slow the voltage step etc), and the interval between voltage steps must allow for complete charging/discharging of C_m. This therefore limits the resolution of this technique to estimate C_m to a frequency of 1 Hz (for further details see Lindau and Neher 1988; Gillis 1995).

2.4.2.3 The PRBS technique

Similar to the time domain technique square-wave voltage pulses are applied, however the duration of the voltage step is now a random variable. The resulting stimulus spectrum approximates white noise. The spectrum of the resulting current signal is directly related to the admittance spectrum, from which C_m can be derived (Fernandez et al. 1982). This method relies on fitting the admittance to theoretical

algorithms to determine C_m, if these are not accurate then the estimation of the cellular parameters will be inaccurate (Neher and Zucker 1993).

2.4.2.4 Sinusoidal Excitation

This is the most commonly used technique and involves applying a sine wave about a hyperpolarised potential. The principle of this technique is shown schematically in figure 2.4.2.5).

2.4.2.5 Schematic representation of sinusoidal excitation
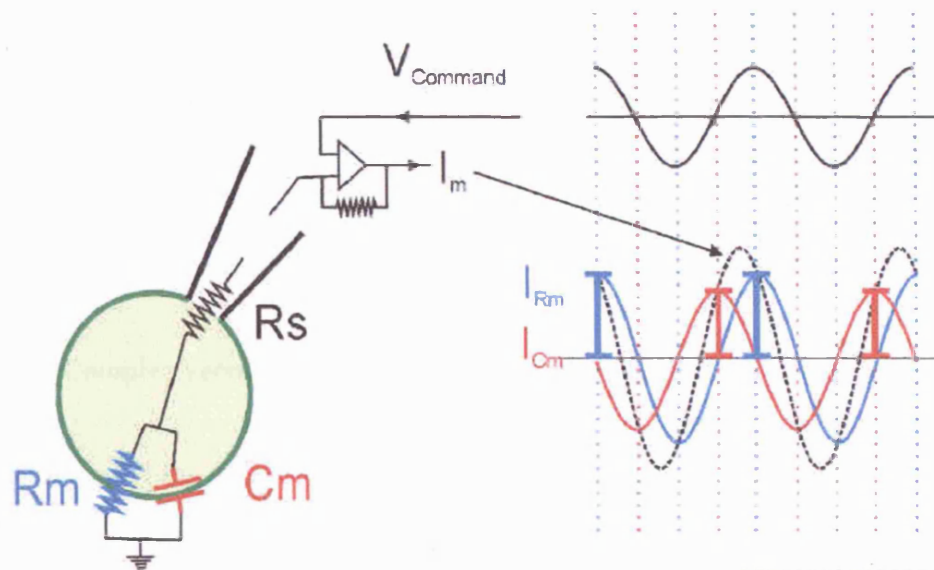
Figure taken from the Schweizer lab web page

http://neurobionet.neurobio.ucla.edu/~felixs/capacita.htm

If a sine wave is applied ($V_{Command}$ top black) to a cell then the resulting current (I_m) will contain both a resistive and capacitative component. It is possible to split up these components. When there is no change in voltage (peak of sine wave, blue dashed line), there is no capacitative current. Therefore all the current will be resistive and we know the voltage, allowing the determination of R_m. Likewise when the voltage changes most, (at the inflection point of the sine wave, red dashed line). There is no net applied voltage and thus no resistive current. At this point all the current will be capacitative. As the voltage and current are known it is possible to calculate membrane capacitance.

As shown in figure 2.4.2.5, I_m (the resultant sinusoid current) is shifted with respect to the voltage stimulus, the magnitude and degree of phase shift can be analysed

62

using a phase sensitive detector to produce estimates of C_m. The first studies using a hardware based phase sensitive detector (lock in amplifier) were developed by (Neher and Marty 1982). Since then a software-based phase detector has been developed (Joshi and Fernandez 1988; Filder and Fernandez 1989). I have used a software-based detector in my studies and will describe this method in more detail below.

2.4.2.6 Software-based phase-tracking technique for cell membrane capacitance measurements.

To measure changes in cell membrane capacitance a 15mV, 1.3 kHz sine wave was added to the holding potential of -80mV ($V_{command}$). This applied sinusoidal voltage produced a sinusoidal current which was phase shifted with respect to the $V_{command}$. This current can be represented in complex space as a vector, and separated into a component in phase with the stimulus voltage (real part) and a component 90° out of phase with the voltage (imaginary part) using a software-based phase-sensitive detector.

2.4.2.7 Complex vector of capacitance and conductance

Imaginary axis

ΔC_m

Real axis

ΔG_m
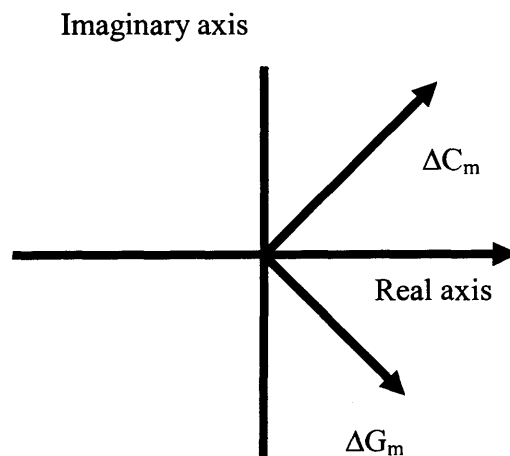
Usually with the voltage clamp configuration the ground is connected directly to the cell bathing solution. With the 'phase-tracking' technique a resistor (in our set up 500kΩ) is placed between the bath and ground. By switching this resistor in and out

63

during the sinusoidal stimulation different phase angles are scanned until one is attained that will result in a deflection of the conductance trace that is not observed on the C_m trace. This phase angle is selected and then visually inspected by the experimenter. The phase angle is judged to be correct if a 100fF calibration step, obtained by temporarily unbalancing the C_{slow} compensation viewed on the C_m trace does not induce a corresponding change on the conductance trace. Similarly placing a 500kΩ resistor in series with the cell will cause a deflection in the conductance trace which should not be visible on the C_m trace (figure 2.4.2.8). Exocytosis is triggered by interrupting the sinusoidal stimulus and applying a variable depolarizing step. The potential is then returned to -80mV for 15-50 ms before re-starting the sine wave stimulus. The phase angle was also deemed to be correct if changes in C_m due to exocytosis were not reflected in the conductance trace. Using the phase tracking method it is possible to check for artefactual changes in C_m at any point in the experiment. Parallel (or anti-parallel) changes in C_m and resistive parameters are indicative of either an incorrect phase setting or imply that the cell is not modelled by a simple electrical circuit.

2.4.2.8 Experimentally recorded capacitance and conductance traces, indicating that the correct phase angle was set.
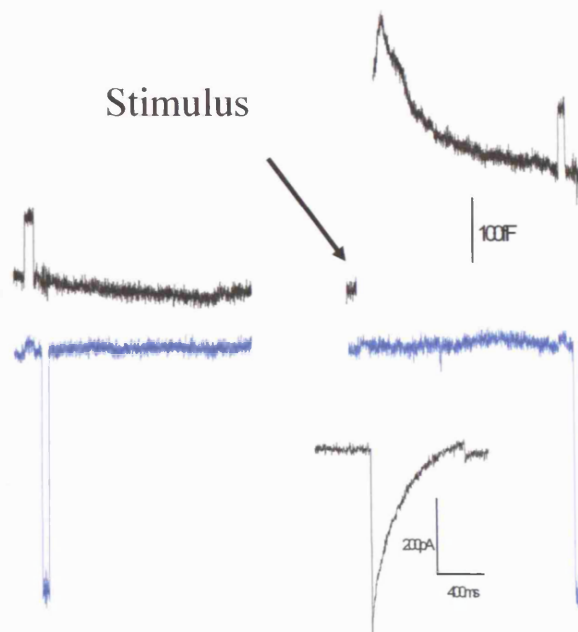
Capacitance traces are shown in black, conductance in blue. On the left a pre-stimulus 100fF calibration in the capacitance trace is applied, note there is little corresponding change in the conductance trace. Similarly a resistor is temporally placed into the circuit causing a deflection in the conductance trace with no change in the capacitance trace. This indicates that the correct phase angle has been found and applied. On the right are capacitance and conductance traces before and after a stimulus (an 800ms depolarization, current trace shown below). Towards the end of the traces capacitance and conductance are calibrated again.

2.4.2.9 Limitations and errors associated with C_m measurements.

Although a very powerful and useful technique, there are several limitations associated with measuring exocytosis by monitoring cell membrane capacitance. C_m measurements report the net rate of exocytosis and endocytosis. Secretion is a dynamic process with the possibility of exocytosis and endocytosis occurring at the same time, especially during a train of depolarisatons. The speed of endocytosis depends on local calcium concentration with a rapid mode reported at elevated calcium concentrations (Neher and Zucker 1993). Therefore slow C_m increases may well represent a mixture of both exo- and endocytosis and lead to an underestimation of the rate of exocytosis. Capacitance measurements by definition are only reporting changes in cell membrane surface area, and not actual detection of neurotransmitter.

65

Therefore any mixing of intracellular membranes with the plasma membrane will lead to an increase of capacitance regardless of whether neurotransmitter is released or not. Also mobilization of charges during gating of voltage-dependent channels can produce a change in specific capacitance (Fernandez et al. 1982; Horrigan and Bookman 1994). Therefore C_m changes are not normally resolved during a depolarization. The sinusoidal wave stimulus is usually paused during the actual depolarization and the rate of secretion is inferred from the difference between pre- and post-stimulus C_m measurements. Usually a delay of a few ms before recommencing the sine wave stimulus after the depolarization is necessary as the voltage-dependence of gating charge movement can shift upon channel inactivation (Horrigan and Bookman 1994). Another potential problem is a change in pipette capacitance (C_p) due to alterations in fluid level within the recording chamber (Gillis 1995). C_p is subtracted by the amplifier when calculating ΔC_m changes, therefore changes in C_p would produce either an increase or decrease in C_m. Amperometry avoids these complications as the carbon fibre electrode measures the actual secreted product, however amperometry as a technique to measure exocytosis has its own inherent limitations (section 2.4.1.1). Some labs now combine capacitance and amperometry to obtain a more complete measurement of exocytosis.

2.5 Drugs

All drugs were made up as a concentrated stock in distilled filtered water and stored as aliquots at $-20^{\circ}C$ until use unless stated differently. Stocks were thawed and added to external solution to obtain the required concentration. This solution was then added to either a 10 or 50 ml tube connected to the superfusion system (see section 2.2.8). ω-Conotoxin GVIA and ω-Agatoxin IVA were obtained from Alomone laboratories (Jerusalem, Irasel). Nifedipine was obtained from Alomone and dissolved in 99% ethanol. Aliquots were wrapped in silver foil to protect them from light inactivation until use. Cyclosporin A (Sigma) was dissolved in 99% ethanol and stored at $-20^{\circ}C$. Peptides that were introduced to the cell via the patch pipette were

66

dissolved as a concentrated stock in standard internal solution, kept at -20°C until needed, then added to fresh internal solution to obtain the required concentration.

2.6 Data analysis

2.6.1 Calcium currents

Sodium currents were not routinely eliminated (due to artefactual influences on C_m traces caused by channel blockers and the expense associated with continued application of blockers to external solution). Sodium currents in bovine adrenal chromaffin cells completely inactivate by 3ms after a depolarizing pulse to potentials greater than 0mV (Neher and Marty 1982, chapter 3, section 3.1.2). Therefore limits were set between 3ms after the start of the pulse and 1ms from the end to avoid contamination from sodium and tail currents respectively. Calcium currents were analysed in one of two ways (figure 2.6.11). A computer program was written to scan the current trace and identify the maximum current within the set limits. Additionally calcium entry could be determined by integration of the calcium currents, again between the defined limits. A caviat to this is that the small amount of calcium entry which occurs during the first three milliseconds, or the last millisecond (including the tail current) will not be accounted for.

2.6.1.1 Measurement of calcium currents
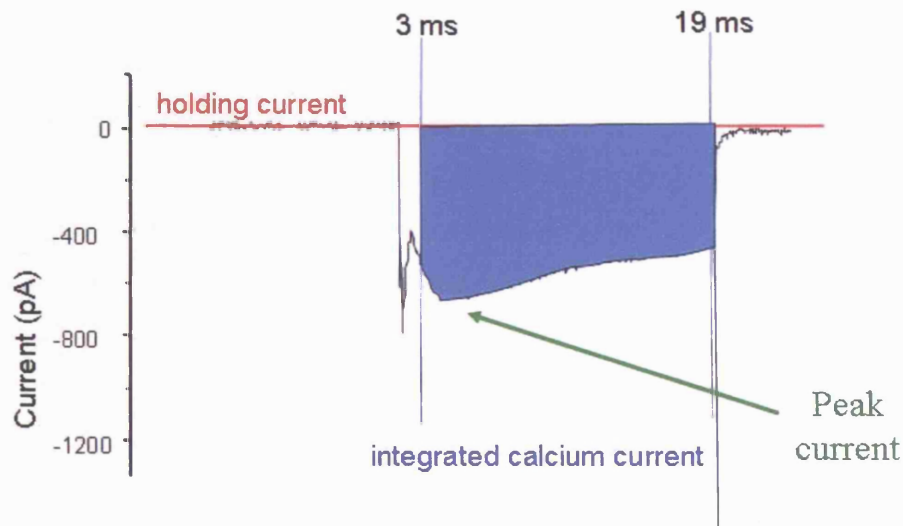
Integrated calcium was derived using Faraday's law:

$$Q = \int idt$$

$$1pA = 1pC/sec$$

$$i = C/secs$$

$$\int pC/s = pC/Fc/mol = mols \; x \; N_A$$

$$pC \; x \; N_A \; / \; 2 \; x \; F = 10^7 \; x \; 0.31 \; ions = x \; .10^7 \; ions$$

Where:

Q = Integrated Ca^{2+} (Number of ions)

C = Coulombs

F = Faraday's constant (charge/mole electrons)

N_A = Avogadro's number

Due to limitations in the software, the sampling rate for acquisition of currents evoked by square voltages depended on the length of the step depolarization. A 10ms voltage step was sampled at 40 kHz, a 40ms voltage step at 10 kHz, a 100ms voltage step at 4 kHz, a 200msec voltage step at 2 kHz and an 800ms voltage step at 0.5 kHz.

2.6.2 Capacitance measurements

ΔC_m was determined relative to a 100fF calibration signal switched into the circuit before and after a depolarization. The total ΔC_m triggered by each voltage pulse was calculated offline as the difference between an averaged value before depolarization and an averaged value after depolarization (4 points before and 4 points after were averaged). With trains of depolarisations drifts in C_m between pulses were assessed by averaging the first 4 points acquired immediately after the voltage pulse and subtracting them from the average of four points taken immediately before the next voltage pulse. This was true for all train protocols except one (a train of 50 x 10ms with an interval of 50ms, in which case only 2 points were averaged). The temporal resolution of C_m measurements was between 10-12 ms per point. Exocytotic efficiency was determined by dividing the size of the capacitance increase by the value obtained for integrating the corresponding calcium current.

2.7 Statistics

Statistical significance was determined using InStat 3 (Graphpad). All statistical tests performed in this thesis were unpaired Student's t-tests unless specifically stated, with significance considered if $p<0.05$. Data shown is the mean $\pm$ standard error of the mean (s.e.m).

2.8 Production of an adenovirus

It became apparent after exhaustive failed attempts to efficiently transiently transfect bovine adrenal chromaffin cells with plasmids encoding genetically altered proteins (electroporation, lipofectamine, fugene 6 etc), that a viral approach would be necessary, particularly if I wished to transfect acute rat slices. The details of viral production and results are contained in appendix 2 of this thesis.

Chapter 3: Characterisation of calcium channels in bovine adrenal chromaffin cells.

Chromaffin cells have been used extensively for many years as a model to study regulated exoytosis (Douglas and Poisner 1967). Since the development of the patch clamp technique in the early 1980's (Neher and Marty 1982; Fenwick et al. 1982), it has been possible to study directly the coupling of calcium channels to neurotransmitter and peptide release. The first part of my research was to characterise the basic biophysical properties of the calcium channels expressed in bovine adrenal chromaffin cells.

Electrophysiological recordings were performed using either the whole-cell or the perforated patch recording configuration. For all the experiments described the cells were held at -80 mV, and depolarised to +20 mV unless stated otherwise. A liquid junction potential of +15mV was not corrected. The calcium channel current was isolated from potassium conductances by using a cesium-based internal solution to block their contribution to evoked currents (see chapter 2, section 2.2 for composition). TEA was omitted from the external solution to prevent cells from depolarizing due to block of potassium channels. It was discovered however that during prolonged depolarisations (800ms), that a calcium-activated outward conductance of unknown identity was being recruited preventing complete isolation of calcium channel currents. This outward current could be greatly reduced by addition of 10mM TEA to the external solution (see appendix 1). Therefore it became routine to establish voltage clamp in TEA-free external and then to perfuse with external solution containing 10mM TEA. Figures presented in chapters 3 and 4 may contain data derived from cells in which 10mM TEA was not added to the external solution. When this is the case it is noted in the figure legend. A fast rate of perfusion was applied to minimize the effects of secretory products from surrounding non voltage-clamped cells exerting modulatory effects on the cell under investigation (Currie and Fox 1996). Multiple recordings from a coverslip were only permitted if external containing 10mM TEA had not been used. As I was simultaneously

recording membrane currents and capacitance, tetrodotoxin (TTx) was omitted from the external solution for the majority of experiments as it slows Na^+ channel gating kinetics 10-fold, resulting in a potential contamination of the membrane capacitance (C_m) trace (Horrigan and Bookman 1994), and would inflict a substantial financial burden if used routinely throughout the duration of my PhD studies.

3.1 Chromaffin cells express voltage-dependent sodium channels.

Chromaffin cells express voltage-dependent sodium channels (Neher and Marty 1982). These channels begin to activate at potentials greater than -40mV and their rate of activation and inactivation are dependent on the membrane voltage (figure 3.1.1). To record sodium currents brief (10ms) depolarisations were applied from a holding potential of -80mV and a current/voltage (I/V) relationship determined. Standard intracellular and extracellular solutions were used except that extracellular calcium was replaced with magnesium, therefore maintaining the extracellular divalent charge. Calcium channel permeability to monovalent ions increases when the external divalent concentration is reduced below the micromolar level (Almers and McCleskey 1984). Under optimal conditions, (low millimolar extracellular calcium), calcium channels display greater than 1000-fold selectivity for calcium over sodium (Catterall 1993, Sather and McCleskey 2003 and references within). However in figure 3.1.1, small tail currents can be observed at the end of depolarisations to positive potentials implying that despite maintaining extracellular divalent concentration by addition of magnesium open calcium channels exhibit some permeability to sodium ions under these conditions.

3.1.1 Sodium current recordings from bovine chromaffin cells.

-50mV   -40mV

-30mV   -20mV

-10mV   0mV

500pA

+10mV   3ms   +20mV
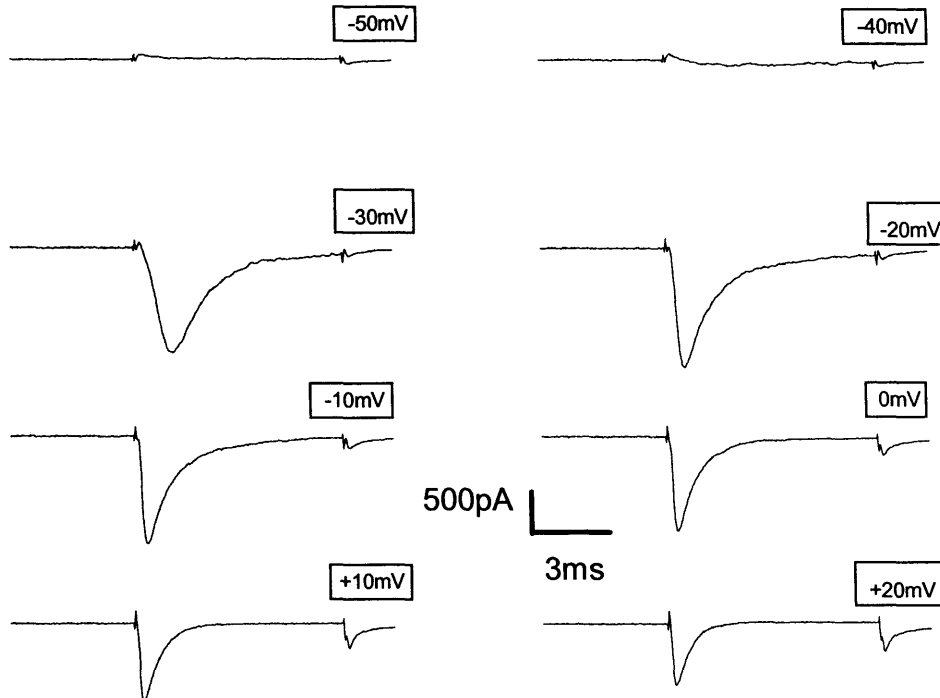
Sodium currents were isolated from calcium currents by replacement of extracellular calcium with magnesium. Short (10ms) depolarisations were elicited from a holding membrane potential of -80mV to +20mV in 10mV increments at 0.1 Hz. Sample traces are shown above.

To address questions asked about calcium channel properties it was necessary to be able to isolate the calcium current from the sodium current. The sodium current can be blocked or eliminated by application of $1\mu M$ TTX or replacement of extracellular sodium with TEA (figure 3.1.2). However, experiments were designed so that information about both membrane currents and changes in capacitance could be recorded from each cell. Therefore neither application of TTX or sodium replacement with TEA was desirable due to their affects on measuring capacitance changes or from depolarisation of unclamped cells and release of neuromodulators respectively. With depolarisations to +20mV the sodium current rapidly inactivates (~2ms), (figure 3.1.2.c). Therefore as explained in section 2.6.1.1, when measuring either peak calcium currents or integrated calcium values resulting from depolarisations to +20mV temporal limits were set 3ms after the start of the

depolarisation. When measuring peak currents at other potentials, for example when examining I/V relationships, then temporal limits were set individually for each membrane potential to eliminate the majority of the sodium current.

3.1.2 The sodium current can be blocked by application of TTX or by replacement of extracellular sodium by TEA.
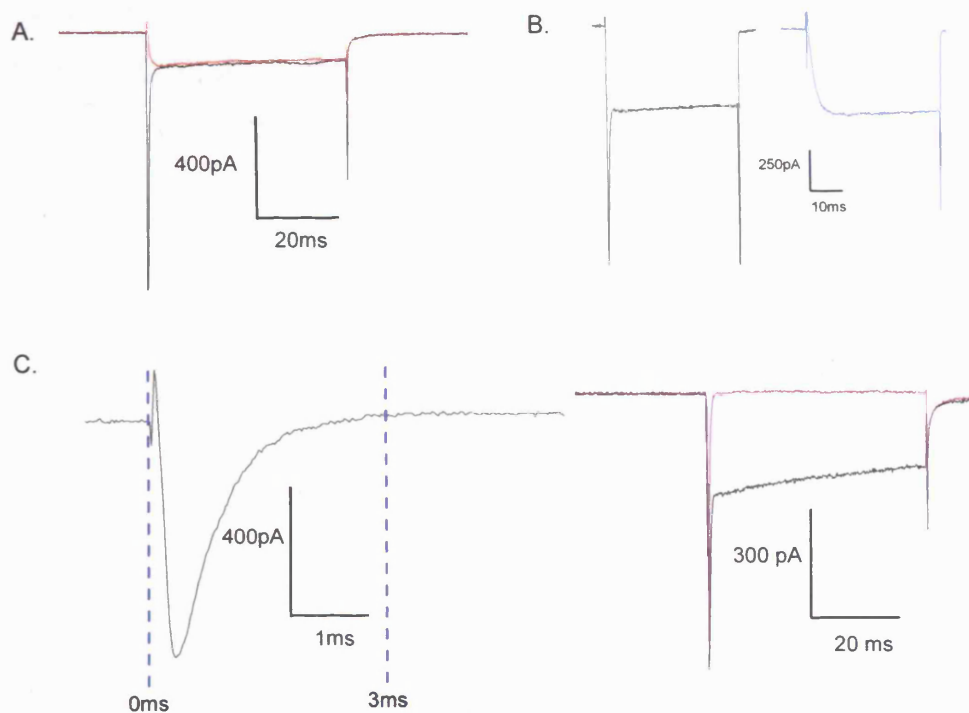
A. A 40ms depolarisation to +20mV before (black) and after (red) application of 1μM TTX.
B. A 40ms depolarisation to +20mV in either standard 150mM NaCl external solution, left in black, and after total extracellular replacement of sodium with TEA (right in blue).
C. The sodium current trace on the left corresponds to a 10ms step depolarisation to +20mV with extracellular calcium replaced with magnesium. Temporal limits of 0 and 3ms are superimposed in blue. Note that at this potential the sodium current has completely inactivated before 3ms. On the right is a 40ms depolarisation to +20mV in standard extracellular solution containing 2.5mM calcium (black). Superimposed is the current trace recorded after extracellular calcium has been replaced with equimolar magnesium (purple).

3.2 Voltage dependence of calcium channel activation.

To study the voltage-dependence of calcium channel activation, brief (50ms) depolarisations were elicited from a holding potential of -80mV to test potentials

from -40mV to +60mV at 10mV increments at a frequency of either 0.1 or 0.03 Hz. A single step depolarisation (to potentials greater than -10mV) resulted in a dual component membrane current consisting of a larger amplitude, rapidly inactivating component which corresponded to the sodium current and a sustained current, which corresponds to activation of calcium currents (figure 3.2.1). Using this protocol, and by setting limits to exclude the majority of the sodium current[1], calcium channel I/V relationships were obtained from both cultured bovine chromaffin cells and from acute rat adrenal slices. As there was no sustained current with depolarisations to -40 mV this suggests that low voltage activated (LVA) calcium currents are not present in chromaffin cells. Chromaffin cells from different species are known to express different levels of calcium channel α_1 subtypes, (Artalejo et al. 1994; Kitamura et al. 1997; Gandia et al. 1998; Lukyanetz and Neher 1999), and there are also reports of differences in the quantity of channel subtypes expressed from the same species when cells are recorded from a slice preparation or after isolation and several days of culture (Albillos et al. 2000). In these experiments I am recording the total membrane calcium current and found that in both preparations the peak current was recorded at +10mV (-388pA ± 164 n=6 and -467pA ± 65 n=13 for rat and cow, respectively). However the rat I/V displays more outward current at highly positive potentials (+149pA ± 49 n=6, and +34pA ± 14 n=13 at +60mV). There are several possibilities which could account for this difference. Firstly in the slice preparation voltage clamp of the cell may not be as good due to electrical coupling between cells. Alternatively different species could express different α_1 subtypes of calcium channel, or couple to different β subunits, or that channel subtype expression changes in culture. Direct pharmacological investigation of the α_1 channel subtypes for the rat preparation was not conducted, whereas the calcium current in bovine cells is mediated by N and P/Q type channels (see chapter 5). The measured reversal potential for both species (~+55 mV) and amplitude of the outward currents is different from the predicted value calculated using the Nersnt equation. As intracellular calcium is usually kept much lower (>15,000 times) than extracellular

---

[1] A previous study, recorded an I/V with sodium channels blocked with TTX (Fenwick et al 1982). This resulted in an I/V with the same characteristics (peak current voltage, reversal potential etc) as the I/V recorded here with sodium current contamination removed by applying temporal limits.

calcium, it seems unlikely that outward calcium flow through the channel could result in a large outward current even at highly positive membrane potentials when the outward electrochemical driving force is large, as the number of free intracellular calcium ions would be low. Secondly the predicted reversal potential for calcium (E_{Ca}) with my solutions (2.5mM extracellular calcium, and assuming intracellular calcium is ~100nM) using the Nersnt equation is calculated to be +123mV. The measured reversal potential here is unlikely to reflect outward current contamination from a separate channel. An explanation for the measured E_{Ca} differing from the calculated one is that monovalent ions can move outward through calcium channels at highly positive membrane potentials (Hille 1992 and references within). The outward current observed at highly depolarised potentials (> +50mV) in my experiments is most likely to reflect cesium ions flowing through open calcium channels (Fenwick et al. 1982). From measurement of tail current amplitudes recorded after depolarisations to different membrane voltages, it was possible to calculate the voltage-dependence of activation. The activation curve for the total calcium current from bovine chromaffin cells produced a V_{50} (half channel activation voltage) of +15 ± 2 mV n = 6 (figure. 3.2.1D). This value may contain a small error as the tail current is proportional to the number of channels open at the end of a depolarisation. During a 50ms depolarisation to +20mV around 20% of the calcium channels will inactivate (figure 3.4.1). Brief (~10ms) depolarisations in which channel inactivation is minimal would have been a preferential length of depolarisation for determination of the voltage-dependence of activation by analysis of tail currents. The V_{50} value of +15 ± 2 mV derived here is similar to the V_{50} value of +11.0 ± 3.0mV which has been reported from tail current analysis from bovine adrenal chromaffin cells in which shorter (20ms) depolarisations were evoked (Powell 2000).

3.2.1 Characterisation of the whole cell calcium current in bovine chromaffin cells.
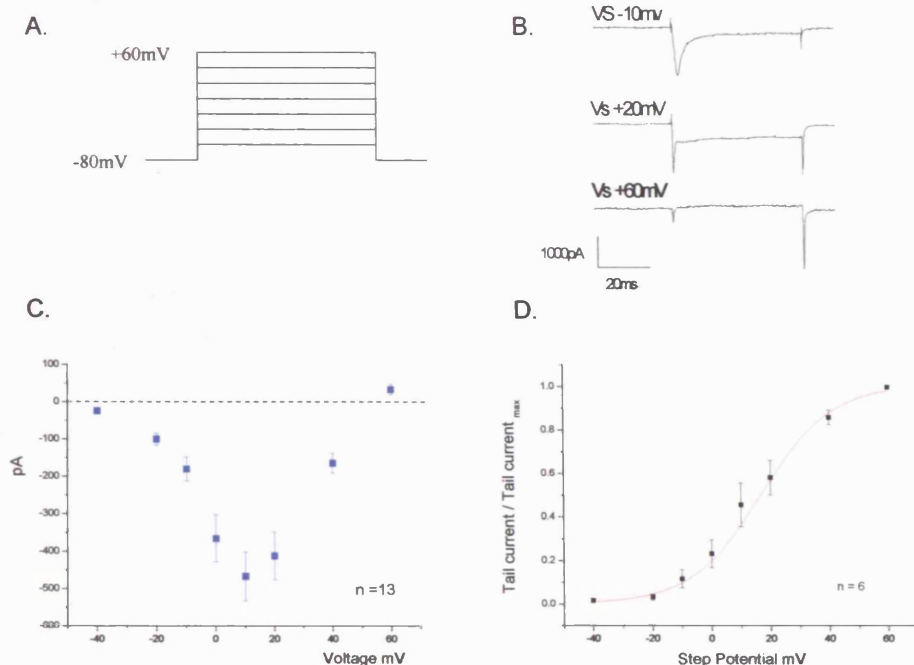
A. The total membrane current in a single cell was evoked every 10 or 30s from a holding potential of -80 mV. 50 ms duration step depolarisations from -40 mV to +60 mV were applied to the cell in 10 mV increments.
B. Sample current traces from a bovine chromaffin cell corresponding to the indicated voltages.
C. Current-voltage relationship (blue) from cultured bovine chromaffin cells. Peak current plotted against depolarising step potential. The peak current was measured using limits that exclude the major component of the sodium current, (n=13).
D. Voltage dependence of activation of the bovine current where tail currents were normalised to the peak tail current and expressed as a function of the depolarisation potential. Data was fit by a Boltzmann sigmoidal curve, $y = A_1 - A_2 / (1 + e^{(x-x0)/dx}) + A_2$, yielding a V_{50} of $+ 15 \pm 2mV$ (n=6).

To assess differences in calcium-dependency of either channel inactivation or stimulus-coupled exocytosis barium was sometimes used as the extracellular divalent charge carrier. It was observed that when extracellular calcium was substituted with equimolar barium the I/V relationship was shifted slightly (~10mV) to the left and that peak currents were augmented. Peak current was -503pA $\pm$ 74 at +10mV in calcium and -644pA $\pm$ 72 at 0mV in barium, n=6 from matched cells in which extracellular calcium was replaced with equimolar barium (figure 3.2.2B). The increase in current amplitude is indicative of a greater permeability for barium verses calcium flowing through the channels (Sather and McCleskey 2003 and references within).

76

3.2.2 Current voltage relationship with extracellular substitution of calcium with barium.
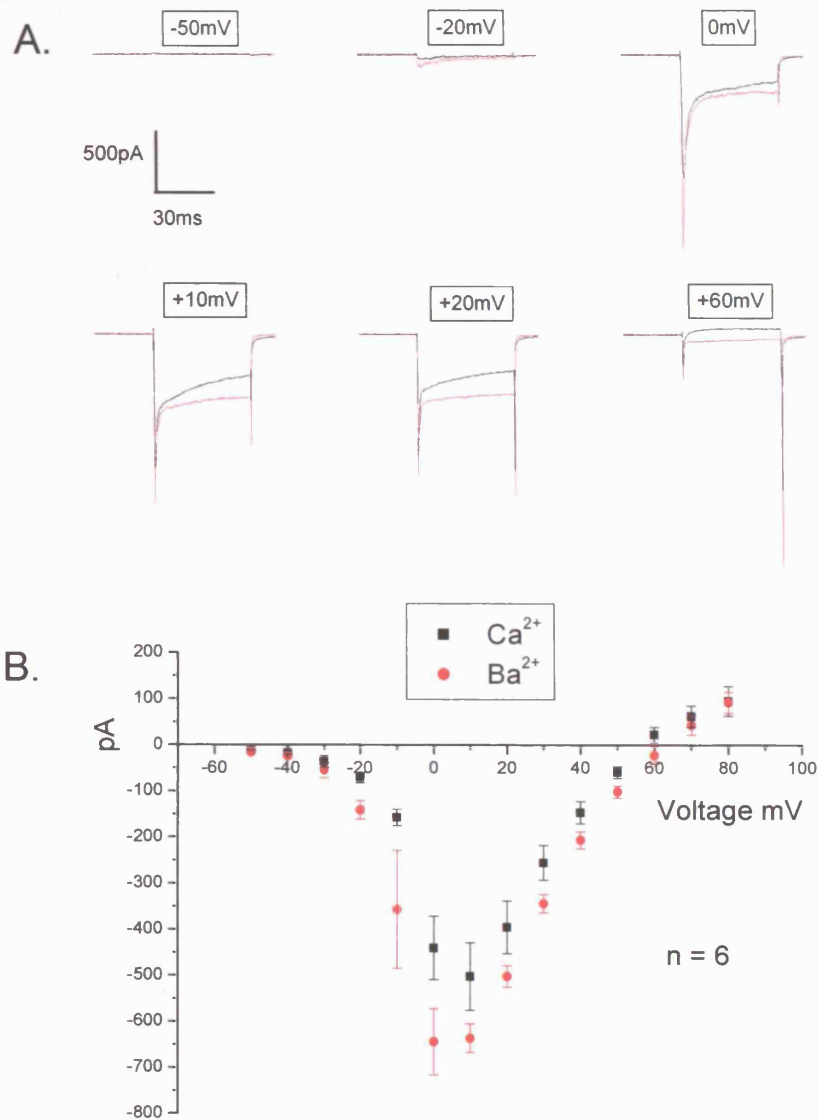
A. Sample traces from 50ms depolarisations from a holding potential of -80mV to the stated membrane potential, in calcium (black), and overlaid with the trace recorded when extracellular calcium was replaced with equimolar barium (red).

B. An I/V plot of the peak current (excluding sodium current contamination) in response to 50ms depolarisations from a holding potential of -80mV to test potentials from -50mV to +80mV at 10mV increments and recorded at 0.1Hz. I/V's were recorded in external solution containing calcium (black) and then again with extracellular calcium replaced with equimolar barium (red) Data is expressed as the mean ± s.e.m of 6 cells.

3.3 Voltage dependence of inactivation.

There are three different conformational changes in which a given calcium channel can inactivate; a fast, and slow voltage-dependent inactivation and also a calcium-dependent process. The voltage dependence of inactivation was investigated using barium as the charge-carrier to insure that only voltage dependent processes were being assessed with out the complication of calcium-dependent inactivation (Eckert and Chad 1984). By raising the holding potential in 10mV increments, and holding at the new potential for 30 seconds before applying a brief test pulses to +20mV, steady-state voltage-dependent inactivation can be assessed. The inactivation curve for the total barium current (figure 3.3.1C) produced a V_{50} (half channel inactivation voltage) of -38 mV ± 1 n = 5. It is possible that a degree of steady state inactivation occurs at the holding potential of -80mV. This could have been assessed by stepping down to more hyperpolarized potentials ie (-120mV) and applying a test pulse from there to investigate this possibility.

3.3.1 Voltage-dependence of inactivation.

A.
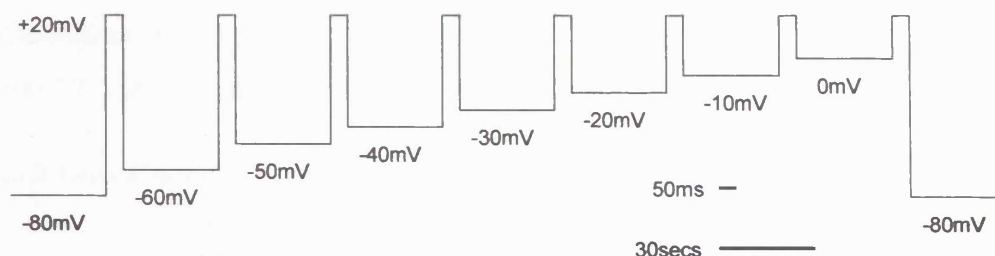
B.
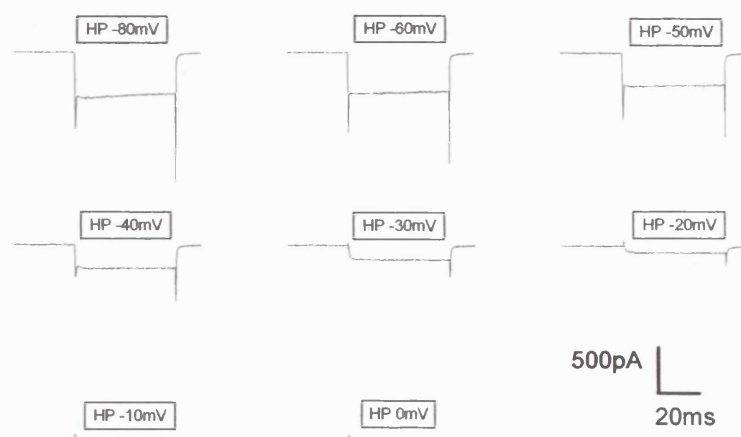
C.
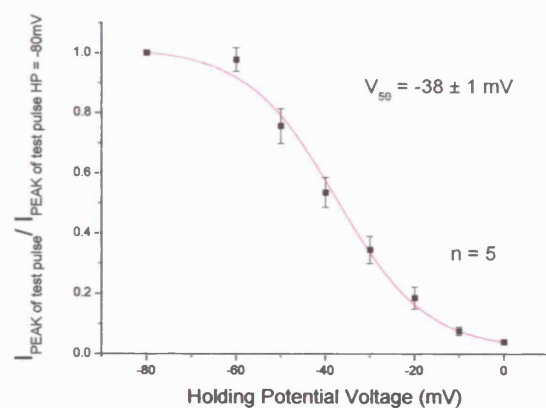
A. Voltage protocol used for determination of the voltage-dependence of inactivation. After obtaining a peak amplitude test current at +20mV with a holding potential of -80mV, the holding potential was raised consecutively from -60mV to 0mV in 10mV increments every 30seconds. Before each change in membrane holding potential a brief (50ms) test depolarisation to +20mV was evoked.
B. Sample traces of 50ms depolarisations to +20mV from differing holding potentials
C. The peak current of the test pulse was plotted against membrane holding potential and fitted with a Boltzmann sigmodial curve, $y = A_1-A_2 / (1 + e^{(x-x0)/dx}) + A_2$. The results are the mean ± s.e.m for 5 cells.

79

Throughout the course of my PhD studies membrane current traces were not leak subtracted. The typical holding current at the holding potential of -80mV was <15pA and never > than 50pA. Figure 3.3.2 displays the leak current observed over a range of membrane voltages when sodium channels have been blocked by application of 1μM TTX and calcium channels blocked by 100μM $CdCl_2$.

3.3.2 Leak Current
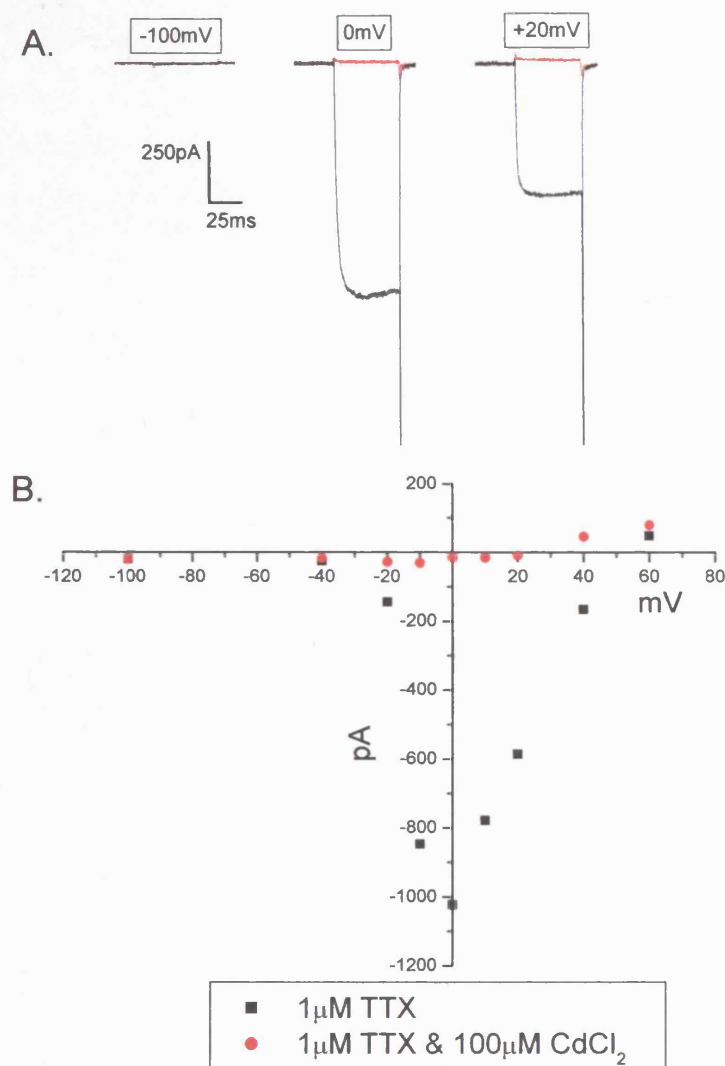
A. Sample 50ms traces recorded at the indicated membrane potential, recorded in extracellular solution containing 1μM TTX and using barium as the divalent charge carrier, before (black) and after (red) application of 100μM $CdCl_2$.
B. I/V of peak current recorded before (black) and after (red) application of 100μM $CdCl_2$.

80

3.4 Calcium channel inactivation.

To prevent excess calcium entry, which would be detrimental to the cell, calcium channels have evolved mechanisms to inactivate. A brief (40ms) current will inactivate during the course of a depolarisation such that $78.9 \pm 1.0 \%$ n = 38, of the peak current remains just prior to termination of the depolarisation (figure 3.4.1). As the pulse duration is increased, the degree of inactivation also increases, such that at the end of an 800ms depolarisation only $5.4 \pm 1.2 \%$ n = 49, of the peak current remains.

3.4.1 Inactivation increases with pulse duration.
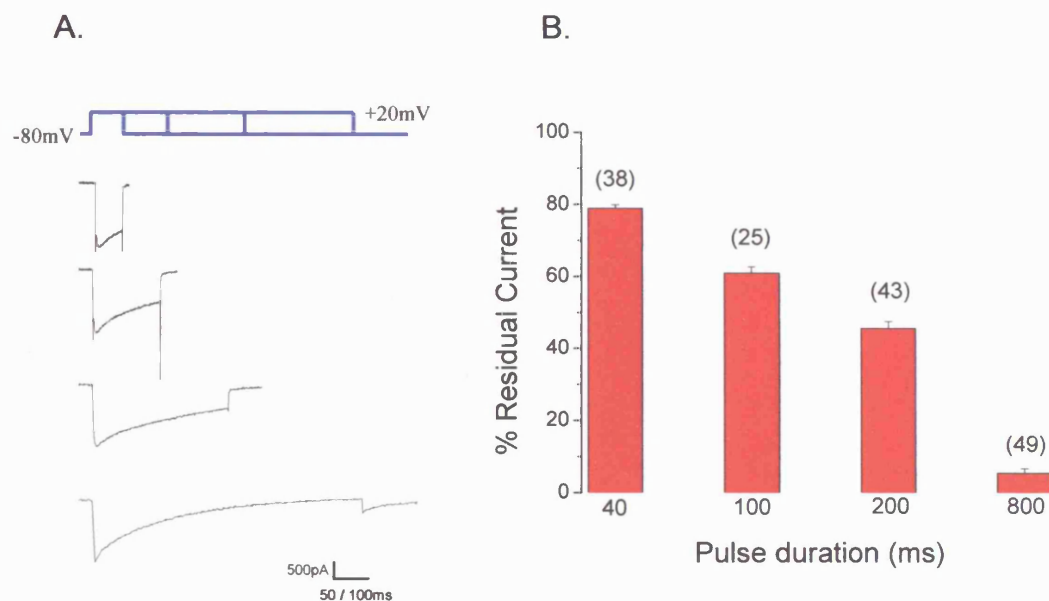
A. Sample current traces resulting from either, 40, 100, 200 or 800ms depolarisation from a holding potential of -80mV to a test potential of +20mV.
B. Bar chart displaying the mean ± s.e.m % residual current just prior to the end of the pulse normalized to the peak current (I_{END} was measured 1-2ms before the end of the pulse to avoid contamination from tail currents). Parenthesis above the columns displays the sample number analysed for each pulse duration. A 40ms depolarisation inactivates such that $78.9 \pm 1.0 \%$ n = 38 of the peak current remains just prior to termination of the pulse, with a 100ms depolarisation $60.9 \pm 1.8 \%$ n = 25 of the peak current remains. With a 200ms pulse $45.6 \pm 1.9 \%$ n = 43 remains, and $5.4 \pm 1.2 \%$ n = 49 of the peak current remains at the end of an 800ms pulse.
The mean result includes data from cells recorded in the presence and absence of 10mM TEA-Cl in the extracellular solution.

81

The rate of inactivation from an 800ms depolarisation could be described by a double exponential time course with mean time constants of τ_1 48 ± 9 and τ_2 257 ± 11 ms, n = 41 (figure 3.4.2). This could imply that there are either two populations of channels, which inactivate with different time courses, or that two independent processes underlie inactivation of a single channel.

3.4.2 Exponential fit of inactivation.
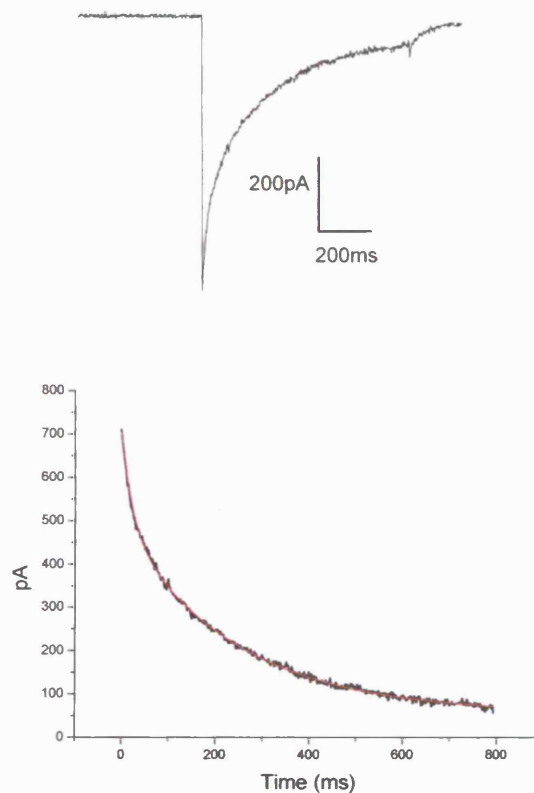
A. Representative current trace resulting from an 800ms depolarisation from a holding potential of -80mV to +20mV.
B. The current trace in A has been constrained within the standard temporal limits (3ms and 798ms, to avoid contamination of sodium and tail currents respectively), inverted and fitted with a double exponential curve $y = y_0 + A_1 e^{-x/t1} + A_2 e^{-x/t2}$ (red line). Mean time constants from fitting individual traces of τ_1 48 ± 9 and τ_2 257± 11 ms n = 41 were derived.
The mean result includes data from cells recorded in the presence and absence of 10mM TEA-Cl in the extracellular solution.

3.5 Rate of recovery from inactivation

Having determined that the total calcium current in bovine chromaffin cells almost completely inactivates over an 800ms depolarisation to +20mV (94.6 ± 1.2%, n = 49), the time taken for recovery from inactivation was assessed. To do this, an 800ms prepulse to +20mV was applied and then a brief (40ms) test pulse to +20mV applied 1, 3 or 10 seconds after the termination of the prepulse. The peak amplitude of the test pulse was then compared to the peak amplitude of the prepulse to assess the degree of recovery from inactivation.

3.5.1 Recovery from inactivation
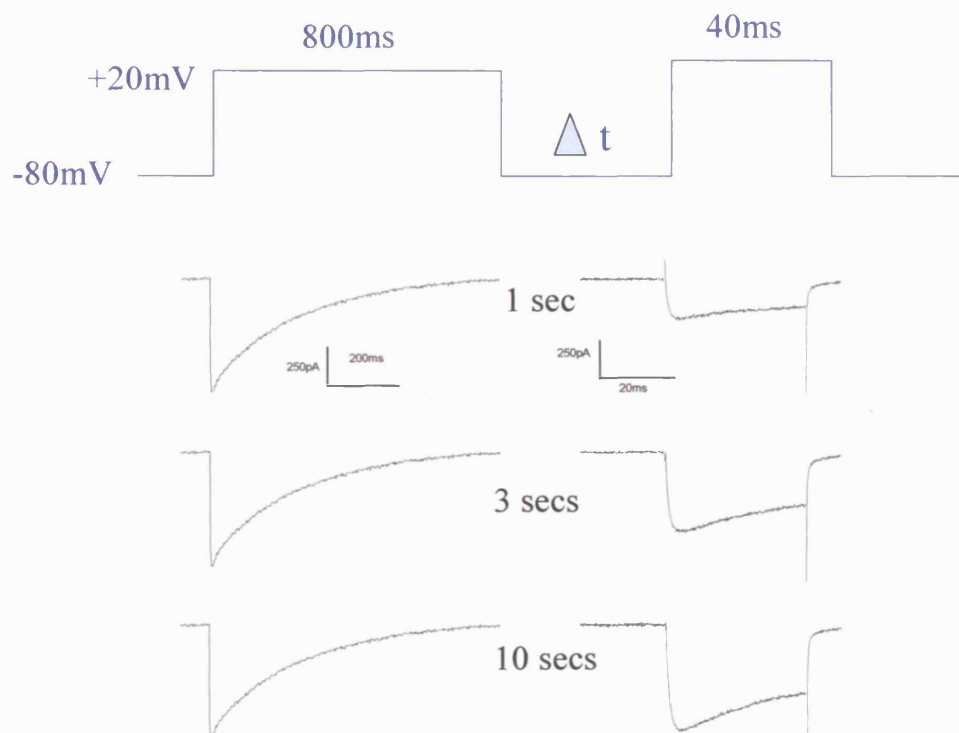
An 800ms prepulse to +20mV was applied and then a 40ms test delivered 1, 3 or 10 seconds after the termination of the prepulse. Sample current traces from each time interval are displayed.

As shown in figure 3.5.2, with an interpulse interval of 10 seconds the peak amplitude of the test pulse has recovered to 94.0 ± 2.9 %, n=7 of the peak amplitude

of the prepulse. The time course for recovery could be fit with a mono-exponential yielding a τ of 3.3 secs, n=7 and a semi-logarithmic (Log$_{10}$) plot of the same data could be fit with a straight line supporting a mono-exponential time course for recovery from inactivation (figure 3.5.2). However it is possible that a fast rate of recovery has been missed, as approximately a third of the channels have recovered by the first interpulse interval of 1 second.

3.5.2 Exponential fit of recovery from inactivation.
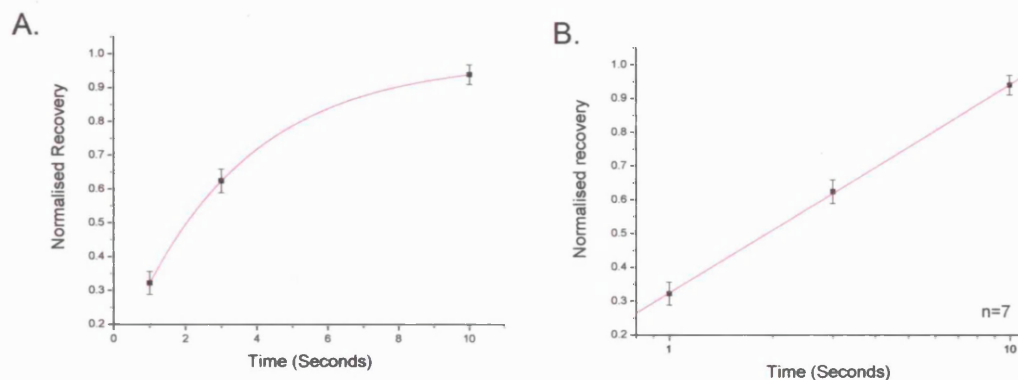
A. The mean data ± s.e.m, n = 7 of the normalized recovery from inactivation after an 800ms depolarisation at 3 time intervals, 1,3 and 10 seconds is displayed. The peak of the test pulse is expressed as a fraction of the peak of the prepulse. With an interpulse interval of 1 sec recovery is 0.32 ± 0.03; after 3 secs is 0.62 ± 0.04 and after 10 secs is 0.94 ± 0.03 %. Data is fit with a mono-exponential, $y = y_0 + Ae^{-x/t}$ (red line) yielding a τ of 3.3 ms.
B. When time is plotted on a semi-logarithmic axis, data points can be well fit with a straight line, $y = a + b^x$, supporting a mono-exponential rate of recovery.
The mean result includes data from cells recorded in the presence and absence of 10mM TEA-Cl in the extracellular solution.

In summary, bovine adrenal chromaffin cells contain a population of high voltage activated (HVA) calcium channels. They also contain sodium channels, which are activated by depolarisations that activate calcium channels but rapidly inactivate. Under standard recording conditions the degree of calcium channel inactivation is correlated to the length of the depolarising pulse, with channels almost completely inactivated after an 800ms depolarisation (96.4 ± 1.2 % n = 49). Channels recover from inactivation with a mono-exponential time course, τ_1 = 3.3 seconds.

Chapter 4: Characterisation of stimulus-secretion coupling in bovine adrenal chromaffin cells.

To investigate the basic secretory properties of the chromaffin cell, capacitance (C_m) measurements were used to monitor exocytosis and endocytosis. Unless stated otherwise the perforated patch configuration was used as exocytosis and endocytosis have been shown to run down in the whole cell configuration (Seward and Nowycky 1996; Smith and Neher 1997). The perforated configuration prevents rundown (Horn and Marty 1988), allowing reproducible responses for periods of several hours. Voltage steps were used to depolarise the cell and elicit exocytosis. Depolarisations of varying lengths were evoked with an interpulse interval of 3-4 minutes as this time period was discovered necessary to produce reproducible recordings of capacitance changes to the longest stimuli (800ms depolarisations).

4.1 Capacitance increases are triggered by calcium entry through voltage-gated calcium channels.

In the perforated patch recording configuration a 200ms pulse to +20mV evoked mean calcium entry of 233 ± 15 x 10^6 Ca^{2+} ions, with a corresponding ΔC_m of 170 ± 17 fF, n = 38. Exocytosis could be effectively inhibited by either blocking calcium channels with 100µM $CdCl_2{}^2$, or by using a high concentration (10mM) of the fast calcium chelator BAPTA in the intracellular solution. Application of 100µM $CdCl_2$ reduced calcium entry to 20 ± 7 x 10^6 Ca^{2+} ions and ΔC_m to 9 ± 5 fF n= 4 (p = 0.001). In whole cell configuration experiments changing intracellular BAPTA concentration from 0.3mM to 10mM increased calcium entry from 165 ± 14 n = 22, to 269 ± 34 x

---

2

Cadmium ions non-specifically block all types of high voltage activated calcium channels by physical occlusion of calcium permeation (Doering and Zamponi and references within). It appears that a ring of glutamic acid residues in the p-loop region is critical for pore block by cadmium (Cloues et al 2000).

10^6 Ca^{2+} ions n = 7 (p = 0.003), but ΔC_m was reduced from 145 ± 27 n = 22 to 7 ± 2 fF n = 7 (p = 0.001), (figure 4.1.1).

4.1.1 Exocytosis is dependent on calcium inflow through voltage-gated calcium channels.
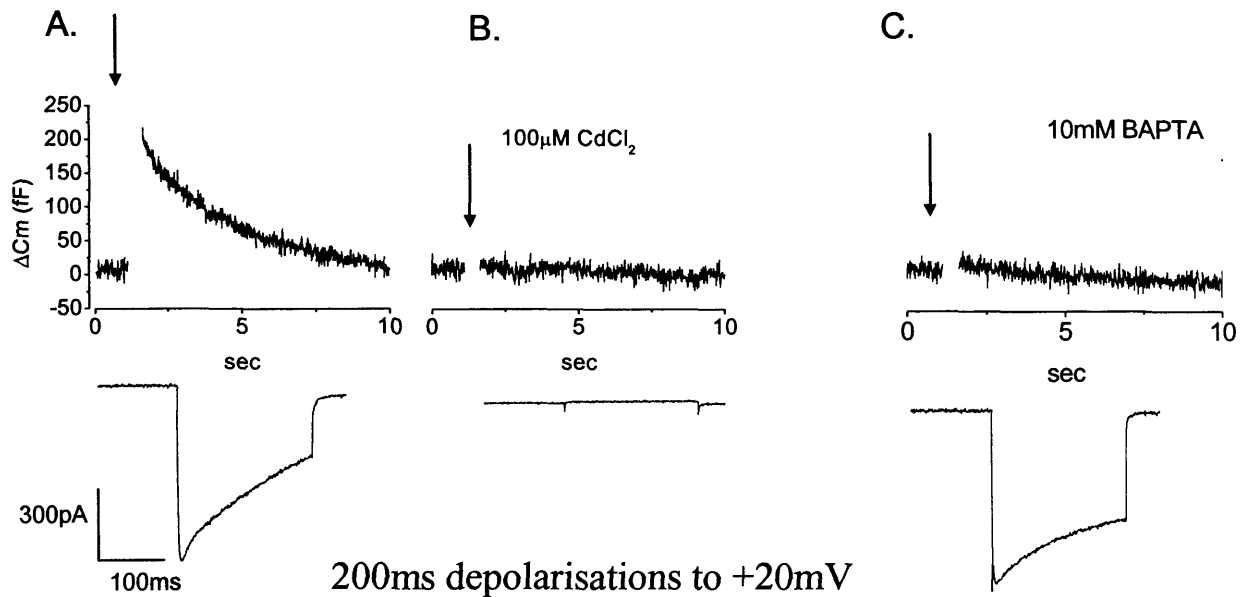
A. Sample capacitance (top) and current (bottom) traces resulting from a 200ms depolarisation. The mean calcium entry was 233 ± 15 x 10^6 Ca^{2+} ions, with a corresponding ΔC_m of 170 ± 17 fF, n = 38.

B. Application of 100µM $CdCl_2$ to the extracellular solution abolishes both ΔC_m and calcium entry in response to a 200ms depolarisation. Mean calcium entry was 20 ± 7 x 10^6 Ca^{2+} ions and ΔC_m 9.0 ± 4.5 fF n= 4.

C. In whole cell patch clamp experiments increasing intracellular [BAPTA] from 0.3mM to 10mM increases calcium entry from 165 ± 14 n = 22 to 270 ± 34 x 10^6 Ca^{2+} ions n = 7, but ΔC_m is reduced from 145 ± 27 fF, n = 22 to 7 ± 2 fF n = 7. The mean result includes data from cells recorded in the presence and absence of 10mM TEA-Cl in the extracellular solution.

4.1.2 Capacitances rise is dependent upon total calcium entry.

The calcium-dependency of exocytosis was further examined by changing the amount of calcium entering by evoking depolarisations of differing length. In response to 10ms pulses to +20mV the mean evoked calcium entry was 11 ± 1 x 10^6 Ca^{2+} ions, with a ΔC_m of 15 ± 3 fF, n = 29. Increasing the pulse duration to 40ms evoked mean calcium entry of 55 ± 4 x 10^6 Ca^{2+} ions, with a corresponding ΔC_m of 29 ± 4 fF, n =

36. Further pulse increases similarly increased calcium entry and ΔC_m. A 100ms pulse evoked mean calcium entry of $122 \pm 11 \times 10^6$ Ca^{2+} ions, with a ΔC_m of 84 ± 20 fF, n = 25, and an 800ms pulse elicited mean calcium entry of $489 \pm 38 \times 10^6$ Ca^{2+} ions, with a ΔC_m of 368 ± 23 fF, n = 51 (figure 4.1.3).

4.1.3 Increasing pulse duration increases calcium entry and ΔC_m.
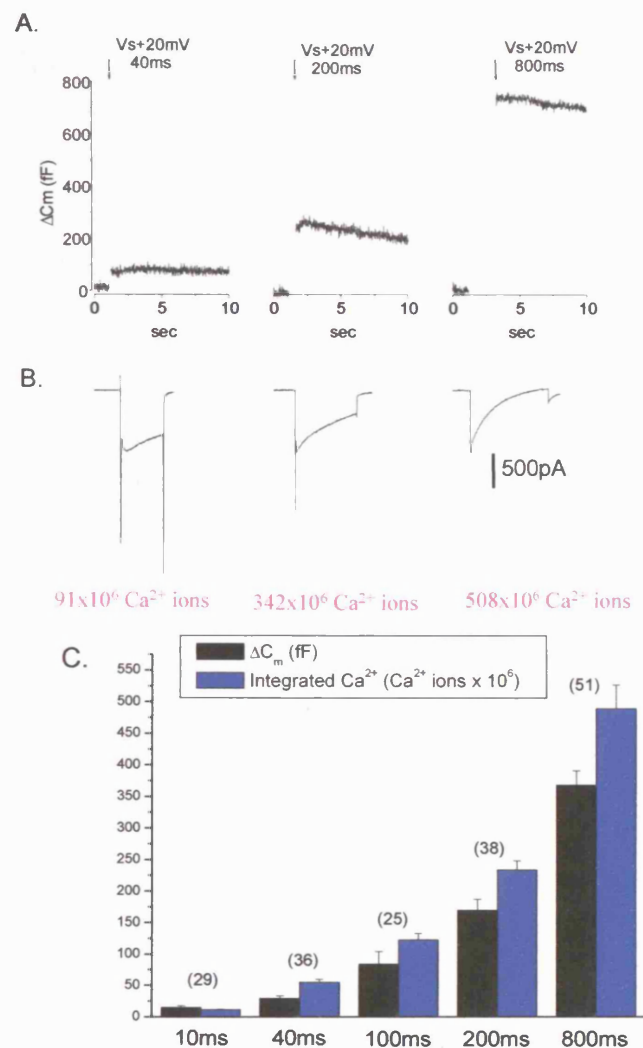
A. Characteristic capacitance traces evoked by 40, 200 or 800ms depolarisations to +20mV from a single cell.
B. Typical 40, 200 and 800ms current traces which correspond to the capacitance traces shown in A. The intergrated calcium values for these individual traces are shown below in magenta.
C. Bar chart displaying the mean ΔC_m and calcium entry resulting from a range of depolarisations. Sample numbers for each pulse duration are shown above in the paretheneses.
The mean result includes data from cells recorded in the presence and absence of 10mM TEA-Cl in the extracellular solution.

A previous report has described the calcium-dependence of large dense-core vesicle fusion in bovine chromaffin cells in response to single pulse step depolarisations as a simple transfer function of summed calcium entry (Engisch and Nowycky 1996). By maintaining pulse duration and varying extracellular calcium concentration they show that exocytosis is related to a second order function of the integrated calcium value. Plotting the ΔC_m of 40,100,200 and 800ms pulses from a single cell against calcium entry resulted in a curve that could be fitted by a Marquardt-Levenberg, nonlinear least-squares fitting algorithm (Origin software, Microcal, Northampton, MA) using the equation $\Delta C_m = g * (\Delta Ca^{2+})^x$. In the fitting routine, iterations were continued until a minimum, non-changing χ^2 value was achieved and data were constrained to pass through the origin (figure 4.1.4). Data from 14 cells was plotted and fit with the algorithm, the best fit was obtained with a proportionality constant $g = 0.05$ and power $x = 1.51$ (figure 4.1.4). The power value obtained by fitting data from individual cells with the allometric function ranged from $x = 0.87$ to 2.40, mean = 1.69 ± 0.13. Similar variability and values were reported by (Engisch and Nowycky 1996). The same data plotted on logarithmic coordinates could be well fit with a linear regression suggesting that regulated exocytosis is related to calcium entry with a power ≤ 2.

4.1.4 Stimulus-coupled exocytosis is a second order function of calcium entry.

A.

B.

C.

D.
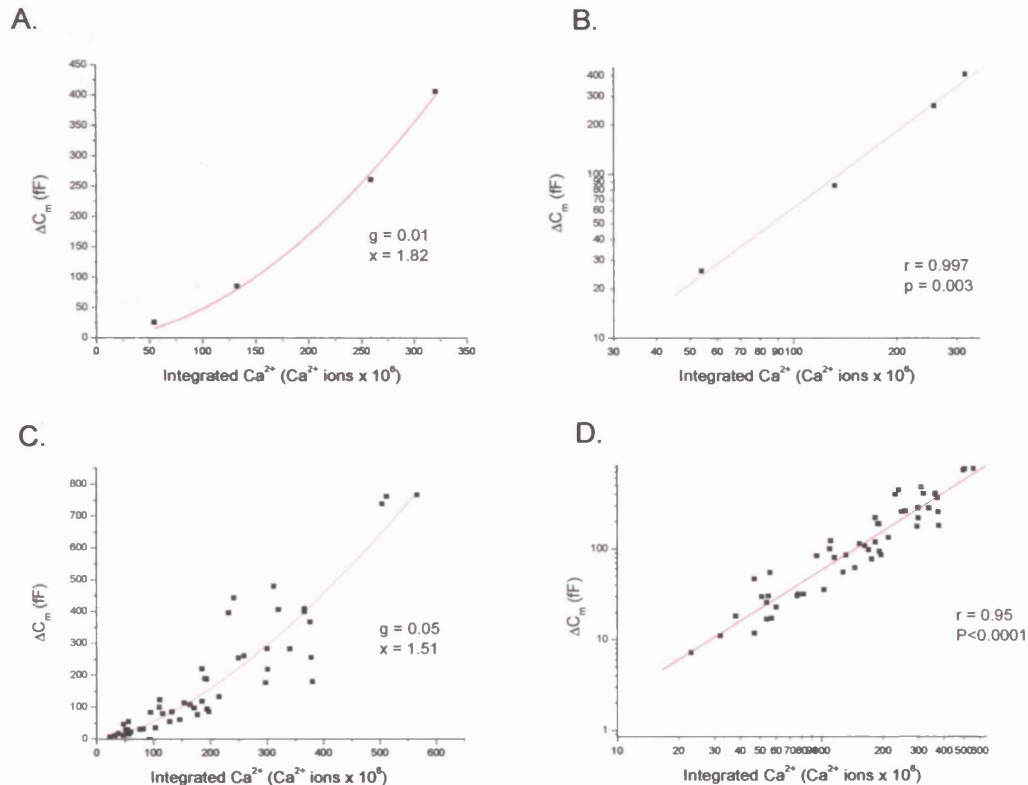
A. ΔC_m evoked by 40,100,200 & 800ms pulses from the same cell is plotted against calcium entry and fit using the equation $\Delta C_m = g * (\Delta Ca^{2+})^x$, $g = 0.01$ and $x = 1.82$. The curve was constrained to pass through $Y = 0$ at 0 calcium entry.

B. Plot of the same data in (A) on logarithmic coordinates. Date was fit with a linear regression, $Y = a + b^x$.

C. Data from 14 cells are plotted together and fit with the same algorithmic equation as in (A). The best fit was obtained with a proportionality constant $g = 0.05$ and power $x = 1.51$.

D. Logarithmic plot of the data from (C), fit with a linear regression.

The mean result includes data from cells recorded in the presence and absence of 10mM TEA-Cl in the extracellular solution.

With depolarisations up to 800ms I did not find evidence to suggest that stimulus-coupled secretion was limited, or available vesicles depleted. However by 800ms, inactivation of the calcium current was almost complete, preventing longer depolarisations from being tested. By normalizing the amount of exocytosis to the amount of calcium entering, the efficiency of calcium-secretion coupling can be assessed. Exocytotic efficiency is not significantly different for pulses ranging in length from 40 to 800ms in duration, 0.67 ± 0.14 n = 36, 0.62 ± 0.13 n = 25, $0.76 \pm$

0.08 n = 38, & 0.75 ± 0.11 n = 51 for 40,100,200 & 800ms pulses respectively (figure 4.1.5). Therefore with long depolarisations there is not a decrease in coupling efficacy that might reflect depletion or depression. However the exocytotic efficiency resulting from 10ms pulses is significantly higher, 1.45 ± 0.25, n = 29 (p ≤ 0.007 for all pulse lengths). This larger ratio of ΔC_m per calcium ion was also observed by (Engisch and Nowycky 1996) in response to 5ms depolarisations and was similarly variable in response, yielding large error bars. They suggest that it may reflect fusion of a larger population of small vesicles. An alternative hypothesis is that it may represent fusion from a small pool of vesicles with a very high release probability, or vesicles in very close proximity to the calcium channels. The large error bars in my data reflect cell to cell variability with a proportion of cells failing to respond (5 out of 29) and a subset of cells with a large ΔC_m yielding an exocytotic efficiency > 4 (4 out of 29). If these cells are excluded from analysis then the mean exocytotic efficiency in response to a 10ms depolarisation is still significantly enhanced relative to other pulse durations, 1.1 ± 0.16 n=20, (p < 0.05).

4.1.5 Exocytotic efficiency in response to differing pulse durations.
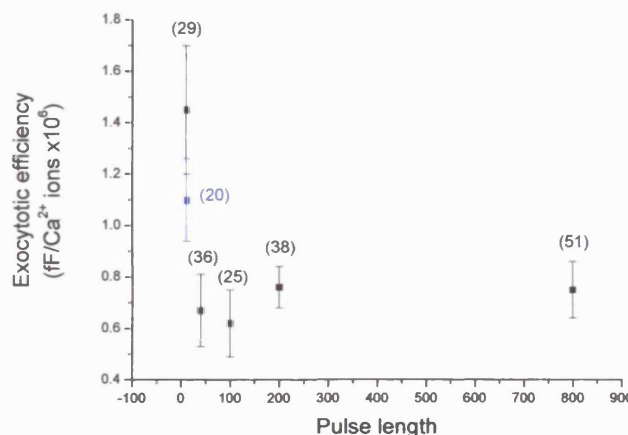
Calcium secretion coupling was similar for pulses ranging from 40 to 800ms in length, suggesting that available vesicles were not depleted as pulse duration increased. The large ratio for 10ms may represent fusion of a pool of small vesicles, a pool of vesicles with a higher release probability or contamination from a non-vesicular source of capacitance (Horrigan and Bookman 1994). Points represent the mean exocytotic efficiency ± s.e.m from 5 different pulse durations. Sample numbers for each pulse duration are shown in the parenthesis above data points. Data point shown in blue for 10 ms depolarisation is the mean exocytotic efficiency once cells which failed to respond, or gave an unusually large ΔC_m were excluded from analysis (see text for details). The mean result includes data from cells recorded in the presence and absence of 10mM TEA-Cl in the extracellular solution.

4.2 Trains of depolarising pulses trigger exocytosis.

In situ, splanchnic nerve stimulation causes release of acetylcholine onto nicotinic channels on adrenal chromaffin cells triggering bursts of action potentials resulting in activation of voltage-dependent channels and exocytosis (Douglas and Poisner 1967, Duan et al. 2003). Previous reports from neuroendocrine, endocrine or large nerve terminals suggest that when confronted by a train of depolarisations, individual C_m jumps initially increase and then decrease in amplitude during the train, (Horrigan and Bookman 1994; Seward et al. 1995; Seward and Nowycky 1996). The initial increase has been interpreted as calcium accumulation at the start of the train recruiting additional pools with different calcium sensitivity (Horrigan and Bookman 1994; Gillis et al. 1996) or generating the threshold requirement for calcium (Seward et al 1995; Seward & Nowycky 1996). The decline has been attributed to depletion of finite pools of readily releasable vesicles (Neher and Zucker 1993). As the secretory response to single (long) step depolarisations will exhibit composite release, I next examined whether trains of depolarisations would reveal multiple vesicle pools. In response to a train of 10, 100ms depolarisations at 2Hz, the mean cumulative calcium entry was $565 \pm 50 \times 10^6$ Ca^{2+} ions, with a cumulative ΔC_m of 358 ± 43 fF, n = 25. A plot of cumulative capacitance against calcium entry could be well fit with a mono-exponential decay (figure 4.2.1), suggesting that available vesicles are depleting, or that the calcium-dependency for secretion is depressed.

4.2.1 Cumulative ΔC_m in response to a train of 10, 100ms pulses at 2Hz.
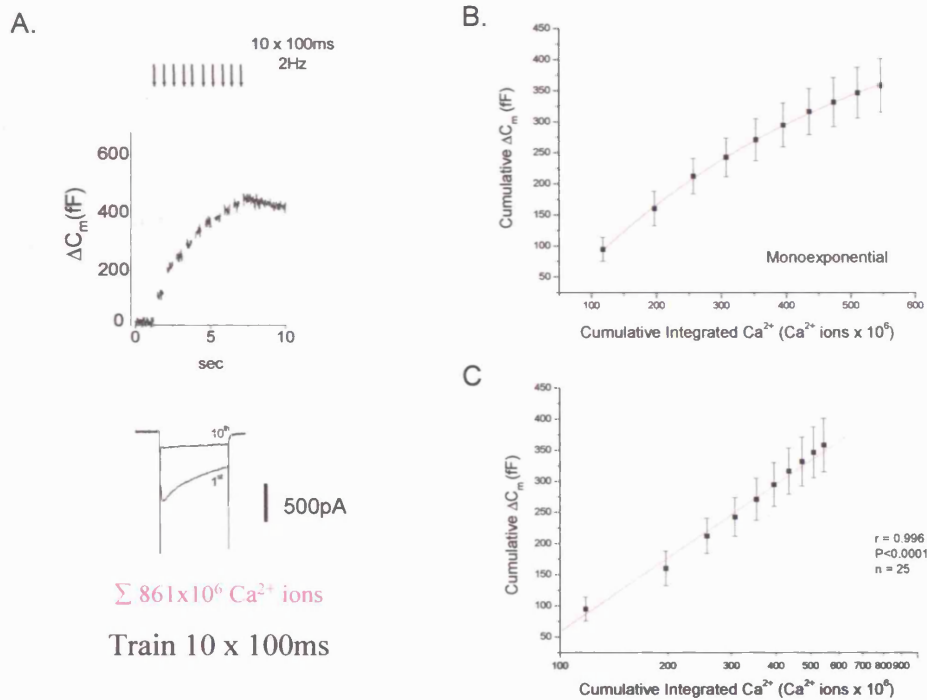
A. Representative capacitance trace in response to a train of 10, 100ms depolarisations to +20mV at 2Hz (top). Corresponding current traces of the 1st and 10th pulse in the train (bottom). The cumulative integrated calcium value for this example is shown underneath in magenta.

B. A plot of mean cumulative capacitance against mean cumulative calcium entry can be well fit with a mono-exponential decay, $y = y_0 + Ae^{-x/t}$. Data points are the mean ± s.e.m, n = 25.

C. A plot of mean cumulative capacitance against mean cumulative calcium on a semi-logarithmic scale. This can be well fit with a straight line, $y = a + b^x$, supporting a mono-exponential rate of decay. The mean result includes data from cells recorded in the presence and absence of 10mM TEA-Cl in the extracellular solution.

However this apparent decrease in calcium efficiency is unlikely to reflect depletion of releasable vesicles as a single long pulse (800ms) from the same cells evoked a larger ΔC_m, 426 ± 50 fF, despite experiencing less calcium entry, $319 \pm 29 \times 10^6$ Ca^{2+} ions, n = 25. In fact the reason that cumulative ΔC_m is getting smaller with each pulse, is because calcium entry is diminishing with each pulse due to channel inactivation (figure 4.2.2). The mean exocytotic efficiency per pulse was variable but not statistically different for any pulse number. When individual pulses in the train were analysed in the same manner as the single step depolarisations, it was apparent

that exocytosis evoked by this train of depolarisations followed a simple transfer function of summed calcium entry. Mean data for each pulse was plotted using the equation $\Delta C_m = g * (\Delta Ca^{2+})^x$. The best fit of the curve generated by this algorithm, yielded a proportionality constant $g = 0.05$ and power $x = 1.50$, which is almost identical to the values found by plotting the mean data from single pulses of varying length (figure 4.1.4).

4.2.2 Exocytosis is related to calcium entry in response to a train of 10, 100ms depolarisations at 2Hz.
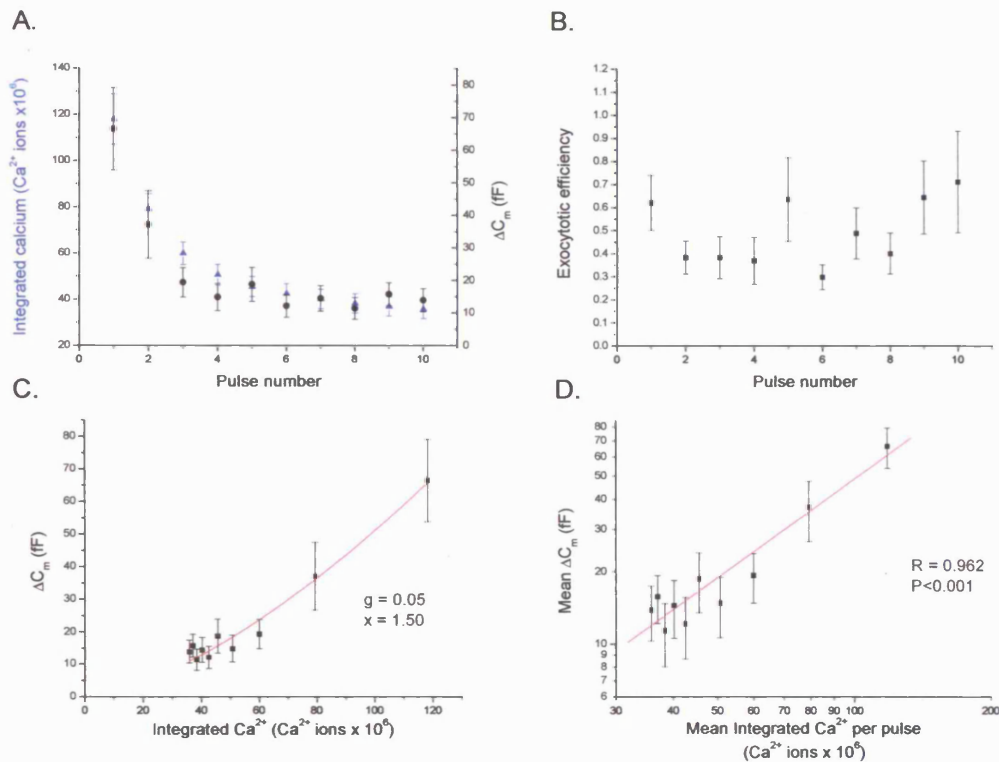
A. Plot of individual ΔC_m (black) and individual integrated calcium values (blue) per pulse. As the train develops less calcium enters and ΔC_m get smaller. Data points correspond to the mean values ± s.e.m, n = 25.
B. Plot of exocytotic efficiency per pulse. Although there is large variability, there is no significant difference in the efficiency ratio between pulses. Data is the mean ± s.e.m of 25 cells.
C. Plot of individual ΔC_m against integrated calcium entry. Data points correspond to the mean values ± s.e.m, n = 25. Data points can be fit with an algorithmic equation using the equation $\Delta C_m = g *$ $(\Delta Ca^{2+})^x$, with a proportionality constant $g = 0.05$ and power $x = 1.50$. The curve was constrained to pass through $Y = 0$ at 0 calcium entry.
D. Logarithmic plot of the data from (C) is well fit with a straight line, $y = a + b^x$, $r = 0.96$.
The mean result includes data from cells recorded in the presence and absence of 10mM TEA-Cl in the extracellular solution.

A train of 100ms depolarisations is a very un-physiological stimulus. As these cell *in situ* respond to bursts of action potentials, a train of brief (10ms) depolarisations was applied to assess exocytosis in response to a stimulation that was closer to the physiological stimulus. A train of 50, 10ms pulses at 20Hz results in a calcium-exocytosis relationship that could be fit using the same algorithm used earlier for single step pulses or a train of long (100ms) depolarisations. Mean data of cumulative capacitance against cumulative integrated calcium from 10 cells was plotted and fit using the equation $\Delta C_m = g * (\Delta Ca^{2+})^x$. The best fit of the curve generated by this algorithm, yielded a proportionality constant $g = 0.05$ and power $x = 1.60$, which again is very similar to the values found by plotting the mean data from single pulses of varying length, or from individual pulses from a train of long (100ms) depolarisations (figure 4.1.4 & 4.2.2). The power value obtained by fitting data from individual cells with the algorithm ranged from $x = 0.6$ to 2.96, mean $n = 1.68 \pm 0.18$. However, as figure 4.2.3 shows, the first few pulses in the train resulted in a capacitance 'hump' that was not well fit by the curve generated for the whole train. This hump was visible in 8 out of the 10 cells analysed and the duration of the hump varied from 5 to 14 pulses in these cells. When the mean data for the first 11 pulses is plotted alone it is better fit with a mono-exponential than the usual algorithm (which yields a proportionality constant $g = 1.2$ and power $x = 0.86$). The remaining pulses (11 to 50) however are well fit by the algorithm yielding a proportionality constant $g = 0.03$ and power $x = 1.66$ (figure 4.2.4).

4.2.3 Calcium-exocytosis relationship in response to a train of brief (10ms) depolarisations.
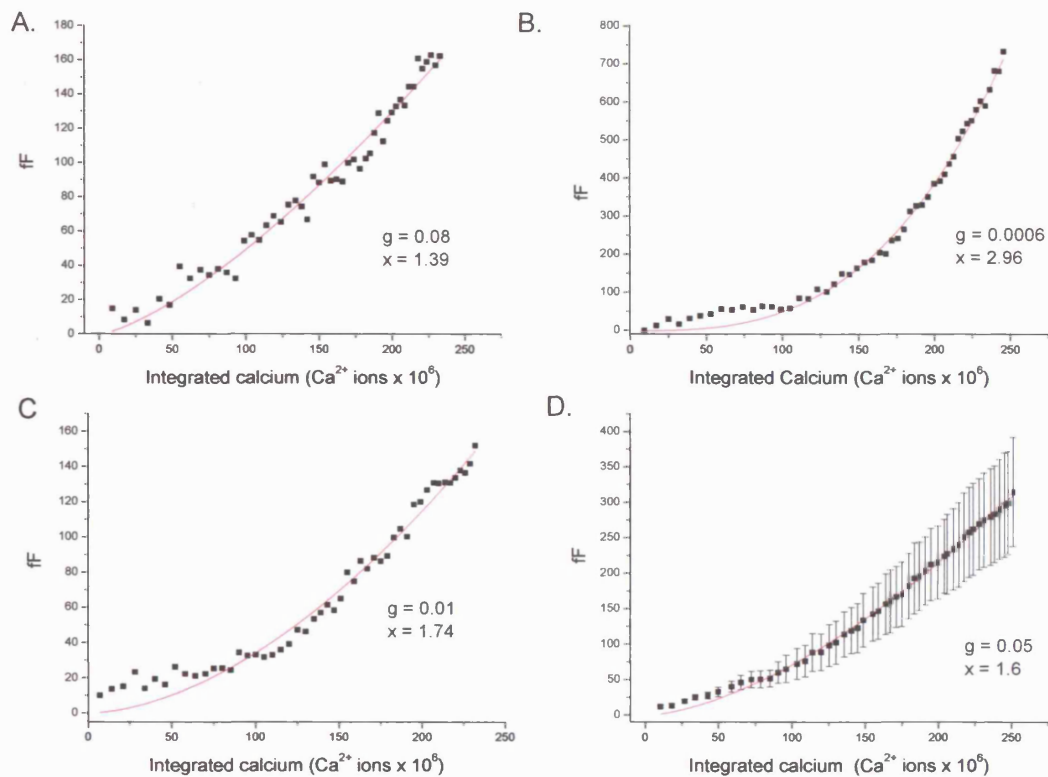
Cumulative capacitance is plotted against cumulative integrated calcium and fit with the equation ΔC_m = $\mathbf{g} * (\Delta Ca^{2+})^x$. The proportionality constant g and power, x for each figure is shown.

A. Sample plot from a cell in which no 'hump' that deviates from the best fit curve (red line) within the first few pulses is observed.

B. Sample plot of cumulative capacitance against cumulative integrated calcium from a cell in which a very obvious 'hump' deviates from the best fit curve (red line) during the first 14 pulses of the train.

C. A typical response, in which a small 'hump' deviates from the best fit curve (red line) at the start of the train.

D. Mean cumulative $\Delta C_m \pm$ s.e.m is plotted against mean cumulative calcium n = 10. The best fit curve is represented by the red line, again the first few pulses in the train deviate slightly from this line.

4.2.4 The first part of the train can be fit with a mono-exponential curve.
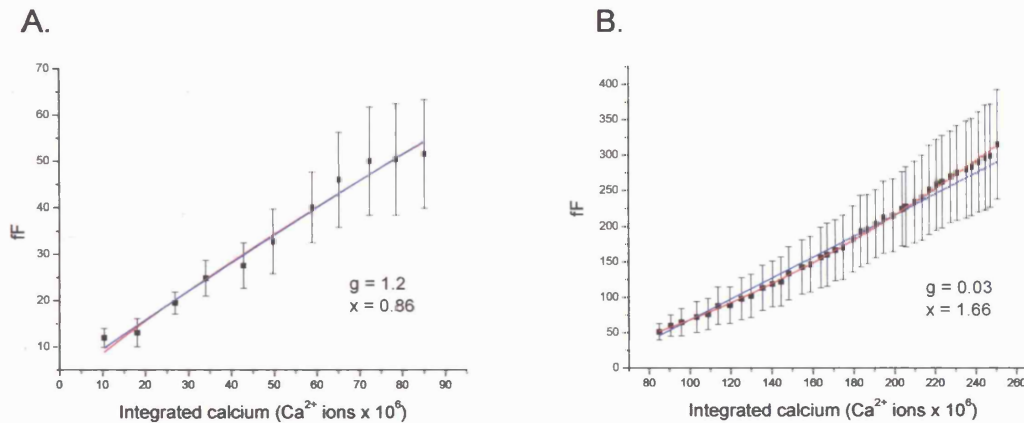
A. The first 11 pulses are plotted and fit using the equation $\Delta C_m = g * (\Delta Ca^{2+})^x$ which gives a proportionality constant, $g = 1.2$ and a power, $x = 0.86$ (red line). Although this is a good fit, the g and x values are very different from the values previously obtained and the data is equally well fit by a mono-exponential, $y = y_0 + Ae^{-x/t}$ (blue line).

B. The second part of the train (pulses 11-50) can be fit with the equation $\Delta C_m = g * (\Delta Ca^{2+})^x$ to give a proportionality constant, $g = 0.03$ and a power, $x = 1.66$ (red line) which are similar values for g and x previously reported in this thesis. This data is better fit with the algometric function than a mono-exponential (blue line).

Previous groups have reported that in chromaffin cells across species, capacitance jumps evoked in response to a train of brief (10-25ms) depolarisations is biphasic, with the rate of exocytosis declining during the first few pulses, and then increasing again (Horrigan and Bookman 1994; Voets et al. 1999). Vesicles in the IRP are able to fuse in response to very brief depolarisations in which the required elevation of intracellular calcium for exocytosis is restricted to the immediate proximity of the calcium channels (Neher 1998). A 10 ms depolarisation has been suggested in adult bovine chromaffin cells to lead to a calcium gradient restricted to a region less than 1μm from the cell membrane (Marengo and Monck 2000). Vesicles in the SRP do not fuse in response to single depolarisations up to 100ms duration (Voets et al. 1999; Voets 2000), but do fuse during trains of brief depolarisations (Voets et al. 2001). It is likely that in response to a train of 50, 10ms pulses, the first few pulses represent fusion of the IRP, the 'hump' at the start of the capacitance trace, subsequent pulses represent fusion from the remainder of the RRP, and fusion from later pulses in the

later pulses in the train represents release from the SRP and possibly from re-filling of the RRP. It is possible to quantitate the size of the IRP and RRP using a dual-pulse protocol (Gillis et al. 1996; Voets et al. 1999), using the following equation:

$$B_{max} = S / (1-R^2)$$

Where S represents the capacitance sum of the first (ΔC_{m1}) and second (ΔC_{m2}), and R is the ratio $\Delta C_{m2}/\Delta C_{m1}$. The upper limit of the pool size is assumed to be the value derived for B_{max} and a lower pool size estimate is given by S. This determination of pool size is reliant on two factors. Firstly, refilling of the pool does not occur between pulses (RRP recovery in chromaffin cells occurs with a time constant of ~10 seconds, (Moser and Neher 1997; Smith et al.1999). Secondly, the amount of calcium entering must be equivalent for both pulses. If both criteria are met, then an R value of < 1, will represent secretory depression, presumably due to partial pool depletion. Substantial pool depletion is a prerequisite for accurate pool determination, therefore previous studies have only analysed cells with an R value < 0.7 in this manner (Gillis et al. 1996). A previous study has used this protocol to define the size of the IRP from mouse chromaffin cells using a double pulse of 10ms depolarisations, and determined its size to be ~ 45fF (Voets et al. 1999). Using this protocol, I analysed my data to obtain a size for the IRP of 40 ± 10 fF n = 18. Out of 29 cells, 18 had an R value < 0.7 and were used for determination of pool size (of the remaining 11 cells, 5 displayed no change in capacitance in response to the first pulse and the other 6 had an R value > 0.7). To determine the size of the RRP a pair of 100ms depolarisations has been used (Gillis et al. 1996). With 100ms pulses appreciable calcium current inactivation occurs, which reduces the amount of calcium entering during the second pulse, therefore invalidating the use of this protocol (a reduction from 118 ± 11 to 79 ± 7 x 10^6 Ca^{2+} ions, n = 25 when pulses are 400ms apart). A way to avoid this problem is to adjust the test potential for the two pulses to ensure that equivalent calcium influx is delivered in response to both pulses. I found cell to cell variability in the test potentials required to match calcium entry, but by keeping the second pulse amplitude fixed at +14 mV and changing the first pulse amplitude between +20 and +28mV a pair of currents with equivalent calcium entry could be obtained. Using this protocol, a pool size for the RRP was estimated at 194

± 27 fF, n=9 (figure 4.2.5). This value again is close to the size of the RRP reported for mouse chromaffin cells using this protocol (Voets et al. 1999), but larger than the RRP size (~100fF) previously reported for bovine adrenal chromaffin cells (Gillis et al. 1996).

4.2.5 Determination of the IRP and RRP size.

A.

C.

B.
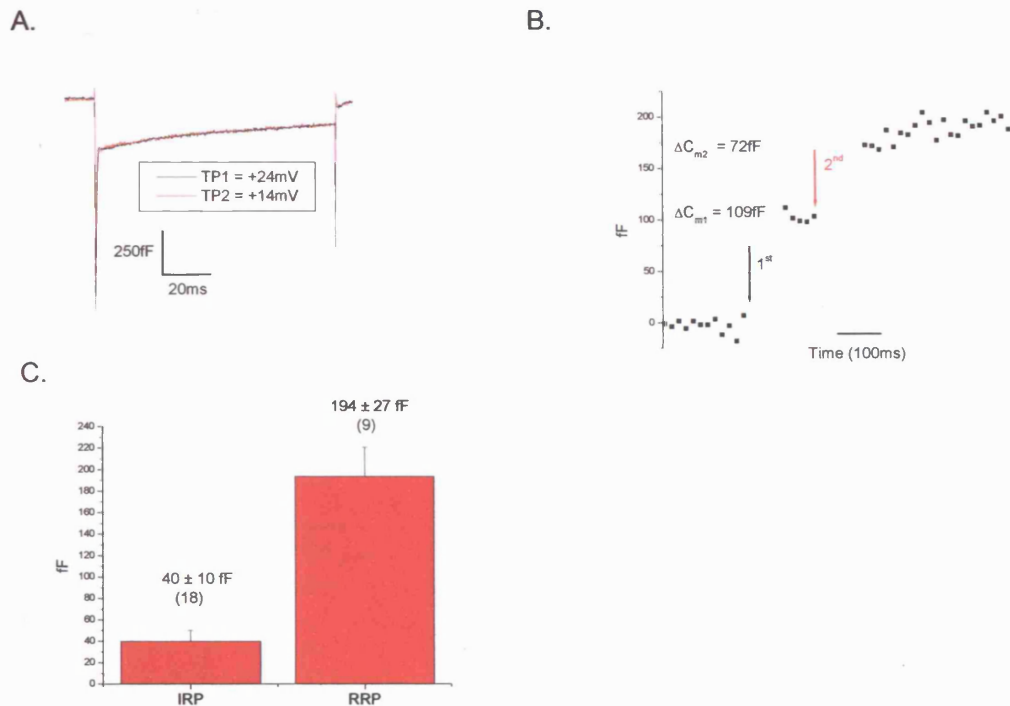
A. Sample current traces from a pair of 100ms depolarisations given 100ms apart to different membrane potentials to ensure identical calcium entry during the depolarisation.
B. Sample capacitance points, displaying the ΔC_m in response to each depolarisation.
C. Bar chart of mean pool size ± s.e.m for the IRP (double 10ms pulse) and the RRP (double 100ms pulse). Sample size for each condition is shown above the bar chart in the parenthesis.

Another protocol was utilized to look at different pools, this is referred here and later in this thesis as 'the pool protocol'. This consisted of a train of 6, 10ms pulses, followed by 4, 100ms pulses. With this protocol the 10ms stimuli will result in a ΔC_m that reflects fusion of the IRP, the further 4 longer pulses result in a second bout of secretion which reflects fusion of the remainder of the RRP and a fraction of the SRP (Voets et al 2001). The size of the IRP can be determined from this protocol,

98

unfortunately it can not be used to accurately determine the size of the RRP as significant calcium channel inactivation occurs during the last 4, 100ms pulses. However this protocol does allow the ΔC_m against calcium entry to be fit by the equation $\Delta C_m = g * (\Delta Ca^{2+})^x$ to assess whether the calcium-dependency of secretion is altered, and the exocytotic efficiency of each pulse can be calculated (figure 4.2.6). Initially it was hoped to have the interpulse duration equivalent for both the short and long pulses. However this was not possible due to software limitations. By setting an interpulse duration of 400ms, the actual interpulse interval for the train of 100ms was 300ms (400 – 100), likewise the interpulse duration for the train of 10ms depolarisations was 390ms (400 – 10).

4.2.6 Pool protocol.

A.

6 X 10ms   4 X 100ms

+20 mV

-80mV

I = 390ms   I = 300ms

B.   500pA   C.

1st 6 pulses   5ms

ΔC_m (fF)

Final 4 pulses

500pA

50ms   Time ms
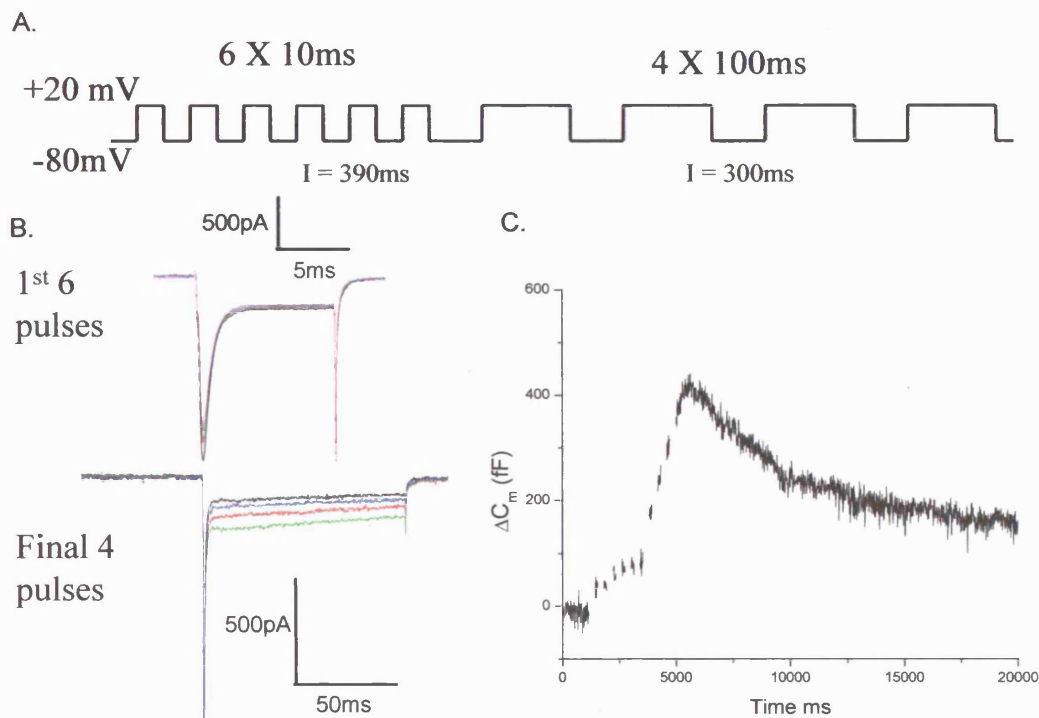
A. The protocol is shown schematically, 6, 10ms depolarisations with an interpulse interval of 390ms were delivered immediately followed by 4, 100ms depolarisations with an interpulse interval of 300ms.
B. Representative calcium currents in response to this protocol, top (6 x 10ms), bottom (4 x 100ms)
C. Corresponding capacitance trace to the calcium currents shown in B. The trace is bipasic, with release in response to the first 6 short pulses becoming depressed, and then increasing again in response to the last 4 longer pulses.
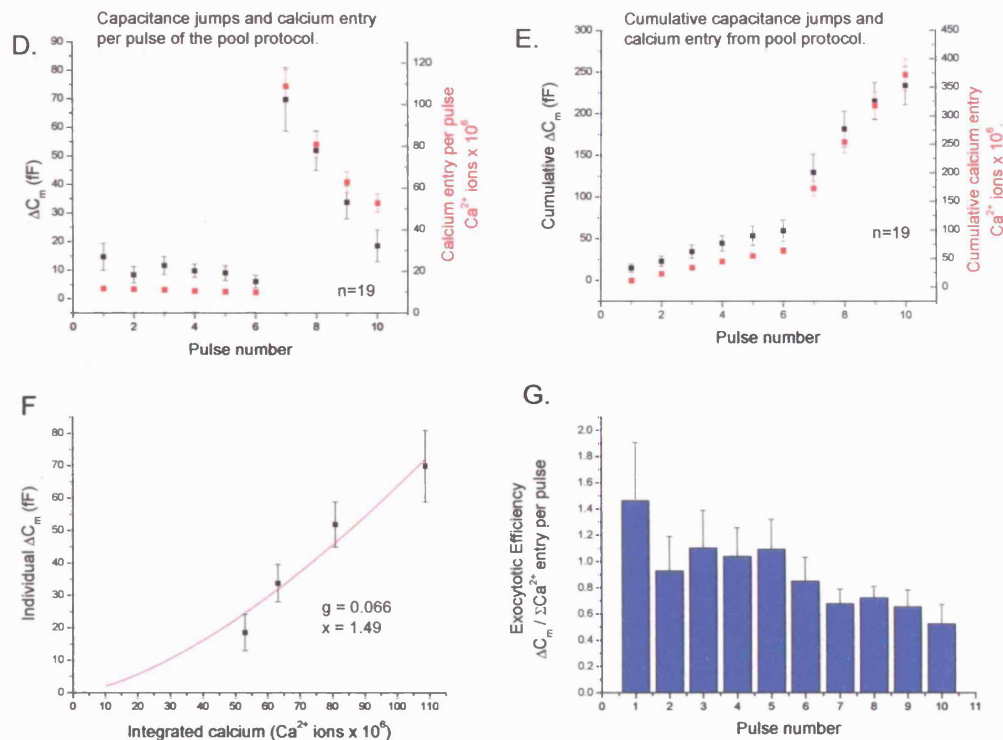
D. Mean data ± s.e.m for individual capacitance and integrated calcium values, n=19.
E. Mean data ± s.e.m for cumulative capacitance and integrated calcium values, n=19.
F. The mean ΔC_m ± s.e.m for the last 4 pulses is plotted against mean calcium entry and fit by the allometric equation $\Delta C_m = g * (\Delta Ca^{2+})^x$. g = 0.07, x = 1.49, n = 19.
G. Mean ± s.e.m exocytotic efficiency of individual pulses in the protocol. The first 10ms pulse has the highest exocytotic efficiency. The remaining 5, 10ms pulses have a reduced by steady state value. As already shown, the exocytotic efficiency to a train of 100ms pulses does not significantly differ with pulse number, but has a lower efficiency than 10ms pulses.

4.2.7 Discussion of stimulus-coupled exocytosis.

I have characterised stimulus-coupled exocytosis from bovine adrenal chromaffin cells and employed stimulation paradigms to investigate the calcium-dependency of exocytosis and the exocytotic efficiency of release in response to differing lengths of single step or trains of depolarisations. My findings correspond well to previous published observations (Engisch and Nowycky 1996; Powell 2000).

A defining feature of calcium-triggered neurotransmitter release is the cooperative relationship between calcium and the amount of neurotransmitter release. This was

100

first described at the frog neuromuscular junction (Dodge and Rahamimoff 1967), who reported that the amplitude of excitatory postsynaptic currents (EPSC's) were related to the forth power of extracellular calcium. This observation has been described from numerous preparations and synapses with the majority displaying a co-efficient, x of 3~4. The power value reported here is lower ($x = 1.51$, figure 4.1.4), this implies that the calcium cooperativity of exocytosis in chromaffin cells is lower than in neurones. However it is possible that the calcium-dependency of exocytosis is altered between the RRP and the SRP. Using the method described here (section 4.1.3) both pools are assessed together with exocytosis from long pulses ($\geq$200ms) being dominated by fusion from the SRP. The calcium cooperativity of exocytosis from the RRP could be higher, with a power function approaching values reported in neurones, but was found to be lower here as this method includes release from SRP which could have a lower calcium cooperativity of release. Other studies performed in bovine adrenal chromaffin cells have investigated the calcium cooperativity of exocytosis using flash photolysis of caged calcium (Sorensen et al. 2002). With this type of experiment the rate constant for release at different calcium concentrations can be plotted against calcium concentration to derive a calcium relationship. These experiments deduced a calcium cooperativity of neurotransmitter release from the RRP in chromaffin cells of $x = 2.5$~3.0, suggesting that release from the RRP retains a similar calcium-dependency of exocytosis to that observed in neurones, and that release from the SRP most likely has a lower power value. Therefore by using the method of (Engisch and Nowycky 1996), fitting the ΔC_m against calcium entry with an allometric function the calcium-dependence of exocytosis derived is a mixture from both releasable pools. This type of analysis will allow me in future experiments to determine whether the calcium cooperativity of exocytosis from both releasable pools is altered for treated groups compared to control, but I will not be able to determine pool specific differences. To investigate release from different pools of vesicles I can apply the pool protocol, and to quantify release from the IRP and the RRP I can employ the double pulse protocol.

4.3 Asynchronous secretion

Exocytosis evoked in response to long ($\geq$100ms) depolarisations often consists of two kinetically distinct components (figure 4.3.1). This corresponds to a fast stimulus-coupled burst of exocytosis, which occurs during the stimulus, and a slow phase of secretion which persists after termination of the stimulus. This slow asynchronous post-stimulus secretion has been described in chromaffin cells, (Horrigan and Bookman 1994; Powell et al. 2000; Thiagarajan et al. 2004) when stimulations evoke large calcium influxes. Asynchronous secretion has also been reported in a variety of neurones as diverse as retinal bipolar neurones (Neves and Lagnado 1999), and hippocampal neurones (Goda and Stevens 1994), suggesting that the mechanism underlying the phenomena is well conserved and not an artifact of the chromaffin cell model. The amount of asynchronous release has been shown to be correlated to calcium entry, increasing with raised extracelluar calcium and decreasing with lowered extracellular calcium (Horrigan and Bookman 1994), leading to the suggestion that residual high levels of cytoplasmic calcium post-stimulus cause fusion from the SRP. I found in response to a 200ms depolarisation that 22 out of 41 cells displayed an increase in capacitance post-stimulus. Visual inspection of capacitance traces indicated that in the majority of cells displaying asynchronous secretion, the peak increase in capacitance occurred 0.5 to 1.5 seconds post-stimulus, before membrane retrieval predominated, and capacitance decreased through endocytotic mechanisms. Therefore I arbitrarily measured capacitance 1 second post-stimulus and related this value to the size of the measured stimulus-coupled exocytotic burst. As this value could be positive (for cells displaying asynchronous release), or negative (for cells in which endocytosis predominated immediately followed the exocytotic burst), the ΔC_m measured 1 second after stimulation was termed post-stimulus drift (PSD).

4.3.1 Asynchronous release after a 200ms depolarisation.
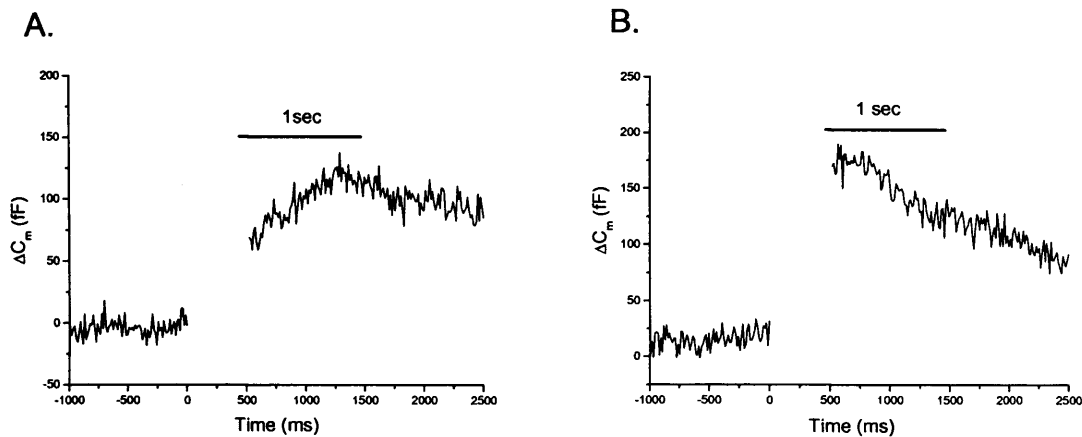
A. In response to a 200ms depolarisation, there is a slow increase in capacitance after the stimulus. This occurred in 22 out of 41 cells with a mean increase measured 1 second post-stimulus of 38 ± 10 fF.

B. In the other 19 cells asynchronous secretion was not detected and the measured PSD 1 second post-stimulus was -93 ± 33 fF, or -62 ± 11 fF if you exclude one cell which displayed an extremely large amount of endocytosis within 1 sec post-stimulation.

I found that the amount and direction of the PSD was not correlated to the size of the exocytotic burst, or degree of channel inactivation during the pulse (figure 4.3.2A & B). In contrast to the results of (Horrigan and Bookman 1994), I did detect a significant trend that suggests increasing calcium entry actually decreased the amount of asynchronous release. Cells displaying a positive PSD had a mean calcium entry of 190 ± 16 x 10^6 Ca^{2+} ions, n = 22, whereas cells displaying a negative PSD had mean calcium entry of 262 ± 23 x 10^6 Ca^{2+} ions, n = 19. This effect was significant, p = 0.01 (figure 4.3.2D). As there is a clear correlation between peak amplitude and calcium entry (figure 4.3.2.E), it was not surprising to detect a significant effect when the direction of the PSD was correlated to the peak amplitude of the current. Cells displaying a positive PSD had a mean peak current of 497 ± 48 pA n = 22, whereas cells displaying a negative PSD had a mean peak current amplitude of 652 ± 54 pA n = 19, (p = 0.04).

4.3.2 Asynchronous secretion is not correlated to immediate ΔC_m, or channel inactivation, but is related to peak current and calcium entry.

A.

B.

C.

D.

E.
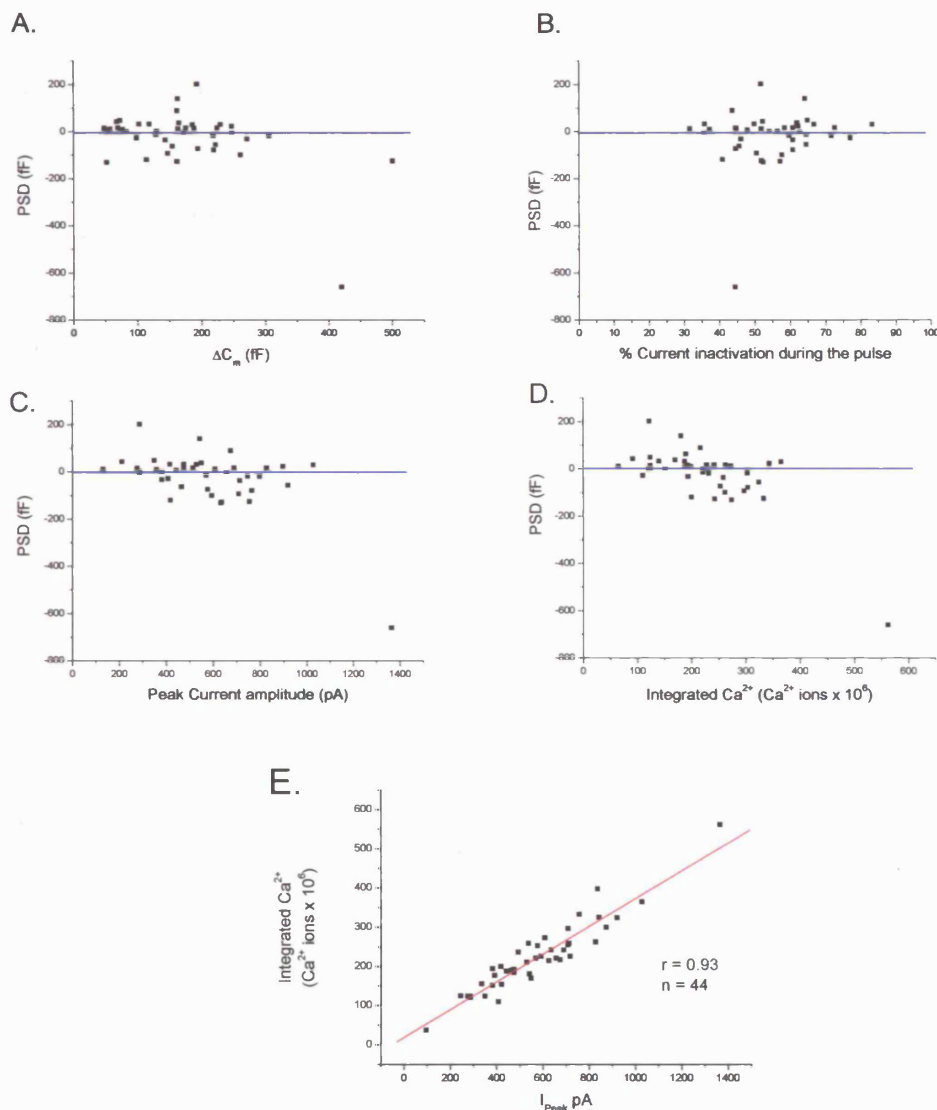
The magnitude and direction of the PSD after a 200ms depolarisation is displayed as a scatter plot against the exocytotic burst (A), the % calcium current inactivation (B), the amplitude of the peak calcium current (C) and the integrated calcium entry during the pulse (D). There is no correlation between the size and direction of the PSD in the first two conditions (A,B) but there is a significant difference between peak current amplitude and calcium entry. Cells displaying asynchronous release had smaller currents and calcium influx during the 200ms depolarisation (C &D). There is a clear correlation between peak current and calcium entry. Figure E shows a scatter plot of I_{Peak} (pA) verses intergrated calcium (Ca^{2+} x 10^6 ions). A linear regression (red line) was applied producing an r value of 0.93. This was considered highly significant p>0.0001, n=41.

104

I next examined asynchronous release in response to repetitive stimulation. After stimulation by a train of 50, 10ms depolarisations at 20 Hz, post-stimulus increases in capacitance were detected in 17 out of 20 cells (figure 4.3.3). The mean positive PSD was +28 ± 6 fF, n = 17 and the mean negative PSD was -11 ± 4 fF, n =3.

4.3.3 Asynchronous release after a train of depolarisations.
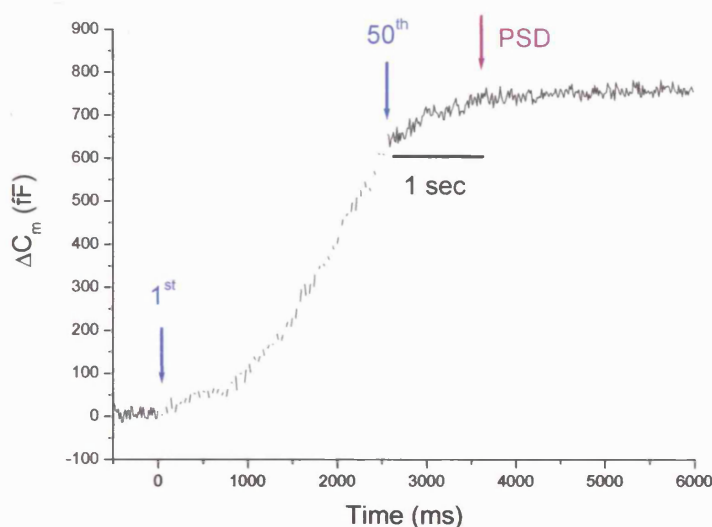
After stimulus-coupled secretion evoked by a train of 50, 10ms depolarisations at 20Hz, asynchronous release was detected in 17 out of 20 cells with a mean increase in capacitance 1 second after stimulation of 28 ± 6 Ff. A typical capacitance trace is shown above.

4.3.4 Discussion of Asynchronous secretion.

In a previous study (Horrigan and Bookman 1994), they found that raising extracellular calcium increased asynchronous release after a 100ms depolarisation. I have evoked secretion from 200ms depolarisations and found that raising extracellular calcium decreased asynchronous release. Cells with larger calcium currents may raise intracellular calcium to a threshold needed to recruit a faster endocytotic pathway (discussed in section 4.4), which may not be reached during 100ms depolarisations even with the raised (10mM) extracellular calcium used in the aforementioned study. Therefore an explanation for the discrepancy in findings could

105

be resolved if increasing calcium entry results in more asynchronous release until a threshold is reached upon which a faster, more dominant membrane retrieval pathway is switched on. An alternative explanation could be species specific differences. Asynchronous release is more apparent in recordings from rat or mouse chromaffin cells (Horrigan and Bookman 1994; Kim et al. 1995; Aldea et al. 2002). Additionally my studies were recorded in the perforated patch configuration whereas those of Horrigan and Bookman 1994, were recorded in the whole cell configuration, which may lead to a rundown of cytoplasmic factors needed for either the regulation of asynchronous secretion or more likely endocytosis. As the kinetics of asynchronous release are slower than release from the RRP, it has been speculated that asynchronous release represents fusion from the SRP in response to elevated prolonged intracellular calcium. Synaptotagmin I is likely to be the calcium sensor for fast release (Fernandez-Chacon et al. 2001), however it is unlikely to mediate asynchronous, slow release (Seward et al. 1996; Voets et al. 2001). Although intrinsically slower than the fast component, asynchronous release is probably induced by lower calcium concentrations (Sudhof 2004). Other synaptotagmin isoforms 3, 6 & 7, exhibit higher calcium affinities (Sugita et al. 2001; Sugita et al. 2002). Consistent with a role for these isoforms in mediating asynchronous release comes from experiments in which over-expression of the C_2 domains of the high affinity synaptotagmins 3 and 7 potently inhibit slow release from permeabilsed neuroendocrine cells, whereas the C_2 domains of synaptotagmin 1 and 2 are inactive (Sugita et al. 2001; Sugita et al. 2002). Recently the role of Rab3A in regulating asynchronous release has also been investigated. Over-expression of Rab3A or a hydrolysis deficient mutant of Rab3A causes significant inhibition of exocytosis, especially during repetitive stimulation. The authors suggest that Rab3A inhibits recruitment of vesicles from a slowly releasable pool (Thiagarajan et al. 2004). Therefore Rab3A may play an important inhibitory role in limiting depletion of the SRP in response to repetitive stimulation, and preventing asynchronous release post-stimulus to ensure phase-locked kinetics of fast neurotransmitter release, a pre-requisite for faithful neuronal transmission.

4.4 Endocytosis

Insertion of vesicle membrane into the plasma membrane during exocytosis is coupled to the process of subsequent membrane retrieval, endocytosis. Endocytosis is a highly regulated process with different rates and molecular mechanisms described (Cousin 2000). I will now describe the types of endocytosis chromaffin cells display to a variety of stimuli.

4.4.1 Monitoring endocytosis in chromaffin cells using the capacitance technique.

The literature regarding stimulus-coupled endocytosis from adrenal chromaffin cells is at present contradictory. This in part probably reflects experimental differences such as, recording solutions (internal and external), age of animals, recording configurations, terminology used and most importantly stimulation paradigms, which dictate the magnitude and temporal properties of raised intracellular calcium. The amount of calcium influx seems to be pivotal. It was shown back in the early 1980's that elevated calcium increases the rate of rapid endocytosis (Neher and Marty 1982). More recently high calcium levels have been reported to shift exocytosis from from full fusion to a kiss and run mode (Ales et al 1999). The last decade has seen an explosion in the number of techniques, biochemical, biophysical and probably most favoured, optical, to study endocytosis. In order to relate my observations on endocytosis to previous published studies an understanding of the language commonly used is required. There is no consistent terminology used to classify the different endocytotic profiles experimentally described from capacitance studies on bovine adrenal chromaffin cells. Endocytosis is usually split up into different modes, some groups use the term rapid endocytosis (RE) to describe quick endocytosis which exceeds pre-stimulus levels (Artalejo et al. 1996; Nucifora and Fox 1998), other groups call this 'excess retrieval' (Engisch and Nowycky 1998), and all the groups have slightly different criteria to define this phase. Other phases include 'compensatory retrieval' which represents endocytosis back to baseline levels after an

exocytotic jump (Engisch and Nowycky 1998). Basal endocytosis rates are normally associated with endocytosis in response to brief action potential trains, ~0.5Hz, intermediate rates are, ~6 Hz, whereas stress-activated rates correspond to endocytosis evoked by trains of action potentials delivered at ~15Hz (Chan and Smith 2001; Chan and Smith 2003).

A 200ms depolarisation resulted in an exocytotic capacitance jump that was then followed by one of four different endocytotic responses. In this study I have measured the amount of endocytosis that occurs 22 seconds post-stimulus. Endocytosis that occurred post-stimulus and resulted in a change of capacitance back towards pre-stimulus levels is termed compensatory endocytosis. This form of endocytosis can be fit with a mono-exponential decay and the amount of membrane retrieval does not exceed pre-stimulus levels 22 seconds post-stimulus. The next type of response I have termed excess retrieval, results in excess membrane retrieval within 22 seconds post-stimulus, this type of response can also be fit by a mono-exponential decay. A third type of response is termed rapid exocytosis, in this case excess retrieval is observed within a few seconds post-stimulus and can be fit by a double-exponential decay. The forth type of response observed is no reduction in capacitance following an exocytotic jump, this group is termed, no endocytosis (figure 4.4.2).

4.4.2 Different endocytotic responses following exocytosis evoked by a 200ms depolarisation.
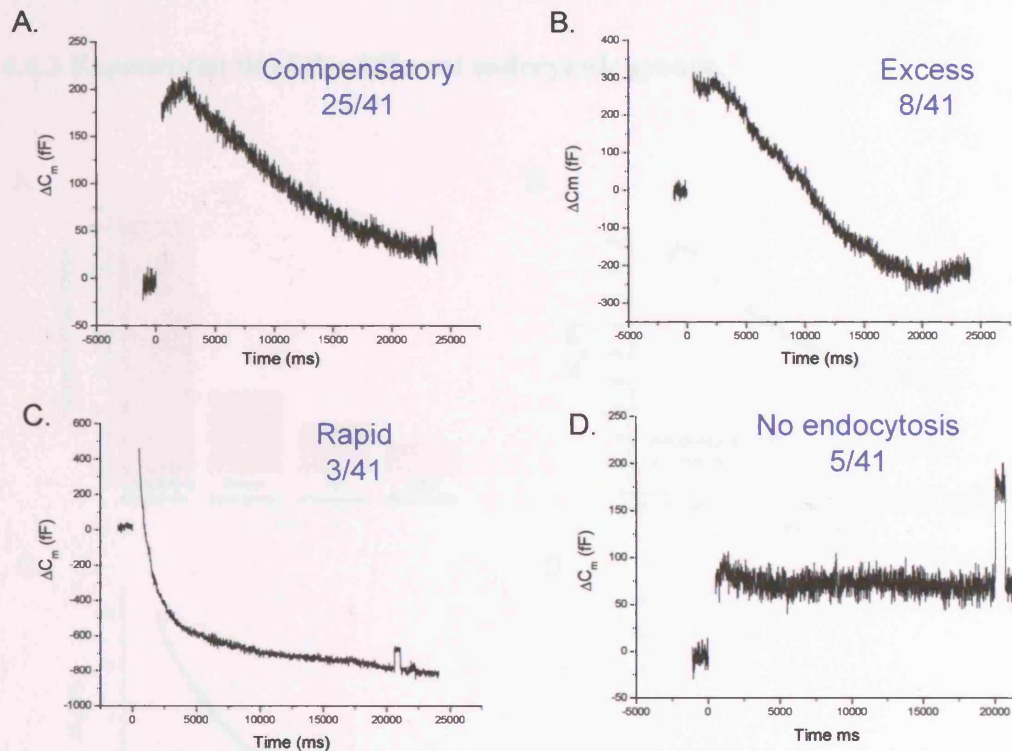
4 different endocytotic responses termed compensatory endocytosis, excess endocytosis, rapid endocytosis and no endocytosis, see text for details. The square upward deflection seen towards the end of some traces represents a 100fF calibration step and are excluded from measurements of endocytosis.

A. A typical capacitance trace from a cell undergoing compensatory endocytosis following exocytosis evoked from a 200ms depolarisation.

B. A typical capacitance trace from a cell undergoing excess retrieval following exocytosis evoked from a 200ms depolarisation.

C. A typical capacitance trace from a cell undergoing rapid exocytosis following exocytosis evoked from a 200ms depolarisation.

D. A typical capacitance trace from a cell in which no endocytosis followed exocytosis evoked from a 200ms depolarisation.

Out of 41 cells, 25 met my criteria for compensatory endocytosis, the average decay in capacitance for this group could be fit by a mono-exponential curve with a average time constant of ~ 6.0 seconds. 8 out of 41 cells met my criteria for excess retrieval, the mean capacitance decay trace for this group could be fit by a mono-exponential curve with a average time constant of ~ 5.2 seconds. 3 out of 41 met my criteria for

rapid endocytosis and the average capacitance trace could be fit by a double exponential, $\tau_1 \sim 0.7$ seconds and $\tau_2 \sim 5.3$ seconds. 5 out of 41 cells exhibited no endocytosis 22 seconds post-stimulation (figure 4.4.3).

4.4.3 Exponential fit of the different endocytotic groups.
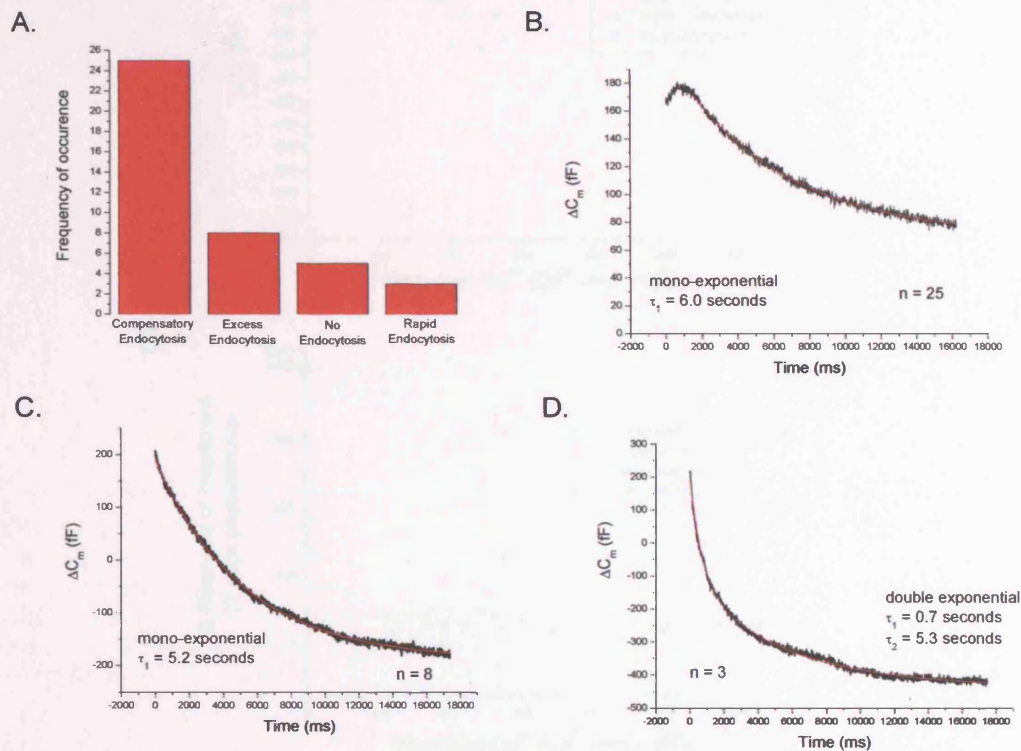
A. Individual endocytosis capacitance traces from 41 cells were examined and binned into 1 of 4 groups, criteria for entry into these groups is defined in the main text. Individual capacitance traces for each group were averaged together and the mean trace fit.
B. The average capacitance trace for cells in the compensatory endocytosis group could be fit with a mono-exponential curve, $\tau_1 \sim 6.0$ seconds, n=25.
C. The average capacitance trace for cells in the excess retrieval group could be fit with a mono-exponential curve, τ_1 5.2 seconds ms, n=8
D. The average capacitance trace for cells in the rapid endocytosis group could be fit with a double exponential curve, $\tau_1 \sim 0.7$ seconds, $\tau_2 \sim 5.3$ seconds n=3.

The relationship between calcium influx and endocytosis was examined by plotting integrated calcium entry versus post-stimulus C_m decrease (figure 4.4.4). This scatter plot shows a trend towards more endocytosis with larger calcium entry. When I examined the frequency of responses observed for each group, it became clear that reduced calcium entry was correlated to an absence of endocytosis (figure 4.4.5).

110

4.4.4 Calcium-dependency of endocytosis.
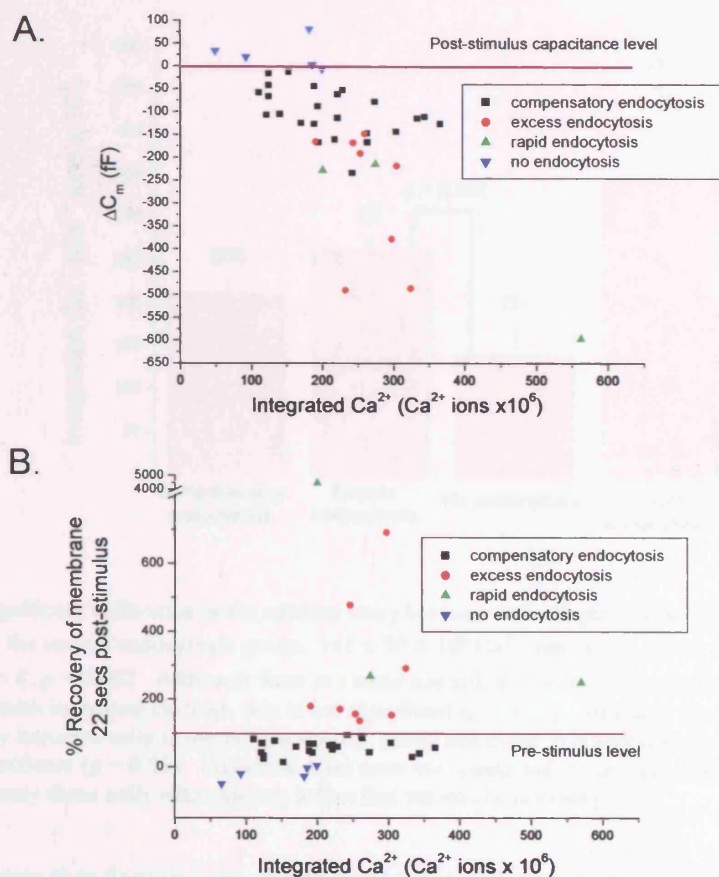
A. The amount of endocytosis (measured as a change in capacitance fF), that occurs 22 seconds post-stimulus was calculated. The magnitude of the exocytotic jump immediately following stimulation has been set at 0fF (purple line) and endocytosis is therefore measured as a decrease in capacitance. This measurement of endocytosis is plotted against calcium influx during the stimulus depolarisation. The amount of endocytosis (fF) is correlated to the amount of calcium entry (Ca^{2+} x 10^6 ions). Individual data points have been colour coded to show which endocytotic profile they belong to.
B. The % recovery from exocytosis, back to pre-stimulus levels is plotted against calcium entry. Individual points have been colour coded to show which endocytotic profile they belong to.

111

4.4.5 Increasing calcium influx during the stimulatory depolarisation increases the chance of a cell displaying excess endocytosis.
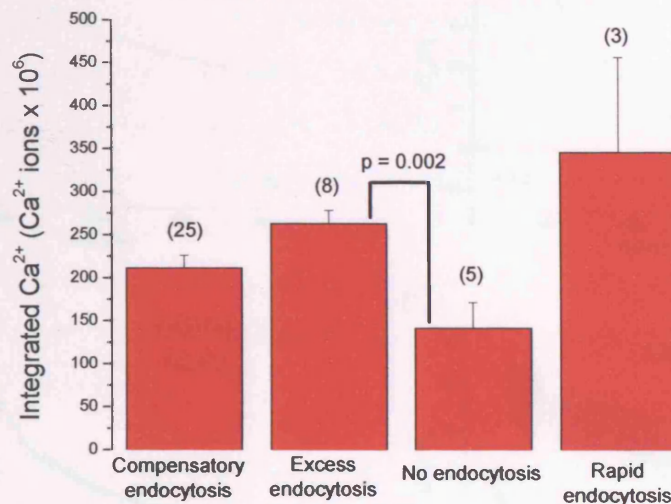
There is a significant difference in the calcium entry between cells displaying no endocytosis and those belonging to the excess endocytosis group. $141 \pm 30 \times 10^6$ Ca^{2+} ions, n = 5 verses $263 \pm 15 \times 10^6$ Ca^{2+} ions, n= 8, p = 0.002. Although there is a trend towards excess endocytosis from compensatory endocytosis with increased calcium, this is not significant (p = 0.07). Similarly the difference in calcium entry between cells in the no endocytosis group and those in compensatory endocytosis was not quite significant (p = 0.06). Statistical tests were not conducted for the rapid endocytosis group, as it contained only three cells with calcium influx that varied considerably.

To investigate this further I measured endocytosis in response to longer (800ms) and shorter (40ms) depolarisations, which will increase and decrease calcium entry respectively. As expected endocytosis was evident in all cells tested in response to an 800ms depolarisation (n = 45), but was also apparent from cells in response to a 40ms depolarisation (n = 24), (figure 4.4.6). This suggests that exocytosis occurs following a brief stimulation, is inhibited with stimulations of increasing length and returns again with long stimulations. This observation has been reported when endocytosis was evoked following action potential-like waveforms (APs), (Chan and Smith 2001). In this study they found that single APs or trains at 0.5 Hz lead to rapid endocytosis, trains delivered at 1.9 to 6 Hz cause a marked reduction in the rate of endocytosis, and trains at 10 – 16 Hz lead to a return to rapid endocytosis.

112

4.4.6 Endocytosis evoked after a long (800ms) or short (40ms) stimulus.
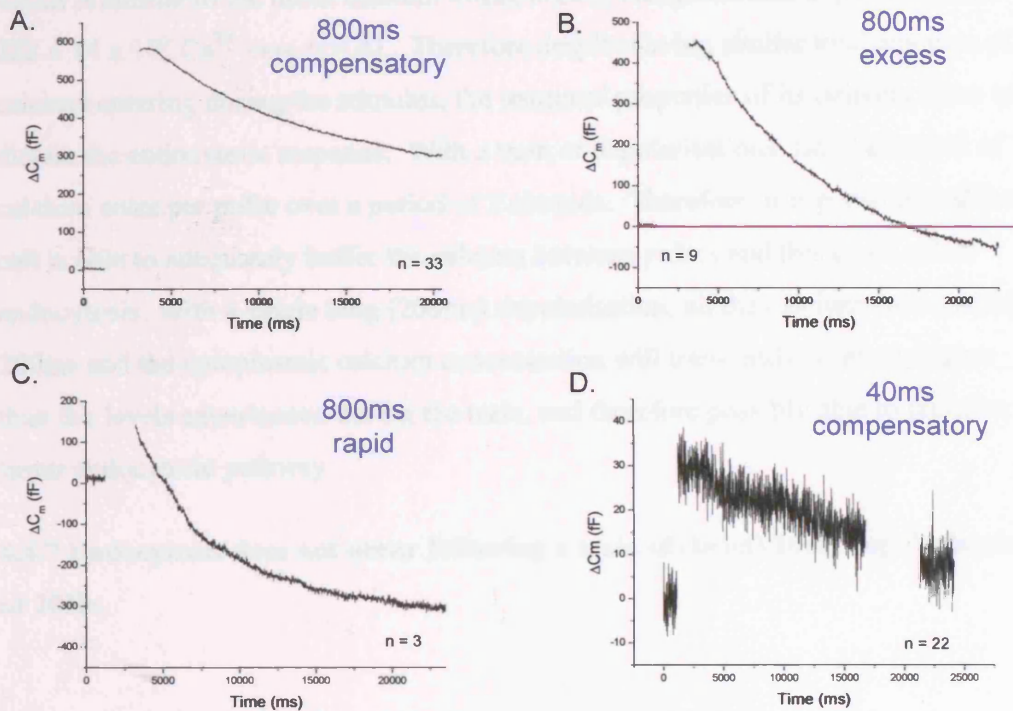
A. After exocytosis evoked from an 800ms depolarisation, membrane retrieval in 33 out of 45 cells fit the criteria for compensatory endocytosis. Shown is the average capacitance trace for cells in this group.

B. 9 out of 45 cells recovered membrane to post-stimulus levels and met the criteria to be classed in the excess retrieval group. Shown is the average capacitance trace for cells in this group.

C. 3 out of 45 cells quickly endocytosed excess membrane and met the criteria for rapid endocytosis. Shown is the average capacitance trace for cells in this group.

D. Cells were able to retrieve membrane after exocytosis evoked from short (40ms) depolarisations. Shown is the average capacitance trace for 24 cells. The gap towards the end represents where a 100fF calibration step was introduced, unfortunately this was not at a standard time for all traces (ranging from 15-22 secs post-stimulus), and therefore this period of time when looking at the average data is messy and has been deleted for clarity and accuracy. Calibration steps were introduced during the capacitance traces evoked from an 800ms depolarisation, however these were introduced after 22 seconds post-stimulus and have been clipped for the figures.

Endocytosis following a train of 10ms depolarisations at 20Hz was next examined. 22 seconds post-stimulus the mean amount of membrane retrieval was only 9 ± 12 fF n =20, despite a mean total exocytotic jump of 259 ± 41 fF. The lack of endocytosis was not related to a large component of asynchronous release as this had a mean value of 28 ± 6 fF n=20 (figure 4.3.3). This corresponds to ~ 3% of the stimulus-

113

evoked membrane insertion being retrieved 22 seconds post-stimulus (figure 4.4.7). The mean total calcium influx during the train was $226 \pm 22 \times 10^6$ Ca^{2+} ions, n = 20, which is similar to the mean calcium influx during a single 200ms depolarisation of $222 \pm 14 \times 10^6$ Ca^{2+} ions, n = 41. Therefore despite having similar total amounts of calcium entering during the stimulus, the temporal properties of its delivery seem to dictate the endocytotic response. With a train of depolarisations, small amounts of calcium enter per pulse over a period of 3 seconds. Therefore, it is possible that the cell is able to adequately buffer the calcium between pulses and this could affect endocytosis. With a single long (200ms) depolarisation, all the calcium enters within 200ms and the cytoplasmic calcium concentration will transiently be much higher than the levels experienced during the train, and therefore possibly able to recruit a faster endocytotic pathway.

4.4.7 Endocytosis does not occur following a train of (brief) 10ms depolarisations at 20Hz.
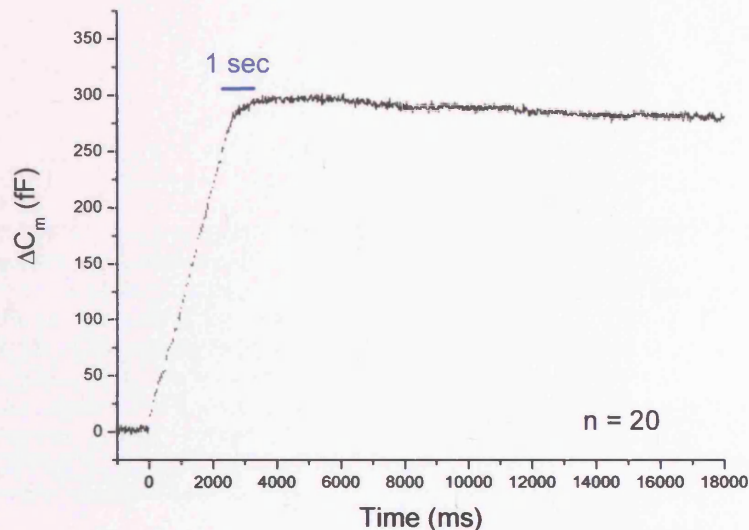
20 individual capacitance traces from separate cells evoked from a train of 50, 10ms depolarisations delivered at 20Hz have been averaged together and the mean trace displayed above. The mean amount of endocytosis that occurs 22 seconds post-stimulus is 9.2 ± 11.9 fF, n =20.

To further examine the calcium-dependency of endocytosis following a train of depolarisations, a train of 10, 100ms depolarisations at 2Hz was applied. This

114

stimulus will increase calcium entry (cumulative calcium entry of 553 ± 50 x 10^6 Ca^{2+} ions, n = 24 verses 226 ± 22 x 10^6 Ca^{2+} ions, n = 20, for the 10ms train). In response to a train of 10, 100ms depolarisations at 2Hz, endocytosis could be classified into 1 of 3 groups. No endocytosis, in which post-stimulus changes in capacitance were no greater that 25fF 22 seconds post-stimulus. Partial endocytosis, where more than 25fF was recovered post-stimulus but less than 50% of the stimulus-evoked membrane insertion was retrieved 22 seconds post-stimulus. Or compensatory exocytosis, with greater than 50 % of the stimulus-evoked membrane insertion retrieved 22 seconds post-stimulus (figure 4.4.8). As shown earlier for single 200ms depolarisations, cells with smaller calcium entry were correlated with an absence of endocytosis (figure 4.4.8).

4.4.8 Endocytosis following exocytosis evoked by a train of 100ms depolarisations at 2Hz.
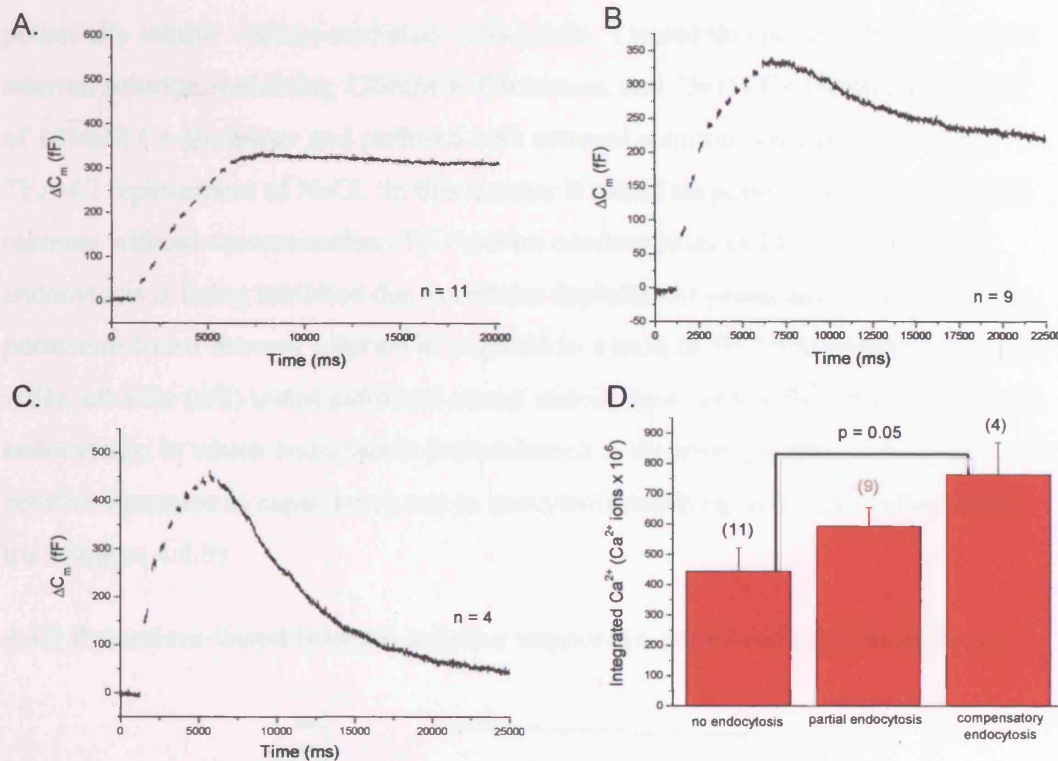
A. In 11 out of 24 cells, no appreciable endocytosis was observed 22 seconds post-stimulus. Shown is the average capacitance trace from cells which were categorised into this group.

B. 9 cells out of 24, displayed a limited amount of endocytosis post-stimulus. Shown is the average capacitance trace for cells within this group.

C. 4 cells out of 24 exhibited compensatory endocytosis, in which membrane capacitance levels fell close to pre-stimulus levels. Shown is the average capacitance trace for cells within this group.

D. There was no significant difference between calcium entry and cells from the partial endocytosis group when compared to either no endocytosis or compensatory endocytosis groups. There was however a significant difference in calcium entry between cells in the no endocytosis group and those in the compensatory endocytosis groups ($p = 0.05$).

Therefore increasing calcium inflow during a train of depolarisations can evoke faster endocytosis, but higher total levels are needed compared to single step depolarisations to induce membrane retrieval, presumably due to effective calcium buffering or extrusion in between pulses.

116

I discovered whilst writing this thesis that clathrin-mediated endocytosis, the pathway believed responsible for retrieval following robust trains of depolarisations (Chan and Smith 2003), has been shown to be dependent on physiological concentrations of intracellular potassium ions (Larkin et al. 1983). I use cesium-based internal solution which would be expected to lead to intracellular depletion of potassium and therefore potentially inhibit clathrin-mediated endocytosis. I tested this possibility by using an internal solution containing 120mM K-Glutamate, and 25mM Cs-glutamate, instead of 145mM Cs-glutamate and perfused with external solution containing complete TEA-Cl replacement of NaCl. In this manner it would be possible to record calcium currents without contamination of potassium conductances and to check whether endocytosis is being inhibited due to cellular depletion of potassium ions. Using the potassium based internal solution in response to a train of 50, 10ms depolarisations at 20Hz, all cells (6/6) tested exhibited robust endocytosis, with 4 cells displaying rapid endocytosis, in which endocytosis predominated as the train progressed masking positive increases in capacitance due to exocytosis resulting from later pulses in the train (figure 4.4.9).

4.4.9 Potassium-based internal solution supports a rapid endocytotic pathway.
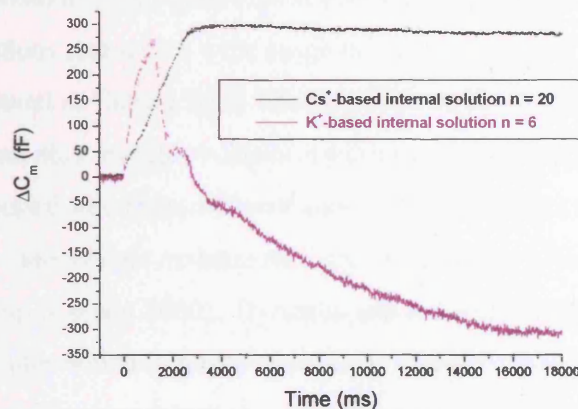
20 individual capacitance traces evoked from a train of 50, 10ms depolarisations delivered at 20Hz have been averaged together and the mean trace displayed above (black). The standard intracellular solution was used (145mM Cs-Glutamate). No individual cell displayed significant endocytosis. The mean amount of endocytosis that occurred 22 seconds post-stimulus was 9 ± 12 fF, n =20. In contrast, when an internal pipette solution designed to maintain a physiological intracellular potassium concentration (120mM K-Glutamate, 25mM Cs-Glutamate) was used, endocytosis was observed in response to the same stimulus from all cells (6/6), with rapid endocytosis evoked in 4 cells. Shown is the average capacitance trace from 6 cells.

117

4.4.10 Discussion of stimulus-coupled endocytosis.

I have found that with a single step 200ms depolarisation, increasing calcium entry is correlated to an increase in endocytosis, which is in agreement with previously published studies (Neher and Marty 1982; Engisch and Nowycky 1998). However when I deliver a robust train of brief (10ms) depolarisations endocytosis is inhibited and longer depolarisations and therefore larger calcium entry is required to elicit compensatory endocytosis. In previous studies endocytosis in response to trains of depolarisations has been reported, however either higher extracellular calcium was used (Nucifora and Fox 1998) 10mM instead of 2.5mM, or calf adrenal chromaffin cells were used with the facilitation channel recruited (Artalejo et al. 1996). This leads to much larger total calcium current amplitudes. Alternatively this could possibly reflect differences between the perforated patch configuration, which I use and the whole cell method employed by some other groups, in which cytoplasmic regulators may diffuse out of the cell up the patch pipette (Artalejo et al. 1996; Nucifora and Fox 1998). So why is endocytosis sometimes inhibited following robust stimulations (200ms and both train protocols)? Even the cells with smaller calcium entry will still experience calcium levels far greater than cells stimulated by single, or trains of action potentials (the physiological stimulus), which have been shown in numerous preparations and with a wide range of techniques to be able to undergo endocytosis (reviewed in Cousin 2000, Morgan et al. 2002, Royle and Lagnado 2003). Calcium can play multiple roles in regulating synaptic vesicle endocytosis. These can be separated into three different steps; a high affinity calcium dependent trigger, a calcium-independent maintenance phase, and a low affinity calcium-dependent inhibition (Cousin 2000). Dynamin and synaptotagmin have been proposed as molecules which (although necessary for endocytosis) may actually inhibit it at high calcium concentrations. Calcium binds both dynamin-1 and dynamin-2 with a low affinity (μM) and inhibits their GTPase activity. Synaptotagmin switches from binding PIP_3 at resting calcium levels to PIP_2 at μM calcium levels. Synaptotagmin could possibly compete with dynamin for vesicle release site PIP_2 when calcium levels rise. A role for PIP_2 interacting with dynamin

has been reported to be essential for synaptic vesicle endocytosis (Cousin 2000 and references within). Perhaps calcium entry during a 200ms depolarisation or the two train protocols previously described is high enough to inhibit endocytosis, and then another endocytotic pathway is switched on when calcium levels are raised even higher. Evidence to support this idea comes from the observation that endocytosis is always observed after exocytosis evoked from a very long (800ms) depolarisation, and that it is also observed following short (40ms) depolarisations when calcium influx will be high and small respectively (figure 4.4.6). However an alternative explanation for inhibition of endocytosis following a train of brief depolarisations is due to inhibition of a clathrin-dependent endocytotic pathway reliant on intracellular potassium. Intracellular depletion of potassium dramatically reduces the number and size of clathrin coated pits on the plasma membrane as assessed by imunofluorescence and electron microscopy (Larkin et al. 1983). In this study they also showed that replacement of intracellular potassium with cesium, lithium, or TEA could not support clathrin-mediated endocytosis, assessed by either ^{125}I-LDL or ^{125}I-EGF uptake, however rubidium could (Larkin et al. 1983). Further studies have shown that intracellular potassium depletion leads to formation of clathrin microcages under the plasma membrane where clathrin coated pits were located previously (Heuser and Anderson 1989). These clathrin microcages are no longer able to show clathrin exchange, and hence endocytosis via this pathway is inhibited (Wu et al. 2001). This has important implications, since the vast majority of published studies investigating endocytosis using the capacitance technique have used cesium based internal pipette solutions (to block potassium contamination of calcium currents), which will lead to intracellular potassium depletion (Artalejo et al. 1996; Nucifora and Fox 1998; Engisch and Nowycky 1998; Chan and Smith 2001; Chan and Smith 2003). A recent study using the capacitance technique shows that endocytosis following brief trains of depolarisations is not affected, but endocytosis following robust trains of depolarisations is blocked when a cesium based internal is used. This inhibition during robust trains did not occur when internal solutions designed to maintain a physiological concentration of potassium were used (Artalejo et al. 2002). However one group believe they are able to specifically study a clathrin-mediated

endocytotic pathway when using a cesium-based internal solution (Chan and Smith 2003). They report endocytosis following robust trains of action potential-like depolarisations (15Hz) and that this endocytosis is blocked after introduction of clathrin/dephosphin-disrupting peptides (Chan and Smith 2003). In my recordings I usually use cesium-glutamate based internal solutions, and therefore expect depletion of potassium from the cell. This could explain why endocytosis is inhibited in some cells, but not why it resumes again with increasing calcium concentration, unless this high calcium-dependent pathway is clathrin independent. When I used a potassium-based internal solution endocytosis was no longer inhibited following a train of depolarisations. Therefore, by using cesium-based electrode solutions, I (and the vast majority of other groups studying endocytosis with the capacitance technique) have excluded an endocytotic pathway, presumably mediated by clathrin. This may also explain previous studies using cesium-based internal solutions which report that rapid endocytosis is usually only observed with the first stimulation after going whole cell (Artalejo et al. 1996). This was interpreted as cytoplasmic factors necessary for this endocytotic pathway being dialysed out of the cell. My studies suggest that the molecular basis for this could be potassium depletion and inhibition of clathrin-mediated endocytosis.

4.5 Stimulus-coupled secretion with barium.

Numerous neuronal preparations show that substituting extracellular calcium for barium reduces the rapid component of stimulus-coupled exocytosis and increases slower asynchronous release (Goda and Stevens 1994; Seward et al. 1996; Neves, et al. 2001). This asynchronous slow release is not due to a slow emptying of internal calcium stores by barium, as it is insensitive to high calcium chelation or thapsigargin pretreatment (Seward et al 1996). I found that barium altered stimulus-evoked exocytosis in relation to control responses in calcium. Figure 4.5.1 shows a typical response resulting from a 200ms depolaristaion or from the pool protocol (6, 10ms depolarisations followed by 4, 100ms depolarisations), when calcium or barium was the extracellular divalent. In the case of the 200ms depolarisation, the size of the

immediate exocytotic jump is well reduced in barium, but asynchronous release is much larger and continues for the duration of the trace (22 seconds), there was no measurable endocytosis within the time frame of this recording. It is possible that endocytosis is occurring but is masked by a continual and larger amount of exocytosis. This possibility cannot be ruled out with the capacitance technique as it only detects total changes in membrane surface area. An imaging approach or capacitance combined with amperomery would be able to investigate this scenario. In response to the pool protocol barium does not evoke secretion from the 10ms pulses, designed to assess the size of the IRP. Exocytosis evoked from the longer 100ms depolarisations is also reduced from the responses seen in calcium, but again asynchronous slow release is increased in barium with no measure of endocytosis occurring within the time frame of the recording (figure 4.5.1).

4.5.1 Barium reduces stimulus-coupled release, but evokes larger sustained asynchronous release.
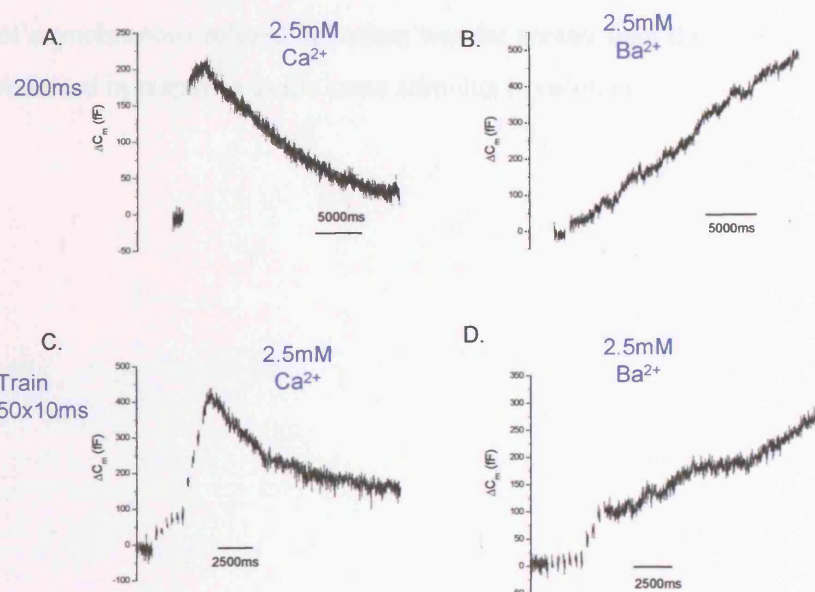
Sample capacitance traces of exocytosis evoked from a 200ms depolarisation with either calcium (A) or barium (B) in the extracellular solution. The size of the exocytotic burst is well reduced with barium compared to calcium, but asynchronous release is much higher. Barium does not support stimulus-coupled secretion in response to a brief train of 10ms depolarisations (D), suggesting that it can not support secretion from the IRP, whereas calcium can (C).

The size of the RRP in barium was investigated. As expected from the results of other studies (Neves et al. 2001) the size of the RRP was significantly reduced when calcium was replaced with barium. The size of the RRP in calcium was calculated using the double pulse method (section 4.2.6) as 194 ± 27 fF n = 9. Similar calculations in barium estimate a RRP size of 43 fF $\pm$ 7fF, n = 3. This reduction in the pool size was statistically significant p = 0.05. However this may be an overestimate of pool size in barium as the protocol was only applied to 5 cells and 2 of these did not evoke a change in capacitance in response to the double pulse and were hence discarded from analysis. The ΔC_m in response to release from the SRP was next investigated by applying longer depolarisations. From paired cells the size of the initial exocytotic jump following an 800ms depolarisation was 470 ± 122 fF n= 5, reduced to 64 ± 29 fF when extracellular calcium was replaced with equimolar barium (figure 4.5.2). This was statistically significant in a paired t-test (p = 0.01). Again there was a large continuous asynchronous release in barium that lasted the duration of the recording. In response to a train of 10ms depolarisations at 20Hz the amount of asynchronous release in barium was far greater than the stimulus-coupled release observed in response to the same stimulus in calcium.

4.5.2 Comparison of calcium and barium evoked ΔC_m in response to an 800ms depolarisation or train of 50, 10ms depolarisations at 20Hz.

A.

B.
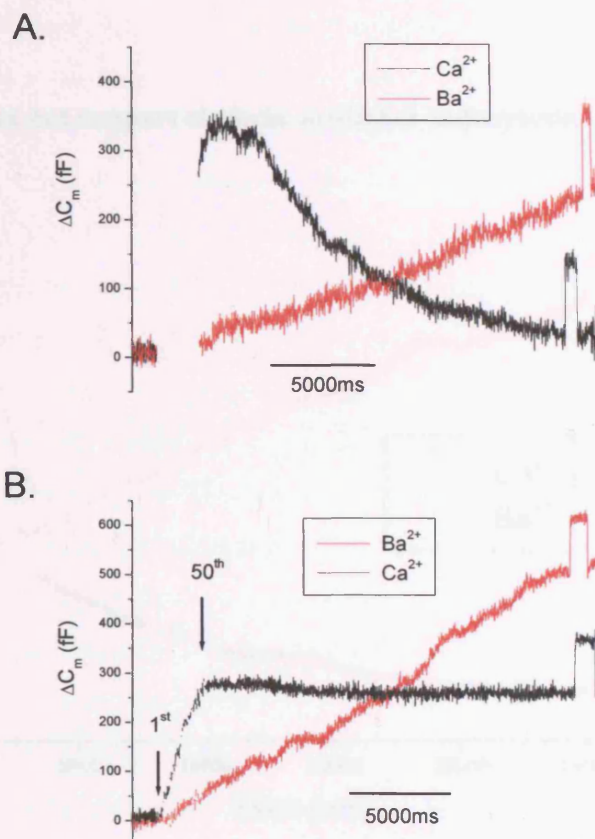
A. A typical ΔC_m evoked from an 800ms depolarisation with calcium (black) and then again when extracellular calcium was exchanged with an equivocal concentration of barium (red). The upward deflects at the end of the capacitance traces represent a 100fF calibration step.
B. A typical ΔC_m evoked from a train of 50, 10ms depolarisations delivered at 20Hz in calcium (black) and then again in barium (red).

I next investigated whether barium could support clathrin-mediated endocytosis, which is inhibited when cesium-based pipette solutions are used (figure 4.4.9). Using a potassium-based internal solution, replacing extracellular calcium with barium, results in a reduction in exocytosis, large asynchronous release and no measurable endocytosis. This therefore suggests that barium does not substitute for calcium and trigger clathrin-mediated endocytosis (4.5.3). However it should be noted that

123

although I did not detect decay in the capacitance trace, this does not confirm that endocytosis is inhibited, as ΔC_m monitor the net result of both exocytosis and endocytosis. Therefore it is possible that barium can support endocytosis but this is masked using the capacitance technique as slow exocytosis persists and dominates the ΔC_m.

4.5.3 Barium does not support clathrin-mediated endocytosis.
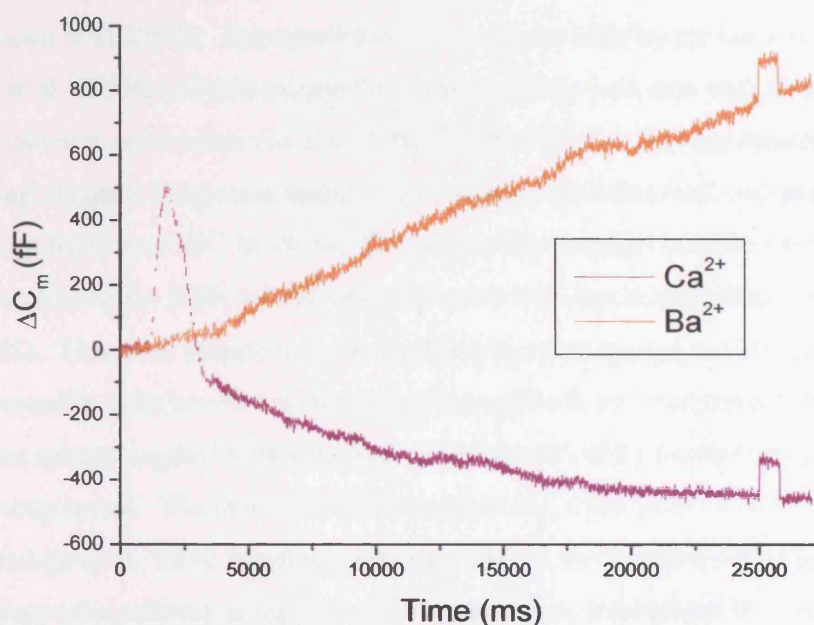
A cell was stimulated with a train of 50, 10ms depolarisations delivered at 20Hz, using a potassium based internal solution. Endocytosis is observed with extracellular calcium (purple), but is not supported when calcium is replaced with equimolar barium (orange).

4.5.4 Discussion of Stimulus-coupled secretion with barium.

Information about the calcium sensor(s) for fast exocytosis can be gained from barium substitution experiments. It was suggested that barium potentiates asynchronous release because the calcium sensing molecule controlling this mode of exocytosis has a higher affinity for barium (Goda and Stevens 1994). Alternatively it has been argued that barium potentiates asynchronous release because it accumulates

124

in the cell and is less effectively buffered or extruded. After moderate stimulation barium is cleared from the synaptic terminals of bipolar retinal neurones 10-100 times slower than calcium (Neves et al. 2001). There is evidence to suggest that barium causes release from a molecularly distinct population of vesicles (Seward et al. 1996; Duncan et al. 2003). Recently a clever imaging approach showed that nicotine and barium selectively cause release of different pools of fluorescently labelled vesicles in chromaffin cells (Duncan et al. 2003). It is now widely accepted that synaptotagmin I, is the calcium sensor for fast stimulus-coupled release (Fernandez-Chacon et al. 2001). Synaptotagmin I has a lower affinity for barium than calcium (Li et al. 1995), and this protein has many different isoforms with different affinities for calcium and barium (Li et al. 1995; Sudhof 2002). This has lead to the idea that synaptotagmin I regulates fusion from the RRP and other isoforms may regulate fusion from the SRP. In chromaffin cells synaptotagmin knockout mice lack fast release from the RRP, but maintain slow calcium-dependent release (Voets et al. 2001). This slow release may be regulated by other synaptotagmin isoforms which chromaffin cells have been shown to possess (Roth and Burgoyne 1994). Whether other synaptotagmin isoforms mediate fusion evoked by barium has not yet been directly tested. The role of barium in supporting endocytosis is controversial (Artalejo et al. 1996; Nucifora and Fox 1998), it would seem that at least one endocytotic pathway is highly calcium-dependent, whereas another may be supported by either divalent. My data confirms previously published observations that substituting extracellular calcium for barium reduces the rapid component of stimulus-coupled exocytosis and increases slower asynchronous release. I found no evidence to suggest that any endocytotic pathway is supported by barium within 22 seconds post-stimulus.

4.6 Summary of stimulus-coupled secretion.

Capacitance increases are triggered by calcium entry through voltage-activated calcium channels. Increasing pulse duration increases calcium entry and ΔC_m which can de described as a simple transfer function of summed calcium, suggesting that

regulated exocytosis is related to calcium entry with a power ≤ 2. This is also true for exocytosis evoked from trains of depolarisations. Exocytotic efficiency ($\Delta C_m / \Sigma\, Ca^{2+}$ ions) is not significantly different for pulses ranging in length from 40-800ms in duration. However 10ms pulses show an enhanced exocytotic efficiency. The size of the IRP and RRP were calculated using a double pulse protocol. The size of the IRP was estimated at $40 \pm 10fF$ n = 18, and the RRP at 194 ± 27 fF n = 9. Asynchronous release was not correlated to the size of the exocytotic burst, peak current amplitude, or degree of channel inactivation. However it was sensitive to calcium, decreasing with elevated levels. Whether this is a true reduction in asynchronous release or an increase in endocytosis was not determined. Post-stimulus endocytosis could be binned into one of four groups. The amount of calcium influx during stimulation determined the endocytotic response. Using a potassium-based internal solution compared to cesium-based, revealed an endocytotic pathway that had previously been inhibited. This pathway is likely to be clathrin-dependent. The size of the RRP is reduced in barium, although asynchronous release is greatly increased. There is no evidence to suggest that barium supports endocytosis following stimulus-coupled exocytosis using any of my standard protocols.

Chapter 5: Characterisation of calcium channel subtypes controlling exocytosis.

Chromaffin cells are reported to possess many subtypes of high voltage-activated calcium channels (L, P/Q, N & R). The role of individual calcium channel subtypes in controlling exocytosis from chromaffin cells is unclear. Some groups have suggested that exocytosis is coupled to calcium entry through specific calcium channel subtypes, although their published findings differ considerably (Artalejo et al. 1994; Lopez et al. 1994; Kim et al. 1995; Lara et al. 1998; Albillos et al. 2000; Aldea et al. 2002). Others find no preferential calcium channel coupling (Engisch and Nowycky 1996; Lukyanetz and Neher 1999). The disparity in results may be due to species differences in density of channel subtypes expressed, differences between cultured cells and acute slices, the recording configuration (whole cell or perforated patch), the intensity and type of stimulation and the method used to detect secretion. The aim of this section of work was to investigate the functional role of individual calcium channel subtypes in the control of neurotransmitter release from adult bovine adrenal chromaffin cells. I have used the perforated patch configuration of the voltage-clamp technique to maintain the cytosolic milieu and have measured secretion by monitoring changes in membrane capacitance. I have used a physiological concentration of extracellular calcium (2.5mM), and elicited stimulus-coupled secretion using a range of single step depolaristions (10 to 800ms), or trains of depolariations.

5.1 Pharmacological isolation of calcium channel subtypes.

In these studies I have discriminated between different molecular channel subunits by using specific toxins. The overall pharmacological profile of a given calcium channel conductance is primarily defined by the α_1 subunit, as this contains the binding sites for multivalent cations, interaction sites for peptide blockers, and receptor sites for small organic molecules (Doering and Zamponi 2003; McDonough 2004 and references within). I have used several specific channel blockers which can be

classified into one of two groups; peptide blockers and small organic molecules from the dihydropyridine family.

5.1.1 Peptide blockers

Peptide toxins isolated from the venom of a wide range of predatory animals have been shown to block a variety of voltage and ligand gated ion channels. Some of these have been found to be highly specific for individual calcium channel subtypes. Of particular relevance to my studies are toxins found in the venom of marine hunting sea snails (ω-conotoxins) and funnel web spiders (ω-agatoxins). These peptides share a rigid structure, as they are spatially confined by numerous disulfide bonds, which act to give them a high degree of specificity in target interactions (Doering and Zamponi 2003).

ω-conotoxin GVIA (ω-CTX GVIA) is a prototypical calcium channel blocking peptide isolated from *Conus geographus*, a carnivorous sea snail (Cruz and Olivera 1986). This peptide is highly selective for N-type calcium channels inhibiting currents with a 1:1 stoichiometry, causing a fast, irreversible block in the mid nanomolar range under physiological ionic conditions (Cruz and Olivera 1986). ω-CTX GVIA acts by physically occluding the channel pore. Site-directed mutagenesis experiments have identified a number of amino acid residues within the S5-S6 region in domain III of the α_{1B} pore subunit as essential for ω-CTX GVIA binding (Ellinor et al. 1994; Feng et al. 2001).

ω-agatoxin IVA (ω-Aga IVA) isolated from the venom of the funnel web spider *Agenelopsis aperta* is a specific blocker of P- and Q-type calcium channels (Mintz et al. 1992), although low affinity block of N-type calcium channels has been reported at micromolar concentrations (Sidach and Mintz 2000). P-type channels are blocked at low nanomolar concentrations, whereas block of Q-type channels requires concentrations of several hundred nanomolar (Bourinet et al. 1999). Block by this toxin is slow (compared to ω-CTX GVIA) and poorly reversible after washing, but

128

the channel can recover from block following strong repetitive membrane depolarisations (Mintz et al. 1992; Powell 2000; Bourinet et al. 1999). This suggests that voltage sensor movement may physically dislodge the toxin from its binding site. ω-Aga IVA is thought to interact with the α_{1A} pore domain IV S3-S4 region (Bourinet et al. 1999), and insertion of an asparagine and proline into this region by alternative splicing shifts ω-Aga IVA sensitivity from high affinity (P-type) to low affinity (Q-type), (Bourinet et al. 1999).

5.1.2 Dihydropyridines.

Dihydropyridines (DHPs) are a group of small organic compounds which are based on a core pyridine structure. They are usually specific for L-type calcium channels, although T-type channels show sensitivity to some DHPs (Kumar et al. 2002), reviewed by (Triggle 2004). DHPs bind to the L-type α_1 subunits at two independent sites on domains III and IV (Striessnig et al. 1991). The detailed molecular basis of block is not clear, however it appears that DHPs can induce an inactivated conformation (Eller et al. 2000) as well as open channel block (Handrock et al. 1999). It has also been shown that some DHPs preferentially bind to inactivated channels, (Triggle 2004). Members of the DHP family can either block (nimodipine, nicardapine, nifedipine etc), or facilitate calcium flow through L-type channels (- Bay K 8644). (-)-Bay K 8644 increases current amplitude, shifts activation to a more negative potential and prolongs tail currents. (-)-Bay K 8644 interacts with the same 'microsite' as other antagonistic DHPs in the S5 region of domain III, although it appears that different DHPs require interactions with different amino acids within this microsite to mediate their effects (Doering and Zamponi 2003). Although the binding sites for DHPs are present on the α_1-subunit, auxillary β subunits can profoundly influence drug sensitivity (reviewed in Hering 2002).

5.2 L-type calcium channels do not contribute significantly to either calcium entry or regulated-exocytosis.

Previous reports have suggested that approximately 30-50% of the calcium current from bovine adrenal chromaffin cells corresponds to activation of L-type calcium channels, as defined by sensitivity to DHP antagonists (Artalejo et al. 1994; Lopez et al. 1994; Kim et al. 1995). Moreover, L-type calcium channels have been suggested to couple more efficiently to exocytosis than other calcium channel subtypes (Artalejo et al. 1994; Lopez et al. 1994; Kim et al. 1995). Previous work conducted in our laboratory by Andrew Powell concluded that chromaffin cells in our preparation do not contain significant L-type calcium currents nor do they contribute to stimulus-coupled secretion. He investigated the role of L-type channels in exocytosis evoked by 200ms step depolarisations using DHP allosteric modulators (Powell 2000). In the absence of nimodipine, a 200 ms step depolarisation resulted in entry of $401 \pm 47 \times 10^6$ Ca^{2+} ions, which produced a C_m change of 240 ± 14 fF (n = 3). Superfusion of nimodipine (10 μM) for 4 minutes, did not significantly reduce either Ca^{2+} entry or ΔC_m $375 \pm 40 \times 10^6$ Ca^{2+} ions and 228 ± 17 fF, p = 0.16 and 0.15, respectively. This corresponds to a reduction in calcium entry and capacitance of 6.5% and 5% respectively. I investigated the effect of a different DHP, nifedipine on calcium currents. Similar results were observed. In response to 40ms depolarisations superfusion of 10μM nifedipine resulted in a reduction in peak calcium current amplitude and integrated calcium entry of 6.4% ± 2.2 and 4.2% ± 2.2, respectively n=3, this difference was not significant (figure 5.2.1). In addition to DHP antagonist sensitivity, L-type calcium channel activity can be potentiated by the DHP agonist (-) Bay K 8644 (Triggle 2004). To confirm the lack of L-type calcium channels under our recording conditions, the effect of (±) Bay K 8644[3] was tested. In agreement with the observations that nimodipne and nifedipine were ineffective, previous work in our lab found that (-) Bay K 8644 at various concentrations (1nM to 1μM) did not

---

[3] (±) – Bay K8644 is a mixture of two optical isomers: the (-)-enantiomer has potent calcium channel agonist properties, whereas the (+)-enantiomer has weak calcium channel antagonist properties. The net activity of the racemic mix is that of the (-)-enatiomer, agonist activity. (Alomone data sheet, Triggle and Rampe 1989).

significantly alter the calcium current (Powell 2000). I repeated part of this experiment by measuring calcium currents before and after application of 1μM (±)-Bay K 8644. I found that the peak current and calcium entry after drug application were not significantly different from control. In response to 40ms depolarisations peak current and calcium entry were, $511 \pm 64pA$ and $56 \pm 6 \times 10^6 Ca^{2+}$ ions reduced to 506 ± 59 pA and $53 \pm 4 \times 10^6 Ca^{2+}$ ions, (n = 3) respectively, after application of (±)-Bay K 8644 at 1μM. (figure 5.2.1).

5.2.1 DHP allosteric modulators do not alter calcium entry.
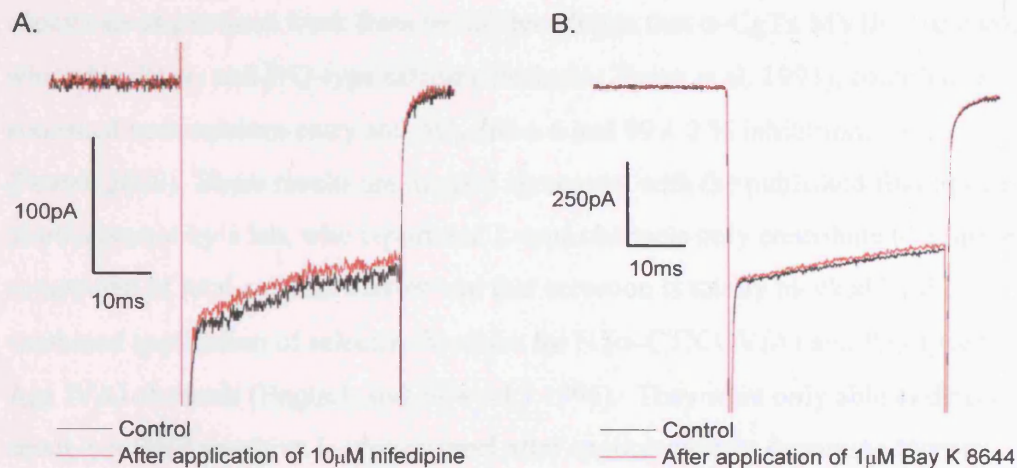
A. Superfusion of 10μM nifedipine does not significantly reduce peak current (6.4 ± 2.2%) or calcium entry (4.2 ± 2.2%, n = 3). Displayed is a sample current trace before (black) and after (red) drug application.

B. Superfusion of (±)-Bay K 8644 at a concentration of 1μM, did not significantly alter peak current (1%) or calcium entry (1%), n = 3. Displayed is a sample current trace before (black) and after (red) drug application.

A possible criticism of these experiments is that there is no positive control for ensuring activity of the drugs. I should have tested the ability of the drugs to block/enhance calcium currents on a cell line or native cell that is known to express functional L-type channels (eg cardiac myocytes). However I find it highly unlikely that the two drugs I used, nifedipine and (±)-Bay K 8644 and both the drugs previously used in the lab, nimodipine and a different batch of (-) Bay K 8644 had all

131

degraded before experimentation. Another more pertinent criticism related to this experiment is that a key feature associated with DHP block is a strong state dependence (Doering and Zamponi 2003). L-type channel block is reportedly sensitive to hyperpolarized membrane potentials, with blocking affinity increasing by several orders of magnitude at more depolarised potentials (Kumar et al 2002). Therefore we may not have observed a significant effect on calcium currents and secretion after DHP application as we hold at a membrane potential of -80mV. Experiments examining the effect of DHP modulators on putative L-type currents could have been conducted from a more depolarised holding potential ($\sim$-60mV) to test this possibility. Despite this we do not believe that L-type calcium channels contribute to either the total membrane calcium current or stimulus-coupled exocytosis as previous work from the lab has shown that ω-CgTx MVIIC (10 μM), which blocks N- and P/Q-type calcium channels (Zhang et al. 1993), completely abolished both calcium entry and ΔC_m (94 $\pm$ 6 and 99 $\pm$ 2 % inhibition; n = 3), (Powell 2000). These results are in good agreement with the published findings from Martha Nowycky's lab, who report that L-type channels only contribute to a minor component of total calcium current and that secretion is totally blocked by the combined application of selective blockers for N (ω-CTX GVIA) and P/Q-type (ω-Aga IVA) channels (Engisch and Nowycky 1996). They were only able to detect a small, but DHP sensitive L-type channel after application of a dopamine receptor agonist, SKF-38393. Also the lab of Arron Fox conclude that L-type channels are normally 'quiesent' and that combined application of ω-CTX GVIA and ω-Aga IVA blocks 95% of calcium currents, the remaining current was insensitive to nitrendipine (1-2μM), suggesting that is not carried by an L-type current (Currie and Fox 1997; Currie and Fox 2002). However they perfuse with 1-2μM nitrendipine to prevent recruitment of an L-type/facilitation channel after strong depolarizing pulses (they were stepping to +100mV to assess G-protein inhibition of channels). This suggests that in their and our cultures, the L-type /facilitation channel reported by other groups (Artalejo et al. 1994) is normally surreptitious and only contributes significantly to current amplitude and secretion after agonist or voltage protocol induced recruitment. This may reflect developmental differences in ion channel expression and regulation

132

as reports of a large L-type calcium current that couples efficiently to exocytosis have been observed from experiments on calf chromaffin cells (Artalejo et al. 1994), whereas we and the labs of Noywecky and Fox record from adult bovine chromaffin cells.

5.3 N and P/Q-type calcium channels mediate calcium entry and couple to exocytosis.

The observation that ω-CTX MVIIC abolished both calcium entry and C_m increases, suggests that stimulus-secretion coupling is mediated solely by N- and P/Q-type channels in cells under our culture conditions (Powell 2000). To confirm this, the effects of selective calcium channel blockers, ω-CgTX GVIA (1μM), to block N-type channels (Fox et al. 1987) and ω-Aga IVA (300nM), to block P/Q-type channels (Mintz et al. 1992; Zhang et al. 1993) were examined. Combined application of these toxins inhibited calcium entry by 94.3 ± 1.0 % and inhibited ΔC_m by 93.1 ± 2.3 %, n=3 (figure 5.3.1).

5.3.1 Calcium entry and exocytosis is coupled to N and P/Q-type channels.
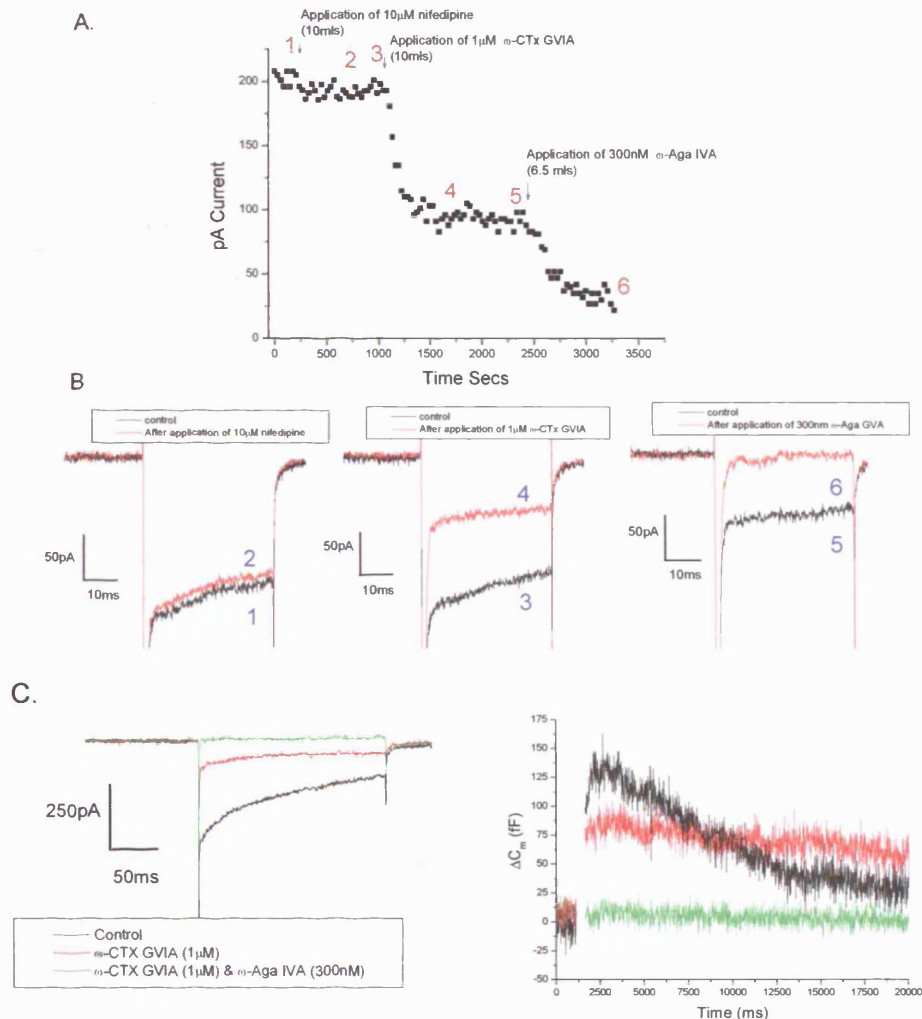
A. Data from a single cell from which 40ms depolarisations were elicited every 25 seconds. The peak current (I_{3ms}) is plotted before, during and after sequential application of 10μM nifedipine, 1μM ω-CTX GVIA and 300nM ω-Aga-IVA.

B. Corresponding current traces from the same experiment at the time indicated by the numbers (blue). 10μM nifedipine has little effect on the current amplitude, whereas 1μM ω-CTX GVIA results in around a 50% decrease in current amplitude and 300nM ω-Aga-IVA further inhibits the current so that after combined application of toxins only ~10% of the current remains. This current could be due to unblocked L-type channels (nifedipine was not perfused for the duration of the experiment), incomplete block by ω-Aga-IVA (time to achieve full block was variable but typically took 5 – 10mins). Or perhaps the residual current is mediated by a current resistant to these toxins. R-type calcium channels have been reported to contribute to membrane calcium currents in mouse chromaffin cells (Albillos et al. 2000).

C. In a separate cell membrane calcium currents (left) and capacitance (right) were monitored after sequential application of 1μM ω-CTX GVIA and 300nM ω-Aga-IVA in response to a 200ms depolarisation. Combined application of these toxins blocked mean calcium entry by 94.3 ± 1.0 % and inhibited ΔCm by 93.1 ± 2.3 % (n=3).

134

5.4 Characterisation of pharmacologically isolated calcium currents

Having established that the majority of calcium entry and stimulus-coupled secretion in bovine chromaffin cells is mediated by N and P/Q-type channels, characterisation of the isolated channel subtypes was conducted. In response to a 200ms depolarisation calcium entry was reduced from 236 ± 24 to 136 ± 21 x 10^6 Ca^{2+} ions after application of $1\mu M$ ω-CTX GVIA, n = 9, p = 0.007. Similarly calcium entry was reduced from 232 ± 27 to 113 ± 19 x 10^6 Ca^{2+} ions n = 6, p = 0.004, after application of 300nM ω-Aga IVA. It was next determined whether data on both channel subtypes could be obtained from each toxin, ie is the current remaining after one toxin similar to the subtracted current (determined by subtracting the residual current after toxin application from the control current) from the other toxin? To test this idea, calcium entry remaining after ω-CTX GVIA application was compared to calcium entry calculated from the subtracted current from control after application of ω-Aga IVA and vice versa. This approach is valid since the amount of calcium entry before toxin application was similar for both groups. No significant difference was found (figure 5.4.1), therefore toxin isolated and toxin subtracted currents were summed together for analysis. As there is no significant difference in calcium entry between toxin isolated and toxin subtracted currents this is further evidence to suggest that calcium entry is mediated solely by N and P/Q-type channels. If an extra channel were present one would expect the remaining calcium entry to be significantly larger than the subtracted value. Peak current, calcium entry and % inactivation evoked from a 200ms depolarisation were then compared for N and P/Q-type channels. There was no difference in peak current amplitude, 309 ± 37 pA n = 15 for N-type currents and 310 ± 55 pA n = 15 for P/Q-type currents. Although there was a trend towards less calcium entry and increased current inactivation for N-type channels over 200ms, this was not found to be significant, p = 0.16 and p = 0.17 respectively. Calcium entry of 105 ± 10 x 10^6 Ca^{2+} ions, n = 15 and 129 ± 14 x 10^6 Ca^{2+} ions, n = 15 for N and P/Q type respectively. Current inactivation of $60.3 \pm 7.2\%$ n= 15 and $47.1 \pm 5.9\%$ n = 15 for N and P/Q type respectively.

5.4.1 Calcium entry evoked from a 200ms depolarisation following application of either ω-CTX GVIA or ω-Aga IVA.
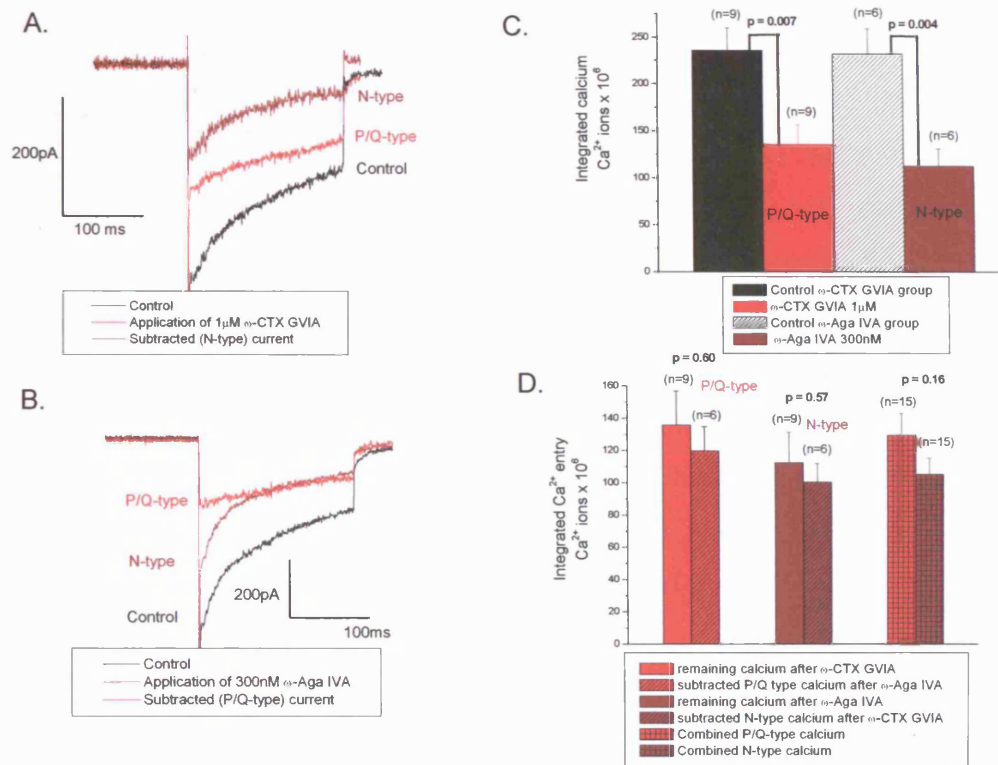
A. Sample currents evoked by a 200ms depolarisation, before (black) and after (red) application of 1μM ω-CTX GVIA. The pharmacologically sensitive N-type current (wine) was determined by subtracting the residual current remaining after toxin application from the control current.
B. Sample currents evoked by a 200ms depolarisation, before (black) and after (wine) application of 300nM ω-Aga IVA. The pharmacologically sensitive P/Q-type current (red) was determined by subtracting the residual current remaining after toxin application from the control current.
C. Bar chart depicting the reduction in calcium entry after application of either toxin.
D. Bar chart illustrating that calcium entry occurring from either residual current after application of one toxin or the subtracted current from the other current are not significantly different.

A similar approach was taken to compare N and P/Q type currents evoked from longer depolarisations (800ms). In response to an 800ms depolarisation calcium entry was reduced from 354 ± 40 to $229 \pm 39 \times 10^6$ Ca^{2+} ions after application of 1μM ω-CTX GVIA, n = 10, p = 0.04. Similarly calcium entry was reduced from 419 ± 35 to $189 \pm 32 \times 10^6$ Ca^{2+} ions n = 6, p = 0.002, after application of 300nM ω-Aga

136

IVA. Mean calcium entry was 155 ± 19 x 10^6 Ca^{2+} ions, n = 16 and 225 ± 25 x 10^6 Ca^{2+} ions, n = 16 for N and P/Q type respectively, the difference was statistically significant, p = 0.03 (figure 5.4.2). This suggests that N-type channels undergo significantly more inactivation following long depolarisations (800ms), than P/Q-type channels, which limits calcium entry. To evaluate this further, the time course for inactivation was derived by fitting N or P/Q-type current traces with double exponentials. Individual current traces were averaged together for each channel subtype and the mean current trace fit with a double exponential (figure 5.4.3). This resulted in near identical τ_1 for both N and P/Q-type channels, τ_1 = 26 ms and 27ms respectively. However the second τ was considerably different, with a faster time-course for N-type channels τ_2 = 173 ms compared to 302 ms for P/Q-type channels. This suggests that both channels share the same fast mode of inactivation; however there are channel specific differences in the determinants of the slower mode of inactivation (figure 5.4.3). A double exponential fit of the mean control current (n=16), yielded a τ_1 of 26 ms and a τ_2 of 254 ms, which is almost exactly the difference between N and P/Q-type currents (τ_2 = 238ms).

5.4.2 Calcium entry evoked from an 800ms depolarisation following application of either ω-CTX GVIA or ω-Aga IVA.

A.

P/Q-type

N-type

Control

200pA

200ms

— Control
— Application of 300nM ω-Aga IVA
— Subtracted (P/Q-type) current

B.

P/Q-type

N-type

Control

200pA

200ms

— Control
— Application of 1μM ω-CTX GVIA
— Subtracted (N-type) current

C.

Integrated Calcium Ca^{2+} ions x 10^6

(10) p = 0.04

(6) p = 0.002

(10)

(6)

P/Q-type

N-type

■ Control ω-CTX GVIA group
■ ω-CTX GVIA 1μM
▨ Control ω-Aga GVA group
■ ω-Aga IVA 300nM

D.

Integrated calcium Ca^{2+} ions x 10^6

p = 0.82
(n=10) P/Q-type
(n=6)

p = 0.06
(n=6) N-type
(n=10)

* p = 0.03
(n=16)
(n=16)

■ remaining calcium after ω-CTX GVIA
▨ subtracted P/Q type calcium after ω-Aga IVA
■ remaining calcium after ω-Aga IVA
▨ subtracted N-type calcium after ω-CTX GVIA
▦ Combined P/Q-type calcium
▦ Combined N-type calcium

A. Sample currents evoked by an 800ms depolarisation, before (black) and after (wine) application of 300nM ω-Aga IVA. The pharmacologically sensitive P/Q-type current (red) was determined by subtracting the residual current remaining after toxin application from the control current.
B. Sample currents evoked by an 800ms depolarisation, before (black) and after (red) application of 1μM ω-CTX GVIA. The pharmacologically sensitive N-type current (wine) was determined by subtracting the residual current remaining after toxin application from the control current.
C. Bar chart depicting the reduction in calcium entry after application of either toxin. Sample numbers are shown in the parenthesis, and the calculated probability shown above the columns.
D. Bar chart illustrating that calcium entry is significantly reduced for N-type channels compared to calcium entry through P/Q-type channels. 155 ± 19 x 10^6 Ca^{2+} ions, n = 16 and 225 ± 25 x 10^6 Ca^{2+} ions, n = 16 for N and P/Q type, p = 0.03.

138

5.4.3 N-type channels inactivate faster than P/Q-type channels.
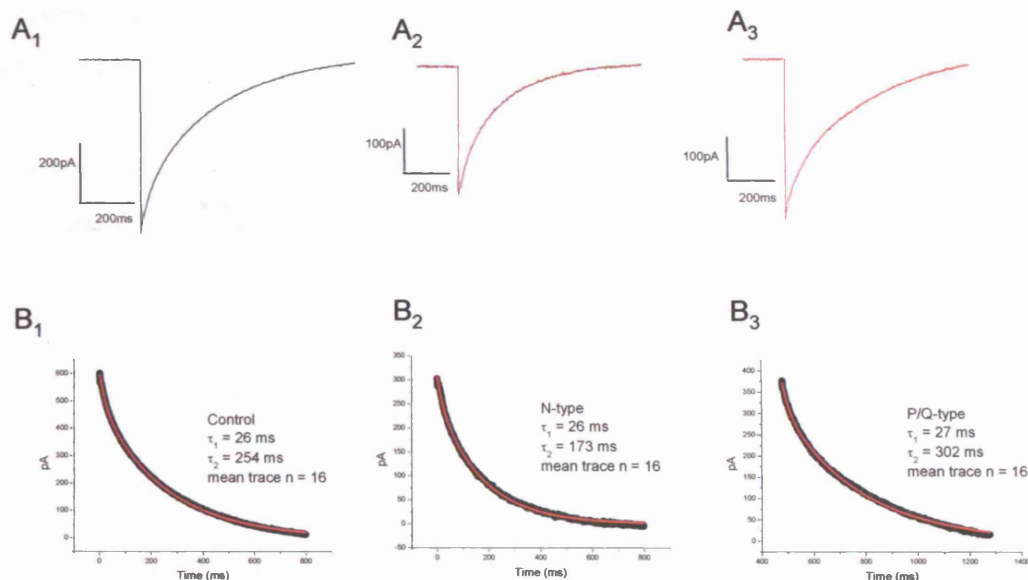
A. Mean current traces (n=16) for control (A_1, black), N-type (A_2, wine) and P/Q (A_3 red).
B. Double exponential fit of mean current traces red line, $y = y_0 + A_1e^{-x/t1} + A_2e^{-x/t2}$. Control (B_1), $\tau_1 =$ 26 ms, $\tau_2 = 254$ ms, N-type (B_2), $\tau_1 = 26$ ms, $\tau_2 = 173$ ms, P/Q-type (B_3), $\tau_1 = 27$ ms, $\tau_2 = 302$ ms.

5.5 Inactivation following trains of depolarisations.

Inactivation observed following long, single step depolarisations is a useful way to detect differences between channel subtypes, however these are very un-physiological stimuli, which a cell would never normally encounter. To assess differences in channel subtype inactivation following a more physiological stimulus, inactivation was monitored in response to currents evoked by a train of 50, brief (10ms) depolarisations delivered at 20Hz. Inactivation was monitored in one of two ways, a reduction in peak current, or a reduction in calcium entry. To quantify inactivation, the peak current of each pulse in the train was normalized to the amplitude of the first pulse, similarly calcium entry was normalized by dividing the integrated calcium value (ΣCa^{2+}) for each pulse by the ΣCa^{2+} entering during the first pulse. In both cases residual current remaining after toxin application was analysed separately to subtracted currents from the other toxin, as no significant difference was

139

observed data from both toxins were grouped together to give a mean value for N and P/Q-type currents respectively (figure 5.5.1). Significantly more channel inactivation occurred by the end of this train (pulse 50), for N-type channels compared to P/Q-type channels. Fractional inactivation, measured as a reduction in peak current amplitude or calcium entry was 0.25 ± 0.04, and 0.21 ± 0.03 n = 10, for N-type channels and 0.60 ± 0.05, and 0.58 ± 0.05, n=10 for P/Q-type channels, both tests were highly significant, $p < 0.001$ (figure 5.5.1).

5.5.1 Inactivation induced by a train of brief (10ms) depolarisations.
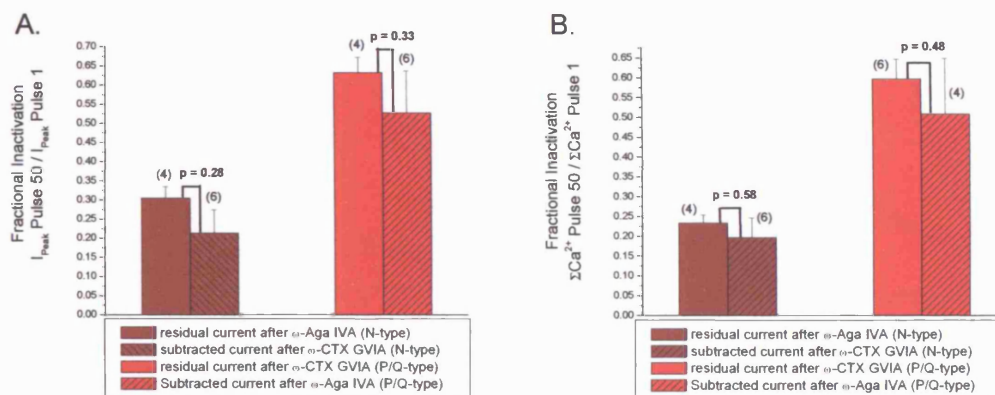
Cells were stimulated with a train of brief depolarisations, (50 x 10ms, from –80mV to +20mV at 20 Hz). Fractional inactivation was determined by dividing the peak current or ΣCa^{2+} entry (after 3ms to exclude contributions from sodium currents) of each pulse in the train by the peak current or ΣCa^{2+} entry of the first pulse. Fractional inactivation is a measure of how much the current inactivates during the course of the train.

A & B. Bar charts depicting the amount of fractional inactivation that occurs at the end of the train (pulse 50) from toxin isolated currents. There was no significant difference in the degree of inactivation for N-type channels whether they were recorded as the residual current left after ω-Aga IVA application, or whether the current data was derived from subtracting the current remaining after application of ω-CTX GVIA from the control current. The same was true for P/Q-type current inactivation. Sample numbers are shown in the parenthesis, and the calculated probability shown above the columns.

140
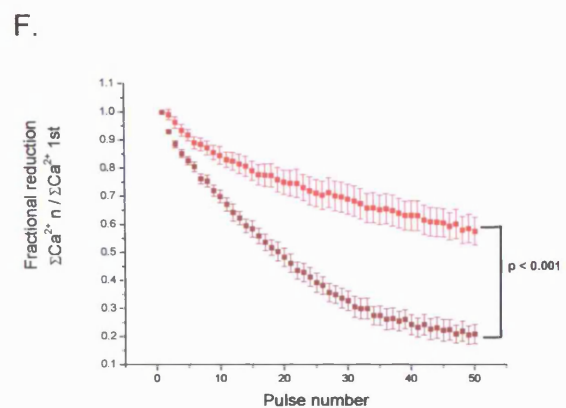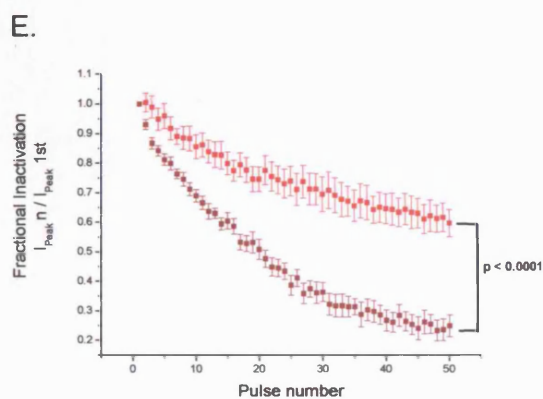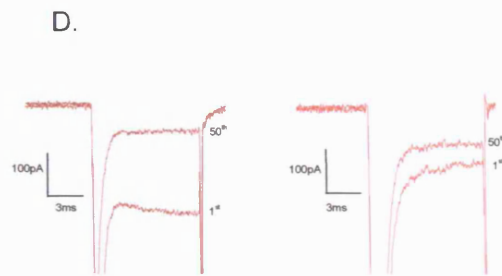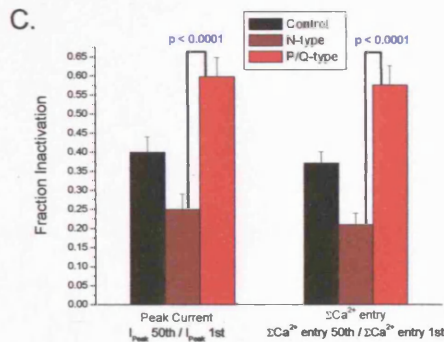
C. Mean fractional inactivation, ± s.e.m at pulse 50 for each channel subtype is plotted. Significantly more channel inactivation occurred for N-type channels compared to P/Q-type channels. Fractional inactivation, measured as a reduction in peak current amplitude or calcium entry was 0.25 ± 0.04, and 0.21 ± 0.03 n = 10, for N-type channels and 0.60 ± 0.05, and 0.58 ± 0.05, n=10 for P/Q-type channels, both tests were significant, $p < 0.001$.

D. Sample current traces for pharmacologically isolated N (wine) and P/Q-type (red) channels. Shown are the 1st and last (50th) currents in the train.

E & F. Fractional inactivation for each pulse in the train is plotted for N and P/Q-type channels. Each point is the mean ± s.e.m n = 10.

5.6 Molecular mechanisms underlying differences in voltage-dependent inactivation between N and P/Q-type channels.

Inactivation of calcium channels can occur by either voltage (fast and slow) or calcium-dependent processes. Calcium-dependent processes are discussed in detail in chapter 6. Here I will discuss some of the literature pertaining to voltage dependent inactivation that may account for the difference in inactivation observed for N and P/Q-type channels.

141

Firstly, intrinsic properties of the two α_1 pore subunits could underlie the difference in inactivation kinetics. N & P/Q-type channels share greater than 70% amino acid sequence identity (Catterall 1998), however amino acid differences between channels in key sites, or changes introduced by alternative splicing can profoundly affect inactivation. Alternative splicing of exon 10 of the P/Q- type α_1 subunit allows insertion of either G or VG residues (Bourinet et al. 1999). The isoform containing $V_{(2421)}$ shows slowed inactivation. Whether bovine chromaffin cell P/Q type channels express this insertion is not known.

Inactivation is not only dependent on the α_1 pore forming subunit, but can be strongly influenced by interactions with intracellular proteins and auxiliary subunits, especially β subunits (Stotz and Zamponi 2001). Bovine chromaffin cells express RNA for at least 5 different β subunits (β_{1b}, β_{1c}, β_{2a}, β_{2b} & β_{3a}). Recombinant expression of these cloned subunits with the α_{1B} subunit display currents with different degrees of inactivation (Cahill et al. 2000). Therefore it is possible that different β subunits associate preferentially with N and P/Q-type channels and underlie the observed difference in inactivation.

Both N and P/Q-type channels have been shown to interact with SNARE proteins such as syntaxin. This interaction increases voltage dependent inactivation (Bezprozvanny et al. 1995). The interaction greatly promotes slow inactivation but has little or no effect on the onset (or recovery) from fast inactivation (Degtiar et al. 2000). In expression systems such as the Xenopus oocyte model, co-expression of syntaxin with the calcium channel leads to diminished currents from the very beginning of the test depolarisation because of decreased availability of calcium channels (Degtiar et al. 2000), however in native systems studying endogenous expression of SNARES when botulinum C (BoNtC1) is applied to cleave syntaxin, or antibodies or peptides introduced to disrupt its function there appears to be little effect on the calcium entry. These systems include the squid giant synapse (Marsal et al. 1997; Sugimori et al. 1998) and the rat superior cervical gangion neurones (Mochida et al. 1995; Mochida et al. 1996). These studies measured the calcium current milliseconds after application of a depolarising voltage-clamp, or made recordings from the cell body rather than from the presynaptic site where the

physiological interaction between syntaxin and calcium channels is believed to occur. When syntaxin was cleaved by BoNtC1 in synaptosomes there was a lack in significance on early calcium entry, however calcium currents evoked by persistent or repetitive depolarisations uncovered syntaxin modulation of the channel (Bergsman and Tsien 2000). These results suggest that modulation of calcium channels by syntaxin is unlikely to account for short-term inactivation, however it may be suited to control synaptic strength during a strong stimulus. It may be the case that channel gating and vesicle turnover may be required to initiate the syntaxin stabilisation of the inactivated state *in vivo*. Further work has shown that although the region of syntaxin that binds the synprint site of the channel is important for an anchoring interaction, the transmembrane domain of syntaxin is involved in mediating the modulatory effects of syntaxin (Bezprozvanny et al. 2000). They have shown by mutagenesis that two amino acids (Ala-240 and Val-244) are critical for the channel modulation. The effect of these two amino acid substitutions in a native system has not been addressed yet.

It is interesting to note that both N and P/Q-type channels have splice isoforms that lack the 'synprint' (syntaxin binding) site in their domain II-III linker (Rettig et al. 1996; Kaneko et al. 2002). In the N-type isoform lacking this site, syntaxin is unable to bind and the voltage-dependence of inactivation is shifted towards a more depolarised potential (Kaneko et al. 2002). One would expect the same observation to be valid for the P/Q-type isoform lacking the synprint site and again may underlie differences in inactivation if expressed. The voltage-dependence of inactivation was assessed for control cells (chapter 4, figure 4.3.1). It would have been prudent for me to have repeated those experiments with toxin isolated channels to assess whether the steady state inactivation differs between the two channels at the standard holding potential of -80mV.

The voltage dependence of activation has been shown to be slight but significantly different for toxin isolated channels in bovine chromaffin cells (Currie and Fox 1997). There is a hyperpolarized shift (~7mv) in the peak of the I/V curve for the P/Q-type current relative to the N-type current. In my experiments the test potential amplitude was not altered after toxin application but would only have had to be

143

changed by 3-4mV in either direction to account for the difference in the I/V curve. Therefore this error is unlikely to have a large effect on inactivation of evoked currents.

5.7 Molecular mechanisms underlying differences in voltage-dependent inactivation between N and P/Q-type channels following a train of depolarisations.

In response to a 200ms depolarisation inactivation (measured as the reduction of the peak current by the end of the pulse) was greater for N-type channels 60.3 ± 7.2 % n= 15 than P/Q-type channels 47.1 ± 5.9 % n = 15 although this was not found to be significant (p = 0.17). However as can be seen in figure 5.5.1e, in response to a train of brief (10ms) depolarisations at 20Hz a significant difference in inactivation occurs within the first few pulses (fractional inactivation of 0.81 ± 0.02 and 0.96 ± 0.04, n = 15, p = 0.004 at pulse 5, for N and P/Q-type channels respectively). The observation that inactivation during single step square pulse depolarisations is slower compared to trains of action potentials (AP's) has been described for recombinantly expressed channels (Patil et al. 1998). They propose a model where by repetitive depolarisation induces a greater amount of cumulative inactivation because channels preferentially inactivate from intermediate closed states along the activation pathway (Patil et al. 1998). They also show that N-type channels are more susceptible to cumulative inactivation in response to a train of AP's than P/Q-type channels, and that the amount of N-type inactivation is critically dependent on β-subunit expression. Recently a splice variant of the N-type channel (exon 18a) which inserts 21 amino acids into a region of the II-III domain loop has been shown to protect the channel from entering a closed-state inactivation resulting from trains of AP's (Thaler et al. 2004). This insertion does not directly alter the synprint motif, however whether interaction of syntaxin with the synprint site still occurs or is weakened by addition of 21 extra amino acids in the close vicinity has not been addressed. This could be important as trains of AP's are more effective than steady depolarisations in stabilizing the slow inactivated state mediated by syntaxin (Degtiar et al. 2000).

144

Many molecular determinants underlying inactivation appear to be mediated by key amino acid residues in numerous different parts of the α_1 subunit, which are targets for alternative splicing. The α_{1B} subunit has been cloned from bovine adrenal chromaffin cells (GenBank AF174417), (Cahill et al. 2000). Currently there is no available clone for the P/Q-type channel expressed in these cells, although this should soon be available (personal communication with Dr J Weiss). It will be interesting to compare the sequences encoded by these cloned channels to identify whether key sites involved in mediating inactivation eluded from studies of recombinantly expressed channels are present or missing.

N and P/Q-type channels have also been shown to be differentially modulated by G proteins. Binding of G-protein $\beta\gamma$ subunits directly to the α_1 subunit shifts gating from a 'willing', readily opened mode, to a 'reluctant' mode of opening (Zamponi and Snutch 1998). Facilitation in current amplitude can occur during trains of action potentials because at depolarised potentials there is a decrease in the affinity of the $\beta\gamma$ channel interaction resulting in disassociation of the $\beta\gamma$ subunit and relief of inhibition. Free $\beta\gamma$ subunits will re-associate with the channel ($\tau < 100$ms) at more negative potentials shifting the channel back towards a reluctant state. However if the frequency of AP firing is fast enough, then $\beta\gamma$ subunits dissociated from one AP will not have time to rebind before the next AP and apparent facilitation of current amplitude occurs (Catterall 2000). The time constant for dissociation of $\beta\gamma$ subunits differs between the two channel types at physiological membrane voltages (Colecraft et al. 2000). Whereas the τ for P/Q-type is relatively constant over a wide range of voltages (-10-+100mV), the N-type τ is significantly slower and only speeds up at potentials > +30mV (Colecraft et al. 2000). During a train of depolarisations autocrine inhibitors are co-released with neurotransmitter. For example, co-released ATP can feed back and inhibit the calcium channels (Currie and Fox 1997; Powell et al. 2000). In chromaffin cells not only is the N-type current inhibited twice as much as the P/Q-type current by ATP (Currie and Fox 1997), but by stepping to +20mV, a degree of inhibition will be lost from $\beta\gamma$ subunit dissociation from P/Q-type channels but not N-type during subsequent pulses in the train. Therefore a greater degree of

inhibition and less relief from inactivation by activation of G-proteins during a train of depolarisations could account for the increased inactivation observed for N-type compared to P/Q in response to this train of depolarisations. However I do not believe that I have a great degree of current inhibition due to negative feedback on the calcium channels by autocrine modulators released during the train as I perfuse at a fast rate (typically $\geq$ 2mls/min), and patch isolated cells. However if a certain percentage of channels are tonically inhibited by $\beta\gamma$ subunits at rest then this train of depolarisations may induce some relief of inhibition for P/Q-type channels but not for N-type, therefore reducing the overall amount of inactivation observed for P/Q-type channels. I could have delivered a double pulse consisting of a prepulse to +100mV and a test pulse to +20mV to assess whether toxin isolated channels possess any basal $\beta\gamma$ subunit voltage-dependent inhibition, or pretreated cells with pertussis toxin to inhibit Gi/o-protein coupled receptors.

5.8 Summary of pharmacologically isolated calcium currents.

Bovine adrenal chromaffin cells express functional P/Q and N-type channels as assessed by current block by specific peptide toxins, ω-Aga IVA (300nM) and ω-CTX GVIA (1μM). I have found no evidence to suggest that they contain a functional L-type current (although I did not specifically look to induce an L-type/facilitation current by applying agonists or strong depolarizing prepulses), which is in accordance with previous work from our lab (Powell 2000) and from the labs of Martha Noweycky, (Engisch et al. 1997) and Arron Fox, (Currie and Fox 1997; Currie and Fox 2002) who conclude that L-type channels are normally quiescent or absent in adult bovine chromaffin cells. The rate of inactivation for toxin isolated currents could be described with a double exponential time-course. There was no difference in the first time constant (τ_1 = 26 or 27 ms), however P/Q-type channels displayed a slower second time constant (τ_2 = 302ms verses 173ms), which corresponds to significantly more calcium entering during a long (800ms) depolarisation (155 $\pm$ 19 x 10^6 Ca^{2+} ions, n = 16 and 225 $\pm$ 25 x 10^6 Ca^{2+} ions, n = 16 for N and P/Q type respectively, p = 0.03). There was also a significant difference in

the reduction of peak current amplitude and calcium entry between the two channel subtypes following a train of brief (10ms) depolarisations at 20Hz.

5.9 Exocytosis evoked by calcium entry through P/Q-type calcium channels is more efficient than through N-type calcium channels.

In response to a control 200ms depolarisation, calcium entry of 246 ± 23 Ca^{2+} ions x 10^6, evoked a ΔC_m of 181 ± 20 fF, n = 11. Calcium entry and ΔC_m through pharmacologically defined N-type channels (toxin isolated and toxin subtracted) was 111 ± 14 Ca^{2+} ions x 10^6 and 55 ± 14 fF, n=11. Calcium entry and ΔC_m through pharmacologically defined P/Q-type channels was 135 ± 22 Ca^{2+} ions x 10^6 and 125 ± 28 fF, n=11. The difference in the reduction in ΔC_m between N and P/Q-type channels was significant (p = 0.04), although the reduction in calcium entry was not. Similarly in response to an 800ms depolarisation control calcium entry of 390 ± 29 Ca^{2+} ions x 10^6, evoked a ΔC_m of 549 ± 61 fF, n = 14. Calcium entry and ΔC_m through pharmacologically defined N-type channels was 158 ± 21 x $10^6 Ca^{2+}$ ions and 160 ± 24 fF, n = 14. Calcium entry and ΔC_m through pharmacologically defined P/Q-type channels was 231 ± 29 x $10^6 Ca^{2+}$ ions and 390 ± 61 fF, n=11. The difference in the reduction in ΔC_m between N and P/Q-type channels was highly significant (p = 0.002), and this time there was also a significant difference in calcium entry (p = 0.05). This suggests that exocytosis is preferentially coupled to P/Q-type channels (figure 5.9.1)..

5.9.1 Exocytosis evoked from calcium entry through N and P/Q-type channels
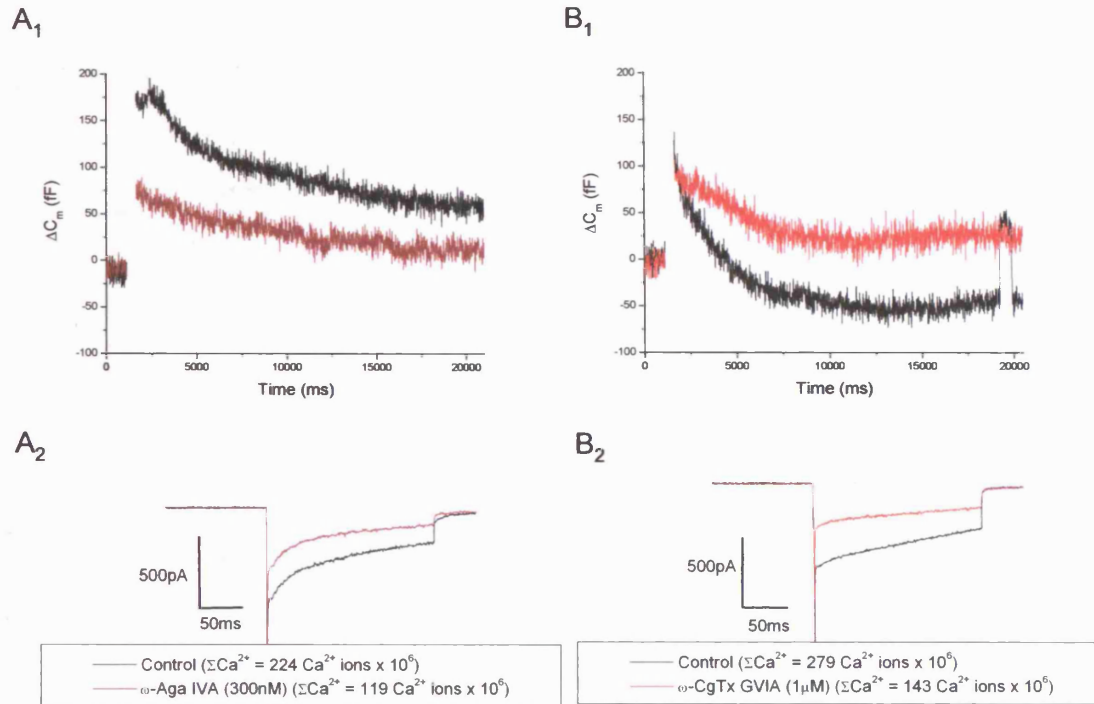
A. A control ΔC_m and calcium current evoked from a 200ms depolarisation (black) and the N-type ΔC_m and calcium current (wine) are overlaid after application of 300nM ω-Aga IVA to block contributions from P/Q-type currents. Calcium entry for this example is indicated below the current trace. Mean calcium entry and ΔC_m for N-type channels is $111 \pm 14 \times 10^6 \, Ca^{2+}$ ions and 56 ± 14 fF, n=11.

B. A control ΔC_m and calcium current evoked from a 200ms depolarisation (black) and the P/Q-type ΔC_m and calcium current (red) are overlaid after application of 1μM ω-CTX GVIA to block contributions from N-type currents. Calcium entry for this example is indicated below the current trace. Mean calcium entry and ΔC_m for P/Q-type channels is $135 \pm 22 \times 10^6 \, Ca^{2+}$ ions and 125 ± 28 fF, n=11. The difference in the reduction in ΔC_m between N and P/Q-type channels was significant (p = 0.04), although the reduction in calcium entry was not.

148
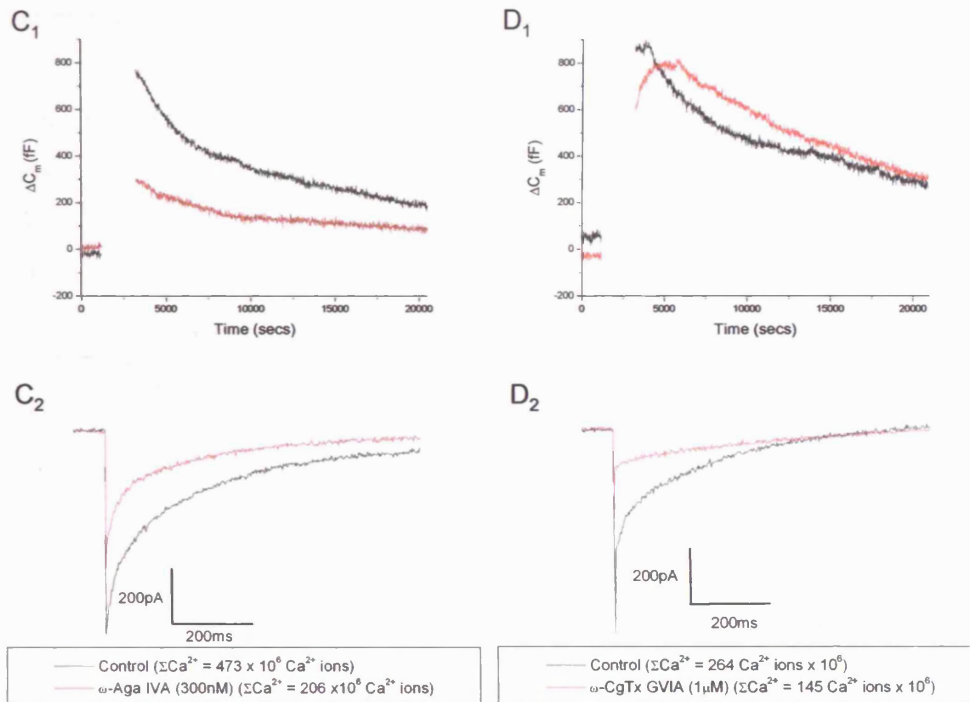
C. A control ΔC_m and calcium current evoked from an 800ms depolarisation (black) and the N-type ΔC_m and calcium current (wine) are overlaid after application of 300nM ω-Aga IVA to block contributions from P/Q-type currents. Calcium entry for this example is indicated below the current trace. Mean calcium entry and ΔC_m for N-type channels is $158 \pm 21 \times 10^6$ Ca^{2+} ions and 160 ± 24 fF, n=14.

D. A control ΔC_m and calcium current evoked from an 800ms depolarisation (black) and the P/Q-type ΔC_m and calcium current (red) are overlaid after application of 1μM ω-CTX GVIA to block contributions from N-type currents. Calcium entry for this example is indicated below the current trace. Mean calcium entry and ΔC_m for P/Q-type channels is $231 \pm 29 \times 10^6$ Ca^{2+} ions and 390 ± 61 fF, n=11. The difference in the reduction in ΔC_m between N and P/Q-type channels is highly significant (p = 0.002), and there is also a significant difference in calcium entry (p = 0.05).

To quantify whether exocytosis is triggered by preferential calcium entry through individual calcium channel subtypes, the mean exocytotic efficiency was calculated. Exocytotic efficiency is calculated as ΔC_m/Ca^{2+} ions x 10^6. Under control conditions, a 200 ms step depolarisation evoked C_m increases with a mean exocytotic efficiency of 0.62 +/- 0.07 fF/ x 10^6 calcium ions, n = 11. The calcium channel toxins exerted different effects on the exocytotic efficiency, such that exocytosis evoked by N-type channels had a mean exocytotic efficiency of 0.47 +/- 0.1 fF/ x 10^6 calcium ions, n = 11. In contrast, calcium entry through P/Q-type channels, evoked exocytosis that was significantly more efficient than the corresponding calcium entry through N-type

149

calcium channels. The mean exocytotic efficiency for P/Q-type channels was 0.80 +/- 0.1 fF/ x 10^6 calcium ions, n = 11. This difference in exocytotic efficiency between N and P/Q-type channels was statistically significant (p = 0.04). Exocytotic efficiency was also significantly greater for P/Q-type channels compared to N-type channels, in response to longer (800ms) and shorter (10ms) depolarisations (figure 5.9.2).

5.9.2 Exocytotic efficiency of N and P/Q-type channels.
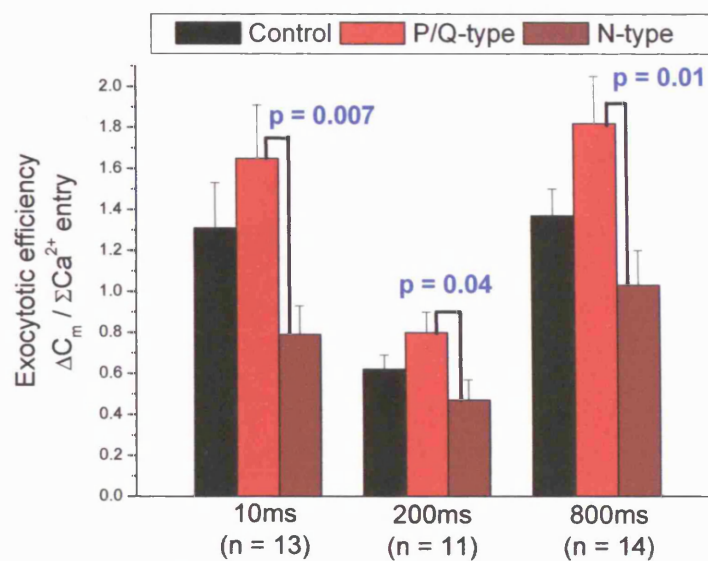
Exocytotic efficiency was calculated as $\Delta C_m/Ca^{2+}$ ions x 10^6. In response to a 10ms depolarisation exocytotic efficiency was 1.31 ± 0.22, for control cells. The exocytotic efficiency was reduced for N-type channels, 0.79 ± 0.14, and increased for P/Q-type channels 1.65 ± 0.26, n = 13. The difference between N and P/Q-type channels is highly significant, p = 0.007. In response to a 200ms depolarisation exocytotic efficiency was 0.62 ± 0.07, for control cells. The exocytotic efficiency was reduced for N-type channels, 0.47 ± 0.10, and increased for P/Q-type channels 0.80 ± 0.10, n = 11. The difference between N and P/Q-type channels is significant, p = 0.04. In response to an 800ms depolarisation exocytotic efficiency was 1.37 ± 0.17, for control cells. The exocytotic efficiency was reduced for N-type channels, 1.03 ± 0.17, and increased for P/Q-type channels 1.82 ± 0.23, n = 14. The difference between N and P/Q-type channels is significant, p = 0.01.

5.10 P/Q-type channels couple to exocytosis more efficiency than N-type in response to a train of depolarisations.

It was next assessed whether exocytosis was preferentially coupled to P/Q-type channels in response to a more physiological stimulus. Exocytosis was evoked by a

150

train of 10ms depolarisations delivered at 20Hz. ΔC_m was reduced 59.5 % with a reduction in calcium entry of 34.1% after application of 300nM ω-Aga IVA, p = 0.04. In contrast application of 1μM ω-CTX GVIA reduced ΔC_m 3.3% and calcium entry 30.3 %. This ΔC_m was not considered significant (figure 5.10.1). Therefore P/Q-type channels couple to exocytosis more efficiently than N-type channels in response to a train of brief (10ms) depolarisations.

5.10.1 ω-Aga-IVA inhibits stimulus-coupled secretion evoked from a train of depolarisations more efficiently than ω-CTX GVIA.

A.
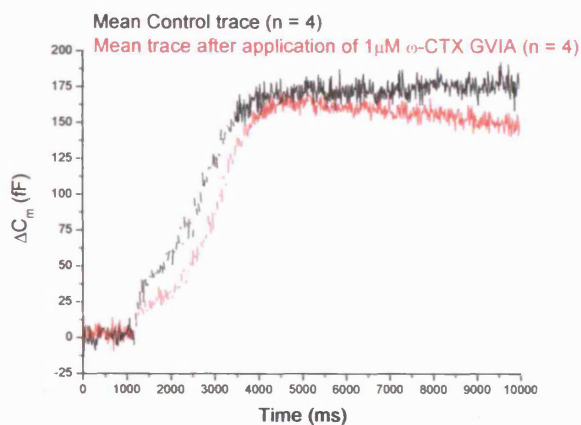
B.
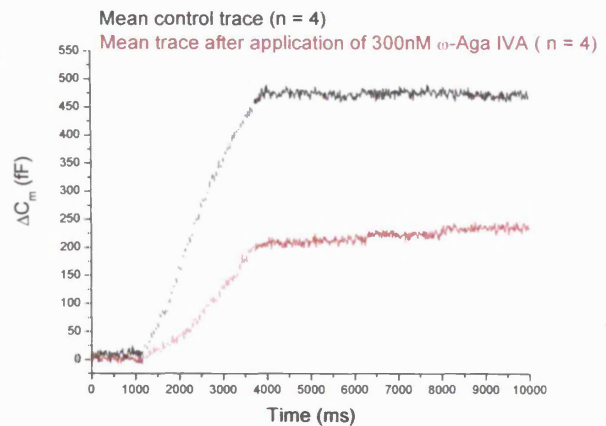
A. Mean capacitance trace before (black) and after application if 1μM ω-CTX GVIA (red). Despite reducing calcium entry, (236 ± 39 to 165 ± 36 x 10^6 Ca^{2+} ions), blocking N-type calcium channels does not significantly reduce the cumulative ΔC_m evoked by a train of 50, 10ms depolarisations at 20Hz. ΔC_m reduced from 150 ± 17 to 145 ± 41 fF, n = 4.
B. Mean capacitance trace before (black) and after application of 300nM ω-Aga IVA (wine). Blocking P/Q-type calcium channels does significantly reduce the cumulative ΔC_m evoked by a train of 50, 10ms depolarisations at 20Hz. ΔC_m reduced from 472 ± 83 to 191 ± 7 fF, n = 4, p = 0.04

It was shown in chapter 4, (figure 4.75) that in control cells exocytosis is related to calcium entry with a power ≤2. It was next investigated whether exocytosis evoked by the different channel subtypes retained the same function of integrated calcium found for control cells. Plotting the cumulative ΔC_m during a train from a single cell against calcium entry before and after toxin application resulted in curves that could be using the equation $\Delta C_m = \mathbf{g} * (\Delta Ca^{2+})^{\mathbf{x}}$. Data from 8 cells (4 before and after

application of 1μM ω-CTX GVIA and 4, before and after application of 300mM ω-Aga IVA) were fit with the alogarithm. The best fit for control cells before application of ω-Aga IVA resulted in a mean proportionality constant $g = 0.07$ and power $x = 1.56$ and after toxin addition this changed to $g = 0.002$ and $x = 2.24$, n=4. The power value obtained by fitting data from individual cells with the alogarithm after toxin application ranged from $x = 2.16$ to 2.42. The best fit for control cells before application of ω-CTX GVIA resulted in a mean proportionality constant $g = 0.04$ and power $x = 1.50$ and after toxin this changed to $g = 0.13$ and $x = 1.36$, n=4. The power value obtained by fitting data from individual cells with the alogarithm after toxin application ranged from $x = 1.25$ to 1.68 (figure 5.10.2). Therefore the calcium-dependency of exocytosis is raised for N-type channels compared to P/Q-type. This may occur because with long pulses more calcium enters through P/Q-type channels compared to N-type channels. Sustained depolarisations will result in exocytosis dominated by release from the SRP and release from the SRP may have a lower calcium dependency of exocytosis (discussed chapter 4, section 4.2.7). In both control groups the first few pulses in the train deviate from the best fit curve and I have attributed this to reflect fusion of the IRP, (discussed in section 4.2.4). As can be seen in figure 5.10.2, exocytosis triggered by calcium entry through P/Q-type channels retains a 'hump' that deviates from the best fit line at the start of the train whereas ΔC_m evoked by calcium entry through N-type channels does not. This implies that P/Q-type channels preferentially couple to the IRP. This was further investigated by analyzing data from the pool protocol.

5.10.2 The calcium-dependency of exocytosis is raised for N-type channels.
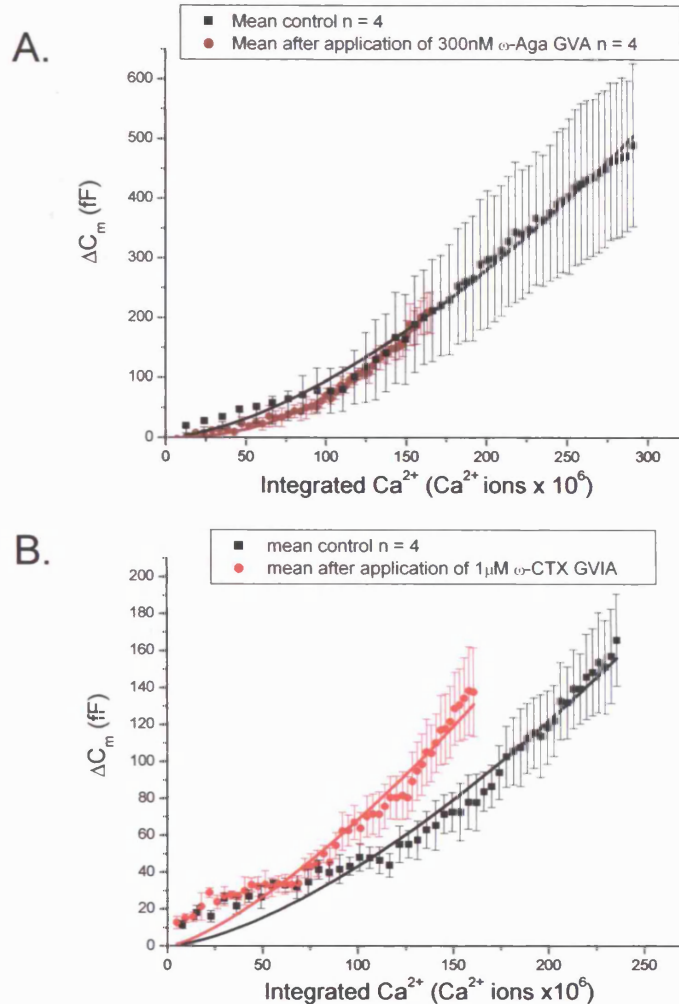
Cumulative capacitance is plotted against cumulative integrated calcium and fit with the equation $\Delta C_m = g * (\Delta Ca^{2+})^x$. Data points represent the mean $\Delta C_m \pm$ s.e.m. The curve was constrained to pass through Y = 0 at 0 calcium entry.

A. In control cells (black) the mean proportionality constant $g = 0.07$ and power $x = 1.56$, $n = 4$. There is a slight deviation from the best fit line at the start of the train. After application of 300nM ω-Aga-IVA (wine) the power function increases to a mean value $x = 2.24$, $n = 4$. There is no longer a deviation from the best fit line at the start of the train.

B. In control cells (black) the mean proportionality constant $g = 0.04$ and power $x = 1.50$, $n = 4$. There is a large deviation from the best fit line at the start of the train. After application of 1μM ω-CTX GVIA (red) the power function decreases to a mean value $x = 1.36$, $n = 4$. The deviation from the best fit line at the start of the train is retained.

Exocytosis was more efficient for P/Q-type than N-type in coupling to secretion in response to the pool protocol (6 x 10ms, 4 x 100ms). In control cells the ΔC_m after

153

the first 6 (10ms) pulses was 30 ± 7 fF, n = 3, reduced after application of 1μM ω-CTX GVIA to 25 ± 15 fF n = 3. In contrast, control cells had a mean ΔC_m of 65 ± 19 fF, n =3 reduced after 300nM ω-Aga IVA to only 5 ± 3 fF n=3. Similarly the ΔC_m at the end of the train was 265 ± 62 fF, n = 3 for control cells, reduced to 242 ± 90 fF after application of 1μM ω-CTX GVIA, n = 3 and a ΔC_m of 165 ± 4 fF, n =3 for control cells reduced to 60 ± 29 fF after application of 300nM ω-Aga IVA, n = 3 (figure 5.10.3). There is practically no exocytosis in response to the first 6 (10ms) depolarisations after P/Q-type channels have been blocked suggesting that P/Q-type channels alone mediate release from the IRP.

5.10.3 P/Q-type channels couple more efficiency to exocytosis evoked by the pool protocol.
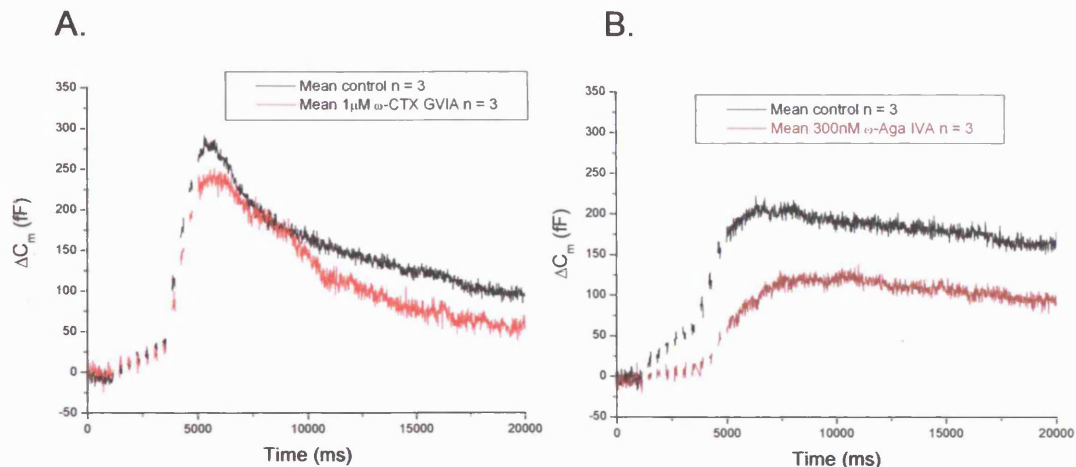
The pool protocol is, 6, 10ms depolarisations with an interpulse interval of 390ms immediately followed by 4, 100ms depolarisations with an interpulse interval of 300ms.
A. The mean capacitance trace from 3 cells before (black) and after application of 1μM ω-CTX GVIA (red). The ΔC_m after the first 6 (10ms) pulses was 29 ± 7 fF, n = 3, reduced after application of 1μM ω-CTX GVIA to 25 ± 15 fF n = 3. The ΔC_m after pulse 10 was 265 ± 62 fF, n = 3 for control cells, reduced to 242 ± 90 fF after application of 1μM ω-CTX GVIA, n = 3.
B. The mean capacitance trace from 3 cells before (black) and after application of 300nM ω-Aga IVA (wine). The ΔC_m after the first 6 (10ms) pulses was 65 ± 19 fF, n = 3, reduced after application of 300nM ω-Aga IVA to 5 ± 3 fF n = 3. The ΔC_m after pulse 10 was 165 ± 4 fF, n = 3 for control cells, reduced to 60 ± 29 fF after application of 1μM ω-CTX GVIA, n = 3.

154

5.11 Release from the IRP is more efficient through P/Q-type channels.

In chapter 4 (figure 4.2.5), the double pulse protocol was used to determine the size of the IRP. It was not possible to accurately determine the size of the IRP when P/Q-type channels were blocked, as the majority of cells failed to evoke a ΔC_m in response to the first 10ms pulse. Therefore one can conclude that calcium entry through N-type channels does not couple to the IRP. Also the size of the IRP calculated using the double pulse was not significantly different from control after application of ω-CTX GVIA (38 ± 2 fF n = 4, 30 ± 3 fF n = 4, p = 0.08), indicating that fusion from the IRP is mediated solely by P/Q-type channels.

5.12 Discussion of exocytosis experiments.

Unlike fast synapses where calcium channels are thought to very closely associate and even physically interact with vesicles, it was traditionally thought that the relationship between calcium channels and secretory vesicles in chromaffin cells was much looser, with the distance between calcium channels and the majority of vesicles much larger (~300nm), (Klingauf and Neher 1997; Neher 1998). However a subset of vesicles may well be closer to the channels, as a recent imaging study suggests that calcium microdomains selectively trigger release of fusion-competent granules that are docked within 300nm (Becherer et al. 2003).

With brief depolarisations, endogenous buffers are believed to spatially restrict calcium entry to within 1μm of the plasma membrane in chromaffin cells (Marengo and Monck 2000; Marengo and Monck 2003). This suggests that only vesicles that are fusion-competent and very close to the source of calcium entry will fuse in response to a 10ms depolarisation. Such a pool of vesicles has been described as the IRP (Horrigan and Bookman 1994; Voets et al. 1999). I find that this pool of vesicles is preferentially coupled to P/Q-type channels. This is slightly surprising given the results of single channel studies conducted on these cells. Analysis of single channel recordings show that N-type calcium channels have a larger conductance and longer mean open time than P/Q-type channels (A.D.Powell, unpublished observation). If

155

calcium channels and docked, primed vesicles are randomly distributed in the plasma membrane one would expect N-type channels to be more efficient than P/Q-type channels at evoking stimulus-coupled secretion in response to brief depolarisations. As this is not the case, it may suggest that vesicles are able to dock closer to P/Q-type channels than N-type, or that P/Q-type channels cluster together, increasing the size of the calcium microdomain, or that P/Q-type channels are closer to specific release sites in the membrane. There is evidence to suggest that secretion is spatially mapped to hot spots of calcium entry in chromaffin cells (Robinson et al. 1995). In this study they mapped sites of calcium entry using a pulsed-laser system to sites of release determined from amperometric detection of catecholamine secretion. They did not use calcium channel toxins to discriminate whether specific channel subtypes preferentially couple to this localised secretion. Biochemical studies in neuroendocrine cells suggests that SNARE proteins necessary for secretion are localised to lipid rafts, maybe allowing spatial regulation of exocytosis (Chamberlain et al. 2001). Recently it has been shown that P/Q-type channels co-localise with SNARE protein complexes within lipid microdomains in rat brain (Taverna et al. 2004). Additionally palmitoylation of some proteins results in localization to lipid rafts. The β_{2a} subunit is palmitoylated and is present in bovine adrenal chromaffin cells (Cahill et al. 2000) and inhibition of palmitoylation by tunicamycin increases steady state inactivation in chromaffin cells (Hurley et al. 2000). There is growing evidence to suggest that spatial regulation by inclusion or exclusion from lipid rafts is an important regulator of exocytosis. Agents that disrupt lipid rafts have been shown to inhibit exocytosis (reviewed in Salaun et al. 2004). Therefore in chromaffin cells P/Q-type channels may specifically co-localise with the secretory machinery within lipid rafts. The co-localisation of SNARE's and P/Q-type channels in raft domains may contribute to the increased exocytotic efficiency observed for P/Q-type channels compared to N-type, particularly in response to brief depolarisations.

Other groups may have missed this preferential coupling in response to brief stimuli due to the high concentration of extracellular calcium in their recording system (ie Lukyanetz and Neher 1999, used 60mM extracellular calcium). With a low concentration of extracellular calcium, calcium ions entering through channels distant

156

to the vesicles will be effectively sequestered by local endogenous buffers. Only vesicles close to the channel will fuse. With high extracellular calcium, calcium ions entering through distant channels will saturate local buffers and therefore be able to fuse these vesicles. Our observation is in good agreement with another study, which used a low concentration of extracellular calcium and concludes that P/Q-type channels are coupled more tightly to exocytotic active sites than other channel subtypes (Lara et al. 1998).

As pulse duration increases, or during a train of depolarisations, local buffers will start to saturate and the calcium gradient will spread from discrete hotspots to a ringlike pattern beneath the plasma membrane (Robinson et al. 1995; Marengo and Monck 2000; Marengo and Monck 2003). Therefore vesicles, which are further away from sites of calcium entry and are fusion-competent, will be able to sense the increase in calcium and fuse. In the case of the train of depolarisations, after the first few pulses, which deplete the IRP, one would then expect N-type channels to become as efficient as P/Q-type channels in evoking release as intracellular calcium levels will rise fairly uniformly and vesicles will fuse regardless of whether a more or less efficient channel subtype is being activated. Also vesicles from the SRP are likely to be released, and the SRP has a lower dependency on calcium than the RRP (Sudhof 2004). Therefore exocytosis will be less dependent on the site of calcium entry and more dependent on total intracellular calcium concentration. However as the train of depolarisations progresses or the length of a single step depolarisation increases, N-type channel inactivation also significantly increases limiting calcium entry. This is observed nicely at the single channel level, with P/Q-type channels flickering open and shut for the duration of a long single pulse. N-type channels open at the start of the depolarisation, albeit with a longer mean open time, but then rapidly inactivate, resulting in very little activity by the end of the pulse (A.D. Powell unpublished observation).

Therefore I propose that the enhanced exocytotic efficiency and lowered calcium-dependency of exocytosis observed for P/Q-type channels results initially from preferential coupling to release sites/fusion-competent vesicles and secondly from a slower rate of channel inactivation compared to N-type channels.

There is a lot of disparity in the literature regarding whether certain subtypes of voltage-gated calcium channels preferentially couple to release from chromaffin cells. This inconsistency could arise from differences in stimulus paradigms.

The use of particular stimulations are likely to dictate the involvement of a given channel subtype in secretion. Stimulations which cause recruitment of channels through facilitation or inhibition of channels through inactivation may alter the degree to which a channel can couple and participate in eliciting secretion. For example (Artalejo et al. 1994) propose that L-type channels couple most efficiently to exocytosis in calf chromaffin cells, but in this study the facilitation/L-type channel was recruited prior to stimulation by applying a train of depolarizing pre-pulses or agents that raise intracellular cAMP. The facilitation channel is normally quiescent in calf cells until recruitment (Artalejo et al. 1994) and non-functional or surreptitious in adult bovine chromaffin cells (Engisch and Nowycky 1996; Currie and Fox 1997). Alternatively, (Lopez et al. 1994), using cultured bovine chromaffin cells propose a role for Q and L–type but not N-type channels in secretion. Secretion was induced in this study by application of a depolarising high potassium solution for 10 seconds. N-type channels inactivate quicker than Q or L-type, therefore their experiments will highlight the role of slowly or non-inactivating channels in the participation of sustained secretion.

Recording in the voltage clamp configuration has the advantage of allowing us to accurately measure calcium influx through voltage-gated calcium channels and to relate this calcium influx to the amount of secretion observed. We can also detect whether there is a preferential coupling of one channel subtype over the others to elicit secretion. However the physiological stimulus to elicit exocytosis is action potential (AP) firing. There are many different ionic channels contributing to the size and duration of the AP, and some of these conductances are calcium-regulated. It may be that certain calcium channel subtypes preferentially spatially couple to these calcium-regulated conductances while others are located to specific sites of release. In voltage clamp experiments only the importance of the latter will be assessed. If one was to perform current clamp experiments other channel subtypes may become

158

more dominant in regulating secretion, by affecting the duration of the AP. Studies have shown that in hippocampal neurones N-type calcium channels are co-localised with BK channels and activation of BK channels is only triggered by calcium influx through N-type calcium channels and not P/Q-type (Marrion and Tavalin 1998).

5.13 Endocytosis following toxin application.

It was observed following single step depolarisations (particularly 200ms depolarisations) that the rate of endocytosis was slowed after toxin (either ω-Aga IVA or ω-CTX GVIA) application (figure 5.9.1). I have previously characterized endocytosis in these cells and have shown in agreement with other studies (Neher and Marty 1982; Smith and Neher 1997; Engisch and Nowycky 1998) that increasing calcium increases the rate of endocytosis (section 4.4). Therefore the reduced rate in endocytosis is likely to reflect less calcium entry after toxin application. Previous work in our lab has investigated this possibility by reducing calcium entry proportionally to the reduction induced by toxin application with cadmium and monitoring the rate of endocytosis. These experiments conclude that the calcium channel toxins inhibit membrane retrieval to a similar extent as would be predicted by a simple reduction in calcium entry (Powell 2000).

However in these experiments cesium-based pipette solutions were used which would deplete the cell of intracellular potassium and inhibit clathrin-mediated endocytosis (Larkin et al. 1983; Heuser and Anderson 1989; Wu et al. 2001, see figure 4.4.9) therefore only examining the contributions of clathrin-independent endocytosis. Key regulators of clathrin-mediated endocytosis have been shown to directly interact with calcium channels (Chen et al. 2003). Disruption of an endophilin-N-type calcium channel interaction significantly reduces endocytosis (Chen et al. 2003). Although these authors show biochemically that endophilin is also capable of binding to P/Q-type channels the functional consequence of this interaction has not been examined. Differences in mediating endocytosis may occur, especially if splice-variants lacking the endophillin binding site are expressed in chromaffin cells. Therefore an examination of endocytosis after toxin application using pipette solutions permissive

to clathrin-mediated endocytosis may result in a preferential coupling between membrane retrieval and a particular calcium channel subtype. This possibility has not been explored.

Chapter 6: Molecular mechanisms underlying N-type calcium channel inactivation

6.1 Putative mechanisms underlying inactivation.

I have shown in bovine adrenal chromaffin cells that exocytosis is preferentially coupled to P/Q-type channels and that N-type channels inactivate quicker and to a greater extent than P/Q-type channels (chapter 5). Therefore it was deemed important to assess differences in the mechanisms of inactivation between the two channel subtypes. Several sites on the α_1 pore of Ca_V2 family channels (which include N and P/Q-type channels) have been implicated in regulating channel inactivation properties. These include regulation by G proteins, protein kinases, SNARE proteins, association of different β subunits and calcium (see introductory chapter and discussion in chapter 5 for review of the literature pertaining to this). Differential regulation by one or more of these modulators could result in enhanced inactivation of N-type channels and subsequently limit the channels ability to support stimulus-coupled secretion. In this chapter I investigate the role of calcium-dependent inactivation in mediating the inactivation of the two channel subtypes and explore the molecular mechanisms underlying this form of channel regulation.

6.2 Calcium-dependency of inactivation

The calcium-dependency of inactivation of total calcium currents was first examined by cation substitution, intracellular dialysis with calcium chelators and by employing a double pulse protocol to probe inactivation after long pulses to various membrane potentials. A train of depolarisations (50 x 10ms, from −80mV to +20mV at 20 Hz) results in pronounced inactivation. Fractional inactivation was determined by dividing the peak of the calcium current of each pulse by the peak calcium current of the 1st pulse in the train. In perforated patch control cells the mean inactivation by the 50th pulse was 0.45 ± 0.02, n = 20. Equimolar replacement of extracellular

calcium with barium attenuated the level of fractional inactivation to 0.86 ± 0.03, n = 3, p < 0.0001 (figure 6.2.1a). Responses to a single 200ms depolarisation show that inactivation is quicker in calcium than in barium. % inactivation was derived from the following equation, $100-(I_{End}/I_{Peak})\times100$, where I_{End} is the current remaining after 199ms (1ms from the end of the pulse to avoid contamination from tail currents) and I_{Peak} is the peak amplitude found after 3ms (to avoid contamination from sodium currents). Under perforated conditions with extracellular calcium the % inactivation over a 200ms depolarisation is 54.4 ± 1.9, n = 43, reduced to 9.2 ± 3.6, n = 6, p < 0.0001, following equimolar barium replacement (figure 6.2.1a). In chapter 3 (figure3.2.2), I show that replacing calcium with barium induces a 10mV negative shift in the I/V relationship. Although the peak amplitude of the current was increased, I found no significant difference in the amount of inactivation detected from barium currents in response to either single pulses, or trains of depolarisations when the step potential was at +20mV (the standard depolarizing potential), compared to a step potential of +10mV. Therefore for the remainder of my studies I maintained the same step potential (+20mV) regardless of which divalent was being employed. In whole cell experiments increasing the concentration of BAPTA in the electrode solution from 0.3mM to 10mM decreased fractional inactivation from 0.42 ± 0.03, n = 7 with 0.3mM BAPTA to 0.74 ± 0.03, n = 5 with 10mM BAPTA, p < 0.0001. Similarly inactivation in response to a single 200ms depolarisation was greatly reduced from 45.1 ± 5.5 %, n = 7 for 0.3mM BAPTA to 29.7 ± 1.7, n = 3, p = 0.04 for 10mM BAPTA. Therefore cation substitution and intracellular dialysis with calcium chelators reveal a calcium-dependent component to the inactivation of the total calcium current (figure 6.2.1).

6.2.1 Calcium-dependent inactivation investigated by examining cation substitution and intracellular dialysis with calcium chelators.
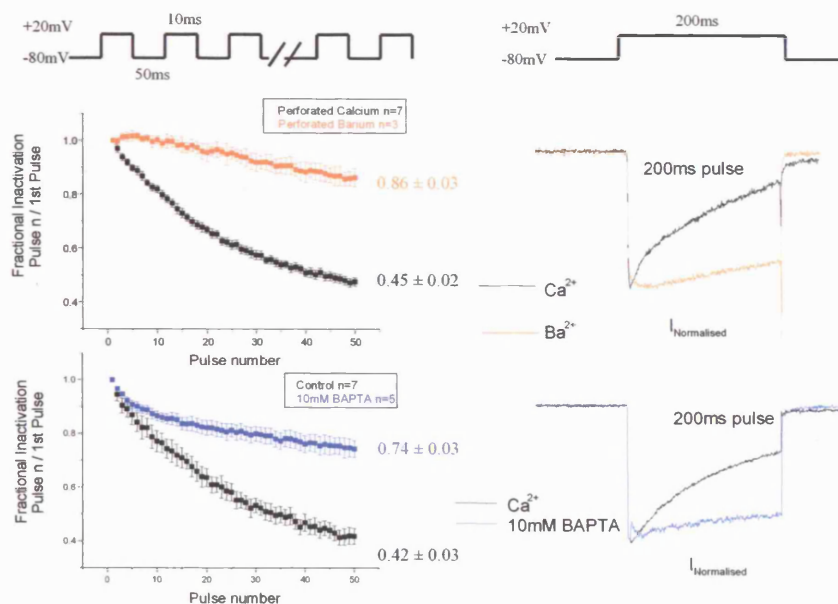
Fractional inactivation was determined by dividing the peak current (after 3ms to exclude contributions from sodium currents) of each pulse in the train by the peak current of the first pulse. % inactivation is a measure of how much the current inactivates during the course of the train. Each point is the mean ± s.e.m.

A. The left panel shows mean data from the train protocol in the perforated patch configuration with either calcium (black) or barium (orange) as the extracellular divalent charge carrier. The mean fractional inactivation of the 50th pulse was 0.45 ± 0.02, n =20 for calcium, attenuated to 0.86 ± 0.03 n=3, p <0.0001 when extracellular calcium was replaced with equimolar barium. The right panel shows typical current traces in response to a 200ms depolarisation with calcium, % inactivation 54.4 ± 1.9, n = 43 (black) or 9.2 ± 3.6, n = 5, p < 0.0001 with barium as the external divalent charge carrier (orange).

B. The left panel shows mean data from the train protocol in the whole cell configuration with either 0.3mM (black) or 10mM (blue) BAPTA in the intracellular pipette solution. The mean fractional inactivation of the 50th pulse was 0.42 ± 0.03, n = 7 with 0.3mM intracellular BAPTA, and 0.74 ± 0.03 with 10mM intracellular BAPTA, n=5. The right panel shows typical current traces in response to a 200ms depolarisation with 0.3mM BAPTA (black) and 10mM BAPTA (blue). In response to a single 200ms depolarisation inactivation was greatly reduced with 10mM BAPTA in the patch pipette, % inactivation 45.1 ± 5.5, n = 7 for 0.3mM BAPTA and 29.7 ± 1.7, n = 3 for 10mM BAPTA.

Next the voltage dependence of inactivation was investigated. A U-shaped voltage dependence of inactivation which parallels calcium entry has been described as a way to detect calcium-dependent inactivation (Jones 1999), (although see Patil et al. 1998; Gera and Byerly 1999). At strongly depolarised voltages (ie +60mV), the apparent

reversal potential for calcium, in these experiments is exceeded and there is no net inflow of calcium (see I/V fig 4.2.1 chapter 4). The fractional inactivation resulting from a prepulse to +20mV is 0.36 ± 0.01, n = 3, reduced to 0.52 ± 0.02, n = 3, p = 0.001 when the prepulse potential is +60mV. Therefore the voltage dependence of inactivation parallels calcium entry and provides further support for a calcium-dependent component to the inactivation of calcium channels in bovine adrenal chromaffin cells (figure 6.2.2).

6.2.2 Voltage dependence of inactivation after a long prepulse.
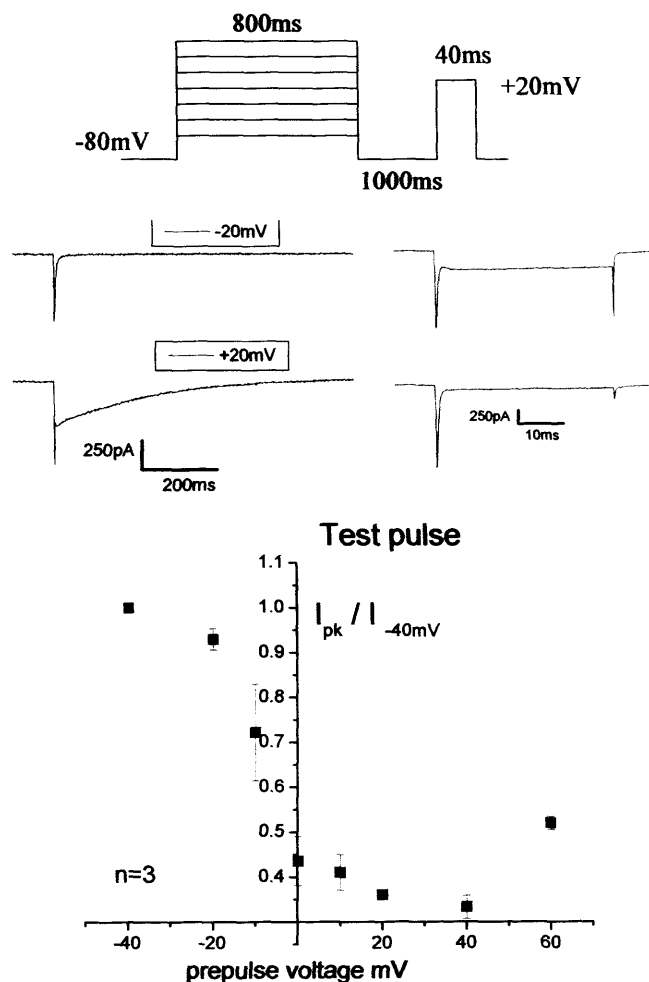
The protocol consists of applying an 800ms prepulse from a holding potential of -80mV to a range of potentials from -40mV to +60mV, followed a second later by a brief (40ms) test pulse from -80mV to +20mV. The top panel shows sample traces (prepulse and corresponding test pulse) in response to a prepulse of either -20mV or +20mV. Fractional inactivation of the test pulse (compared to a test pulse after a prepulse at -40mV) is plotted against the membrane voltage of the prepulse. The level of inactivation decreases at strongly positive potentials (ie +60mV), therefore decreasing in parallel with calcium entry.

6.3 Calcium-dependency of recovery from inactivation

I have previously shown that recovery from channel inactivation occurs mono-exponentially with a τ of 3.3 seconds (chapter 3, figure 3.5.2). The calcium dependency of recovery from inactivation was next investigated. The group of Professor Catterall has monitored the calcium-dependency of recovery of recombinantly expressed channels by applying a train of brief test pulses after a long inactivating prepulse (Lee et al. 1999; Lee et al. 2000). I used an 800ms prepulse from -80mV to + 20mV to completely inactivate all the calcium channels (figure 6.3.1a and b) followed by a train of 30, 10ms pulses to +20mV. Initially experiments were conducted with an interpulse duration of 500ms. However it was noted that full recovery was not possible with this protocol, as a steady state inactivation remained un-recovered. Under perforated patch recording configuration the mean fractional recovery (determined by dividing the peak of each pulse in the train by the peak of the prepulse) at the end of the train was 0.65 ± 0.05, n = 6 (figure 6.3.1c). It was experimentally observed that an interpulse duration of 2000ms was required before full recovery was observed using this protocol (figure 6.3.1d). By simultaneously monitoring intracellular calcium levels with the ratiometric dye fura-2, it was noted that intracellular calcium was maintained at an elevated level for the duration of the protocol when the interpulse duration was 500ms (figure 6.3.1e). Therefore one explanation for incomplete recovery could be that maintained, elevated calcium levels keep a fraction of the channels inactivated. Alternatively, the steady state inactivation observed could be due to slow recovery from voltage dependent processes. To investigate this possibility extracellular calcium was replaced with barium. (In this case it should be noted that a greater degree of inactivation occurs during the 800ms prepulse with calcium). Although there is a difference in the rate of recovery at the start of the protocol, the first current had a fractional recovery of 0.23 ±0.03, n = 6 in calcium and 0.59, n = 2 in barium this probably represents recovery from the calcium-dependent component of inactivation induced during the prepulse as the final pulse fractional inactivation was identical under both conditions, 0.65 ±

0.05, n = 6 in calcium and 0.65, n = 2 in barium. Therefore it seems more probable that slow voltage dependent inactivation (Hering et al. 2000; Degtiar et al. 2000) initiated by the 800ms prepulse is the rate limiting factor in determining full recovery. Recovery in calcium shows two components, a fast recovery which coincides with a fall in cytoplasmic calcium (figure 6.3.1 e&f) and then the same steady state inactivation observed with barium. So although a component to recovery is calcium-dependent, it seems that relatively high cytosolic levels are required to inhibit or slow recovery and that after a long (800ms) prepulse a significant proportion of the channels enter a slow voltage inactivated state which is the rate limiting step. In the previous studies which used this protocol (Lee et al. 1999; Lee et al. 2000), test pulses were delivered at 0.2Hz and recovery monitored over a time period of minutes. The calcium channels in my cells completely recover from inactivation within 10 seconds (chapter 3, figure 3.5.2). This illustrates that protocols designed to test channel function in recombinant expression systems cannot automatically be applied to studies of native channels *in situ*, in which the intracellular environment is not as easily controlled and many separate processes can feed into the overall process.

6.3.1 Calcium-dependency of recovery from inactivation.
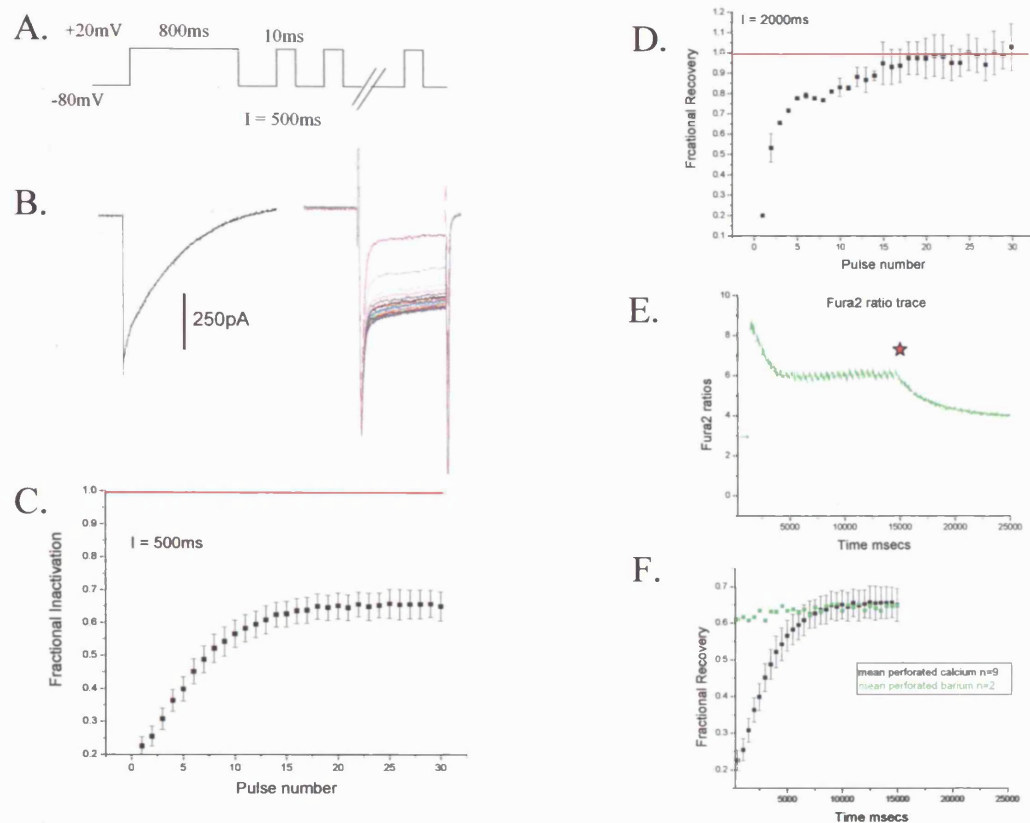
A. Recovery protocol, after an 800ms depolarisation to completely inactivate the calcium channels, a total of 30, 10ms depolarisations were elicited every 500ms.

B. (left) the 800ms prepulse, (right) traces of the 10ms pulses, the brown trace is the first and therefore most inactivated.

C. A plot showing the recovery from inactivation, 100% recovery is not achieved in the time this protocol runs for. The fractional recovery at the 30th pulse is 0.65 ± 0.05, n = 6.

D. It was experimentally found that the interval between pulses had to be increased to 2000ms before complete recovery was observed. The red horizontal line in C and D indicates full recovery.

E. A typical fura 2 ratio (340/380) trace (I = 500ms), note that an 800ms depolarisation induces a large increase in the fura-2 ratio indicative that cytosolic calcium levels have increased in response to this stimulus. The trace suggests that intracellular calcium levels then begin to fall, but are kept elevated compared to resting for the duration of the protocol. The star indicates the time when the protocol finished and the cell was allowed to rest.

F. The calcium dependency of recovery was determined by comparing recovery with either calcium or barium as the extracellular divalent charge carrier. Using the protocol with an interpulse interval of 500ms there is a significant difference between calcium and barium at the start of the recovery train. The first current had a fractional recovery of 0.23 ±0.03, n = 6 in calcium and 0.59, n = 2 in barium. However by the end of the train in both conditions the final pulse fractional inactivation was identical, neither condition resulted in full recovery, 0.65 ± 0.05, n = 6 in calcium and 0.65, n = 2 in barium.

6.4 N-type channels display robust calcium-dependent inactivation.

Once it had been determined that the total calcium current in bovine adrenal chromaffin cells inactivated with a calcium-dependent component, we wanted to assess whether the altered rate of inactivation observed between N and P/Q-type channels was due to differential sensitivity to calcium-dependent inactivation. Channel subtypes were pharmacologically isolated using specific toxins (described in chapter 5). A train of depolarisations (50 x 10ms, from -80mV to $+20$mV at 20 Hz) was then applied to assess inactivation. Figure 6.4.1 shows that replacing extracellular calcium for equimolar barium unmasks a pronounced calcium-dependence to the inactivation of N-type currents (mean fractional inactivation at pulse 50 of 0.25 ± 0.07, $n = 10$ in calcium, which was reduced to 0.89 $n = 2$ in barium), in contrast a smaller calcium-dependent component to the inactivation of P/Q-type currents is detected (mean fractional inactivation at pulse 50 of 0.60 ± 0.05, $n = 10$ in calcium, reduced to 0.85, $n = 2$ in barium). N-type channels display rapid and pronounced inactivation in response to a single 200ms depolarisation in calcium, inactivating $60.3 \pm 7.2\%$ $n = 15$, but are practically non-inactivating in barium, 2.3 % $n = 2$. With P/Q-type channels, the difference in inactivation after changing divalents is significant but less severe than that observed with N-type channels. The currents inactivated 47.1 ± 5.9 % $n = 15$ in calcium and 16.2 ± 3.3 %, $n = 5$, ($p = 0.01$) in barium (figure 6.4.2). This implies that both channels are susceptible to calcium-dependent inactivation, but N-type channels display more sensitivity.

6.4.1 Calcium-dependent inactivation of N and P/Q-type calcium channels in response to a train of depolarisations.
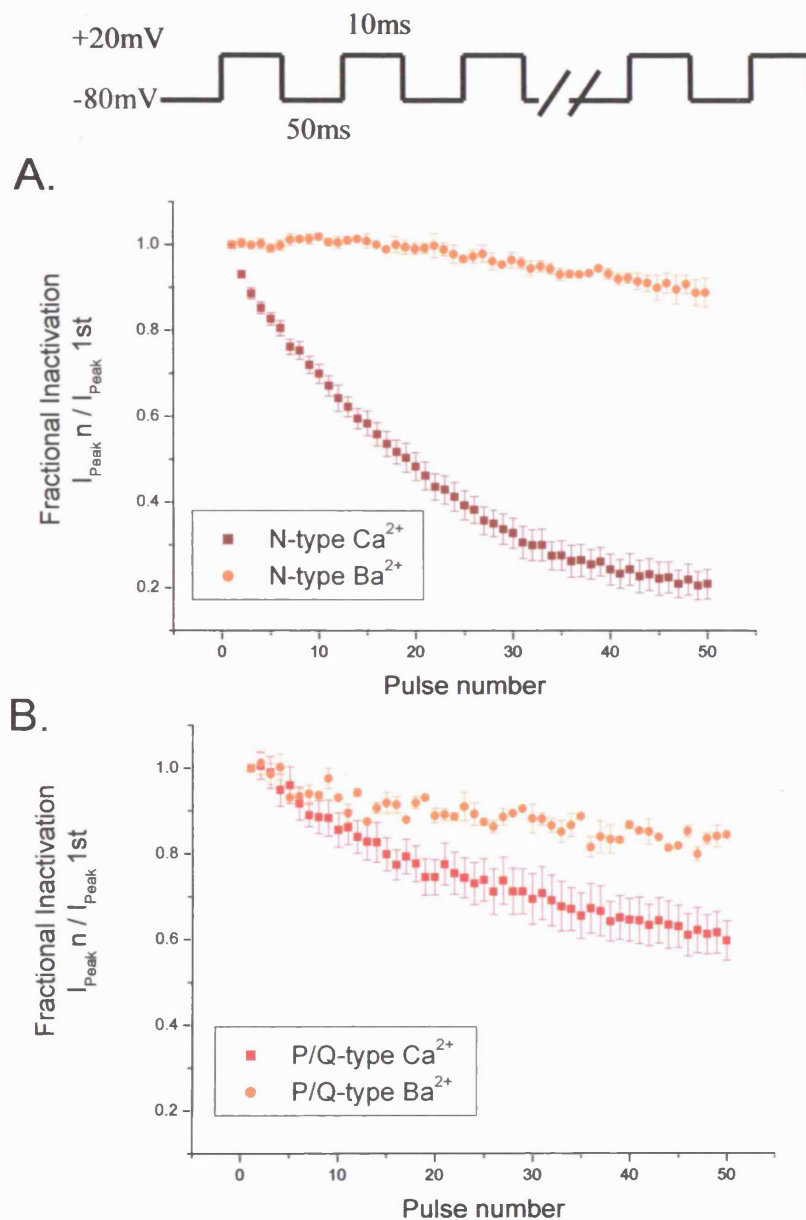
A. In response to a train of depolarisations N-type channels display robust inactivation in calcium (wine). Mean fractional inactivation at pulse 50 of 0.25 ± 0.04, n = 10, which was reduced to 0.89 n = 2 when extracellular calcium was replaces with equimolar barium (orange).
B. P/Q-type channels had a mean fractional inactivation at pulse 50 of 0.60 ± 0.05, n = 10 in calcium (red), reduced to 0.85, n = 2 in barium (orange).

6.4.2 Calcium-dependent inactivation of N and P/Q-type calcium channels in response to a 200ms depolarisation.
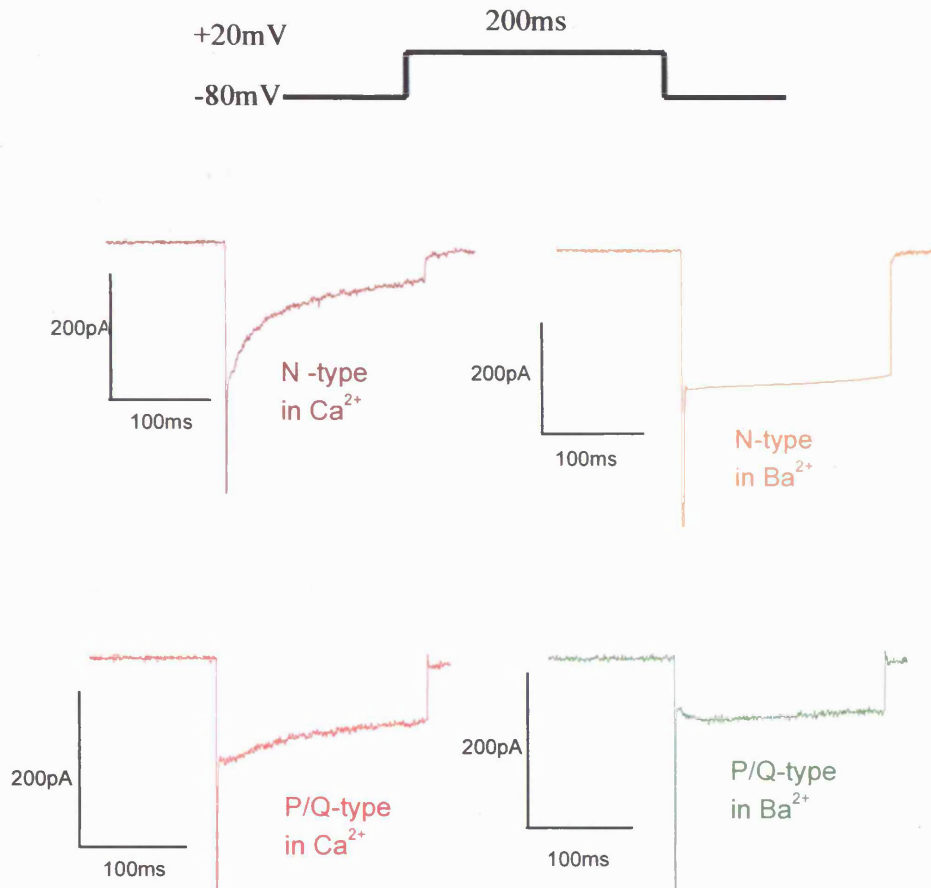
Shown are sample current traces of N-type channels inactivating in response to a single 200ms depolarisation in calcium (wine), or barium (orange), or P/Q-type channels inactivating in calcium (red), or barium (green). N-type channels display rapid and pronounced inactivation in calcium, inactivating $60.3 \pm 7.2\%$ n= 15, but are practically non-inactivating in barium, 2.3 % n = 2. With P/Q-type channels currents inactivated 47.1 ± 5.9 % n = 15 in calcium and 16.2 ± 3.3 %, n = 5, (p = 0.01) in barium.

6.5 Calcium-dependent inactivation of calcium channels is independent of calcineurin.

As there is a pronounced difference in the calcium-dependency of inactivation between the two channel subtypes, the molecular mechanisms underlying this were investigated. Different mechanisms have been proposed for calcium-dependent

inactivation of neuronal calcium channels. Although it is apparent that calmodulin plays an essential and direct role in initiating calcium-dependent inactivation of L-type channels, the evidence for calmodulin mediating the same direct effects on non-L-type channels is less conclusive. Calcium-dependent inactivation of L-type channels is insensitive to raised intracellular calcium chelators (Peterson et al. 1999). As I initially found that raised intracellular BAPTA slowed the rate of inactivation (figure 6.2.1), this suggested that a different mechanism was responsible for calcium-dependent inactivation in chromaffin cells. Calcineurin (protein phosphatase 2B), a calcium/calmodulin-dependent protein phosphatase has been reported to mediate calcium-dependent inactivation of N-type channels in NG108-15 cells (Burley and Sihra 2000). However studies in GH_3 cells and chick dorsal root ganglion neurones argue against a role for calcineurin in mediating calcium-dependent inactivation of N-type channels (Zeilhofer et al. 2000). Calcineurin is rapidly activated upon calcium entry across neuronal membranes (Sihra et al. 1992) and has been proposed to regulate several voltage-gated and ionotrophic ion channels (see Yakel 1997 for review). Cyclosporin A is a fungal compound commonly used to inhibit calcineurin activity. Cyclosporin A is cell permeable and forms a complex with endogenous cyclophilins (Yakel 1997), this complex then binds to and inhibits calcineurin with nanomolar affinity. Initially I performed whole cell experiments to determine fractional inactivation after a train of depolarisations (50 x 10ms, from –80mV to +20mV at 20 Hz) with cells matched from the same culture with or without 15 min preincubation with 100nM cyclosporin A. There was no significant difference between control and cyclosporin A treated cells, mean fractional inactivation at pulse 50 of 0.39 ± 0.02, n = 4 for control and 0.34 ± 0.07, n = 4 for cyclosporin A treated cells. Although cyclosporin A is reported to act with nanomolar affinity, I decided to increase the concentration to 1µM and to incubate the cells for > 20 mins before patching. Under these conditions cyclosporin A treated cells again failed to produce a significant difference from control cells. The mean fractional inactivation at pulse 50 was 0.47 ± 0.04, n = 11 for control cells, and 0.51 ± 0.03, n = 11 for cell culture matched controls (figure 6.5.1). The % inactivation over a 200ms depolarisation was 53.4 ± 5.3, n = 8 for control cells and 57.5 ± 3.5, n = 9 for cells pretreated with

cyclosporin A at 1μM. There was no statistical difference between the peak current amplitude or integrated calcium entry values between control and cyclosporin A cells. Mean peak current 479 pA ± 63, n = 8, and 446 pA ± 37, n = 9, integrated calcium 180 ± 17 x 10^6 Ca^{2+} ions and 167 ± 15 x 10^6 Ca^{2+} ions for control and cyclosporin A treated cells respectively.

6.5.1. Cyclosporin A (1μM) does not significantly reduce the level of calcium-dependent inactivation.
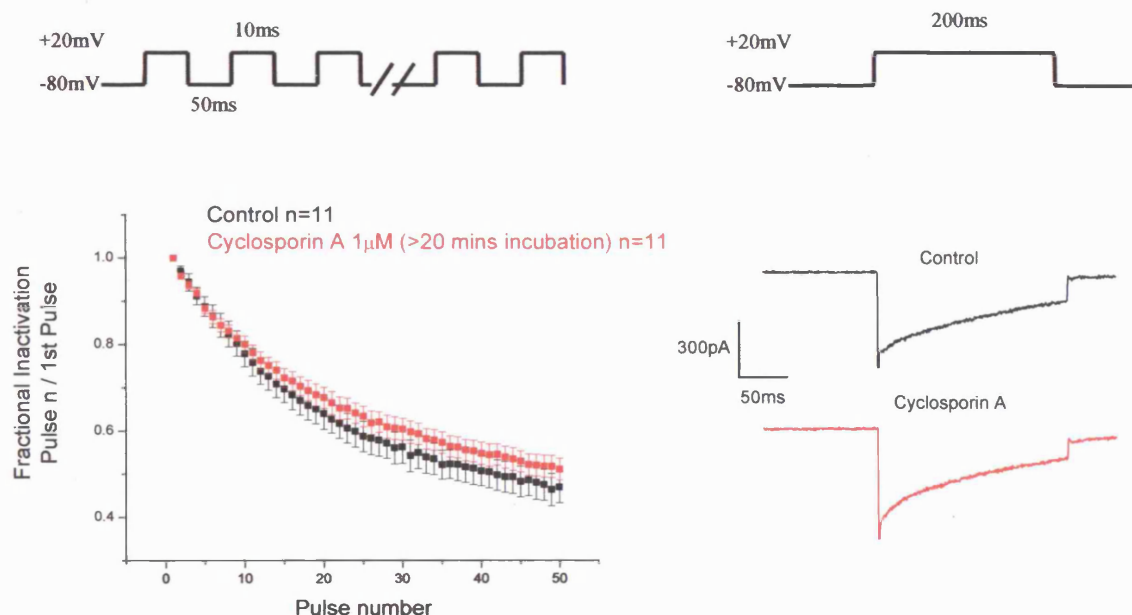
On the left is a response to a train of depolarisations, the mean fractional inactivation at pulse 50 was 0.47 ± 0.04, n = 11 for control cells (black), and 0.51 ± 0.03, n = 11 for cell culture matched cells which were preincubated > 20 mins before patching with 1μM cyclosporin A (red). On the right are sample traces in response to single 200ms depolarisations, in control % inactivation 53.4 ± 5.3, n = 8 (black) and from a cells pretreated with 1μM cyclosporin A, % inactivation 57.5 ± 3.5, n = 9 (red).

As cyclosporin A acts as an inhibitor of calcineurin by forming a complex with cyclophilins I wondered whether there were firstly endogenous cyclophilins in bovine adrenal chromaffin cells and secondly whether the reason I failed to see an effect was due to dialysis of cyclophilins out of the cell and up the patch pipette. A literature search discovered papers in which the activity of endogenous cyclophilins in bovine

adrenal chromaffin cells were monitored (Shiraishi et al. 2000) ruling out the first possibilty. To address the second concern, I performed perforated patch recordings and compared inactivation from a control train with later trains from the same cell after addition of 1μM cyclosporin A to the external solution. Under these conditions there was no change in the peak amplitude and inactivation actually increased. Fractional inactivation at pulse 50 was 0.35 ± 0.01, $n = 3$ for the control recording dropping to 0.27 ± 0.03, $n = 3$ after 15-20 minutes application of 1μM cyclosporin A, this increase was not significant ($p = 0.06$). This finding is in agreement with two other reports in which cyclosporin A was applied to bovine adrenal chromaffin cells (Engisch and Nowycky 1998; Chan and Smith 2001), who similarly found a modest, yet significant increase in calcium channel inactivation under perforated patch conditions. This could imply that calcineurin is important in recovery from inactivation. This possibility was not directly tested. Other tools that are commonly used to inhibit calcineurin include the immunosuppressant drug FK506 (whose mode of action is similar to cyclosporin A), or calcineurin auto-inhibitory peptides (which interact with the catalytic core of the calcineurin A subunit), (Yakel 1997). These compounds were not tested during the course of my studies. Therefore I cannot definitively rule out an involvement of calcineurin, but my findings support previous published results and suggest that in chromaffin cells calcineurin is unlikely to be the sensor that mediates calcium-dependent inactivation of calcium channels.

6.6 Calmodulin regulation of calcium-dependent inactivation of calcium channels

Several groups suggested that calmodulin was the calcium sensor for inactivation of L-type calcium channels with calmodulin directly binding to the channel (Peterson et al. 1999; Zuhlke et al. 1999). Initially commercial peptides based on the myosin light chain kinase binding site on calmodulin were introduced via the patch pipette to determine the involvement of calmodulin in calcium-dependent inactivation in chromaffin cells (figure 6.61). Calmodulin is an abundant protein reaching concentrations of 1-10μM in the cell (Saimi and Kung 2002), therefore a saturating

173

concentration of 30μM calmodulin inhibitory peptide was dialysed into the cell. Six minutes after obtaining access, trains of depolarisations were delivered to assess inactivation (6 minutes is predicted to give sufficient time for a 17aa peptide to diffuse into the cell from the patch pipette and reach equilibrium. Series resistance in these experiments was always less than $10M\Omega$). In response to a train of depolarisations the mean fractional inactivation at pulse 50 was 0.42 ± 0.03, n = 7 for control cells, and 0.48 ± 0.04, n = 5 for cell culture matched cells which were dialysed with 30μM calmodulin inhibitory peptide. The % inactivation over a 200ms depolarisation was 45.1 ± 5.5, n = 7 for control cells and 53.4 ± 3.5, n = 5 for cells dialysed with 30μM calmodulin inhibitory peptide. The difference between the peak current amplitude and integrated calcium entry values between control and cells dialysed with calmodulin inhibitory peptide were, peak current 302 pA ± 65, n = 7, and 496 pA ± 87, n = 5, integrated calcium values of 125 x 10^6 Ca^{2+} ions and 187 x 10^6 Ca^{2+} ions, respectively. As mean peak current and integrated calcium values were slightly higher for the treated group this could explain the slight but non-statistically significant increase in inactivation observed over a 200ms depolarisation from cells dialysed with calmodulin inhibitory peptide.

6.6.1 CaM Inhibitory Peptides (30μM) do not significantly reduce the level of calcium-dependent inactivation.
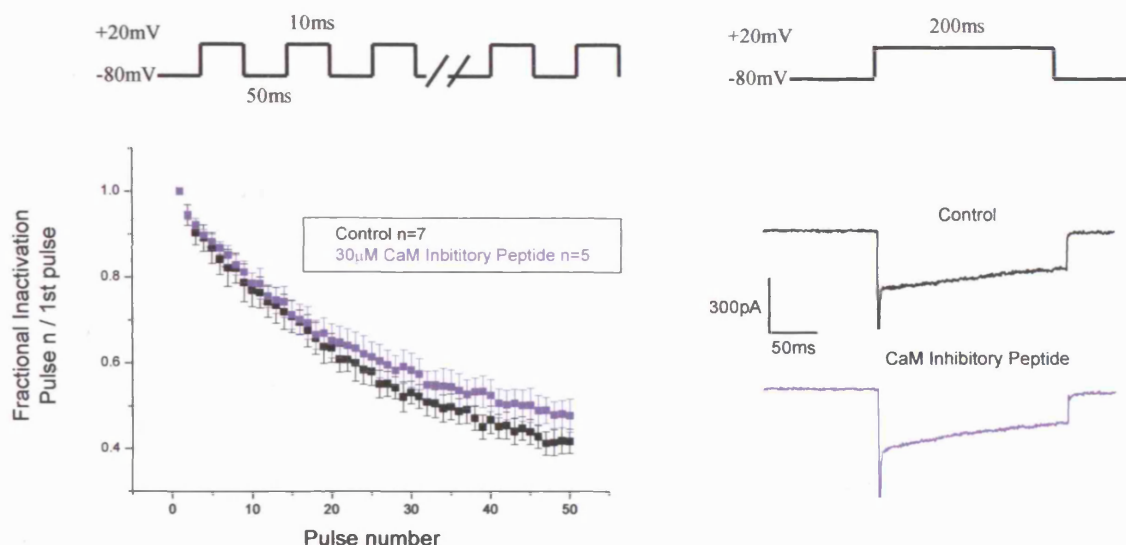
On the left is a response to a train of depolarisations, the mean fractional inactivation at pulse 50 was 0.42 ± 0.03, $n = 7$ for control cells (black) 6 mins after the whole cell configuration was obtained, and 0.48 ± 0.04, $n = 5$ for cell culture matched cells which were dialysed with 30μM calmodulin inhibitory peptide for 6 minutes after obtaining access to the cell interior (magenta). On the right are sample traces in response to single 200ms depolarisations, in control (black) and from a cell dialysed with 30μM calmodulin inhibitory peptide (magenta). The % inactivation over a 200ms depolarisation was 45.1 ± 5.5, $n = 7$ for control cells and 53.4 ± 3.5, $n = 5$ for cells dialysed with 30μM calmodulin inhibitory peptide.

The lack of effect of the calmodulin peptide actually adds weight to the argument against calcineurin mediating calcium-dependent inactivation, as the calcium-dependent activation of calcineurin is dependent upon calcium-calmodulin binding (Yakel 1997). By introducing the inhibitory peptide, free calmodulin should effectively be sequestered, leaving only calmodulin constitutively associated with target proteins (and therefore presumably protected from inhibition) able to respond to changes in calcium. Although these experiments fail to demonstrate an effect of the inhibitory peptide on calcium-dependent inactivation, a role for calmodulin cannot be ruled out if it is constitutively and tightly associated with the channel. Calmodulin has been shown to be the calcium sensor for small calcium-activated potassium channels and L-type calcium channels despite the absence of effects by

175

pharmacological or peptide inhibitors (Xia et al. 1998; Zuhlke et al. 1999). In these studies and others, the role of calmodulin was examined by over-expression of dominant mutant forms in which, one, several or all four of the EF calcium binding hands were mutated, rendering them incapable of binding calcium.

To test for a role of calmodulin using a dominant negative strategy, plasmids encoding either wild type (WT) calmodulin, or a version of calmodulin in which all four EF hands were mutated (aspartate to alanine, named 1,2,3,4 CaM) rendering them incapable of binding calcium, but able to bind to other target proteins were transiently transfected in chromaffin cells (plasmids kind gift from Dr Adelman, the Vollam Institute, Portland). Using either electroporation, or liposome based reagents like fugene-6 or lipofectamine 2000 transfection efficiency was very poor (<1-2%). In contrast adenovirus infection of wild type or mutant calmodulin worked very well with greater than 90% of cells infected (adenovirus kind gift of Dr Yue, John Hopkins Medical School, Baltimore). Full details of adenovirus construction and amplification are described in appendix 2 of this thesis.

6.6.2 Infection of cells with Adenovirus

It was important to assess whether adenoviral infection alone would alter the inactivation properties of the calcium channels endogenously expressed independently to the effects of the desired protein they are encoded to produce. Cells were initially infected with an adenovirus designed only to produce green fluorescent protein (GFP) (kind gift from Dr Herbet, University of Leicester). Cells were usually infected one day after plating, immediately after exchange of feeding media and the virus left in the media until the cells were used. Cells were used 24-72 hrs after infection. Positively infected cells were identified by fluorescent microscopy. In response to a train of depolarisations the mean fractional inactivation at pulse 50 was 0.42 ± 0.03, n = 7 for control cells, and 0.46 ± 0.05, n = 4 for culture matched cells which had been successfully infected with GFP adenovirus (figure 6.6.3). The % inactivation over a 200ms depolarisation was 45.1 ± 5.5, n = 7 for control cells and 51.8 ± 6.6, n = 4 for cells infected with GFP adenovirus, this difference was not

significant. Therefore adenoviral infection, does not affect channel inactivation properties in response to single step or trains of depolarisations.

6.6.3 Adenovirus infection alone does not affect channel biophysical properties.
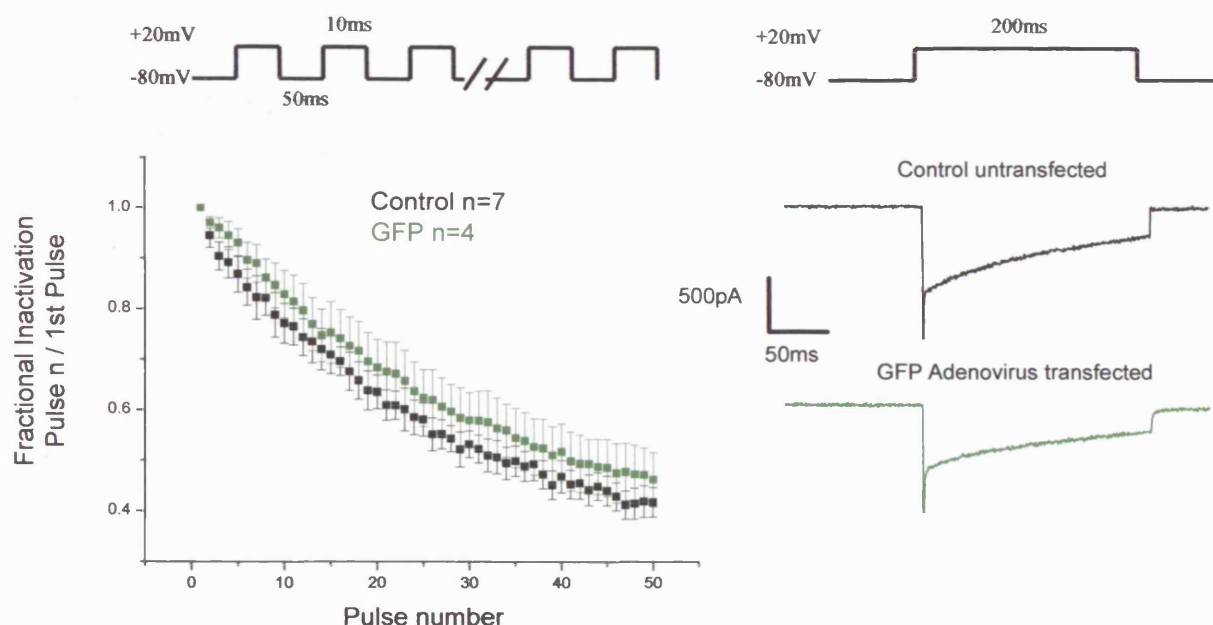
On the left is a response to a train of depolarisations, the mean fractional inactivation at pulse 50 was 0.42 ± 0.03, n = 7 for control cells (black) and 0.46 ± 0.05, n = 4 for culture matched cells which were successfully infected with GFP adenovirus (green). On the right are sample traces in response to single 200ms depolarisations, in control (black) and from a cell infected with GFP adenovirus (green). The % inactivation over a 200ms depolarisation was 45.1 ± 5.5, n = 7 for control cells and 51.8 ± 6.6, n = 4 for cells infected with GFP adenovirus.

6.6.4 The I/V relationship and voltage-dependence of inactivation are not altered between WT and Mutant CaM expressing cells.

Before assessing whether over-expression of mutant calmodulin would prevent calcium-dependent inactivation, it was first assessed whether the I/V relationship or voltage-dependence of inactivation were altered after infection with either the WT or mutant calmodulin. There was no shift in the I/V relationship for either virus, peak inward current was recorded at +10mV and currents reversed ~ +50mV, which matches the relationship observed for uninfected cells (chapter 3, figure 3.2.1). The

177

voltage-dependence of inactivation (using barium as the charge carrier) was also investigated. In identical experiments to the ones described earlier (chapter 3, figure 3.3.1) a Boltzmann fit of the data yielded a V_{50} of -38 mV for WT expressing cells, n = 3 and a V_{50} of -38 mV for mutant expressing cells, n = 4. This is identical to the V_{50} value of -38 mV, n = 5 obtained from uninfected cells.

6.6.4.1 Current voltage relationship and voltage-dependence of inactivation of WT and Mutant calmodulin over-expressing cells.
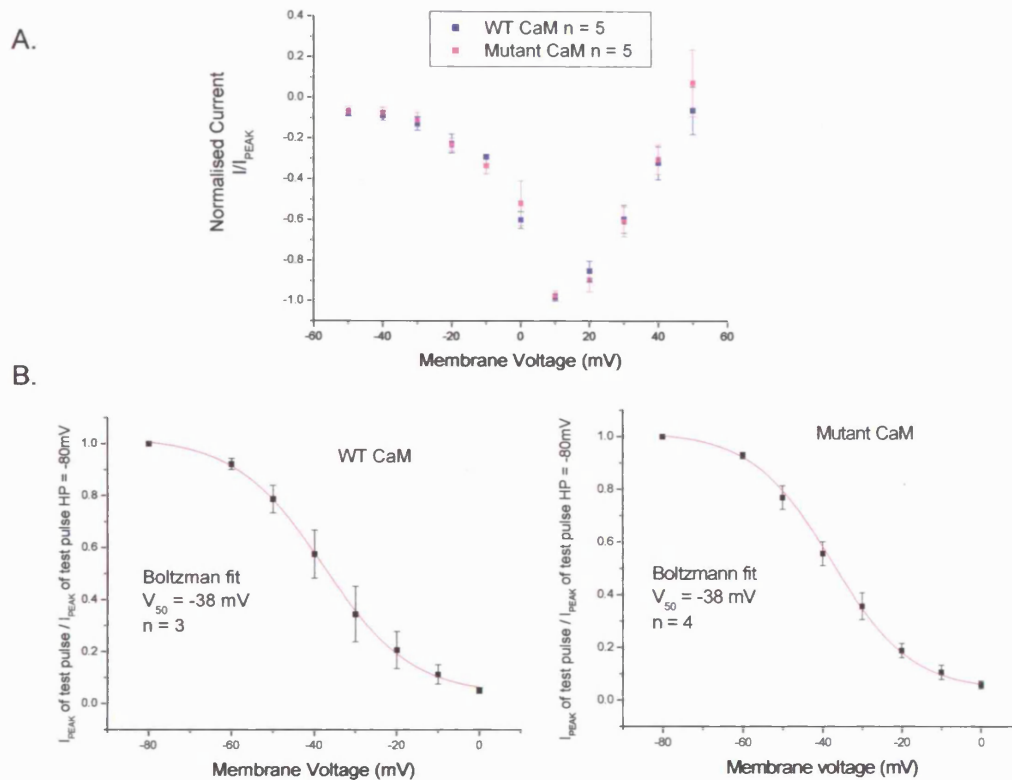
A. I/V relationship for WT (blue) and Mutant (magenta) over-expressing cells. The total membrane current in a single cell was evoked every 10 seconds from a holding potential of -80 mV. 50 ms duration step depolarisations from -40 mV to +60 mV were applied to the cell in 10 mV increments. Plotted is the peak current at each potential normalized to the peak current recorded at +10mV. Data points are the mean ± s.e.m, n = 5.

B. The voltage-dependence of inactivation was investigated. After obtaining a peak amplitude test current at +20mV with a holding potential of -80mV, the holding potential was raised consecutively from -60mV to 0mV in 10mV increments every 30seconds. Before each change in membrane holding potential a brief (50ms) test depolarisation to +20mV was evoked. The peak current of the test pulse was plotted against membrane holding potential and fitted with a Boltzmann sigmodial curve, $y = A_1 - A_2 / (1 + e^{(x-x0)/dx}) + A_2$. The results are the mean ± s.e.m, n = 3 for WT, n = 4 for mutant.

6.6.5 Over-expression of WT calmodulin does not significantly alter inactivation.

In response to the standard train of brief (10ms) depolarisations, fractional inactivation of the peak current amplitude at pulse 50 for cells over-expressing WT calmodulin was 0.44 ± 0.02, n = 26 recorded in the whole cell configuration or 0.39 ± 0.04, n= 13 recorded in the perforated patch configuration. As these values were not significantly different data was pooled together to give a mean value of 0.42 ± 0.02, n = 39. This is not significantly greater than the value observed from uninfected cells, 0.45 ± 0.02, n = 20. Cation replacement experiments reveal that inactivation is attenuated to a similar degree as uninfected cells when calcium is replaced by barium. Fractional inactivation at pulse 50 of 0.83 ± 0.03, n = 12, and 0.86 ± 0.03, n = 3 for WT and uninfected cells respectively (figure 6.6.5.1). In addition to assessing fractional inactivation by a reduction in peak current amplitude, integrated calcium entry was also measured for each pulse in the train and a fractional inactivation derived from dividing the ΣCa^{2+} entry per pulse by the ΣCa^{2+} entry during the first pulse. The amount of fractional inactivation whether it was measured by a reduction in peak current amplitude, or by a reduction in calcium entry consistently yielded values that were not significantly different from each other. Fractional inactivation at pulse 50 for WT cells measured by a reduction in peak current amplitude was 0.42 ± 0.02, n = 39, whereas a value of 0.39 ± 0.02, n = 39 was derived by calculating the reduction in calcium entry per pulse (figure 6.6.5.1). In response to a 200ms depolarisation cells infected with WT calmodulin adenovirus inactivated $57.8 \pm 2.3\%$, n = 33, which was attenuated to $15.5 \pm 5.5 \%$, n = 8 when barium was used as the extracellular divalent ($p < 0.0001$). There was no statistical difference in the amount of inactivation observed by the end of the pulse for cells infected with WT calmodulin compared to uninfected cells, $57.8 \pm 2.3\%$, n = 33, and $54.4 \pm 1.9\%$, n = 43 respectively. However, there was a significant difference in the amplitude of the peak current recorded, 391 ± 26 pA, n = 33 for WT and 551 ± 31 pA, n = 43 for uninfected cells ($p = 0.0003$). This reduction in peak current has previously been described when chromaffin cells were infected by semliki-forest virus (Pan et al. 2002). The molecular mechanisms underlying this are unknown. The decrease in

179

current amplitude may be due to reduced production of new channels which normally happens to maintain membrane density. This could occur as the protein synthesis machinery of the cell is 'highjacked' after viral infection to over-express the protein of interest and normal protein synthesis may consequently be down-regulated. Despite this, the biophysical properties (I/V, voltage-dependence and calcium-dependent inactivation) of the channels from WT infected cells is indistinguishable from uninfected cells suggesting that the channels present after adenoviral infection, albeit reduced in membrane density behave identically to uninfected cells (figure 6.6.5.2). To directly assess whether the reduction in peak current amplitude is due to a reduction in channel membrane density, additional experiments could be performed. Firstly, surface biotinylation of membrane calcium channels could be conducted and subsequent quantitative blot analysis performed. Alternatively it is possible that the reduction in peak current does not result from a reduction in membrane channel density but from a direct affect on the α_1 subunit resulting in a smaller unitary conductance from individual channels. Single channel recordings could be performed to investigate this possibility. Additionally, the magnitude of calcium currents is not only determined by the α_1 pore-forming unit, but can be modulated by its association with auxiliary subunits. Perhaps after adenoviral infection and production of calmodulin, protein synthesis of these proteins is down-regulated which consequentially leads to a reduction in peak current. Indeed Dolphin and co-workers have determined that the total complement of β subunits in DRG are turned over with a half life of around 50hrs (Berrow et al. 1995), and I record from cells 24-72hrs post-infection. In these studies knocking down β-subunits by injection of antisense sequences reduced calcium currents by 47%. Quantitative western blotting, or immunohistochemistry could be applied to monitor the cellular protein levels of β, $\alpha_2\delta$ and γ subunits after viral infection. These experiments were not conducted.

6.6.5.1 Cells over-expressing WT calmodulin inactivate in calcium-dependent manner.
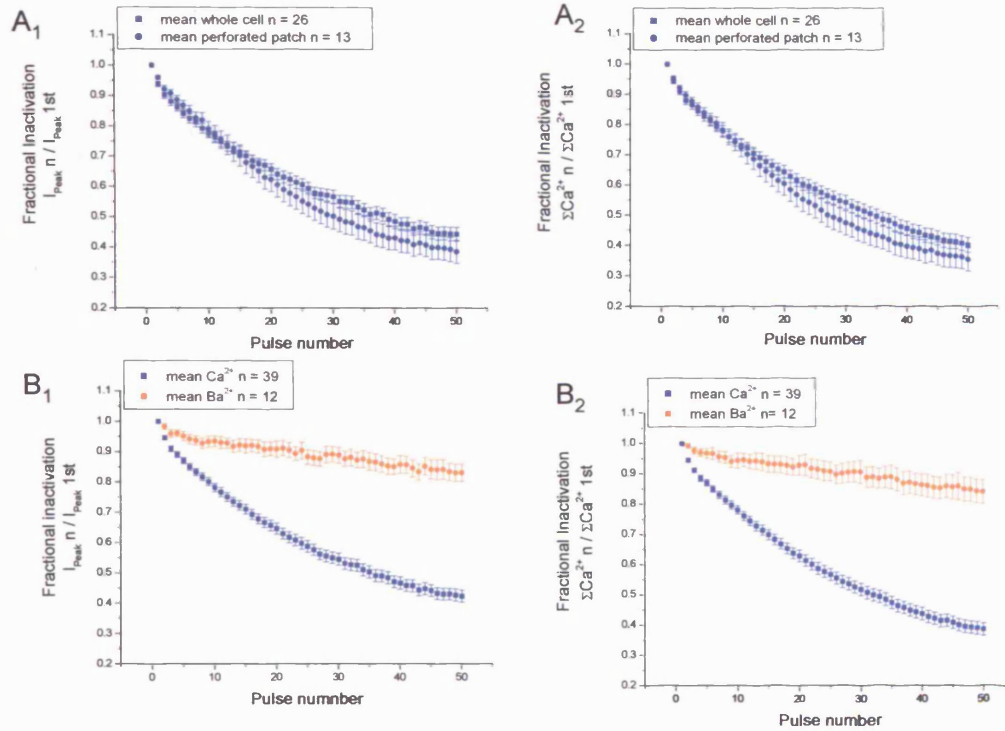
A. Whole cell and perforated patch experiments were initially analysed separately. Fractional inactivation at pulse 50, derived from normalizing either peak current amplitude (A1) or calcium entry (A2) was 0.44 ± 0.02, n = 26 and 0.40 ± 0.02, n = 26 for whole cell recordings and 0.39 ± 0.04, n = 13 and 0.36 ± 0.04, n = 13 for perforated recordings. No significant difference was observed in the degree of inactivation between recording configurations so channel data was pooled together.
B. The mean fractional inactivation at pulse 50 in calcium (blue) was 0.42 ± 0.02, n = 39 for peak currents (B1) and 0.39 ± 0.02, n = 39 for calcium entry (B2), attenuated in barium (orange) to 0.83 ± 0.03, n =12 and 0.84 ± 0.04, n =12 respectively, p < 0.0001.

6.6.5.2 WT Calmodulin over-expressing cells inactivate in an identical manner to uninfected cells.
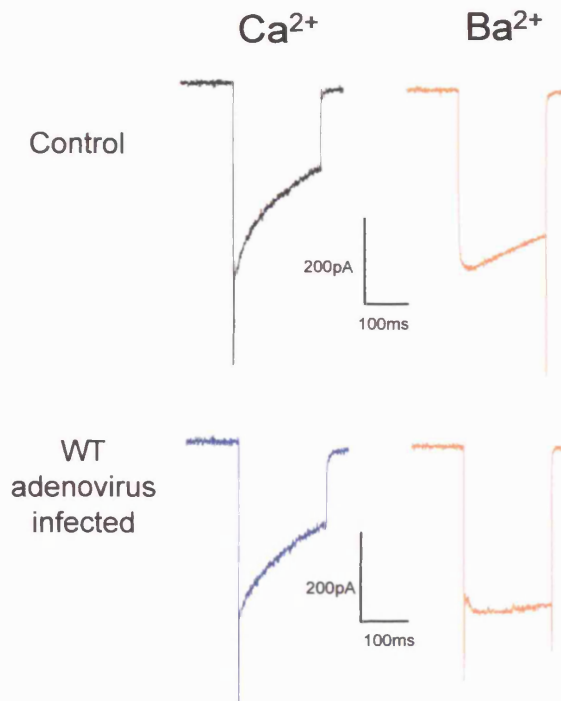
Shown are sample current traces from uninfected cells evoked from a 200ms depolarisation with either calcium (black), or barium (orange) as the extracellular divalent charge carrier. Currents inactivate $54.4 \pm 1.9\%$, n = 43 in calcium, which is attenuated to $9.2 \pm 3.6\%$, n = 6, $p < 0.0001$, in barium. WT calmodulin adenovirus infected cells inactivated $57.8 \pm 2.3\%$, n = 33, in calcium (blue), which was attenuated to $15.5 \pm 5.5\%$, n = 8 in barium (orange), $p < 0.0001$. There is no significant difference between uninfected cells and WT calmodulin cells in the I/V relationship, steady-state voltage-dependent inactivation, inactivation in response to a train of depolarisations or a single step to +20mV, or the magnitude of the calcium-dependent component to channel inactivation.

6.6.6 Over-expression of mutant (1,2,3,4) calmodulin significantly reduces calcium-dependent inactivation.

In response to the standard train of brief (10ms) depolarisations, fractional inactivation of the peak current amplitude at pulse 50 for cells over-expressing mutant calmodulin was 0.69 ± 0.02, n = 18 recorded in the whole cell configuration and 0.72 ± 0.05, n= 7 in the perforated patch configuration. As these values were not significantly different data was pooled together to give a mean value of 0.70 ± 0.02, n = 25. A similar degree of inactivation was detected when calcium entry per pulse

182

was normalized, 0.68 ± 0.02, n = 18 recorded in the whole cell configuration and 0.73 ± 0.05, n= 7 recorded in the perforated patch configuration, mean 0.69 ± 0.02, n = 25 (figure 6.6.6.1). Cation replacement experiments reveal that inactivation is attenuated when calcium is replaced by barium, 0.82 ± 0.04, n = 9, p = 0.006. In response to a 200ms depolarisation cells infected with mutant calmodulin adenovirus inactivated $33.6 \pm 2.2\%$, n = 30, which was attenuated to $19.1 \pm 2.0\%$, n = 13 when barium was used as the extracellular divalent (p = 0.0002).

6.6.6.1 Over-expression of mutant calmodulin reduces but does not eliminate calcium-dependent inactivation.
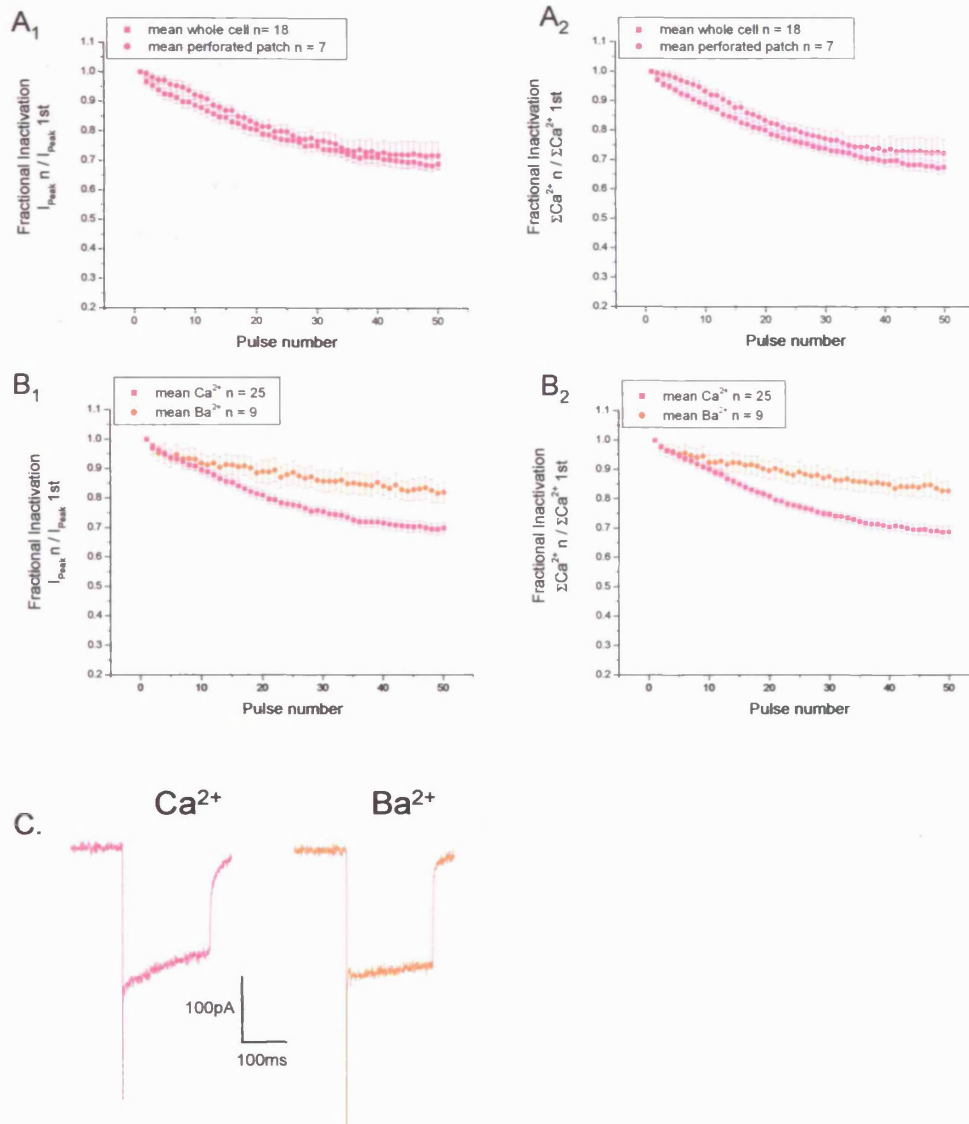
A. Whole cell and perforated patch experiments were initially analysed separately. Fractional inactivation at pulse 50, derived from normalizing either peak current amplitude (A1) or calcium entry (A2) was 0.69 ± 0.02, n = 18 and 0.680 ± 0.02, n = 18 for whole cell recordings and 0.72 ± 0.05, n = 7 and 0.73 ± 0.05, n = 7 for perforated recordings. No significant difference was observed in the degree of inactivation between recording configurations so channel data was pooled together.

B. The mean fractional inactivation at pulse 50 in calcium (magenta) was 0.70 ± 0.02, n = 25 for peak currents (B1) and 0.69 ± 0.02, n = 25 for calcium entry (B2), attenuated in barium (orange) to 0.82 ± 0.04, n =9, p = 0.0006 and 0.83 ± 0.03, n =9, p = 0.0008 respectively.

C. In response to a 200ms depolarisation mutant calmodulin expressing cells inactivate $33.6 \pm 2.2\%$, n=30 with calcium (magenta) as the charge carrier attenuated to 19.1 ± 2.0, n = 13 with barium (orange), p = 0.0002.

184

Significantly less inactivation occurs, measured by either a reduction in peak current amplitude or calcium entry in mutant expressing cells compared to WT, p <0.0001 (figure 6.6.6.2). Similarly in response to 200ms single step depolarisation significantly less inactivation occurs in cells expressing mutant calmodulin compared to those expressing WT, 33.6 ± 2.2%, n= 30 and 57.8 ± 2.3%, n= 33, p <0.0001 respectively.

6.6.6.2 Adenovirus mediated over-expression of mutant (1,2,3,4) calmodulin significantly reduces calcium-dependent inactivation.
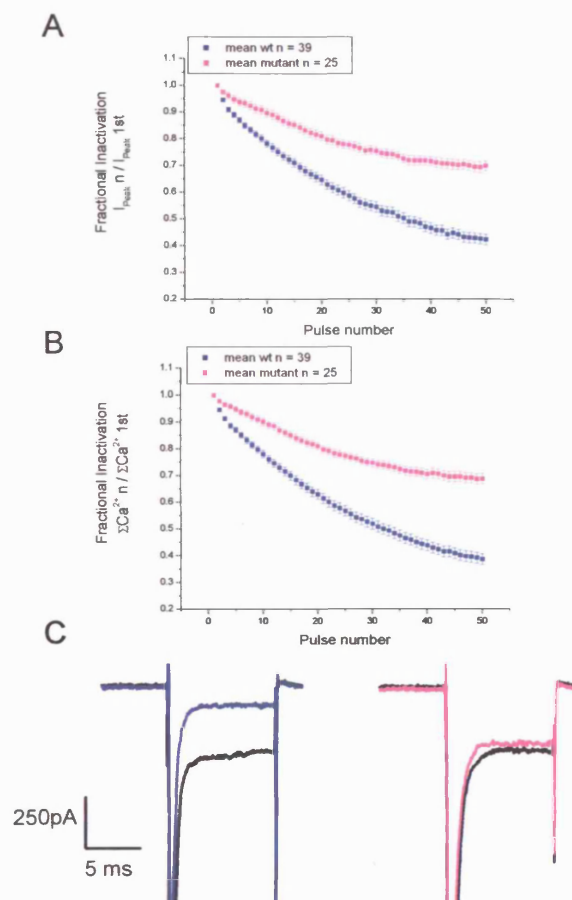
A. The mean fractional inactivation defined by a reduction in peak currents at pulse 50 was 0.42 ± 0.02, n = 39 for WT expressing cells (blue) and 0.70 ± 0.02, n = 25 for mutant expressing cells, p <0.0001.
B. A. The mean fractional inactivation defined by a reduction in calcium entry at pulse 50 was 0.39 ± 0.02, n = 39 for WT expressing cells (blue) and 0.69 ± 0.02, n = 25 for mutant expressing cells, p <0.0001.
C. Sample current traces indicating the 1st (black line) and 50th pulses, (blue for wt, and magenta for mutant) in the train. Sodium currents have been clipped for clarity.

A significant difference is also observed with longer depolarisations. Inactivation occurring during an 800ms pulse is $86.5 \pm 1.9\%$, n = 20 for WT expressing cells and $71.1 \pm 3.4\%$, n = 18 for mutant expressing cells, p = 0.0002. Significantly more calcium entered during an 800ms depolarisation, $268 \pm 27 \times 10^6\,Ca^{2+}$ ions and $359 \pm 35 \times 10^6\,Ca^{2+}$ ions, despite having similar peak current amplitudes, 332 ± 28 pA, n = 20 and 308 ± 36 pA, n = 18 for WT and mutant calmodulin over-expressing cells respectively.

6.6.6.3 More calcium enters through cells over-expressing mutant calmodulin in response to a long depolarisation.
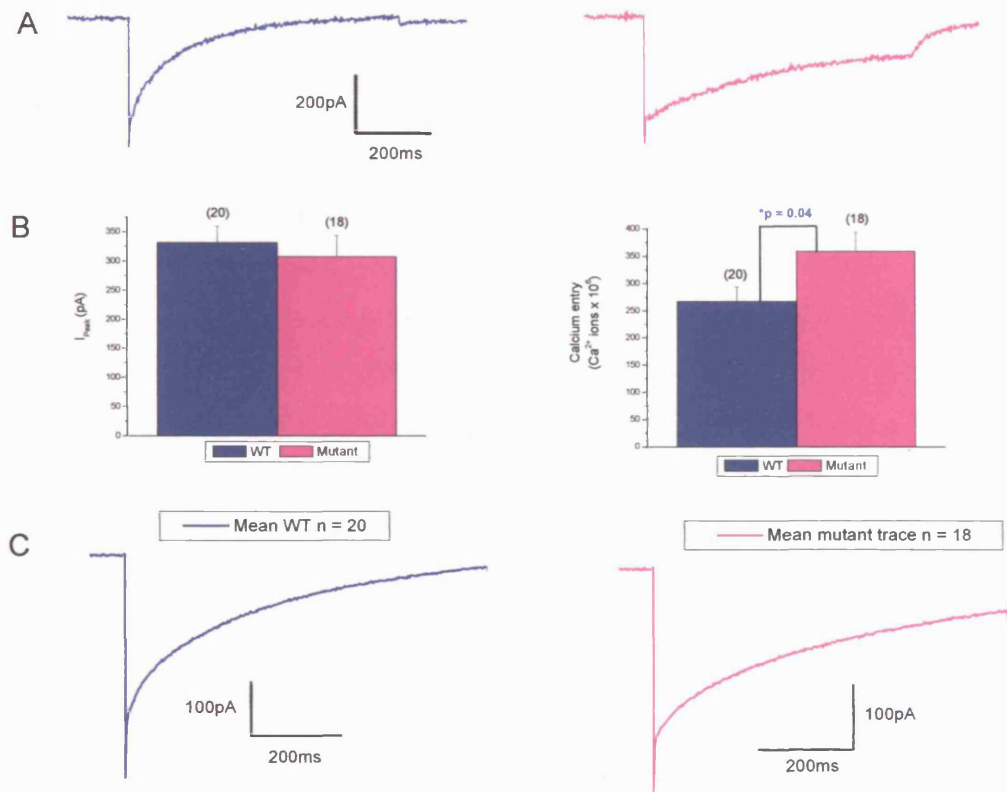
A. Sample current traces from WT (blue) and mutant (magenta) calmodulin over-expressing cells.
B. Bar Charts depicting the mean peak current (332 ± 28 pA, n = 20 and 308 ± 36 pA, n = 18 for WT and mutant calmodulin over-expressing cells respectively) and calcium entry ($268 \pm 27 \times 10^6\,Ca^{2+}$ ions n = 20 and $359 \pm 35 \times 10^6\,Ca^{2+}$ ions n = 18 for WT and mutant calmodulin over-expressing cells respectively). The difference in calcium entry was statistically significant p = 0.04.
C. Mean current traces are displayed. Inactivation occurring during an 800ms pulse is $86.5 \pm 1.9\%$, n = 20 for WT expressing cells and $71.1 \pm 3.4\%$, n = 18 for mutant expressing cells, p = 0.0002.

Over-expression of WT calmodulin did not significantly increase the amount of inactivation observed indicating that in control, normal conditions, calmodulin is not limited and able to direct its regulation to all available channels. Likewise, although over-expression of the mutant calmodulin significantly reduced inactivation it did not completely eliminate it, or reduce it to the level observed when extracellular calcium is replaced with barium. Therefore either a second calmodulin-independent pathway may be involved in calcium-dependent channel inactivation or the dominant negative strategy was incomplete. Calmodulin is an abundant protein, comprising $\sim 0.5\%$ of brain protein (Saimi and Kung 2002). Mammals contain three genes that encode a 100% identical calmodulin protein, resulting in a high level of cell expression. It is probable that even when over-expressing a large amount of mutant calmodulin endogenous calmodulin is still able to compete and bind to the channel. This argument can be strengthened further is one envisions a slow turnover rate and presuming mutant calmodulin can only bind to a channel that does not already have calmodulin pre-associated. Recent studies on L-type channels reveal a 1:1 stoichiometry of calmodulin binding to the channel (Mori et al. 2004).

The above experiments were conducted on cells which had not been toxin treated to isolate the N-type calcium channel. The inactivation observed will contain a component from the P/Q-type channel which displays a small amount of calcium-dependent inactivation and the mechanism underlying this may not be regulated by calmodulin. In fact the mean fractional inactivation of P/Q-type channels was 0.60 ± 0.05, n = 10 which is comparable to the value of 0.70 ± 0.02, n = 25 for cells not treated with toxins but infected with mutant calmodulin adenovirus. Therefore to assess properly calmodulin regulation of N-type channels, recordings from pharmacologically isolated channels were conducted.

6.6.7 N-type but not P/Q-type channel inactivation is regulated by calmodulin

After pharmacological isolation of P/Q-type channels, fractional inactivation of peak currents at the end of a train of depolarisations was 0.63 ± 0.09, n= 5 for WT expressing cells and 0.70 ± 0.05, n= 6 for mutant expressing cells. This difference

was not statistically significant, $p = 0.49$. The same was true when fractional inactivation was derived from normalizing the reduction of calcium entry per pulse, 0.60 ± 0.09, n= 5 for WT expressing cells and 0.70 ± 0.05, n= 6 for mutant expressing cells, $p = 0.34$. In contrast, after pharmacological isolation of N-type channels, fractional inactivation of peak currents in response to a train of depolarisations was 0.35 ± 0.07, n= 8 for WT expressing cells and 0.67 ± 0.04, n= 6 for mutant expressing cells. This difference was highly statistically significant, $p = 0.004$. The same was true when fractional inactivation was derived from normalizing the reduction of calcium entry per pulse, 0.32 ± 0.07, n= 8 for WT expressing cells and 0.67 ± 0.04, n= 6 for mutant expressing cells, $p = 0.002$. Therefore calmodulin mediates calcium-dependent inactivation of N-type channels, but plays little role in promoting calcium-dependent inactivation of P/Q-type channels. It may be possible that other calcium sensing proteins, which interact with calcium channels could mediate the small component of calcium-dependent inactivation observed in P/Q-type channels, (Burgoyne et al. 2004).

6.6.7.1 N-type calcium-dependent inactivation is regulated by calmodulin.
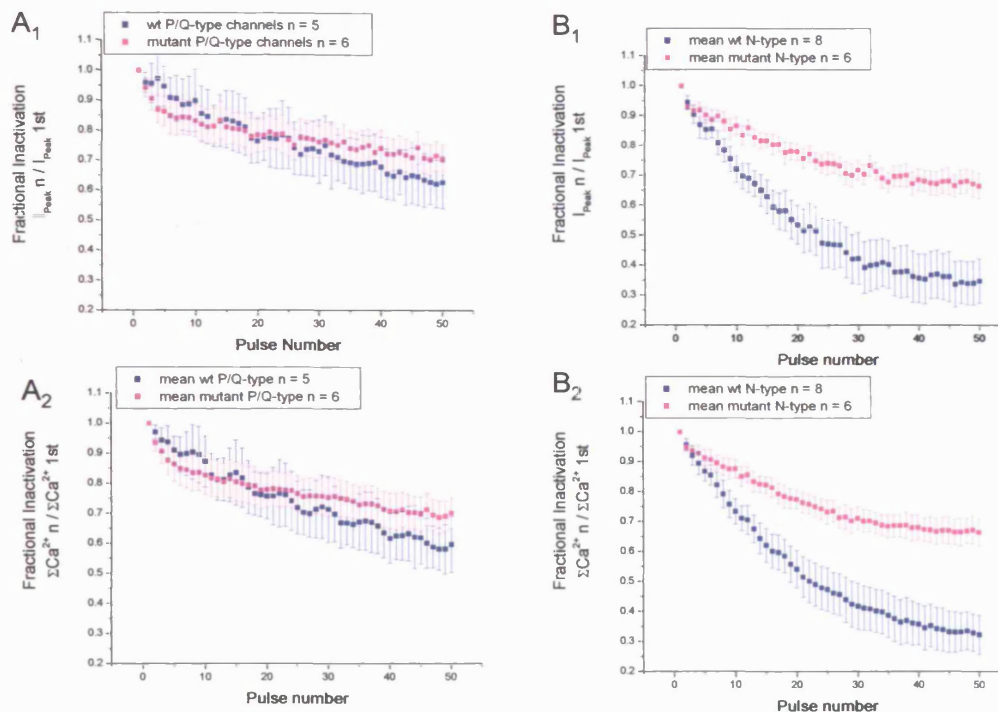
A1. The mean fractional inactivation of P/Q-type channels defined by a reduction in peak currents at pulse 50 was 0.63 ± 0.09, n = 5 for WT expressing cells (blue) and 0.70 ± 0.05, n = 6 for mutant expressing cells (magenta), p = 0.49

A2. The mean fractional inactivation of P/Q-type channels defined by a reduction in calcium entry at pulse 50 was 0.60 ± 0.09, n = 5 for WT expressing cells (blue) and 0.70 ± 0.05, n = 6 for mutant expressing cells (magenta), p = 0.34.

B1. The mean fractional inactivation of N-type channels defined by a reduction in peak currents at pulse 50 was 0.35 ± 0.07, n = 8 for WT expressing cells (blue) and 0.67 ± 0.04, n = 6 for mutant expressing cells (magenta), p = 0.004

B2. The mean fractional inactivation of N-type channels defined by a reduction in calcium entry at pulse 50 was 0.32 ± 0.07, n = 8 for WT expressing cells (blue) and 0.67 ± 0.04, n = 6 for mutant expressing cells (magenta), p = 0.002.

6.7 Discussion

Calcium-dependent inactivation of calcium channels was recognised several decades ago, from a variety of species and preparations (see Eckert and Chad 1984 for a review of early work on this subject). In addition to L-type channels, other non-L-type calcium channels have been described as inactivating in a calcium-dependent

189

manner. Recently the molecular mechanisms underlying this have started to be investigated.

6.7.1 Molecular determinants of calcium-dependent inactivation of P/Q-type channels.

In the Calyx of Held within the rat brainstem the P type presynaptic calcium current rapidly inactivates through a charge carrier-dependent mechanism, that was most pronounced but not specifically dependent on calcium (Forsythe et al. 1998). As the physiological divalent is calcium, this type of channel inactivation could be described as calcium-dependent. Recombinant studies have since shown that P/Q type channels can inactivate in a calcium-dependent manner and that this mode of inactivation is dependent on calmodulin (Lee et al. 1999). This study showed that calmodulin can bind to a site that shows a strong similarity to a region in the Ca^{2+}/Calmodulin-stimulated adenylyl cyclase type 8 (AC8) and that Ca^{2+}/calmodulin initiates first a calcium-dependent facilitation and then a calcium-dependent inactivation of the channel. It was shown that calcium-dependent inactivation but not calcium-dependent facilitation was blocked by 10mM EGTA, but both processes were blocked by 10mM BAPTA (Lee et al. 2000). This suggests that calcium-dependent facilitation is triggered by local calcium, which is intercepted rapidly by BAPTA, whereas calcium-dependent inactivation is induced by global calcium elevations, which can be removed by the slower calcium chelator EGTA. A molecular basis for this could arise from the different calcium binding affinities for the N and C lobes. The C-lobe has a 3-5 fold higher affinity for calcium than the N-lobe (Chin and Means 2000). Further dissection of the calcium binding domains of calmodulin revealed that the N-lobe is responsible for inactivation whereas the C lobe is responsible for facilitation (DeMaria et al. 2001), (figure 6.7.1.1).

6.7.1.1 Model of calcium-dependent facilitation and inactivation of P/Q-type channels by calmodulin.
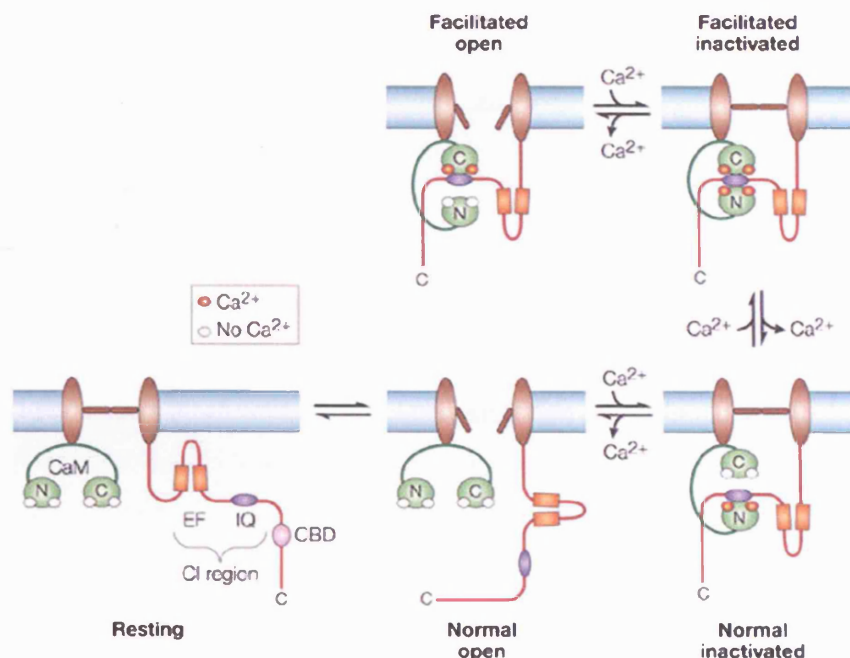
Nature Reviews | Neuroscience

The P/Q-type channel and its C-terminal tail including the EF, IQ and calmodulin binding domain (CBD) which resembles a region of Ca^{2+}/calmodulin-stimulated adenylyl cyclase type 8 are illustrated schematically. As the exact role of the CBD is not fully understood (calmodulin binding to this region is calcium-dependent), this picture depicts calmodulin binding to another unknown site at rest as apoCalmodulin is thought to pre-associate with the channel. Following calcium influx, calcium binding to the C lobe of calmodulin results in an interaction with the IQ region and induces calcium-dependent facilitation of the current. Calcium binding to the N-lobe results in calcium-dependent inactivation. In this model the C-lobe is thought to respond preferentially to fast local calcium concentration changes and the N-lobe detects slower global concentrations of calcium. Taken from (Budde et al. 2002), which itself was adapted from (DeMaria et al. 2001).

6.7.2 Molecular determinants of calcium-dependent inactivation of N-type channels.

Whether N-type channels undergo calcium-dependent inactivation was highly controversial. Previous studies in sympathetic neurones and of recombinant N type channels failed to detect calcium-sensitive inactivation (Patil et al. 1998; Jones et al. 1999) and biochemical methods indicated that apoCalmodulin binding to N-type

channels was either weak (Peterson et al. 1999), or non-existent (Zuhlke et al. 1999). However native studies in the dorsal root ganglia (Morad et al. 1988; Cox and Dunlap 1994) amongst others, favoured a calcium-dependent component to inactivation. In contrast to studies on L-type channels, only a few studies have investigated the molecular mechanisms underlying calcium-dependent inactivation of N-type channels. It has been suggested that calcineurin is implicated (Burley and Sihra 2000), however others argue against this (Zeilhofer et al. 2000), I find no evidence to support this theory. A recent study determined using an imaging technique that apoCalmodulin was constitutively associated with the N-type channel and recombinantly expressed N-type channels could undergo calmodulin mediated calcium-dependent inactivation when a concentration of calcium chelator which resembled physiological buffering conditions was used (Liang et al. 2003). This last observation explains the results from previous studies, as those, which used a low concentration of intracellular calcium chelator usually observed calcium-dependent inactivation whereas those which used a high concentration usually failed to observe this form of inactivation. This implies that there is a fundamental difference in channel regulation by calmodulin between the different channel subtypes as calcium-dependent inactivation of L-type channels is relatively insensitive to raised calcium chelator concentrations. Indeed, the C-lobe of calmodulin is required to mediate calcium-dependent inactivation of L-type channels and responds to local calcium (ie calcium influx through the individual channel), whereas non-L-type channels require the N-lobe to mediate calcium-dependent inactivation in response to a global rise in intracellular calcium (Liang et al. 2003), (figure 6.7.2.1). It also explains why calcium-dependent inactivation is attenuated in my experiments when 10mM BAPTA is included in the patch pipette and why I fail to detect significant calcium-dependent inactivation with very short pulses (10ms) where calcium is restricted locally and quickly buffered, but detect robust inactivation with trains of depolarisations and long (200, or 800ms) depolarisations which would raise cytosolic calcium levels more significantly. A good way to test this hypothesis would be to make adenovirus carrying just lobe specific mutations of calmodulin. The theory would predict that mutations in the N-lobe, rendering it incapable of binding calcium should result in the

same affect as the ones reported here when the calcium binding sites from both lobes have been altered. In contrast, mutations specific to the C-lobe should result in the same affects as WT. It is of interest to note that the observation that calcium chelators can attenuate calcium-dependent inactivation relates back to the original studies in the late 1970's and early 1980's on invertebrate neurones, as current inactivation was slowed after injection of EGTA (reviewed in Eckert and Chad 1984). This implies that invertebrate calcium channels are more closely related to mammalian Ca_v2 family, than to the Ca_v1 with calcium-dependent inactivation triggered by the N-lobe of calmodulin.

6.7.2.1 Schematic representation of calmodulin lobe-specific calcium-dependent inactivation in L-type and non-L-type calcium channels.
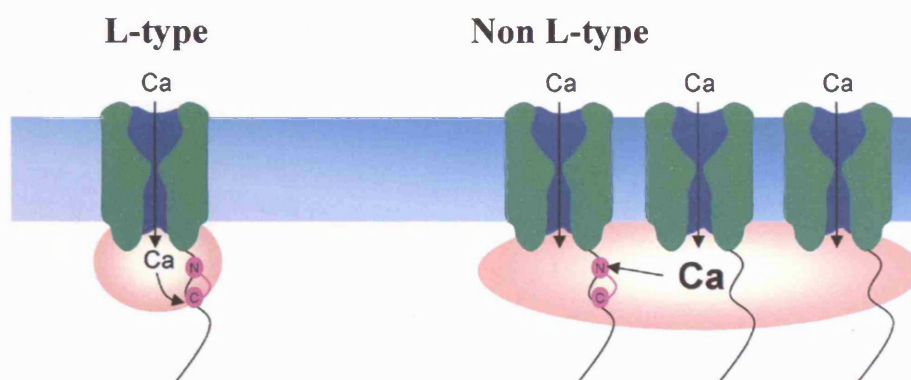
In non-L-type channels calcium-dependent inactivation is mediated by the lower affinity N-terminal lobe of calmodulin which responds to summed global rises in intracellular calcium concentration. For L-type channels, calcium influx through an individual channel is sufficient to trigger calcium-dependent inactivation due to calcium binding to the high affinity C ternminal lobe of calmodulin. Taken from (Zamponi 2003).

Therefore all HVA calcium channels, L,N,P/Q and also R (not previously mentioned), are constitutively associated with apoCalmodulin and able to undergo calmodulin-mediated calcium-dependent inactivation.

6.7.3 Why is calmodulin dependent facilitation and inactivation of P/Q-type channels not observed?

Two groups have published extensively over the last five years examining the role calmodulin plays in mediating calcium-dependent facilitation and inactivation of P/Q-type channels (Lee et al. 1999; Lee et al. 2000; Lee et al. 2002; Lee et al. 2003; DeMaria et al. 2001; Chaudhuri et al. 2004). These studies have been performed solely in recombinant expression systems. Professor Yue's group use human α_{1A} isoforms and have only co-expressed the β_{2a}-subunit (DeMaria et al. 2001; Chaudhuri et al. 2004). Professor Caterall's group have exclusively used the rat α_{1A} subunit and predominantly use the β_{2a}-subunit, in fact they show that co-expression with a different β-subunit, β_{1b}, results in inactivation with minimal calmodulin regulation (Lee et al. 1999; Lee et al. 2000; Lee et al. 2002; Lee et al. 2003). Therefore the first obvious explanation for the lack of calmodulin regulation of P/Q-type channels in my studies could result from differences in the bovine α_{1A} and/or the β-subunits it functionally couples to *in vivo*. In fact the ability of the α_{1A} subunit to alternatively splice may be important in determining the degree of calcium-dependent inactivation. In general the shorter the C-terminus, the greater the current amplitude and the stronger the calcium-dependence of inactivation (reviewed in Jurkat-Rott and Lehmann-Horn 2004). C-terminus mobility is essential for the induction of calcium-dependent inactivation regulated by calmodulin in L-type channels and is also thought to contribute to removing the calcium-calmodulin complex from the inner pore and initiating signal transduction through activation of CREB (Kobrinsky et al. 2003). For both N and P/Q-type channels, exons encoding for distal parts of the C-terminus may potentially be spliced out, exons 43, 44 in P/Q-type and exon 46 in N-type (Jurkat-Rott and Lehmann-Horn 2004). Professor Yue's group have recently investigated the role of alternative splice variants in exon 37 of the human α_{1A} subunit which produce two variants of an EF-hand-like domain, a region implicated in calmodulin regulation of these channels (Chaudhuri et al. 2004). This study determined that splicing at this site regulates calcium-dependent facilitation but does

not alter calcium-dependent inactivation. There is evidence to suggest that bovine chromaffin cells express at least two splice isoforms of the α_{1A} subunit. Immunoprecipitation of the α_{1A} subunit reveals a major polypeptide band of around 190 kDa and a minor polypeptide band at 220kDa (Weiss and Burgoyne 2001). Therefore it would be useful to clone the bovine α_{1A}'s expressed and recombinantly express them with various β-subunits to determine whether calmodulin-dependent regulation can occur. Likewise recombinant studies to investigate the calmodulin-dependent inactivation of the cloned bovine α_{1B} with different β-subunits could prove insightful in determining the β-subunit specificity of this process.

6.7.4 Putative molecular mechanisms underlying calcium-dependent inactivation of P/Q-type channels.

As previously discussed over-expression of a dominant negative mutant calmodulin does not significantly reduce calcium-dependent inactivation of P/Q-type channels. It is possible that other molecular mechanisms account for the calcium-dependent component of inactivation observed with these channels. This regulation could be mediated by other calcium sensing proteins (Burgoyne et al. 2004), or by calcium-dependent alterations of the cytoskeleton (Budde et al. 2002).

6.7.4.1 Calcium-Binding Protien-1 (CaBP1).

CaBP's are a family of proteins that are closely related to calmodulin (Haeseleer et al. 2000). CaBP1 has recently been shown to competitively bind to the same C-terminal region on L-type channels ($Ca_v1.2$) as calmodulin (Zhou et al. 2004). *In vitro* studies show that binding of calmodulin and CaBP1 to the IQ motif was mutually exclusive in that calmodulin could displace CaBP1 if it was in excess and vice versa CaBP1 could displace calmodulin if it was in excess. In contrast to calmodulin binding which results in profound calcium-dependent inactivation, CaBP1 prolongs calcium currents during a train of depolarisations by inhibiting inactivation (Zhou et al. 2004). The authors speculate that the suppression of inactivation could result from the N-

terminal myristoylation of CaBP1 (Haynes et al. 2004), that will create an association between the C-terminal domain of the channel and the plasma membrane. Therefore in cells expressing both calmodulin and CaBP1 their relative protein expression levels and proximity to channels could lead to calcium currents displaying robust calcium-dependent inactivation (all calmodulin associated), or currents that are relatively inactivating (all CaBP1 associated), the potential for a graded response could also be possible. CaBP1 has also been shown to bind to P/Q-type channels, again to the same site utilized by calmodulin (Lee et al. 2002). However recombinant studies co-expressing CaBP1 and P/Q-type channels results in different channel regulation to the observed affect with L-type channels. CaBP1 modulates P/Q-type channels by accelerating inactivation in a calcium-independent manner (Lee et al. 2002). Therefore this protein is unlikely to mediate the effects on P/Q-type currents seen in my studies, unless the complement of α_1 splice isoforms and/or β subunits in chromaffin cells is different from those used in the aforementioned recombinant study and allows CaBP1 regulation of these channels in a manner analogous to its regulation of L-type channels. So far CaBP1 has only been tested on P/Q-type channels containing the β_{2a}-subunit. The functional interaction of CaBP1 with the calcium channel may depend on specific β-subunits, as recently shown for another calcium-binding protein NCS-1 (Rousset et al. 2003).

6.7.4.2 Neuronal Calcium Sensor 1 (NCS-1).

NCS proteins are members of the superfamily of EF-hand binding proteins, which include calmodulin and CaBPs, with expression restricted mainly to neurones and neuroendocrine cells (for reviews see Burgoyne and Weiss 2001, Hilfiker 2003, Burgoyne et al. 2004). A member of this family, NCS1 has been shown to regulate different subtypes of calcium channels (discussed in Weiss and Burgoyne 2002), although there is disparity within these reports, suggesting that NCS-1 regulation of channels is dependent on the co-expression of other proteins.

In chromaffin cells, over-expression of wild type NCS-1 has little effect on calcium currents, however over-expression of a dominant negative mutant (mutated in the 3rd

EF hand) increases calcium currents (Weiss et al. 2000). This is due to the removal of a component of autocrine inhibition of P/Q-type channels and requires the activity of a src-like tyrosine kinase (Weiss and Burgoyne 2001). It is interesting to note that N-type channels in chick DRG and rat hippocampal neurones have a Src-like tyrosine kinase constitutively associated with the channel (Richman et al. 2004), but N-type channels do not show relief from voltage-independent inactivation when a dominant negative mutant of NCS-1 is over-expressed in chromaffin cells (Weiss & Burgoyne 2001). In contrast to the studies in chromaffin cells, experiments in the calyx of Held propose a role for NCS-1 in mediating calcium-dependent facilitation of P/Q-type channels (Tsujimoto et al. 2002). In this study direct application of recombinant NCS-1 protein through the patch pipette leads to a calcium-dependent increase in current activation. Facilitation was blocked by application of a C-terminal NCS-1 peptide. The authors suggest that activity-dependent facilitation of P-type channels previously described in the calyx of Held (Forsythe et al. 1998, Cuttle et al. 1998) is mediated by residual calcium activating endogenous NCS-1. The difference in results between the calyx of Held and chromaffin cells has been argued to result from different coupling to G-protein inhibitory pathways (Weiss and Burgoyne 2002). Other reports have reported equally diverse effects. In neuroblastoma cells over-expression of WT NCS-1 reduces HVA calcium currents but increases LVA calcium currents (Burley et al 2000), whereas those in the Xenopus neuromuscular synapse conclude that NCS-1 facilitates N-type calcium channels, presumably by increasing the number of functional channels (Wang et al. 2001). In hippocampal neurones over-expression of NCS-1 had no effect on the calcium currents (recorded from the cell body), (Sippy et al. 2003). Recently results from recombinant studies in Xenopus oocytes report that NCS-1 regulation of calcium channels is dependent on the β-subunit that is co-expressed (Rousset et al. 2003). They found that when NCS-1 was co-expressed either with just the P/Q-type channel, or with the P/Q-type channel and the β_3 subunit, calcium currents were unaffected. However co-expression with other β-subunits ($\beta_1, \beta_2, \beta_4$) resulted in a marked decrease in calcium current. This reduction in current density was attributed to an inhibition of trafficking and membrane insertion and not protein synthesis. Additionally they found a slight alteration in

197

activation and inactivation parameters when P/Q-type channels were expressed with the β_{2a}-subunit and NCS-1. This last study implies that the NCS-1 regulates calcium channels primarily by controlling surface expression, however the studies in chromaffin cells and the calyx of Held mentioned earlier suggest that calcium-dependent direct protein-protein interactions can dynamically regulate P/Q-type channels. NCS-1 has not been shown to directly bind to the channels (in L-type channels no interaction between NCS-1 and a C-terminal fragment was detected, Zhou et al. 2004). Whether NCS-1 exerts its affects by direct interactions with the calcium channels, reminiscent of calmodulin, or through activation of second messengers remains to be examined. However this molecule could explain the small degree of calcium-dependent inactivation observed for P/Q-type channels and warrants further investigation.

6.7.4.3 Mediation of calcium channel inactivation by calcium-dependent regulation of the cytoskeleton.

Observations from numerous neuronal preparations indicate that calcium-dependent inactivation of calcium channels is sensitive to the state of the cytoskeleton (reviewed in (Budde et al. 2002). This argument centres on the observation that cytoskeletal stabilizers dramatically reduce calcium-dependent inactivation of calcium channels. The molecular mechanisms underlying this are unclear at present but may involve disruption of microtubule and microfilament components by raised intracellular calcium. It has been proposed that β-subunits interact with the cytoskeleton via a Src homology 3-guanylate kinase (SH3-GK) domain similar in sequence to membrane-associated guanylate kinases (MAGUKs), (see Budde et al. 2002). Recently it has been shown that disruption of the SH3-GK module in β-subunits can profoundly affect channel inactivation (McGee et al. 2004; Takahashi et al. 2004). Therefore disruption of the cytoskeleton may exert an affect on the channel through the β-subunit. In support of this hypothesis NMDA receptor channels have been shown to be downregulated by calcium-dependent depolymerisation of the channels from the actin filaments in hippocampal neurones (Rosenmund and Westbrook 1993), a

process however that probably involves calmodulin (Zhang et al. 1998; Krupp et al. 1999). Therefore as cytoskeletal disruption is likely to involve Ca^{2+}/calmodulin then this process is unlikely to account for the calcium-dependent component of P/Q-type channel inactivation as there was not a significant difference in P/Q-type inactivation between cells over-expressing WT or mutant calmodulin.

6.7.5 Could cellular compartmentation underlie the differences in inactivation between N and P/Q-type channel?

A different viewpoint is that both channels share the same ability to undergo calcium-dependent inactivation with localized calcium buffers dictating the degree of channel inhibition. The difference in calcium-dependent regulation could be argued to result from preferential localization of P/Q-type channels to calcium buffers. In addition to their well described role as generators of ATP mitochondria are capable of sequestering calcium, and large numbers of mitochondria are present in synaptic terminals. In chromaffin cells inhibition of mitochondria leads to an increase in the rate of calcium-dependent channel inactivation, although the rate of inactivation was comparable for both P/Q and N-type channels (Hernandez-Guijo et al. 2001). However studies in the calyx of Held report that mitochrondrial inhibition does not alter inactivation of presynaptic (P-type) calcium currents (Billups and Forsythe 2002). Alternatively instead of preferential coupling of P/Q-type channels to calcium buffers the difference in calcium-dependent inactivation could occur from favoured coupling of N-type channels to calcium stores and activation of calcium-induced-calcium-release (CICR). Recent results from experiments on PC12 cells (a tumour cell line derived from rat chromaffin cells), reveals that calcium influx specifically through N-type channels is amplified by CICR from ryanodine sensitive stores (Tully and Treistman 2004). CICR will not only increase the local concentration of calcium, but due to the regenerative nature of CICR maintain a raised calcium concentration for longer. Ryanodine receptors have been found on the extensions of the endoplasmic reticulum that are in very close apposition to the cell membrane (Berridge 1998). Therefore a co-localisation and specific activation of CICR by N-

type channels could occur. Indeed close localization would be required to initiate CICR as elevations in calcium in the micromolar range are required to activate ryanodine receptors (Fill and Copello 2002). Such a concentration would occur within a microdomain surrounding calcium channels, with neither calcium entry from distant channels or residual calcium creating the required concentration for ryanodine channel activation. Functional co-localisation of ryanodine receptors, N-type calcium channels and BK channels has been described in bullfrog sympathetic neurones (Akita and Kuba 2000). Additional functional coupling of calcium channels to other processes that influence local calcium concentrations, such as extrusion by Ca^{2+}-ATPases or store-operated capacitative calcium entry may also exist.

6.7.6 Other channels regulated by calmodulin.

Diverse ion channels from a wide range of species from yeast to man use calmodulin as either a constitutively bound or dissociable calcium-sensing regulator of channel function. The list includes, cyclic nucleotide-gated channels, NMDA receptors, ryanodine and ionositol 1,4,5 triphosphate receptors, small and intermediate calcium-activated calcium channels, transient receptor potential channel family members, connexons (gap junctions) and human EAG potassium channels (Saimi and Kung 2002). I will not attempt to review the literature pertaining to this, however it should be noted that studies investigating the molecular regulation by calmodulin from one channel can be useful in examining its properties on another channel type. Briefly, studies in *Paramecium* initially discovered that mutations in the C-lobe lead to an increase in excitability, whereas mutants in the N-lobe resulted in a reduction in excitability (discussed in Saimi and Kung 2002). This suggested that different lobes of the same molecule could mediate opposite functions. Recently the ability of calmodulin to display functional bipartition with respect to its lobes has been shown again with its regulation of mammalian P/Q-type calcium channels (Lee et al. 1999; Lee et al. 2000; DeMaria et al. 2001). Furthermore, several practical approaches (namely the use of dominant negative mutants in 1or more of the EF calcium binding hands) initially used to detect calmodulin regulation of small conductance potassium

channels (Xia et al. 1998) have been successfully applied to determine a role of calmodulin in regulating different calcium channel subtypes (Zuhlke et al. 1999; Peterson et al. 1999; Lee et al. 1999; Liang et al. 2003).

6.8 Conclusions

In this chapter I have shown that the whole cell calcium current in bovine adrenal chromaffin cells is regulated by calcium. The calcium-dependence of this inactivation was investigated in perforated patch experiments by equimolar replacement of extracellular calcium with barium, or in whole cell experiments by increasing the concentration of BAPTA in the electrode solution from 0.3mM to 10mM. Channels were pharmacologically isolated to assess whether both subtypes possessed the same degree of calcium-mediated inactivation. The pharmacologically isolated N type channels displayed significantly more profound sensitivity to calcium.

The molecular mechanisms underlying this effect were then investigated. Inhibiting calcinuerin by 20 mins preincubation with $1\mu M$ cyclosporin A or by introducing $30\mu M$ calmodulin inhibitory peptides through the patch pipette did not significantly reduce the level of calcium-dependent inactivation. In contrast, adenoviral mediated expression of a mutant calmodulin deficient in calcium binding resulted in a highly significant reduction in inactivation. N-type channel inactivation was significantly reduced with over-expression of a dominant mutant calmodulin whereas P/Q-type inactivation was not. This is the first time that calmodulin has been shown to regulate endogenously expressed non-L-type calcium channels. Taken together, these results are consistent with calmodulin acting directly to control N-type channel inactivation in adrenal chromaffin cells and could account for the reduced exocytotic efficiency observed with these channels during intense stimulation.

Chapter 7. Calmodulin regulation of stimulus-coupled secretion.

Calmodulin is not thought to be the calcium sensor that triggers calcium-dependent exocytosis, distinct from its proposed role as a primary calcium sensor mediating homotypic fusion of early endosomes and yeast vacuoles (Burgoyne and Clague 2003). However there is growing evidence to suggest that it may play important regulatory or modulatory roles in this process. The number of different proteins implicated in exocytosis and endocytosis with which calmodulin has been reported to interact with is considerable. At present, the importance of these interactions and the extent to which calmodulin can modulate neurotransmitter release remains to be fully characterized. In this chapter I describe how over-expression of WT, or mutant calmodulin affects calcium-dependent exocytosis and endocytosis from bovine adrenal chromaffin cells.

7.1 Exocytosis evoked by a 200ms depolarisation.

Unless specifically stated otherwise, all secretion data presented in this chapter results from recordings in the perforated patch configuration. Initially exocytosis evoked from a 200ms depolarisation was characterized. WT infected cells had a mean ΔC_m of 107 ± 37 fF, and a mean calcium entry of 179 ± 16 x 10^6 Ca^{2+} ions, n = 6. This was not significantly higher than the corresponding ΔC_m and calcium entry from cells over-expressing mutant calmodulin, 89 ± 22 fF and 156 ± 18 x 10^6 Ca^{2+} ions n = 7, respectively. Cells infected with either virus evoked less exocytosis to the 200ms stimulus than non-infected cells, ΔC_m of 169 ± 17 fF, n = 38 (figure 4.7.2), however, this can be explained by the reduction in calcium entry observed after viral infection (section 6.6.5).

7.1.1. Mean capacitance traces for cells over-expressing WT, or mutant calmodulin.
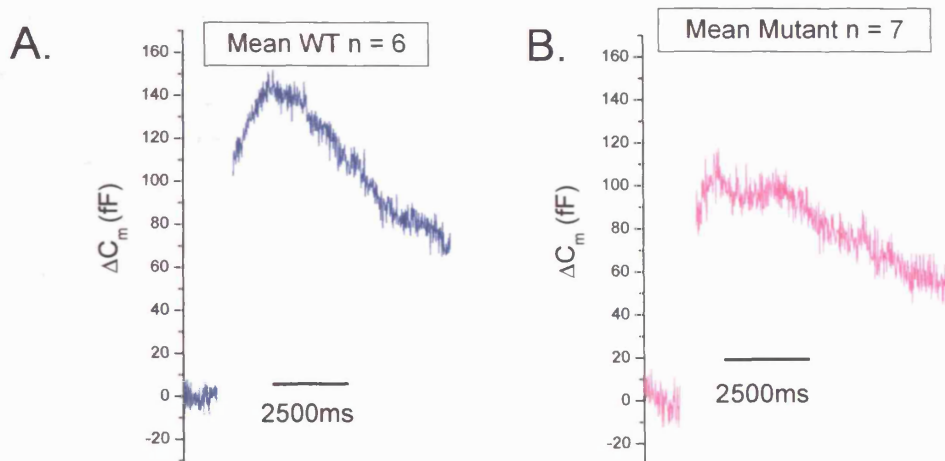
A. For cells over-expressing WT calmodulin the mean ΔC_m resulting from a 200ms depolarisation was 107 ± 37 fF, with a mean calcium entry of $179 \pm 16 \times 10^6$ Ca^{2+} ions, n = 6. Shown is the average capacitance trace (blue).

B. For cells over-expressing mutant calmodulin the mean ΔC_m resulting from a 200ms depolarisation was 89 ± 22 fF, with a mean calcium entry of $156 \pm 18 \times 10^6$ Ca^{2+} ions, n = 7. Shown is the average capacitance trace (magenta).

7.1.2. Asynchronous secretion.

In chapter 4 it was observed that exocytosis evoked by a 200ms depolarisation that cells displayed an increase in asynchronous capacitance post-stimulus (22 out of 41). The ΔC_m measured 1 second post-stimulus was defined as post-stimulus drift (PSD), and could be positive for cells displaying asynchronous release, or negative for cells in which endocytosis predominated immediately following the exocytotic burst. The direction and magnitude of the PSD was related to calcium influx. Cells displaying a positive PSD had a mean calcium entry of $190 \pm 16 \times 10^6$ Ca^{2+} ions n = 22, whereas cells displaying a negative PSD had mean calcium entry of $262 \pm 23 \times 10^6$ Ca^{2+} ions n = 19. This effect was significant, p = 0.01 (figure 4.9.2D). With cells infected with either WT or mutant calmodulin asynchronous secretion (positive PSD) was observed

in 5/6 and 5/7 cells respectively. A scatter plot of the size and direction of the measured PSD 1 second post-stimulus against calcium entry indicates that there were no obvious differences between WT and mutant infected cells. The observation that the majority of cells display a positive PSD is in agreement with previous results from uninfected cells, as the mean calcium entry for WT and mutant cells was $179 \pm 16 \times 10^6\,Ca^{2+}$ ions, n = 6 and $156 \pm 18 \times 10^6\,Ca^{2+}$ ions n = 7, respectively, which is similar to the mean calcium entry of uninfected cells that displayed a positive PSD, $190 \pm 16 \times 10^6\,Ca^{2+}$ ions, n = 22.

7.1.3 Asynchronous release from virally infected cells
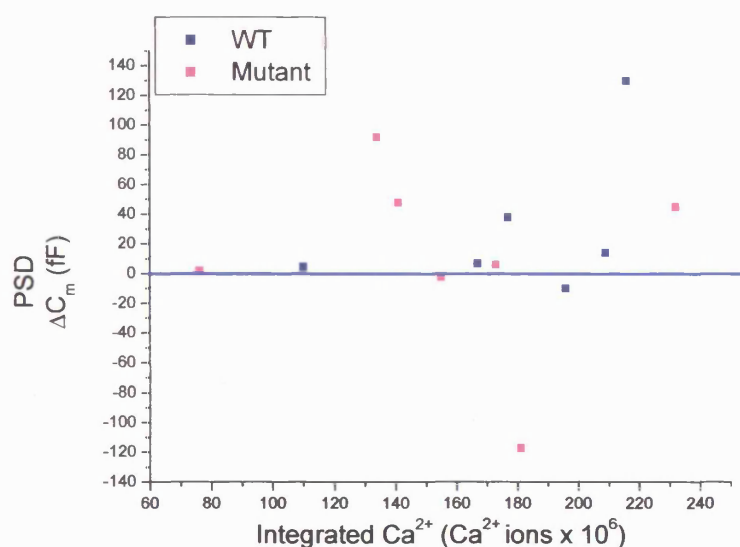
PSD, (the ΔC_m 1 second post-stimulus), is plotted against calcium entry. In relation to the size and direction of the PSD after a 200ms depolarisation cells infected with WT or mutant calmodulin behave in a manner predicted from previous studies on uninfected cells.

However a recent study has suggested that adenoviral infection leads to an increase in asynchronous secretion (Thiagarajan et al. 2004). The molecular mechanism(s) underlying this were not determined, although the authors conclude that it is not due to viral infection altering endocytosis or resting calcium homeostasis. In uninfected cells displaying asynchronous secretion, the peak increase in capacitance occurred 0.5

to 1.5 seconds post-stimulus, before membrane retrieval predominated, and capacitance decreased through endocytotic mechanisms. Therefore I arbitrarily measured capacitance 1 second post-stimulus. It was noted however that in some cells infected with adenovirus post-stimulus asynchronous secretion continued for several seconds. This was observed for both WT and mutant infected cells suggesting a specific affect of viral infection rather than virally-driven gene expression of calmodulin and an explicit role for Ca^{2+}/calmodulin in mediating asynchronous release. The mechanism underlying this increase in asynchronous secretion after viral infection is not known but could result from a signalling cascade activated by viral capsid binding to cell surface receptors and/or trafficking of the virus within the endocytotic pathway.

7.1.4 Longer asynchronous secretion was occasionally detected from virally infected cells.
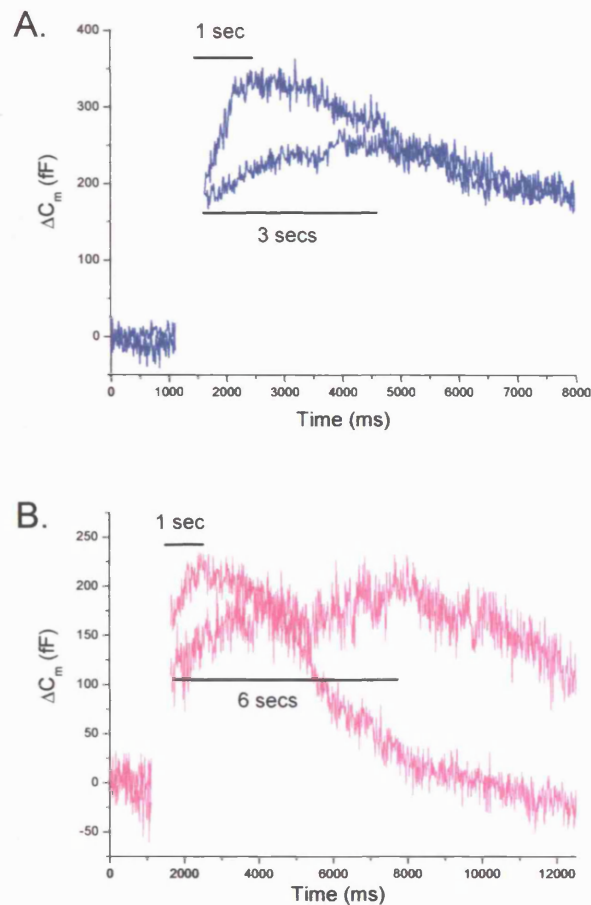
In contrast to uninfected cells, where asynchronous release was temporally restricted to < 1.5 seconds, virally infected cells occasionally displayed longer asynchronous secretion lasting for several seconds.
A. Two capacitance traces evoked by a 200ms depolarisation from cells infected with WT calmodulin adenovirus (blue). One trace exhibits a peak increase in asynchronous secretion within 1 second post-stimulus similar to uninfected cells, whilst the other displays asynchronous secretion lasting several seconds.
B. Two capacitance traces evoked by a 200ms depolarisation from cells infected with mutant calmodulin adenovirus (magenta). One trace exhibits a peak increase in asynchronous secretion within 1 second post-stimulus similar to uninfected cells, whilst the other displays asynchronous secretion lasting several seconds.
The molecular mechanism(s) underlying the increase in asynchronous duration is unknown.

7.2 Calcium-dependency of exocytosis.

In chapter 4, exocytosis was described as a simple transfer function of summed calcium. Individual ΔC_m could be plotted against calcium entry and fit with an allometric function. These results were in good agreement with the published findings of (Engisch and Nowycky 1996) and suggest that regulated exocytosis is related to calcium entry with a power ≤ 2. Plotting the ΔC_m of 40,100,200 and 800ms pulses against calcium entry resulted in a curve that could be fit using the equation $\Delta C_m = g * (\Delta Ca^{2+})^x$. With cells infected with WT calmodulin adenovirus data from 6 cells was plotted and the best fit was obtained with a proportionality constant $g = 0.04$ and power $x = 1.58$. With cells infected with mutant calmodulin adenovirus data from 7 cells was plotted and the best fit was obtained with a proportionality constant $g = 0.04$ and power $x = 1.54$ (figure 7.2.1). This is almost identical to the proportionality constant $g = 0.05$ and power $x = 1.51$ derived from fitting data from 14 uninfected cells (figure 4.1.4). The same data plotted on logarithmic coordinates could be fit with a linear regression suggesting that regulated exocytosis is not altered by either virus and is related to calcium entry with a power ≤ 2.

7.2.1 Stimulus-coupled exocytosis is a second order function of calcium entry.
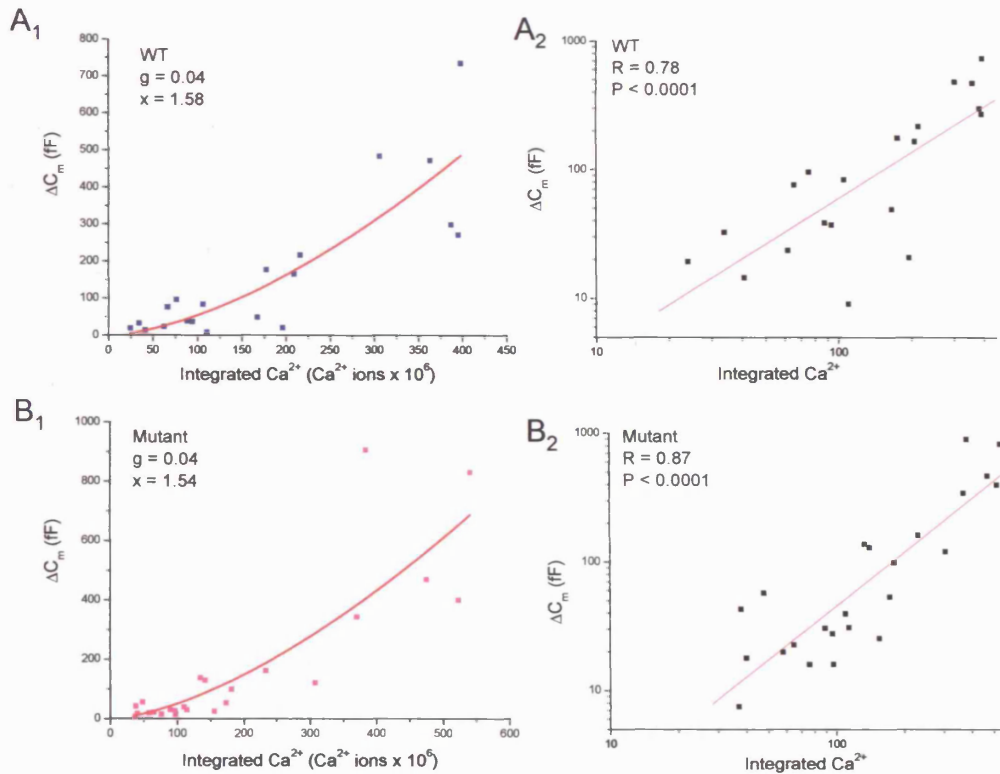
ΔC_m evoked by 40,100,200 & 800ms pulses is plotted against calcium entry and fit using the equation $\Delta C_m = g * (\Delta Ca^{2+})^x$. The curve was constrained to pass through $Y = 0$ at 0 calcium entry.

A_1. Data derived from WT infected cells was best fit with a proportionality constant $g = 0.04$ and power $x = 1.58$.

A_2. Plot of the same data in (A_1) on logarithmic coordinates, and fit with a straight line $r = 0.78$, $p < 0.0001$.

B_1. Data derived from mutant infected cells was best fit with a proportionality constant $g = 0.04$ and power $x = 1.54$.

B_2. Plot of the same data in (B_1) on logarithmic coordinates, and fit with a straight line $r = 0.87$, $p < 0.0001$.

By normalizing the amount of exocytosis for each duration to the amount of calcium entering, the efficacy of calcium-secretion coupling can be assessed. Exocytotic efficiency is not significantly different between WT and mutant calmodulin over-expressing cells for pulses ranging in length from 200ms to 800ms in duration, however with shorter length pulses, cells infected with mutant calmodulin adenovirus were less efficient at evoking exocytosis than WT infected cells (figure 7.2.2).

208

7.2.2 Exocytotic efficiency of cells over-expressing WT or mutant calmodulin.
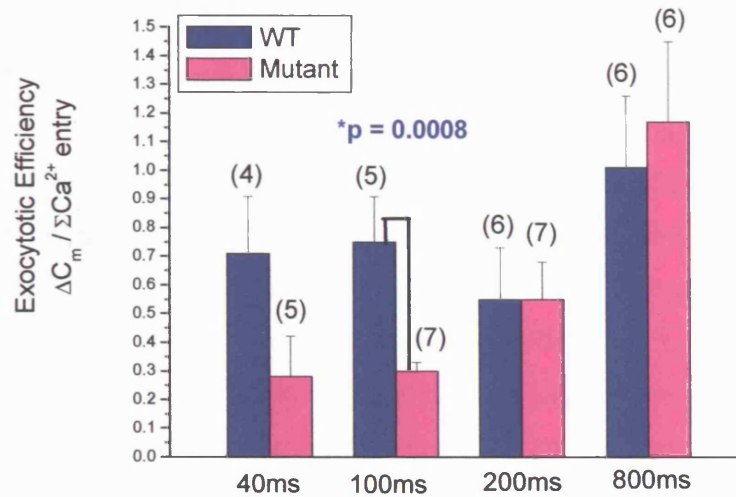
Exocytotic efficiency was derived by dividing ΔC_m by calcium entry per pulse. Displayed is a bar chart of exocytotic efficiency for 40, 100, 200 and 800ms depolarisations from cells expressing either WT (blue), or mutant (magenta) calmodulin. Sample numbers for each condition are shown above in the parenthesis. Exocytotic efficiency at 40ms was calculated as 0.71 ± 0.2, n = 4 and 0.28 ± 0.14, n = 5 for WT and mutant respectively, this was considered not quite significant, p = 0.1. Exocytotic efficiency at 100ms was calculated as 0.75 ± 0.16, n = 5 and 0.30 ± 0.03, n = 7 for WT and mutant respectively, this difference was statistically significant, p = 0.0008. With longer depolarisations exocytotic efficiency was equivocal for WT and mutant expressing cells. Exocytotic efficiency at 200ms was calculated as 0.55 ± 0.18, n = 6 and 0.55 ± 0.13, n = 7 for WT and mutant respectively. Exocytotic efficiency at 800ms was calculated as 1.01 ± 0.25, n = 6 and 1.17 ± 0.28, n = 6 for WT and mutant respectively.

The reduction in exocytotic efficiency with shorter depolarisations implies that the dominant negative mutant calmodulin could differentially affect fusion from different pools of vesicles. Release from the SRP, which will dominate exocytosis in response to long ($\geq$200ms) pulses may not be affected by over-expression of mutant calmodulin, but it could affect release from the IRP, and/or remainder of the RRP. To examine this possibility the size of the IRP/RRP from either WT or mutant calmodulin expressing cells was estimated using the double pulse protocol (see section 4.2.5). Two 10ms depolarisations were elicited and the size of the IRP determined using the following equation:

$$B_{max} = S / (1-R^2)$$

Where S represents the capacitance sum of the first (ΔC_{m1}) and second (ΔC_{m2}), and R is the ratio $\Delta C_{m2}/\Delta C_{m1}$ (Gillis et al 1996). The upper limit of the pool size is assumed to be the value derived for B_{max}. These experiments were conducted in both the perforated patch configuration and the whole cell configuration. In whole cell experiments secretion data is limited to the very first stimulus only, to prevent distortion of results due to dialysis of cytoplasmic factors necessary for maintaining pool sizes. For WT calmodulin over-expressing cells the size of the IRP calculated in the perforated patch configuration was 55 ± 30 fF, n= 7 and 61 ± 17 fF, n = 8 recorded in the whole cell configuration. This gave a total mean value of 58 ± 17 fF, n = 15. It was not possible to calculate the size of the IRP from 4 cells (1 perforated, 3 whole cell), as the ratio $\Delta C_{m2}/\Delta C_{m1}$ was > 0.7 and therefore one can not assume sufficient pool depletion invalidating this use of this test (Gillis et al 1996). For mutant calmodulin over-expressing cells the size of the IRP calculated in the perforated patch configuration was 18 ± 10 fF, n= 8 and 11 ± 3 fF, n = 10 recorded in the whole cell configuration. This gave a total mean value of 14 ± 5 fF, n = 18. It was not possible to calculate the size of the IRP from 3 cells (all whole cell), as the ratio $\Delta C_{m2}/\Delta C_{m1}$ was > 0.7. The difference in the size of the IRP for WT and mutant calmodulin over-expressing cells was significant, p = 0.01. When the pulse duration was increased to 100ms to determine the size of the RRP (Gillis et al. 1996; Voets et al. 1999), the mean size for WT calmodulin over-expressing cells was 210 ± 84 fF, n = 6 and 80 ± 20 fF, n = 6 for mutant calmodulin over-expressing cells. This difference was not significant, p = 0.1 (figure 7.2.3). However 5 out of the 11 WT and 6 out of the 12 mutant calmodulin over-expressing cells were discarded from analysis as the ratio $\Delta C_{m2}/\Delta C_{m1}$ was > 0.7. I believe if I had extended the pulse duration to 150ms I would have depleted the pool sufficiently to have been able to include these cells in this test and would have detected a significant difference in the size of the RRP. An alternative way in which to measure the size of the RRP is by using flash photolysis of caged calcium (Heinemann et al. 1994). In such experiments calcium channels are bypassed and cytoplasmic calcium raised uniformly. This leads to a change in exocytosis with several kinetic components. The fast burst is thought to reflect release of vesicles from the RRP (ie fusion

competent vesicles requiring just a rise in intracellular calcium for release). The slow burst represents a mixture of release from the SRP, refilling of the RRP and contamination from endocytosis (Voets et al. 1999). If I were to conduct flash photolysis experiments I would predict that the size of the fast burst would be smaller for cells over-expressing mutant calmodulin compared to those over-expressing WT calmodulin or uninfected cells. Another advantage of this technique is that it assesses the role of calmodulin in modulating the secretory machinery completely independently of its regulation of calcium channels.

7.2.3 Determining the size of the IRP and RRP.

A.
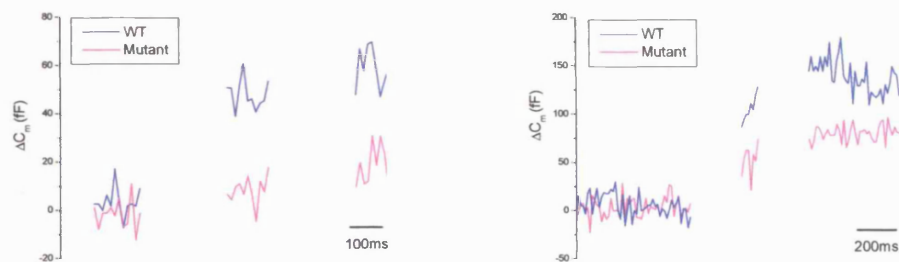
B.
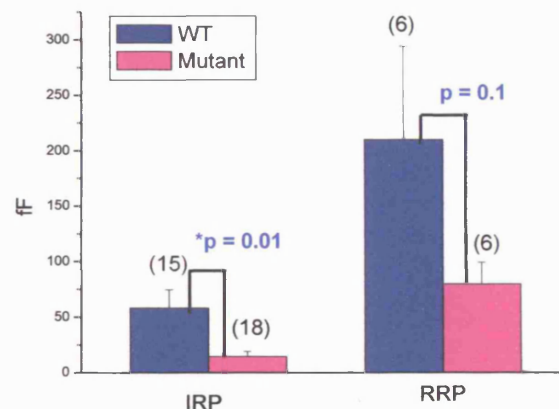
A. Sample capacitance traces of either WT (blue), or mutant (magenta) calmodulin over-expressing cells in response to a either a double 10ms (left), or double 100ms (right) pulse.
B. Bar chart of the mean size of the IRP and RRP. For WT calmodulin over-expressing cells (blue) the size of the IRP was 58 ± 17 fF, n = 15 and the RRP was 210 ± 84 fF, n = 6. For mutant calmodulin over-expressing cells (magenta) the size of the IRP was 14.3 ± 4.6fF, n = 18, and the RRP was 80 ± 20 fF, n = 6. The difference between pool size for the IRP was statistically significant p = 0.01, however the difference in the size of the RRP failed to reach significance p = 0.1.

211

With the pool protocol (6, 10ms depolarisations followed by 4, 100ms depolarisations), the 10ms stimuli will result in a ΔC_m that reflects fusion of the IRP, the further 4 longer pulses result in a second bout of secretion which reflects the fusion of the remainder of the RRP and a fraction of the SRP (Voets, Moser et al. 2001). With cells over-expressing WT calmodulin the cumulative ΔC_m recorded at pulses 1, 6 and 10 were 25 ± 14 fF, 87 ± 41 fF and 438 ± 82 fF, n = 7 for perforated patch recordings and 32 ± 8 fF, 106 ± 32 fF and 498 ± 122 fF, n = 12, for whole cell recordings giving a total mean cumulative ΔC_m of 29 ± 7 fF, 99 ± 25 fF and 476 ± 81 fF, n = 19. With cells over-expressing mutant calmodulin the cumulative ΔC_m recorded at pulses 1, 6 and 10 were 8 ± 3 fF, 34 ± 19 fF and 268 ± 75 fF, n = 8 for perforated patch recordings and 8 ± 2 fF, 25 ± 5 fF and 498 ± 95 fF, n = 13, for whole cell recordings giving a total mean cumulative ΔC_m of 8 ± 2 fF, 28 ± 8 fF and 398 ± 68 fF, n = 21. The difference in the cumulative ΔC_m at pulses 1 and 6 between WT and mutant calmodulin over-expressing cells was highly significant, $p = 0.004$ and $p = 0.007$. The difference in cumulative ΔC_m was not significant at pulse 10, $p = 0.46$. The difference in the cumulative ΔC_m at pulses 1 and 6 was not due to a significant difference in calcium entry. Integrated calcium entry was 12 ± 1 and $9.0 \pm 2 \times 10^6$ Ca^{2+} ions, for WT and mutant over-expressing cells respectively at pulse 1, and cumulative calcium entry of 63 ± 6.4 and $52 \pm 8 \times 10^6$ Ca^{2+} ions at pulse 6 (figure 7.2.4).

7.2.4 Analysis of calmodulin regulation of exocytosis in response to the pool protocol.
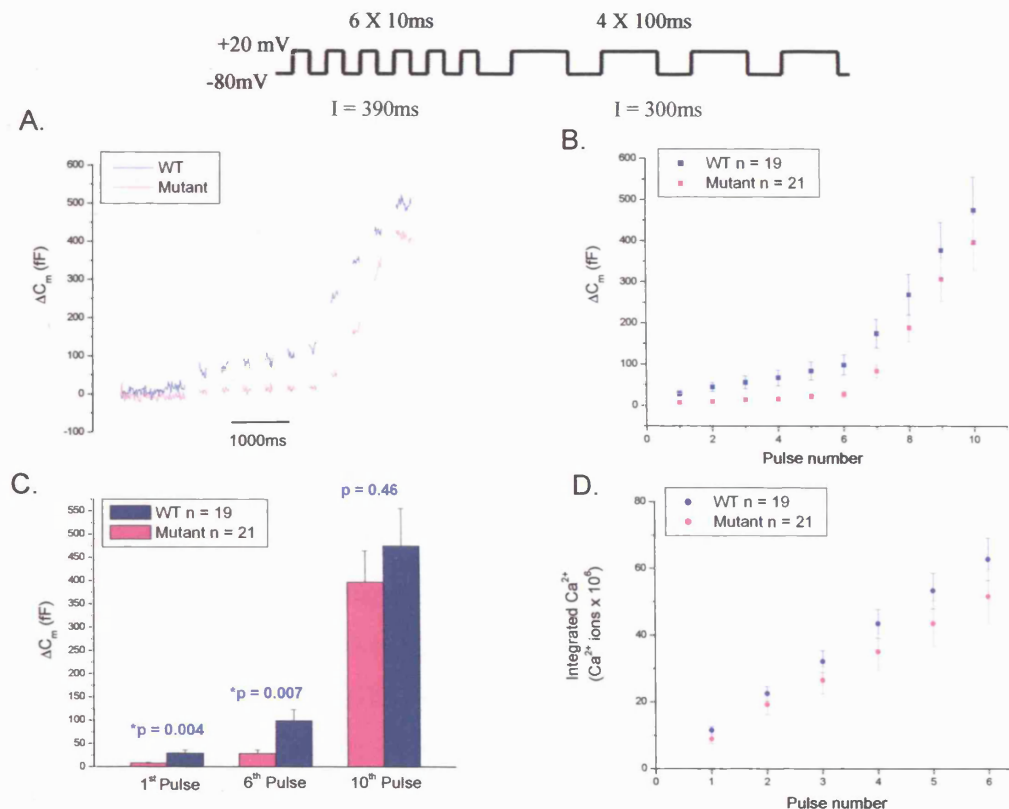
The protocol is shown schematically, 6, 10ms depolarisations with an interpulse interval of 390ms were delivered immediately followed by 4, 100ms depolarisations with an interpulse interval of 300ms.

A. Representative capacitance traces evoked by the pool protocol for WT (blue) and mutant (magenta) calmodulin over-expressing cells.

B. Mean $\Delta C_m \pm$ s.e.m for cumulative capacitance for WT (blue) and mutant (magenta) calmodulin over-expressing cells.

C. Bar chart displaying the mean $\pm$ s.e.m, cumulative ΔC_m calmodulin over-expressing cells at pulses 1, 6 and 10, for WT (blue) 29 ± 7 fF, 99 ± 25 fF and 476 ± 81 fF, n = 19 and mutant (magenta) 8 ± 2 fF, 28 ± 8 fF and 398 ± 68 fF, n = 21. The difference in the cumulative ΔC_m at pulses 1 and 6 between WT and mutant calmodulin over-expressing cells was highly significant, p = 0.004 and p = 0.007. The difference in cumulative ΔC_m was not considered significant at pulse 10, p = 0.46

D. Mean $\pm$ s.e.m of cumulative calcium entry for WT (blue) and mutant (magenta) calmodulin over-expressing cells. Integrated calcium entry was 12 ± 1 and 9 ± 2 x 10^6 Ca^{2+} ions, for WT and mutant over-expressing cells respectively at pulse 1, and cumulative calcium entry of 63 ± 6 and 52 ± 8 x 10^6 Ca^{2+} ions at pulse 6.

213

7.2.5 Is calmodulin the calcium sensor for fast stimulus-coupled release?

I have shown in response to the pool protocol, in uninfected cells, that barium does not evoke secretion from the 10ms pulses, designed to assess the size of the IRP, and although secretion occurs during the last 4, 100ms pulses this is considerably less than the ΔC_m with calcium (chapter 4, section 4.11). The lack of stimulus-coupled exocytosis from mutant calmodulin over-expressing cells in response to brief 10ms depolarisations is reminiscent of secretion from uninfected cells when barium is used instead of calcium as the extracellular divalent. To investigate this further in the perforated patch configuration I stimulated mutant calmodulin over-expressing cells with extracellular calcium and then again with extracellular barium. There was no difference in the amount of exocytosis elicited from the first 6 pulses, however by the last pulse in the train, significantly more exocytosis was evoked with calcium, 294.8 $\pm$ 75.4fF, than with barium 63.1 $\pm$ 33.3fF, n = 3, p = 0.048 (figure 7.2.6).

Could this mean that calmodulin is a calcium sensor for fast calcium-dependent release? The prevailing school of thought at present is that synaptotagmin 1 is the calcium sensor for fast stimulus-coupled release (Fernandez-Chacon et al. 2001), and it has been proposed that other synaptotagmin isoforms regulate fusion from the SRP and could potentially mediate fusion in response to barium entry. However when stimulus-coupled secretion was examined from synaptotagmin 1 deficient chromaffin cells, exocytosis evoked from a train of depolarisations similar to the one in the pool protocol displayed a ΔC_m identical to the one shown in figure 7.2.4 when cells over-express mutant calmodulin (Voets et al. 2001). Therefore the observation that mutant calmodulin inhibits fast stimulus-coupled release could be interpreted as calmodulin being the calcium sensor for fast release. An alternative, hypothesis is that calmodulin plays an important role in priming of vesicles that reside in the IRP and therefore over-expression of mutant calmodulin is simply reducing the number of fusion-competent vesicles ready to respond to brief depolarisations without having a direct effect on the calcium sensor for fusion. The evidence in support of synaptotagmin 1 as the calcium sensor for fast release is considerable (Chapman

214

2002; Sudhof 2004). A key observation in this respect is that strontium ions can efficiently substitute for calcium in triggering exocytosis. Synaptotagmin 1 can bind strontium via its C2-domains, however strontium is a poor activator of calmodulin. Therefore I favour a role for calmodulin in vesicle priming. A suitable control experiment would be to substitute calcium for strontium and monitor exocytosis. If exocytosis from WT calmodulin over-expressing cells is reduced to the same level as mutant calmodulin over-expressing cells then you could propose a role for calmodulin as a calcium sensor for fast calcium-dependent exocytosis in chromaffin cells.

7.2.6 Exocytosis elicited by brief depolarisations from mutant calmodulin over-expressing cells in the presence of calcium or barium.
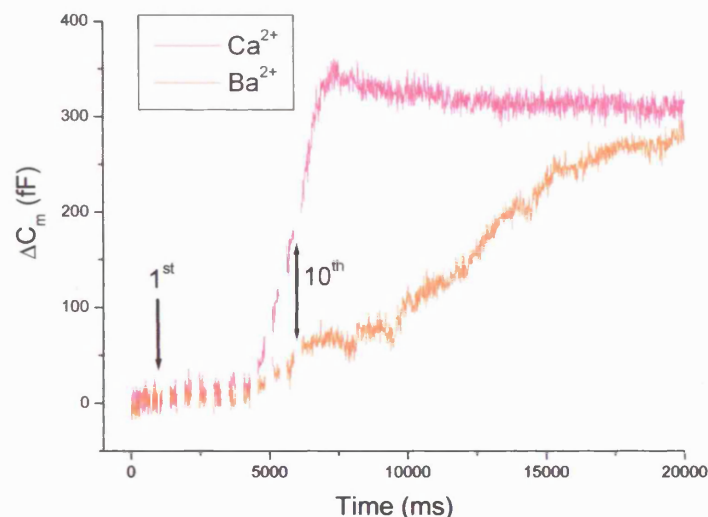
Sample capacitance traces from a single cell over-expressing mutant calmodulin in response to the pool protocol with either calcium (magenta), or barium (orange), as the extracellular divalent. There was no statistical difference in the ΔC_m between calcium and barium during the first 6 brief (10ms) pulses, ΔC_m at pulse 1 was 11 ± 4 fF and 5 ± 3 fF, n = 3, for calcium and barium respectively. However the ΔC_m evoked from the long (100ms) pulses was. ΔC_m at pulse 10 was 295 ± 75 fF and 63 ± 33 fF, n = 3, p = 0.05 for calcium and barium respectively.

7.2.7 Calmodulin does not mediate exocytosis elicited by barium.

There was no statistical difference between WT and mutant over-expressing cells when barium was used as the charge carrier, pulse 1, ΔC_m of 3 ± 1 fF and 5 ± 3 fF, and pulse 10, 46 ± 27 f F and 63 ± 33 fF, n = 5 and n = 3, for WT and mutant calmodulin over-expressing cells respectively (figure 7.2.7). Over-expression of a mutant calmodulin therefore does not inhibit exocytosis when barium is the charge carrier, which adds weight to the argument that barium induces release from molecularly distinct pool of vesicles (Seward et al. 1996; Duncan et al. 2003).

7.2.8 Exocytosis is not altered between mutant and WT calmodulin over-expressing cells when barium is the charge carrier.
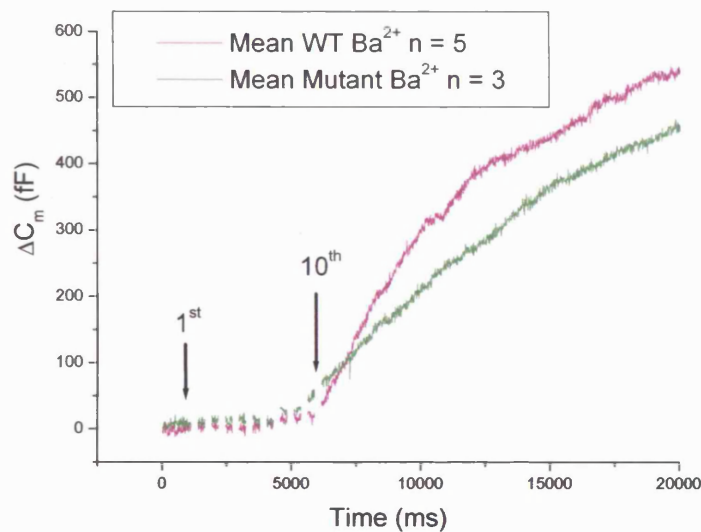
Mean capacitance traces for WT (purple), or mutant (olive) calmodulin over-expressing cells. There was no statistical difference in the ΔC_m evoked from any pulses in the protocol. ΔC_m at pulse 1 was 3 ± 1 fF, n = 5 and 5 ± 3 fF, n = 3 and ΔC_m at pulse 10 was 46 ± 27 fF, n = 5 and 63 ± 33 fF, n = 3, for WT, and mutant calmodulin over-expressing cells respectively.

216

7.3 Exocytosis evoked in response to a train of brief depolarisations.

The physiological stimulus for secretion in chromaffin cells is splanchnic nerve
stimulation, subsequent release of acetylcholine onto nicotinic channels which
triggers bursts of action potentials resulting in activation of voltage-dependent
channels and exocytosis, under stressful conditions a high firing rate can be achieved
(Douglas and Poisner 1967; Duan et al. 2003). To investigate the role of calmodulin
in regulating exocytosis in a more physiological context, trains of brief (10ms)
depolarisations were applied at 20Hz. In response to this stimulation the mean
cumulative ΔC_m at pulse 50 was 307 ± 67 fF and 323 ± 80 fF, for WT and mutant
calmodulin over-expressing cells respectively, with related cumulative calcium entry
of 229 ± 24 and 250 ± 33 x 10^6 Ca^{2+} ions. Therefore over-expression of the mutant
calmodulin does not alter total release in response to a robust train of depolarisations.
The calcium-exocytosis relationship was next investigated. Mean data of cumulative
capacitance against cumulative integrated calcium was plotted and fit using the
equation $\Delta C_m = g * (\Delta Ca^{2+})^x$. For cells over-expressing WT calmodulin the mean
data from 9 cells was plotted and the best fit of the curve generated by the algorithm
yielded a proportionality constant $g = 0.01$ and power $x = 1.84$. The power value
obtained by fitting data from individual cells with the algorithm ranged from $x = 0.85$
to 2.93, mean 1.81 ± 0.2. For cells over-expressing mutant calmodulin the mean data
from 6 cells was plotted and the best fit of the curve generated by the algometric
function yielded a proportionality constant $g = 0.1$ and power $x = 1.45$. The power
value obtained by fitting data from individual cells with the algorithm ranged from x
= 1.06 to 2.29, mean 1.65 ± 0.2. These values are similar to the ones reported in
chapter 4 for uninfected cells, proportionality constant $g = 0.05$ and power $x = 1.60$, n
= 10 (see fig 4.2.3). Taken together this data suggests that calcium-dependence of
exocytosis is not altered when cells over-express either WT or the mutant calmodulin.
However, figure 7.3.1 shows that the first few pulses in the train resulted in a
capacitance 'hump' that was not well fit by the curve generated for the whole train for
WT over-expressing cells, but was not observed in cells over-expressing mutant
calmodulin. I have attributed this 'hump' to reflect fusion of the IRP, (discussed in

217

sections 4.2.4 and 5.10.2). This therefore supports the previous experimental findings and suggests that over-expression of the mutant selectively reduces the efficiency of fusion from the IRP and possibly the remainder of the RRP, but does not affect fusion from the SRP. There is a significant difference between the mean cumulative ΔC_m for WT and mutant cells in the first few pulses in the train. Significance fails (p > 0.05) after pulse 4. It was surprising that after only 4 pulses the difference in the mean cumulative ΔC_m was no longer statistically different between WT and mutant calmodulin over-expressing cells. In figure 7.2.4 I show that there is still a highly significant difference after 6, 10ms pulses. The difference in results could be explained by the protocol interpulse interval. In the pool protocol, the interval between 10ms pulses is 390ms whereas in the train protocol the interpulse interval is only 50ms. Therefore vesicle pools could partially refill in the pool protocol in between pulses and calcium entry could be more efficiently buffered and/or extruded with an interpulse interval of 390ms compared to 50ms. One could envisage that calcium entry is spatially restricted during the 6, 10ms pulses of the pool protocol, as there is time to effectively buffer and extrude calcium in between pulses. During the train protocol this may not be the case and calcium entry per pulse could sum leading to a less spatially restricted area of raised intracellular calcium, which will result in fusion from vesicles no longer limited to the IRP.

218

7.3.1 Calcium-exocytosis relationship in response to a train of brief (10ms) depolarisations.
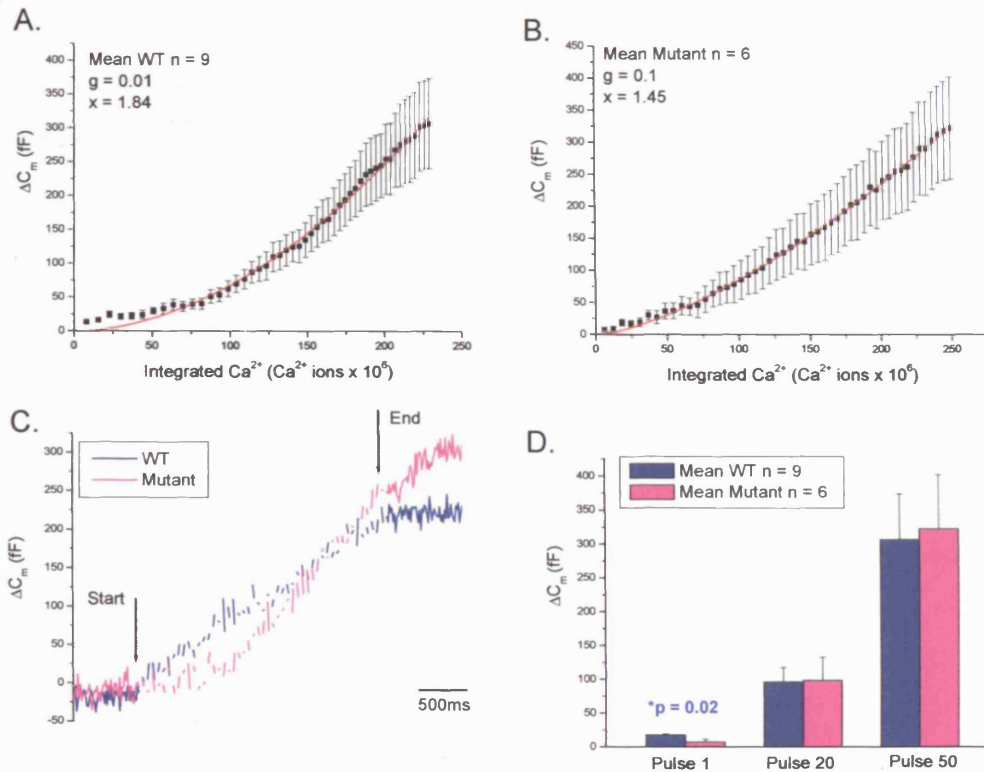
Cumulative capacitance is plotted against cumulative integrated calcium and fit with the equation $\Delta C_m = g * (\Delta Ca^{2+})^x$.

A. Cells over-expressing WT calmodulin. Mean cumulative $\Delta C_m \pm$ s.e.m is plotted against mean cumulative calcium n = 9. The best fit curve is represented by the red line, the first few pulses in the train deviate slightly from this line. The proportionality constant g = 0.01 and power x = 1.84.

B. Cells over-expressing mutant calmodulin. Mean cumulative $\Delta C_m \pm$ s.e.m is plotted against mean cumulative calcium n = 6. The best fit curve is represented by the red line, the first few pulses in the train do not deviate from this line. The proportionality constant g = 0.1 and power x = 1.45.

C. Sample capacitance traces for WT (blue) and mutant (magenta) calmodulin over-expressing cells. The arrows indicate the 1st and last (50th) depolarisation.

D. Bar chart depicting the mean ΔC_m at pulses 1, 20 & 50 for WT (blue) and mutant (magenta) calmodulin over-expressing cells. There is a significant difference between WT and mutant cells for the first few pulses in the train. Significance fails (p > 0.05) after pulse 4, by pulse 20 cumulative ΔC_m is greater for mutant cells compared to WT calmodulin over-expressing cells.

7.4 Summary of exocytosis data

The data presented in this chapter shows that stimulus-coupled secretion is altered after over-expression of mutant calmodulin, (with respect to either WT or uninfected cells) in response to brief depolarisations and not after long single pulses, or robust trains of brief depolarisations. This suggests that the physiological consequence of calmodulin regulation is related to vesicle priming, increasing the number of fusion-competent vesicles (the RRP) able to fuse in response to single or brief trains of action potentials. This type of stimulus dictates basal catecholamine release and is important for maintaining vascular tone. During periods of stress when action potential frequency increases and large quantities of catecholamine are released, the RRP is quickly depleted and secretion is dominated by release from the SRP. My studies indicate that Ca^{2+}/calmodulin is not an important regulator of release from the SRP, nor is it important for regulating the pool of vesicles released when calcium is substituted for barium.

7.5 Discussion of calmodulin regulation of exocytosis.

In this section I discuss potential molecular mechanisms, which may account for my observations of altered exocytosis from chromaffin cells after over-expression of a mutant calmodulin. The majority of previous studies investigating a role for calmodulin regulation of stimulus-coupled secretion have utilised peptide blockers or antibodies, or addition of recombinant protein (see section 1.18 for details). They have measured exocytosis using biochemical methods with poor time resolution and as such are unable to determine whether specific pools of vesicles are targeted. I have refined this experimental approach using capacitance measurements and investigated the effects of additional WT calmodulin expression and expression of a mutant incapable of binding calcium. By varying stimulation paradigms I have assessed contributions from different pools of vesicles and shown that Ca^{2+}/calmodulin specifically regulates the IRP and probably the remainder of the RRP in response to single pulses or brief trains of depolarisations. The specific

220

molecular targets of calmodulin enhancement of exocytosis are beginning to be described, there is now good evidence to suggest regulation of core complex SNARES, proteins essential for vesicle priming, and proteins which limit or recruit vesicles from the reserve pool to the RRP. These are discussed below.

7.5.1 Interactions with members of the core complex.

Trans SNARE complex assembly is an essential step in calcium-dependent exocytosis. Recent evidence suggests that calcium can bind either directly to the complex, or via Ca^{2+}/calmodulin or via CaMKII to participate either directly in secretion or facilitate core complex coupling to the calcium sensor to mediate fusion. These interactions and their physiological relevance are discussed below.

7.5.1.1 Synaptobrevin

Over the last four years Professor Seagars group has published a series of papers reporting an interaction between Ca^{2+}/calmodulin and synaptobrevin (Quetglas et al. 2000; Quetglas et al. 2002; de Haro et al. 2004). The binding sequence (residues 77-90) is situated precisely C-terminal to the tetanus toxin (TeTX) and botulinum B toxin cleavage site close to the transmembrane anchor. This sequence binds both Ca^{2+}/calmodulin and phospholipids in a mutally exclusive manner. Mutation of basic or hydrophobic residues within this motif reduces both Ca^{2+}/calmodulin and phospholipid binding to the same extent. The functional effect of this motif was explored by cleavage of endogenous synaptobrevin by TeTX and subsequent transfection of TeTX resistant synaptobrevin with or without mutations that inhibit Ca^{2+}/calmodulin and phospholipid binding into PC12 cells. Exocytosis was abolished in the latter case, indicating that either Ca^{2+}/calmodulin and/or phospholipid binding to this region of synaptobrevin is required for calcium-dependent exocytosis. They next investigated the mechanisms involved and determined that cis lipid binding

221

(synaptobrevin folding back on itself and into the vesicle lipid bilayer) occurs and that addition of Ca^{2+}/calmodulin totally disrupts cis inhibition, triggering trans lipid binding (insertion into the plasma membrane). They speculate that Ca^{2+}/calmodulin can displace cis phospholipids to induce SNARE pairing and formation of the core complex and insertion of synaptobrevin into the plasma membrane. This would significantly reduce the distance between the opposed bilayers, inducing hemi-fusion (mixing of the outer vesicle leaflet, with the inner plasmalemmal leaflet), thereby reducing the energy required for subsequent full fusion. The difference between the SRP and the RRP has been described as a transition from a loose to a tight trans-SNARE complex (Xu et al. 1998). If the physiological consequence of the Ca^{2+}/calmodulin-synaptobrevin interaction is to facilitate a tight trans-SNARE complex and formation of an RRP then this is a potential mechanism to explain my results. If the Ca^{2+}/calmodulin-synaptobrevin interaction is required upstream of this for the formation of a loose SNARE complex and the construction of an SRP then it is unlikely to be the target affected in my studies.

7.5.1.2 Syntaxin

Exocytosis can be regulated by Ca^{2+}/ATP-dependent binding of autophosphorylated Ca^{2+}/CaMKII to syntaxin 1A (Ohyama et al. 2002). The authors show that autophosphoylated CaMKII specifically bound syntaxin when calcium concentration was $>10^{-6}M$, and bound CaMKII was released when the calcium concentration decreased or CaMKII was dephosphorylated. CaMKII bound to the linker domain of syntaxin, a region separate from other syntaxin binding proteins (Munc18/tomosyn). Immunoprecipitation experiments showed that the CaMKII-syntaxin complex occurs *in vivo* and when reconstituted *in vitro* recruited larger amounts of synaptotagmin and SNAP-25 than syntaxin alone, suggestive that this interaction is important in regulating SNARE complex formation. CaMKII was unable to bind to syntaxin in the presence of munc 18 (ie in the closed conformation), but did bind to a mutant syntaxin (L165A and E166A) with a forced open configuration (Dulubova et al. 1999) in the presence of munc18. This indicates that CaMKII binds to the open form

222

of syntaxin, which is necessary for binding to other SNARE core complex components. Microinjection of chromaffin cells with a fragment of syntaxin that binds CaMKII decreased the frequency of exocytosis monitored by amperometric detection of catecholamine, but microinjection of a mutant fragment of syntaxin (R151G) unable to bind CaMKII had no effect. Likewise microinjection of another CaMKII binding fragment that does not bind to syntaxin was without affect. These findings were supported by injection of SCG neurones with the CaMKII binding fragment of syntaxin in which Excitory Post-Synaptic Potentials (EPSPs) were decreased compared to those microinjected with mutant fragments unable to bind CaMKII. Therefore Ca^{2+}/calmodulin activation of CaMKII could facilitate SNARE complex formation via its interaction with syntaxin and is a possible pathway with which over-expression of mutant calmodulin in chromaffin cells could inhibit exocytosis.

7.5.1.3 SNAP-25

The crystal structure of the synaptic fusion complex revealed a number of potential divalent cation binding sites on the surface (Suttonr et al. 1998). One such site, containing acidic and hydrophilic residues on SNAP-25 and synaptobrevin 2, is close to the cleavage sites of TeTX and botulinum A (Fasshauer et al. 1998). There is evidence to suggest that this potential cation-binding site is involved in calcium-mediated triggering of exocytosis. By mutating three amino acids located to the outside of the SNARE complex, reducing the net charge in SNAP-25 slowed secretion and abolished one calcium-binding site in the calcium sensor for exocytosis (Sorensen et al. 2002). The authors were unable to determine whether the mutation effects pool size (stability of the RRP), or release kinetics. It could potentially affect both. Two mechanisms were proposed to explain the reduction in exocytosis. As the site does not provide the full co-ordination required for direct calcium binding, simultaneous binding of synaptotagmin I may be required to generate a full calcium-binding site. Alternatively the site may be able to bind another protein, which itself binds calcium and mediates the affect on exocytosis. In this respect calmodulin may

223

be worth investigating. To my knowledge investigations of such an interaction have not been published. It is important to note in this respect that a binding pocket mediated by several different proteins in the complex may be required.

7.5.1.4 Synaptotagmin

A calcium-dependent interaction between calmodulin and synaptotagmin has been described (Fournier and Trifaro 1988, Trifaro et al. 1989, Perin 1996), however another group failed to detect a calcium-dependent interaction between these proteins (Chen et al. 1999). The physiological importance of this interaction, if it truly occurs, has not been directly tested. Synaptotagmin 1 is also a substrate for CaMKII *in vitro* (Hilfiker et al. 1999).

7.5.2 Priming proteins

Plasma membrane docking is not a prerequisite for subsequent calcium-stimulated vesicle fusion. In order for exocytosis to be efficient, vesicles are required to undergo maturation, or priming. An essential priming protein is Munc-13, which has recently been shown to directly interact with Ca^{2+}/calmodulin; the physiological consequence of this interaction is described below.

7.5.2.1 Munc-13

Genetic studies in mouse, fly and nematode have established an essential role for munc-13 in vesicle priming, (Augustin et al. 1999; Aravamudan and Broadie 2003; Richmond et al. 1999) via its ability to regulate syntaxin (Betz et al. 1997) and promote SNARE complex formation (Brose et al. 2000; Richmond et al. 2001). Recently Professor Brose's group reported a calcium-dependent interaction between munc-13 and calmodulin (Junge et al. 2004). Putative calmodulin binding sites on munc-13 were investigated and a 1-5-10 binding motif was detected. A 21-residue

peptide representing this motif was found to specifically bind to calmodulin in a 1:1 stoichiometry. With several calmodulin targets the first hydrophobic anchor point in the N-terminal part of the motif is a Trp residue. Mutation of this Trp residue has been shown to severely lower the affinity of target proteins for Ca^{2+}/calmodulin (Chin and Means 2000). Similarly a Trp/Arg mutation in the munc-13 binding motif completely abolished calmodulin binding without additional affects on the integrity and function of the protein (ie binding to RIM, or DAG). They then assessed the effect of the Trp mutation in full length munc-13 protein by virally expressing WT or Trp/Arg mutated munc-13-GFP fusion proteins in hippocampal neurones from munc13 (single and double) knockout mice. Evoked EPSC amplitudes from double knock out neurones rescued by over-expression of WT or Trp/Arg munc-13's were indistinguishable indicating that calmodulin binding to munc-13 is not required for basal vesicle priming. However calcium-dependent refilling of the RRP was severely impaired. Therefore the Ca^{2+}/calmodulin interaction with munc-13 is important during sustained activity to refill the RRP. As only activity-dependent refilling of the RRP was observed in neurones after expression of a calmodulin-binding deficient mutant, munc-13 is unlikely to be the molecular target which is affected by over-expression of a mutant calmodulin in chromaffin cells and leads to inhibition of the IRP and/or RRP.

7.5.3 Ca^{2+}/calmodulin regulation of the cytoskeleton

In chromaffin cells a mesh of filamentous actin is believed to act as a barrier to keep vesicles away from the plasma membrane and sites of exocytosis (Vitale et al. 1995). There are numerous proteins with which calmodulin is believed to interact with, which disrupt the integrity of the cytoskeleton and may be important in refilling vesicle pools after bouts of stimulation. The roles of these proteins and their regulation by calmodulin are discussed below.

7.5.3.1 Myosin

Myosins are actin-based motors that hydrolyze ATP to move along actin filaments. Phosphorylation of the myosin light chain, by myosin light chain kinase (MLCK) is required to activate the actin-dependent ATPase activity of myosin, a process dependent on Ca^{2+}/calmodulin (Matsumura et al. 1999). Several studies, have implicated myosins and MLCK in regulating neurotransmitter release (reviewed in Doussau and Augustine 2000). These studies conclude that myosin works upstream of fusion, as the size of the RRP is not affected by inhibitors but exocytosis is inhibited in a use-dependent manner. This suggests that myosin activation facilitates vesicle movement from a reserve pool, to exocytotic sites on the plasma membrane along a track of actin filaments to refill pools (Doussau and Augustine 2000). Two members of this family are believed to be important in this process, myosin II and myosin V, both of which are expressed in chromaffin cells. Myosin V is thought to be particularly important in chromaffin cells (Rose et al. 2003), as antibodies to myosin V heads where able to inhibit exocytosis but myosin II antibodies were not. In addition to its role as a motor, myosin V could play a central role in Ca^{2+}/calmodulin regulation of the cytoskeleton. Myosin V associates with vesicles in a calcium-dependent manner (Prekeris and Terrian 1997), and calmodulin binds to myosin at low calcium concentrations and partially dissociates at high (micromolar) calcium levels (Nascimento et al. 1996). With myosin bound calmodulin is more efficient at activating Ca^{2+}/CaMK II which can then phosphorylate synaptic vesicle associated substrates (Costa et al. 1999). This could explain the requirement of myosin V during sustained stimulation. The myosin V interaction with Ca^{2+}/calmodulin could facilitate the disruption of the cytoskeleton, releasing vesicles which can then be transported towards the plasma membrane after Ca^{2+}/calmodulin-dependent MLCK activation of myosin to refill the RRP.

7.5.3.2 Rab3A

Rab proteins are believed to regulate several processes including movement of vesicles along cytoskeletal filaments, interacting with tethering and docking factors and controlling the duration of fusion (for review see Zerial and McBride 2001). Rab3A is a GTPase believed to cycle on and off vesicle membranes during the vesicle cycle and acts as an inhibitor of exocytosis. *In vitro* studies have identified that Ca^{2+}/calmodulin can cause Rab3A to dissociate from synaptic membranes (Park et al. 1997), although another group disputes this, as they fail to detect an interaction between Rab3A and calmodulin in pull down assays (Chen et al. 1999). The interaction of Rab3A and calmodulin (and not with other binding partners, rabphilin or RIM) has been shown to be important in mediating an inhibition of exocytosis in PC12 cells (Coppola et al. 1999). A recent study in chromaffin cells concludes that Rab3A inhibits recruitment from the SRP (Thiagarajan et al. 2004). Therefore this could help explain why exocytosis in response to long depolarisations in mutant calmodulin over-expressing cells is as efficient as or greater than WT over-expressing cells. With long depolarisations, one expects release from the RRP and the SRP in WT cells, although the contribution from the SRP could be limited by the effect of the Ca^{2+}/calmodulin-Rab3A interaction. In mutant expressing cells release from the RRP is inhibited (via a different mechanism), but secretion from the SRP is enhanced due to removal of the inhibitory control of the Ca^{2+}/calmodulin-Rab3A interaction. Since the SRP has primarily been defined by flash photolysis of caged calcium, experiments designed to investigate release from the SRP should be performed using this technique.

7.5.3.3 Myrisolyated, alanine-rich, protein kinase C substrate (MARKS)

Calmodulin may play other roles in the regulation of the cytoskeleton. Disassembly of the cortical F-actin by calcium entry and activation of either scinderin or MARKS phosphorylation allows vesicles from the reserve pool to move to the plasma membrane (Vitale et al. 1995; Trifaro et al. 2000; Rose et al. 2001; Trifaro et al.

2002). MARKS has been shown to form a complex with Ca^{2+}/calmodulin (Graff et al. 1989). A region of MARCKS enriched with basic amino acids mediates binding to vesicles containing acidic phosphoglycerides. MARKS dissociates from vesicles after PKC phosphorylation of serine residues within this interaction site (Kim et al. 1994), a process which also greatly reduces its interaction with Ca^{2+}/calmodulin (Graff et al. 1989; Kim et al. 1994). The physiological importance of Ca^{2+}/calmodulin binding to MARCKS is not known.

7.5.3.4 Synapsins

Synapsins are integral synaptic vesicle proteins and are substrates for Ca^{2+}/calmodulin kinases (Hilfiker et al. 1999). Two roles for synapsin have been suggested. Firstly, synapsins are thought to tether vesicles to each other and to the actin cytoskeleton to maintain a reserve pool of vesicles close to the active zone. Ca^{2+}/CaM Kinase II is thought to phosphorylate synapsin, which leads to dissociation of synapsins from the vesicle and vesicle release from the cytoskeleton. Secondly synapsins could play a role downstream of vesicle docking by regulating the time course of neurotransmitter release (Hilfiker et al. 1999). Three isoforms of synapsin are present in neurones, all three bind ATP, but this binding is differentially regulated. ATP binding to synapsin 1 is calcium-activated, ATP binding to synapsin 2 is calcium-independent and ATP binding is calcium-inhibited (Hosaka and Sudhof 1998a; Hosaka and Sudhof 1998b). This calcium sensitivity may be mediated by calmodulin as Ca^{2+}/CaM Kinase 2 phosphorylates synapsin 1, but not synapsin 2 (Sudhof 2004). The exact role synapsins play in the synaptic vesicle cycle and whether synapsin phosphorylation is physiologically relevant remains to be determined (Sudhof 2004). Synapsins are unlikely to be the relevant Ca^{2+}/calmodulin target in my studies as synapsin I is not expressed in chromaffin cells (Senda et al. 1991), and although synapsin II is expressed (Firestone and Browning 1992), this isoform is not phosphorylated by CaMKII (Hosaka and Sudhof 1998a).

Calmodulin regulation of the cytoskeleton is most likely to affect exocytosis by mediating activity-dependent refilling of vesicles. The major finding of my studies over-expressing mutant calmodulin was a reduction in the size of the IRP and/or RRP. However I did not specifically examine pool refilling in these experiments. It is highly likely that over-expression of mutant calmodulin will have an affect on activity-dependent recruitment of reserve vesicles to releasable pools in chromaffin cells, possibly an inhibitory affect analogous to studies employing calmodulin inhibitors in neurones (Sakaba and Neher 2001). The challenge will now be to discriminate the physiological importance that potential different effectors, (myosin, Rab3A, or MARKS) play in this pathway in chromaffin cells. This is particularly interesting, as the Ca^{2+}/calmodulin interaction with myosin V would predict an enhancement of exocytosis, whereas the Ca^{2+}/calmodulin interaction with Rab3A would predict an inhibition of exocytosis.

7.5.4 Other Proteins

There are numerous other exocytotic proteins that calmodulin interacts with which, do not fall into the above defined categories, these are discussed below.

7.5.4.1 Vo sector of the V-ATPase

Intracellular membrane fusion was widely believed to be a constitutative process, fundamentally distinct from regulated calcium-dependent exocytosis. This view has been challenged recently with evidence suggesting that intracellular vesicle fusion can also be calcium-dependent (reviewed in Mayer 2001). The calcium sensor for this, at least in yeast was found to be calmodulin (Peters et al. 2001). In this study they identified release of calcium from the vesicle lumen, calmodulin and protein phosphatase I as essential downstream factors which initiate fusion after trans SNARE formation. They also identified the Vo sector of the vacuolar-ATPase as the Ca^{2+}/calmodulin binding partner and suggest that a Vo-Vo trans complex dilates after

Ca^{2+}/calmodulin binding to become the fusion pore (Peters et al 2001). V-ATPases are found on synaptic vesicles, where they mediate an electrochemical proton gradient needed to concentrate neurotransmitter within vesicles. It has been proposed that the Vo sector of the V-ATPase forms the fusion pore in neurones (Morel et al. 2001; Morel 2003), although at present the evidence to support this hypothesis is sparse. Additionally dicyclohexylcarbodiimide (DCCD), which inhibits vacuole fusion does not affect calcium-dependent exocytosis in chromaffin cells (Holz et al. 1983). An alternative role for the V-ATPase-Ca^{2+}/calmodulin interaction may exist. Once a vesicle is loaded with neurotransmitter the subunits, which make up the functional V-ATPase dissociate leaving the Vo sector in the lumenal membrane. I hypothesize that Ca^{2+}/calmodulin could then bind and through its interactions with other SNARE proteins bring the vesicle to the membrane and initiate SNARE complex formation. This would insure that only vesicles fully filled with neurotransmitter are able to fuse, resulting in efficient stimulus-coupled secretion. However a caveat to this proposal is that in synaptosomes, using Bafilomycin A1 to inhibit the V-ATPase and prevent vesicle refilling, empty vesicles were seen to exocytose and endocytose in response to electrical field stimulation using vesicle specific dyes (Cousin and Nicholls 1997).

Amperometry is a technique which allows the kinetics of the fusion pore be measured (Chow et al. 1992; Chow 1995; Schulte and Chow 1998). Using this method Professor Burgoyne's group have suggested that PKC (Graham et al. 2000) Munc18 (Fisher et al. 2001), csyteine string protein (CSP) (Evans et al. 2001), complexin (Archer et al. 2002) and dynamin (Graham et al. 2002) can all affect the degree and duration of fusion pore expansion. Although a powerful technique it is not without controversy and the method of analysis between groups varies, in as much that other groups using this technique fail to detect changes in the kinetics of single fusion events when over-expressing proteins under similar conditions (see Voets et al. 2001). Recently the groups of Professor Jackson and Professor Chapman using this technique have suggested roles for syntaxin (Han et al. 2004) and synaptotagmin (Bai et al. 2004) in controlling fusion pore kinectics. It will be interesting to determine whether calmodulin can affects fusion pore kinetics, and whether it does this

independently of interactions with other SNARE proteins and/or the V-ATPase on the vesicle.

7.5.4.2 Neuromodulin/GAP43

Interestingly, increasing intracellular calcium may lead to an increase in the local concentration of calmodulin available for calcium-dependent binding to target proteins. Some regions of the brain contain a membrane-associated protein called neuromodulin or GAP43. This protein binds calmodulin *in vitro* in the absence of calcium, and releases it when calcium levels rise or after phosphorylation by PKC (Andreasen et al. 1983; Alexander et al. 1987). Therefore this could be a protein involved in facilitation of neurotransmitter release observed by certain neuromodulators. Activation of Gq-coupled receptors leads to release of intracellular calcium and activation of PKC, and then presumably release of calmodulin from neuromodulin, where it can either directly, or through association with other proteins (ie Munc-13) modulate vesicle priming.

7.5.4.3 Pollux & CRAG

In a screen for drosophila retinal calmodulin-binding proteins several proteins with potential to affect exocytosis were discovered (Xu et al. 1998). These included proteins like unc-13, previously described and novel calmodulin interacting proteins. CRAG may provide a mechanism for calcium-regulated GDP/GTP exchange of Rab3 as it shares homology with other identified Rab GEPs. Pollux shares homology to yeast Rab GAP proteins and was localized to the plasma membrane, raising the possibility that this protein may play a role in regulating exocytosis. The functional consequence of calmodulin binding to these proteins is unknown.

7.5.4.4 Calmodulin as a PLC interacting protein.

Calmodulin may play an important role in regulating responses from extracellular modulators. It has been shown to physically interact with phospholipase C-β, (PLCβ) with calmodulin inhibitors reducing G-protein stimulation of inositol phosphate hydrolysis (McCullar et al. 2003). Neuromodulators like histamine (Currie and Fox 2000) or angiotension II (Teschemacher and Seward 2000) couple to GqPCR's in chromaffin cells and modulate release. Therefore calmodulin via is interaction with PLCβ, will regulate the actions these molecules exert on the secretory machinery. Testing the role that calmodulin plays in the signal transduction of histamine or angiotension to induce facilitation of exocytosis was not conducted. However it is unlikely to require Ca^{2+}/calmodulin, as calmodulin can bind to PLCβ in the absence of calcium (McCullar et al. 2003).

7.6 The role of calmodulin in endocytosis.

Initially it was discovered that synaptic vesicle endocytosis was sometimes inhibited by the substitution of external calcium with other divalent ions such as barium or strontium, but exocytosis remained, albeit with altered kinetics intact (Robinson and Dunkley 1983). This observation suggested that the calcium sensor for endocytosis was different than that for exocytosis and would be mediated by a highly calcium selective molecule. Calmodulin was an obvious target molecule to investigate in this respect. Once a role for calmodulin as the initial calcium sensor was suggested (Artalejo et al. 1996), the hunt for downstream effectors began. Calmodulin is highly promiscuous in the number of proteins it is capable of interacting with. Of note however in the context of vesicle endocytosis are the calmodulin-dependent protein kinases, synapsin-1, calcineurin, GAP-43 or the Arp2/3 complex (Cousin 2000 and references within). It is interesting to note however that some of these proteins can be activated by other molecules than calmodulin, for example NCS-1 can activate calcineurin independently of calmodulin (McFerran et al. 1999). Ca^{2+}-calmodulin can also interact with components of the cytoskeleton, and there are several lines of

evidence to indicate a role of the cytoskeleton in vesicle endocytosis (Doussau and Augustine 2000). Therefore it is possible that calmodulin may have several targets proteins in the regulation of vesicle endocytosis.

7.6.1 The effect of over-expression of WT or mutant calmodulin on endocytosis.

The endocytotic responses to a 200ms pulse and a train of 50, 10ms depolarisations at 20Hz, recorded in the perforated patch configuration were investigated. In this study I have measured the amount of endocytosis that occurs 22 seconds post-stimulus. Figure 7.6.2 shows the mean capacitance trace following a 200ms depolarisation for WT (n = 6) and mutant (n = 7) over-expressing cells. There is no difference between the two groups in their ability to support endocytosis, suggesting that calmodulin is not involved in regulating the mode of endocytosis recruited with this stimulus.

7.6.2 Endocytosis resulting from a 200ms is not altered after over-expression of a dominant mutant calmodulin.
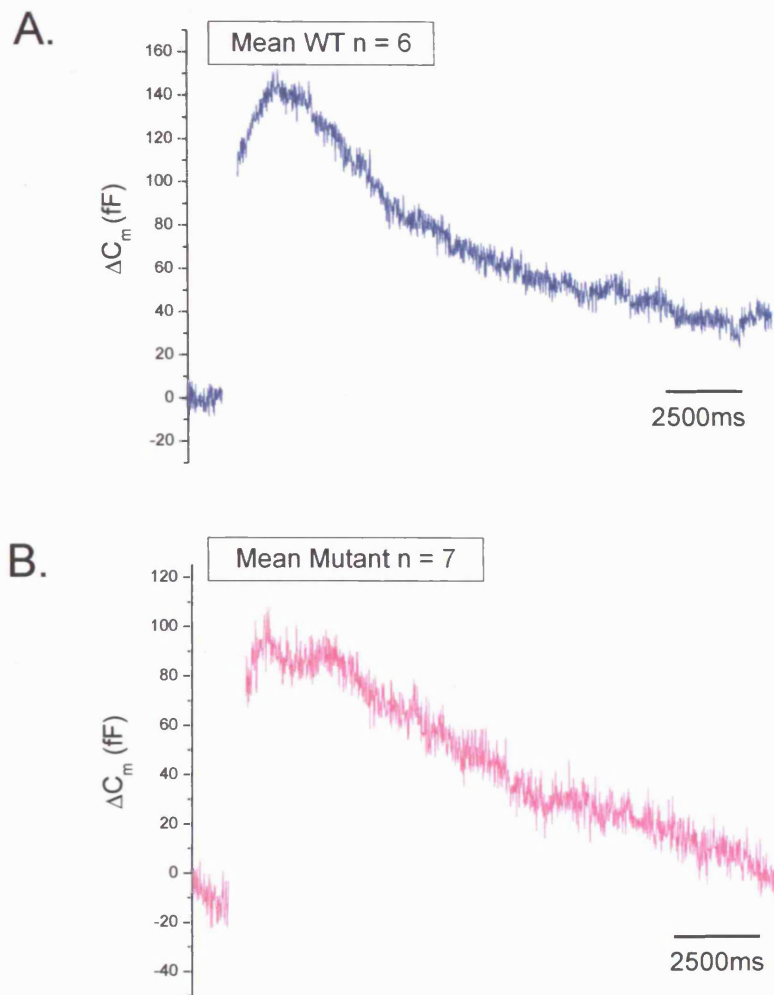
Mutant calmodulin over-expressing cells behave in the same manner as WT or uninfected cells and are able to elicit endocytosis in response to a 200ms depolarisation. Fig A shows the mean capacitance trace for cells over-expressing WT calmodulin (blue), n = 6. Fig B shows the mean capacitance trace for cells over-expressing mutant calmodulin (magenta), n = 7.

In chapter 4, I found that a 200ms depolarisation results in an exocytotic capacitance jump that is then followed by one of several different endocytotic responses. I have described these responses in chapter 4 (section 4.10), briefly endocytosis that occurred post-stimulus and resulted in a change of capacitance back towards pre-

stimulus I have termed compensatory endocytosis. This form of endocytosis can be fit with a mono-exponential decay and the amount of membrane retrieval does not exceed pre-stimulus levels 22 seconds post-stimulus. The next type of response I have termed excess retrieval, results in excess membrane retrieval within 22 seconds post-stimulus, this type of response can also be fit by a mono-exponential decay. A third type of response observed is no reduction in capacitance following an exocytotic jump, this group is termed, no endocytosis. It was discovered with uninfected cells that the amount of calcium influx during stimulation determined the endocytotic response. Increasing calcium influx during the stimulatory depolarisation increases the chance of a cell displaying excess endocytosis compared to no endocytosis. I next wished to examine whether over-expression of calmodulin altered this calcium-dependency and the rate of endocytosis. From the 6 cells over-expressing WT calmodulin 3 cells displayed no endocytosis (mean calcium entry of $158 \pm 25 \times 10^6$ Ca^{2+} ions, n = 3), 2 cells displayed compensatory endocytosis (mean calcium entry of $197 \times 10^6 Ca^{2+}$ ions, n = 2), and 1 cell exhibited excess endocytosis (calcium entry of $209 \times 10^6 Ca^{2+}$ ions). In 7 cells over-expressing mutant calmodulin 2 cells displayed no endocytosis (mean calcium entry of $125 \times 10^6 Ca^{2+}$ ions, n = 2), 3 cells displayed compensatory endocytosis (mean calcium entry of $157 \pm 14 \times 10^6 Ca^{2+}$ ions, n = 3), and 2 cells exhibited excess endocytosis (mean calcium entry of $187 \times 10^6 Ca^{2+}$ ions). These results indicate that similar to uninfected cells increasing calcium influx increases the rate of endocytosis for both WT and mutant calmodulin over-expressing cells, however due to the small sample number statistical tests cannot be applied.

7.6.3 Increasing calcium influx increases the rate of endocytosis for both WT and mutant calmodulin over-expressing cells.
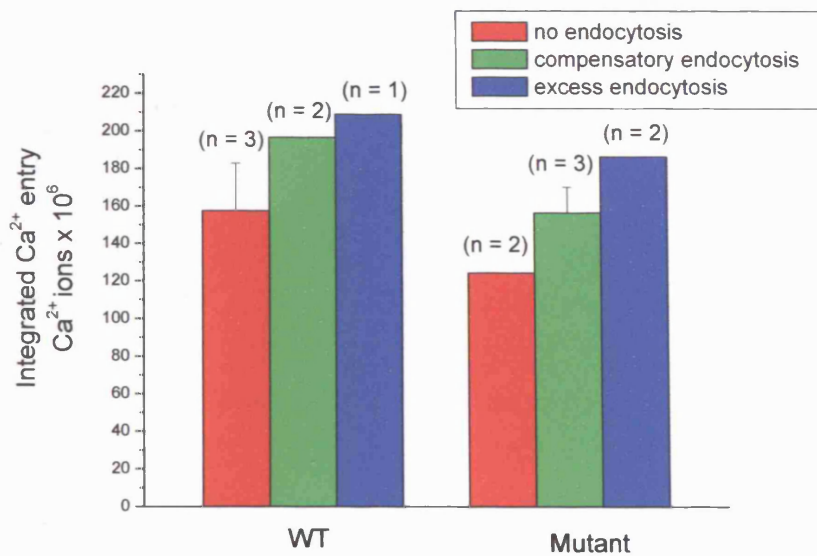
Mutant calmodulin over-expressing cells behave in the same manner as WT or uninfected cells. The rate of endocytosis shows calcium-dependency, increasing with greater calcium influx.

I have also shown in chapter 4 (figure 4.4.5) that increasing calcium entry is correlated to the amount of endocytosis (measured as a ΔC_m 22 seconds post-stimulus). A scatter plot of calcium entry verses ΔC_m 22 seconds post-stimulus show that both mutant and WT over-expressing cells retain this relationship.

7.6.4 Increasing calcium entry increases the amount of endocytosis observed.
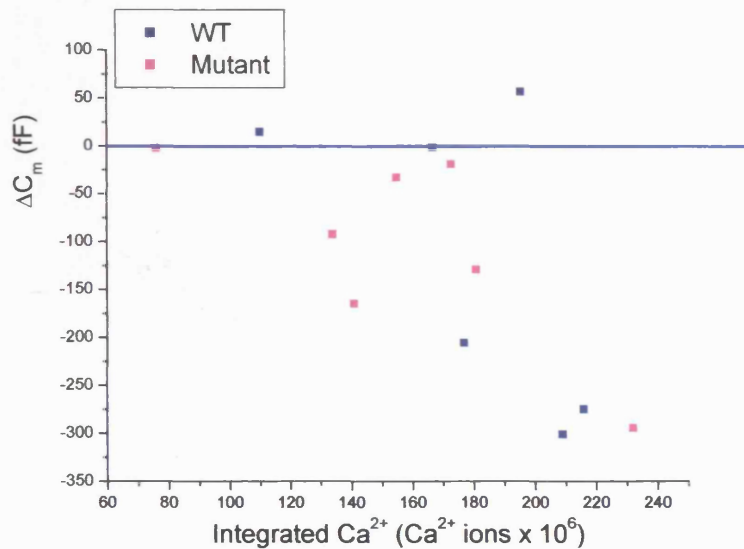
The amount of endocytosis (measured as a change in capacitance fF), that occurs 22 seconds post-stimulus was calculated. The magnitude of the exocytotic jump immediately following stimulation has been set at 0fF (blue line) and endocytosis is therefore measured as a decrease in capacitance. This measurement of endocytosis is plotted against calcium influx during the stimulus depolarisation.

7.6.5 Endocytosis in response to a train of depolarisations.

In chapter 4, I showed that in response to exocytosis evoked by a train of 10ms depolarisations at 20Hz endocytosis was inhibited. 22 seconds post-stimulus the mean amount of membrane retrieval was only 9 ± 12 fF n =20, despite a mean total exocytotic jump of 259 ± 41 fF. The lack of endocytosis was not related to a large component of asynchronous release as this had a mean value of 28 ± 6 fF n=20 (figure 4.4.7). Using cesium-based pipette solutions and the train stimulus no endocytosis was observed (within 22 seconds) in 6 out of 7 WT calmodulin over-expressing cells. Likewise no endocytosis was observed in all cells over-expressing mutant calmodulin in response to the same stimulus, n = 3 (figure 7.6.6). This shows that in response to this stimulus infection by adenovirus or over-expression of either WT or mutant calmodulin results in the same inhibition of endocytosis as uninfected

237

cells when cesium-based pipette solutions are used, implying that calmodulin is not required for clathrin-independent endocytosis.

It was noted that in response to this stimulus slow asynchronous secretion persisted for several seconds in 2 out of 7 WT calmodulin over-expressing cells and 1 out of 3 mutant calmodulin over-expressing cells. One of the WT calmodulin over-expressing cells exhibited asynchronous secretion that was reminiscent of a barium response in the fact that it continued for the duration of the recording (22 seconds). The molecular mechanism(s) underlying asynchronous secretion from virally infected cells is not known (see section 7.1.2 for discussion of this).

7.6.6 Endocytosis in response to a train of depolarisations is inhibited by over-expression of either WT or mutant calmodulin when cesium-based internal solution is used.
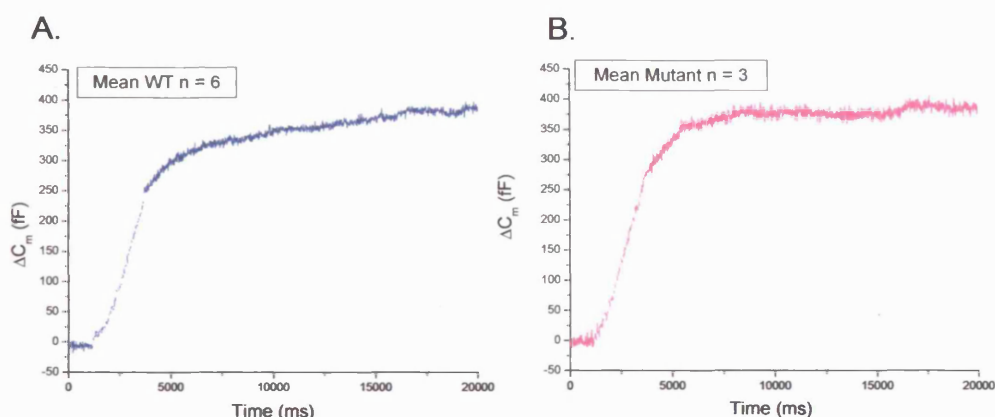
A. In 6 out of 7 WT calmodulin over-expressing cells, no post-stimulus endocytosis was observed 22 seconds after exocytosis was evoked by a train of 10ms depolarisations delivered at 20Hz. Shown is the mean capacitance trace from these cells, n = 6 (Blue).
B. In all 3 mutant calmodulin over-expressing cells tested, no post-stimulus endocytosis was observed 22 seconds after exocytosis was evoked by a train of 10ms depolarisations delivered at 20Hz. Shown is the mean capacitance trace from these cells, n = 3 (magenta).

In uninfected cells it was discovered that inhibition of endocytosis could be ablated when a potassium-based internal solution was used instead of the regular cesium-based one. Using the potassium based internal solution in response to a train of 50, 10ms depolarisations at 20Hz, all cells (6/6) tested exhibited robust endocytosis (figure 4.10.9). Clathrin-mediated endocytosis is dependent on intracellular

potassium (Larkin et al. 1983; Heuser and Anderson 1989; Wu et al. 2001; Artalejo et al. 2002), which is likely to be dialyzed from the cells when cesium-based recording solutions are used. Therefore with this stimulus and by using a potassium-based internal solution the role of calmodulin in regulating clathrin-dependent endocytosis can be assessed. I repeated these experiment with a potassium-based internal recording solution and observed robust endocytosis from all WT calmodulin over-expressing cells (n = 3), which was similar to the response shown for uninfected cells when a potassium-based solution was used (4.4.9), however rapid endocytosis observed from some uninfected cells was not observed . This is likely to result from the amount of calcium entry during stimulation. Virally infected cells have smaller calcium currents and rapid endocytosis is only observed in cells in which a large amount of calcium enters (section 4.4, and Engisch and Nowycky 1998). In contrast to this, no mutant over-expressing cells exhibited endocytosis following this stimulus when potassium-based solutions were used, n = 3 (figure 7.6.7). This suggests that Ca^{2+}/calmodulin is required for clathrin-mediated endocytosis, but not for clathrin-independent endocytosis.

7.6.7 Clathrin-dependent endocytosis is inhibited by over-expression of mutant but not WT calmodulin.
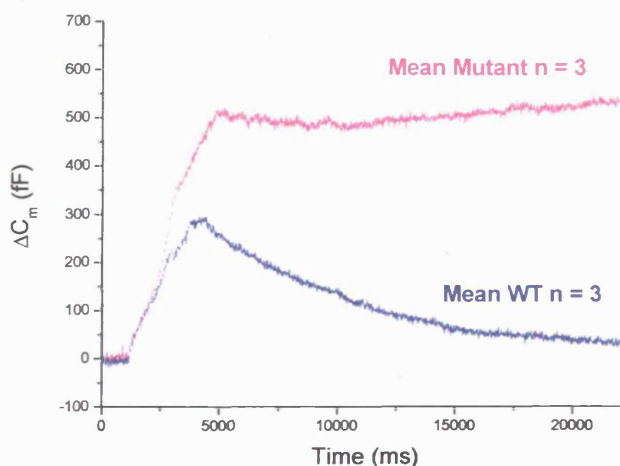
When an internal pipette solution designed to maintain a physiological intracellular potassium concentration (120mM K-Glutamate, 25mM Cs-Glutamate) was used, endocytosis was observed in response a train of 50, 10ms depolarisations delivered at 20Hz for cells over-expressing WT calmodulin n=3, but not from cells over-expressing mutant calmodulin, n = 3. Shown are the averaged capacitance traces.

239

Finally I investigated the possibility that barium could support clathrin-mediated endocytosis from cells over-expressing WT calmodulin. As expected from experiments on uninfected cells, barium was not able to support endocytosis. Using a potassium-based internal, compensatory endocytosis was observed in response to a train of depolarisations, subsequent replacement of extracellular calcium with barium, inhibited endocytosis in response to an identical stimulation.

7.6.8 Barium does not support clathrin-mediated endocytosis.
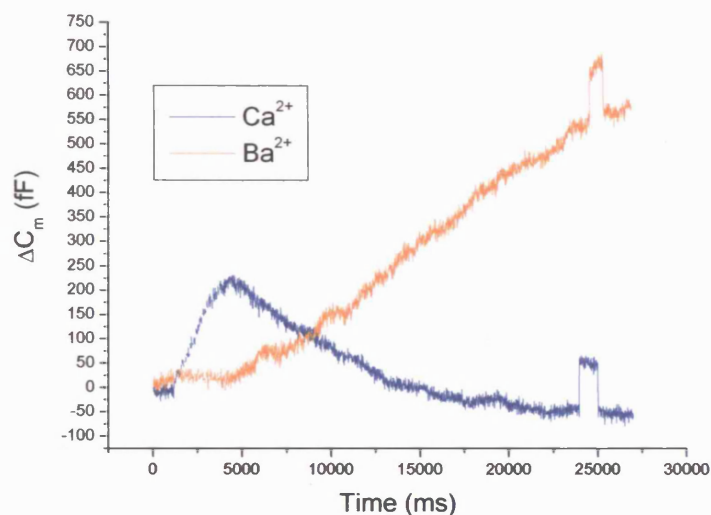
A WT calmodulin over-expressing cell was stimulated with a train of 50, 10ms depolarisations delivered at 20Hz, using a potassium based internal solution. Endocytosis is observed with extracellular calcium (blue), but is inhibited in the same cell when calcium is replaced with equimolar barium (orange).

7.7 Discussion of calmodulin regulation of endocytosis.

A multitude of studies have investigated the molecular mechanisms underlying synaptic vesicle and LDCV endocytosis over the last decade. I will start this section with a resume of what has been published in the last 8 years. I have limited my discussion to studies on bovine adrenal chromaffin cells and experiments which

monitored endocytosis using the membrane capacitance method, as this is the technique and cell type that I have used in my studies.

One of the first papers to look at the molecular mechanisms underlying endocytosis from bovine adrenal chromaffin cells was by Christina Artalejo, (Artalejo et al. 1996). She suggested a role for calmodulin in mediating rapid endocytosis (RE). Her system used calf adrenal glands and the whole cell configuration for introduction of anti-calmodulin antibodies, a host of calmodulin peptide inhibitors and organic calmodulin antagonists. She showed that RE was not supported by barium and was calmodulin dependent. This is in stark contrast to a later paper by Aaron Fox, who using the same cells (calf) and recording configurations and similar stimulation paradigms, (a strong train of depolarisations) shows that barium can support RE and that one of the calmodulin inhibitors used in the previous study, calmadazolium (100nM) had no effect on endocytosis (other inhibitors were not checked). This effect was independent of internal calcium stores as these could be emptied before stimulation, thus ruling out barium activating calcium stores to mediate these effects (Nucifora and Fox 1998). I cannot add to this controversy as rapid endocytosis was never observed from virally infected cells, and only rarely from uninfected cells. Rapid endocytosis is only observed after a high threshold of calcium is reached (Engisch and Nowycky 1998). As I use 2.5mM extracellular calcium and virally infected cells have smaller calcium currents this could explain why I do not routinely observe rapid endocytosis. To address this I could increase the concentration of extracellular calcium to 5-10mM to increase the chance of eliciting rapid endocytosis and then compare WT to mutant to determine a role for calmodulin in mediating this endocytotic pathway. However regardless of the recording stimulation used, I did not detect endocytosis when calcium was replaced by barium.

7.7.1 Downstream targets of calmodulin.

After establishing a role for calmodulin, Artelejo went on to look at downstream targets of calmodulin and through peptides and antagonists ruled out a role for CaM Kinase-2, MLCK or cAMP-dependent protein kinases (Artalejo et al. 1996).

241

Calcineurin, is a protein which is activated by Ca^{2+}-calmodulin and is important in the regulation of many proteins essential for endocytosis, such as dynamin (Cousin and Robinson 2001). Artelego examined a role for calcineurin using 4 approaches, cyclosporin A and FK506 which inhibit cyclophilin and FKBP-12 respectively to inactivate calcineurin and by the introduction of anti-calcineurin antibodies and calcineurin inhibitory peptides. Disruption of calcineurin activation does not inhibit RE and unexpectedly actually increases its kinetics. She concludes that calcineurin is not the relevant target of calmodulin in mediating RE, but that calcineurin is involved in basic, slow membrane retrieval (Artalejo et al. 1996). A couple of years later, the group of Martha Nowycky published a paper examining the calcium dependence of endocytosis from adult bovine adrenal chromaffin cells using the perforated patch technique (Engisch and Nowycky 1998) In contrast to Artalejo's results they found that after cyclosporin A incubation, capacitance decays were slow and often incomplete, and that the rate of endocytosis no longer showed a dependence on calcium. Cyclosporin A did not alter the threshold for excess retrieval, but due to enhanced inactivation of calcium channels, reduced the amount of calcium entering the cell and therefore reduced the probability of a cell reaching the required threshold level for excess retrieval to be switched on. The regulation of calcium channels by calcineurin is itself a debated issue (discussed in chapter 6).

The regulation of endocytosis by calcium and calcineurin in bovine chromaffin cells was investigated again by another group (Chan and Smith 2001). In this study action potential (AP)-like stimulation was used to stimulate the cells. This delivers a very different calcium entry profile to square pulse stimulation. They found a relationship between cell firing (during a physiological range) and the rate of endocytosis. This can be summarised as follows. Single APs or trains at 0.5 Hz lead to rapid endocytosis, 1.9 to 6 Hz trains cause a marked reduction in the rate of endocytosis, trains at 10 – 16 Hz lead to a return to rapid endocytosis. They also found that cyclosporin A left endocytosis characteristics the same at the lower stimulus levels but blocked the resurgence of endocytosis seen in control cells at high AP frequencies. They suggest that there are two mechanisms of endocytosis. One is prevalent at basal and low stimulation frequencies and lessens with increasing

calcium levels and is insensitive to cyclosporin A and another which, is activated by high stimulus frequencies and is blocked by cyclosporin A. More recently they have examined these two modes in more detail (Chan and Smith 2003), and find that blocking clathrin-mediated retrieval with a clathrin/dephosphin disrupting peptide (PP-19), inhibits endocytosis in response to trains at 15Hz, but not to trains at basal rates (~0.5 Hz). They also discover that endocytosis in response to basal firing is sensitive to conventional PKC's, but endocytosis evoked by stressful firing is not. Therefore they conclude that endocytosis evoked under stressful conditions is clathrin-mediated and can be blocked by cyclosporin A (therefore presumably a Ca^{2+}/calmodulin, calcineurin pathway), and that endocytosis in response to basal firing is clathrin-independent and mediated by PKC. I could investigate the possibility of calcineurin as a downstream target of Ca^{2+}/calmodulin, by over-expressing a constitutively active calcineurin with over-expression of mutant calmodulin in the same cell.

Finally a recent paper by Artalejo suggests that two phases of endocytosis, (which she calls rapid and slow) are mediated by different isoforms of dynamin. RE is blocked by anti-dynamin-1 antibodies, (but not anti-dynamin-2 antibodies), substitution of extracellular calcium with barium, and is resisitant to anti-clathrin antibodies. Replacement of calcium with barium however has little effect on slow endocytosis, which is sensitive to anti-clathrin and anti-dynamin2 antibodies but not anti-dynamin1 antibodies (Artalejo et al. 2002). She suggests that rapid endocytosis is associated with kiss and run events and is the more common form of vesicle endocytosis, but under heavy stimulation and full vesicle fusion with the plasma membrane, slow endocytosis which is clathrin mediated is switched on.

However it should be noted that all of the above mentioned studies, except the last one (Artalejo et al. 2002) used cesium-based pipettes, a condition which will lead to intracellular potassium depletion and an inhibition of clathrin-mediated endocytosis (Larkin et al. 1983; Heuser and Anderson 1989; Wu et al. 2001; Artalejo et al. 2002, see chapter 4 section 4.4.9). Therefore care should be taken when interpreting these results, as recorded endocytosis is likely to be dominated by clathrin-independent mechanisms. I have investigated the role of calmodulin in endocytosis in response to

200ms depolarisations and a train of brief (10ms) depolarisations using either cesium-based or potassium-based internal recording solutions. I find that endocytosis from virally infected cells is not altered in response to either stimulus when cesium-based internal solutions are used. Therefore Ca^{2+}/calmodulin is unlikely to regulate this endocytotic pathway. However in response to the train of depolarisations endocytosis is inhibited in cells over-expressing mutant, but not WT calmodulin when a potassium-based internal solution is used. This implies that calmodulin is required for this clathrin-mediated pathway. Further experiments are required to determine the roles of potential downstream targets, such as calcineurin and/or dynamin. However I believe that a valid experimental model now exists to investigate the role of these proteins in clathrin-dependent endocytosis. Namely the train of depolarisations as the stimulus, over-expression of the mutant calmodulin, and the distinction between clathrin-dependent and clathrin-independent endocytosis offered by changing internal solution composition from potassium-based to cesium-based. This approach in combination with an imaging technique to monitor endocytosis is likely to be very informative.

Studies from neurones and neuroendocrine cells suggest that three basic mechanisms of endocytosis can occur; clathrin-dependent retrieval of vesicles, bulk retrieval of large areas of membrane and fast recapture of vesicles that have not fully collapsed into the membrane, colloquially called 'kiss and run' endocytosis (reviewed in Royle and Lagnado 2003). Kiss and run fusion has gained popularity recently as the most common form of endocytosis in central synapses during 'physiological' stimulation, especially from optical fluorescence studies (Aravanis et al. 2003). Interestingly it has been suggested that in response to a nerve impulse, synapses with low release probability primarily use the kiss-and-run mode, whereas high release probability terminals predominantly use the compensatory mode of vesicle retrieval (Gandhi and Stevens 2003). Therefore an understanding at the molecular level of all modes of endocytosis is warranted.

Chapter 8. Final discussion

There are three main conclusions from the experiments presented in this thesis. Firstly, exocytosis is preferentially coupled to P/Q-type channels, secondly calmodulin regulates N-type calcium channel inactivation, and thirdly calmodulin is required for the filling or release of the IRP/RRP. At the end of each chapter I have discussed the relevance of these observations. In this final discussion I will consider four questions which continue from these initial observations and could form the basis of future experiments designed to gain a more thorough understanding of regulation of stimulus-coupled secretion in bovine adrenal chromaffin cells.

8.1 Is there a physical interaction between P/Q-type channels and SNARE proteins?

I have shown that exocytosis in chromaffin cells is preferentially coupled to P/Q-type channels. In the discussion of chapter 5 I offer several mechanisms that could account for this, including preferential inclusion of P/Q-type channels and SNARE proteins within lipid rafts (section 5.12). Here I expand my discussion and consider the possibility of a direct specific coupling between P/Q-type channels and the secretory machinery as a mechanism to explain the enhanced exocytotic efficiency compared to N-type channels. The cytoplasmic loop between domains 2 and 3 of N and P/Q type channels (L_{2-3}) has been shown to be able to bind to SNARE proteins. This 'synprint' site, (*syn*aptic *pr*otein *int*eraction) is found between residues 718-963 and can bind syntaxin 1A and SNAP-25 as well as synaptotagmin reviewed in (Sheng et al. 1998 and Catterall 1998). Targeting of the exocytotic machinery to calcium channels is a mechanism to increase the efficiency of synaptic transmission. As synaptic protein interactions with the synprint site are competitive, they may occur in series and represent steps in the pathway of docking and release (Walker and De Waard 1998). A hypothesis put forward by Professor Catterall and others propose that at resting calcium concentrations P/Q and N type channels can bind to syntaxin and SNAP-25. Calcium influx can greatly increase the affinity of this coupling, and

may therefore contribute to early priming steps of the fusion process. As calcium levels rise and reach threshold for release (20-50 μM), this binding affinity is reduced and syntaxin and SNAP-25 are displaced and allow synaptotagmin to bind in order for membrane fusion to proceed (Sheng et al. 1996). This hypothesis predicts a direct coupling between the source of calcium entry and vesicles. Recently it has been shown that splice isoforms exist for both channels subtypes, which lack this 'synprint' (syntaxin binding) site in their domain II-III linker (Rettig et al. 1996; Kaneko et al. 2002). The bovine adrenal chromaffin cell P/Q-type channel(s) have not yet been cloned but hopefully should soon be available (J. Weiss personal communication). It will be interesting to determine (if the synprint site is present on chromaffin cell P/Q-type channel), how disruption of this site will affect stimulus-coupled secretion. Several groups have studied the effects of calcium channel activity and secretion by either cleaving SNARE proteins with specific toxins or by injecting peptides or antibodies designed to inhibit the interaction between SNAREs and the calcium channels. In neurones, experiments disrupting the physical link between N type channels and SNARE proteins can displace vesicles from the channels and shift the calcium dependence of neurotransmitter release to higher levels (Catterall 1999). As well as spatially coupling vesicles to the source of calcium entry, interactions with SNARE proteins can affect the biophysical properties of the channel, and so in addition to regulation by calmodulin may underlie the difference in inactivation between the two channel subtypes.

8.2 Does calmodulin regulation of N-type channels limit their ability to contribute to stimulus-coupled secretion?

It was hypothesised that calmodulin regulation of N-type channel inactivation could limit the ability of this channel to contribute to exocytosis. It was not possible to test this directly as over-expression of mutant calmodulin not only reduced channel inactivation but also altered exocytosis by acting on the secretory machinery. Ideally a separation of the effects on the channel and secretory machinery would be desirable. This could be investigated by engineering a double mutation in the N-type

channel removing both the calmodulin and ω-CTX GVIA binding sites. In this case the mutant channel could be over-expressed with endogenous N-type calcium channels blocked by application of ω-CTX GVIA. Thus it would be possible to compare the role calmodulin plays in regulating stimulus-coupling exocytosis between the channel subtypes without affects on the secretory machinery.

To investigate this in a more physiological context these studies could be expanded to examine the channel subtypes ability to couple to exocytosis in response to action potential (AP) firing. Firstly secretion could be monitored with AP firing before and after toxin application to assess the contributions of individual calcium channel subtypes. Then the role of calmodulin regulation of N-type channels could be assessed in the same manner previously described for single pulses in voltage clamp, over-expression of the double mutant N-type channel and block of endogenous N-type channels. A problem with this is that simultaneous recording of APs and ΔC_m are not possible. Stimulating with APs requires current clamp and measuring C_m responses requires voltage clamp and it takes time to switch between voltage and current clamp, which would greatly reduce the temporal resolution currently observed by stimulating cells and measuring ΔC_m in voltage clamp. To address this problem mock APs can be generated in voltage clamp by using a series of ramps to mimic an AP (Chan and Smith 2001). However the ability of these mock APs to accurately represent an AP has recently questioned (Duan et al. 2003). In this latter study they measured real APs in current clamp and used this template to reconstitute APs waveforms under whole cell patch clamp.

It will be interesting to determine how calmodulin affects the complete AP duration. Calmodulin activates small conductance potassium channels (Xia et al. 1998) as well as inactivating N-type channels, which themselves regulate BK channel activity (Marrion and Tavalin 1998). Therefore to determine calmodulin regulation of exocytosis specifically through its regulation of membrane conductances, distinct from effects on the secretory machinery AP's could be recorded in current clamp from cells over-expressing WT and mutant calmodulin and then the template from these AP's could be converted into a voltage clamp waveform to mimic AP firing in uninfected cells. Thereby neglecting the need to infect these cells, eliminating

unwanted side effects of viral infection (smaller calcium current amplitudes, and an increase in asynchronous secretion), and the effects the mutant calmodulin exerts on the secretory machinery.

8.3 What is the functional significance of calmodulin regulation of N-type calcium channels?

I have shown that in bovine adrenal chromaffin the vast majority of calcium current is carried by N and P/Q-type channels, and exocytosis is preferentially coupled to P/Q-type channels even in response to brief depolarisations when there is no difference in the degree of inactivation between the two calcium subtypes. The exocytotic response to a train of brief depolarisations is almost the same after blockade of N-type channels as it was before despite a significant reduction in calcium entry. The functional consequence of calmodulin-dependent inactivation of N-type channels may be simply to prevent excess calcium entry, which could be detrimental to the cell and allowing exocytosis to persist via calcium entry through P/Q-type channels. Therefore stimulus-coupled secretion is not compromised and the cell is protected from an overload of calcium. If that is the case, what is the physiological relevance of the N-type channel? I believe that the N-type calcium channels in chromaffin cells have a functional role and a calmodulin interaction may be important for this. In neurones specific calcium channel subtypes appear to be important for delivering the calcium needed for different cellular functions. For example it has been proposed that calcium entry through L-type channels in the cell body primarily leads to gene transcription, whereas calcium entry through P/Q and N-type channels at the synapse initiates neurotransmitter release (West et al. 2002; Deisseroth et al. 2003). L-type channel calcium current preferentially increases CREB phosphorylation, even though other channels support equivocal or greater calcium entry (Dolmetsch et al. 2001). The transduction of the calcium signal to CREB activation is essential on calmodulin binding to the channel and its subsequent activation by calcium flowing through the channel (Dolmetsch et al. 2001; Mori et al. 2004). Therefore the same molecule interacting with different calcium channel subtypes can regulate disperse cellular

events. One could envision the physiological role of calmodulin regulation of L-type channels in the modulation of gene transcription and its regulation of N-type channels by preventing high and possibly dangerous levels of calcium from entering the cell. However the prevailing view that calcium-dependent gene expression is triggered by calcium influx through L-type channels is based predominantly from studies, which used chronic potassium depolarisation to mimic neuronal activity. This stimulation is likely to assess only slowly or non-inactivating channel subtypes ability to couple to gene transcription. N-type channels inactivate quickly and their potential contribution to gene expression would be overlooked in these experiments. Indeed it has been shown that CREB phosphorylation is transient following electrical stimulation but relatively sustained following chronic depolarisation by potassium, indicating a differential regulation of CREB phosphorylation under physiological conditions (Brosenitsch and Katz 2001). An elegant study has shown that both chronic depolarisation by potassium and electrical stimulation of dissociated primary sensory neurons induces expression of immediate early genes Nurr1 and Nurr77 and an increase in tyrosine hydroylase mRNA (a marker for induction of dopaminergic traits), (Brosenitsch and Katz 2001). However the two stimuli rely on calcium entry through different channel subtypes and utilize diverse downstream effectors. Chronic potassium depolarisation requires calcium entry through L-type channels and activation of the MAPK pathway, whereas electrical stimulation (5Hz) requires calcium entry through N-type channels and activation of PKC and PKA (Brosenitsch and Katz 2001). This study shows that physiological stimuli couple calcium entry through non-L-type channels to mediate gene transcription and show that N-type channels can directly link membrane depolarisation to gene expression. With this in mind, a functional interaction of calmodulin with N-type calcium channels in bovine adrenal chromaffin cells may involve mediating gene transcription reminisant of the process described for L-type channels, but missed as non-physiological stimuli were used to assess its involvement. This may specifically be worth investigating as L-type channels only contribute to a small fraction of the calcium current, or are quiescent in cultures of adult bovine adrenal chromaffin cells (Engisch and Nowycky

1998; Currie and Fox 1997; Currie and Fox 2002), yet obviously gene transcription occurs.

A fast calmodulin-dependent kinase and a slow MAP kinase dependent cascade are thought to mediate CREB activation by phosphorylation of its ser-133 residue. Ca^{2+}/calmodulin can lead to local activation of ras, which leads to stimulation and nuclear translocation of MAPK, a process that may involve PKA (reviewed in Deisseroth et al. 2003). It is interesting to note that ras has recently been shown to immunoprecipitate with N-type channels in DRG neurons after GABA receptor stimulation, with subsequent activation of the MAPK pathway, an affect that is inhibited by block of N-type calcium channels with ω-CTX GVIA (Richman et al. 2004). Clustering of calcium channel subtypes and neuronal receptors with specific signalling molecules in microdomains is likely to dictate whether or not a given channel subtype is important in regulating gene expression and this co-localisation is likely to vary for individual cell types. Future experiments could test the hypothesis that activation of gene transcription in bovine adrenal chromaffin cells requires calcium entry through N-type calcium channels with or without an implicit role for calmodulin in this process.

8.4 What is the relevant Ca^{2+}/calmodulin target that regulates release from the IRP/RRP?

In chapter 7 I discuss various different proteins, which may mediate the reduction in exocytosis observed after over-expressing of a mutant calmodulin incapable of binding calcium. The major observation from my experiments was the elimination of the IRP, with no effect on release in response to long depolarisations, or at the end of a train of brief depolarisations suggesting that release from the SRP is not affected. Since the SRP is primarily defined from experiments of flash photolysis of caged calcium, experiments of this nature should be performed to quantify SRP pool size from WT or mutant over-expressing cells to verify this. Additionally pool refilling may be affected through Ca^{2+}/calmodulin regulation of proteins required for this, but as I did not investigate pool refilling I will limit the rest of this discussion to

250

mechanisms, which could account for the alterations in exocytosis observed in my experiments. My results (reduction in release from the IRP/RRP) indicate that Ca^{2+}/calmodulin is required either for priming vesicles to obtain fusion competence, stabilization of the IRP/RRP, calcium sensing, or a combination of these. This is discussed in more detail below.

Munc-13 is a priming protein that is essential for the maturation of vesicles to become fusion-competent in neurones (reviewed in Rosenmund et al. 2003). However, two key pieces of evidence suggest that it is not the relevant Ca^{2+}/calmodulin target in my studies. Firstly, when the calmodulin binding site was mutated in munc-13, and expressed in neurones basal pool sizes were not affected and the importance of this interaction appears to be in mediating refilling of the RRP after bouts of stimulation when cytoplasmic calcium is raised (Junge et al. 2004). Secondly, in contrast to bovine brain, munc-13 expression is low in bovine chromaffin cells (Ashery et al. 2000) and secretion from munc-13 knockout mice is normal (Voets 2000), suggesting that although over-expression can enhance secretion in chromaffin cells, it is not a normal required priming protein in this cell type (although it is possible that other isoforms of the protein are important in chromaffin cells). Therefore I predict that the observed reduction in exocytosis in my studies results from perturbation of a Ca^{2+}/calmodulin interaction with one or more of the SNARE proteins (Synaptobrevin, SNAP-25 or syntaxin). This could be explained either as an inhibition of a tight trans-SNARE complex, a destabilization of the RRP, and/or a reduction in the co-operativity of release.

The SNARE complex consists of a twisted coiled-coil bundle made up of four α-helices (one from synaptotagmin, one from syntaxin and two from SNAP-25). This complex brings vesicle and plasma membranes into close contact and is necessary for fast stimulus-coupled release (Sutton et al. 1998). Recent work has shown that the vesicular lipid bilayer itself inhibits synaptobrevin interactions with syntaxin and SNAP-25 in the absence of calcium (Hu et al. 2002) and that Ca^{2+}/calmodulin is required to allow synaptobrevin to change from cis lipid binding to trans lipid binding (de Haro et al. 2004). Addition of an antibody that prevents full SNARE complex formation results in the loss of the RRP, but not from the SRP, implying that the SRP

may be able to fuse from a 'loose' SNARE complex (Xu et al. 1999). This suggests that Ca^{2+}/calmodulin may be required for conversion of a 'loose' SNARE conformation into a 'tight' one and explains the reduction in release from the IRP/RRP but not from the SRP in my experiments. Alternatively the antibody could result in impaired binding of synaptotagmin and therefore a reduction in the RRP size. Nonetheless there is plentiful evidence to suggest that calcium is required for the formation of a tight trans-SNARE complex (Chen et al. 2001, Matos et al. 2003). Zippering of a loose SNARE complex into a tight trans-SNARE complex increases the rate of vesicle fusion, is calcium-dependent and involves proteins known to be regulated by Ca^{2+}/calmodulin, therefore this may be the relevant target for perturbation after over-expression of mutant calmodulin. Biochemical assays could be performed to assess whether trans-SNARE complexes are altered from cells over-expressing mutant calmodulin.

The RRP is thought to be in equilibrium with the SRP and a potential way for exocytosis to be modulated is by changing the stability of the vesicles residing in the RRP by altering the forward or reverse priming rates (Sorensen 2004). Complexins are an example of proteins that affect the stability of the RRP (reviewed in Rosenmund et al. 2003). They are not thought to change the size of the RRP but are thought to stabilize the tight conformation of the core complex as knock-outs of these proteins reduce the efficiency of calcium-dependent release (Reim et al. 2001; Tokumaru et al. 2001; Chen et al. 2002; Pabst et al. 2002; Bracher et al. 2002). Perhaps a role of the Ca^{2+}/calmodulin interaction with synaptobrevin and CaMKII interaction with syntaxin is to maintain the stability of the RRP. Indeed CaMKII binds to syntaxin in the open form, when it is able to bind to SNAP-25 and synaptobrevin (Ohyama et al. 2002), maybe this interaction stabilises the trans-SNARE complex, and reduces dissembly and munc18 binding to syntaxin. This could be prevented when the mutant calmodulin is over-expressed leading to a reduction in the efficiency of release.

It may be possible that over-expression of mutant calmodulin perturbs the calcium-dependency of exocytosis. The evidence that synaptotagmin1 is the primary calcium-sensor for fast stimulus-coupled transmitter release is convincing (Koh and Bellen

2003; Yoshihara et al. 2003), however whether SNARE proteins either directly themselves, or by interacting with synaptotagmin can alter the calcium cooperativity of release is still a subject of debate. Evidence to suggest that SNARE proteins may themselves sense calcium is now discussed. Reducing the expression levels of syntaxin and synaptobrevin through genetic manipulation in drosophila led to a reduction in the calcium cooperativity from $n = 3.4$, to $n = 2.4$ and 2.6 respectively (Stewart et al. 2000). In this study they ruled out perturbations caused by their mutants on calcium entry through the calcium channels and spatial arrangement of the vesicles and the source of calcium entry concluding that the SNARE proteins themselves were part of the calcium-sensing complex. As discussed earlier (section 7.5.3.3), mutations in a putative divalent cordination site on SNAP-25 leads to slowed secretion presumably due to the deletion of one calcium-binding site in the calcium sensor for exocytosis (Sorensen et al. 2002). Therefore it is conceivable that Ca^{2+}/calmodulin via its interactions with synaptobrevin or CaMKII via syntaxin could also affect the calcium cooperativity of neurotransmitter release. Whether this effect is direct, or involves an indirect effect on synaptotagmin association with the core complex would have to be assessed. Although I found no difference in the calcium-dependency of exocytosis between WT and mutant calmodulin over-expressing cells (figure 7.2.1), the results from the method I used (Engisch and Nowycky 1996), will be dominated by fusion from the SRP. To investigate the calcium-dependency of release from the RRP flash photolysis of caged calcium experiments can be performed (Sorensen 2004). The calcium cooperativity of neurotransmitter release from the RRP in chromaffin cells was calculated as 2.5~3.0 using this technique (Sorensen et al. 2002), which is considerably higher than the value reported here, and by (Engisch and Nowycky 1996), when both pools are assessed together. Therefore using the flash photolysis technique I may detect an alteration in calcium cooperativity between WT and mutant calmodulin over-expressing cells. If this occurs then over-expression of either mutated synaptobrevin or syntaxin (incapable of interacting with Ca^{2+}/calmodulin or CaMKII) could be investigated in a similar way to determine the downstream target of Ca^{2+}/calmodulin. In addition to determining the molecular basis for the reduction in the IRP/RRP, future experiments can be

conducted to investigate whether Ca^{2+}/calmodulin plays a role in pool refilling, and if so characterization of the molecular targets underlying this. Other future experiments include an amperometric analysis of single fusion events to determine whether Ca^{2+}/calmodulin effects fusion pore kinetics.

Furthermore I have described a simple technique to isolate clathrin-dependent from clathrin-independent mechanisms and shown some preliminary evidence to suggest that over-expression of mutant calmodulin specifically affects a clathrin-mediated endocytosis pathway in these cells. Future experiments could be conducted to examine the downstream targets of this regulation.

In summary, Ca^{2+}/calmodulin plays a central role in regulating neurotransmitter release. It regulates several diverse membrane currents to finely tune calcium entry, the trigger for release. It also interacts with many proteins necessary for all stages of the vesicle cycle, (docking, priming, and retrieval of membrane post-fusion). To understand the exact molecular mechanisms and physiological importance of each of these interactions is a challenge for the future.

Appendix 1. Examination of an unidentified calcium-dependent ionic current.

When I started these studies it was noted that with long depolarisations (800ms) the kinetics of the tail current slowed. This suggested that an additional channel was being activated and that I was not recording calcium channels in isolation. This appendix describes experiments I conducted to try to characterise and inhibit this unknown conductance.

A step from –80mV to +20mV will activate a number of calcium channels resulting in an inward calcium current. At the end of the voltage step a calcium current of larger amplitude and smaller duration is recorded (figure A1.1). This 'tail' current corresponds to the current flowing through channels that are not closed at the end of the depolarising step and its amplitude and direction is relative to the size of the voltage step and hence the driving force for calcium ions.

A1.1 Tail current recorded from a 100ms depolarisation.

500pA

500ms
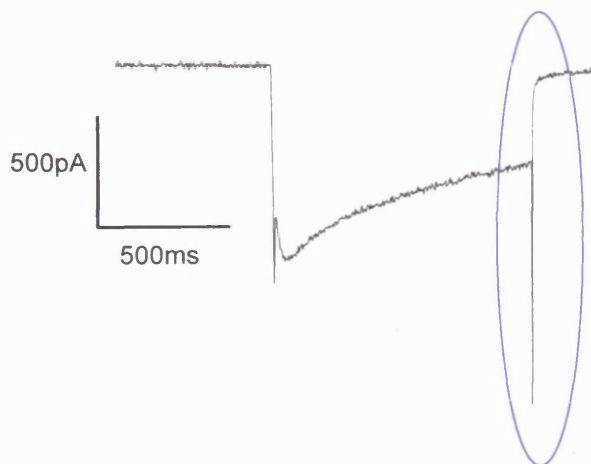
A 100ms depolarisation from -80mV to +20mV evokes a membrane calcium current which begins to inactivate during the course of the depolarisation. At the end of the pulse the membrane voltage is stepped back down to -80mV and a large transient inward current, colloquially termed a 'tail current' is observed (surrounded in this figure by a blue oval).

As the length of the depolarising pulse increases, the tail current and calcium conductance get smaller because calcium channel inactivation has already shut many channels. Therefore one would expect that an 800ms pulse would not induce a significant tail current as the vast majority of calcium channels will inactivate before the end of the depolarisation. However it was observed upon inspection of 800ms pulse traces that a tail current with slow inactivation kinetics was present and occasionally the inactivating 800ms current went positive (figure A1.2). The obvious explanation for this is that I was not recording pure calcium current, but a mixed current that also contained an outward conductance. Therefore the tail current was a result of either calcium flowing through calcium channels that were still open (and therefore not inactivated), or that it resulted from flow of ions through another type of channel that was being switched on, or that it corresponds to a mixture of both these possibilities.

A1.2 Slow tail current recorded from an 800ms depolarisation.
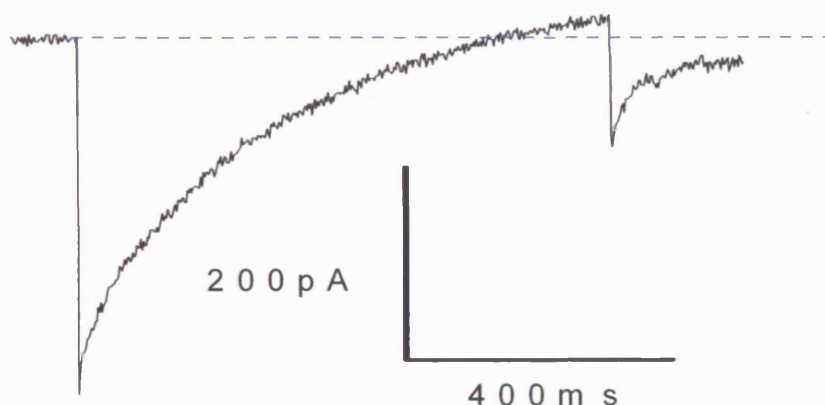
An 800ms depolarisation from -80mV to +20mV in which the current actually goes outward towards the end of the pulse and produces a tail current with slow inactivation kinetics. The blue dashed line represents 0pA.

The calcium-dependency of the tail current was examined. Figure A1.3 displays sample traces resulting from an 800ms depolarisation in either the whole cell

256

configuration with intracellular [BAPTA] raised from 0.3mM to 10mM, or in the perforated patch configuration with either calcium or barium in the extracellular solution. It is apparent that there is less inactivation during an 800ms pulse when calcium is buffered with 10mM BAPTA or calcium is replaced with barium (discussed in detail in chapter 6). However the slow tail current also disappears. A fast tail current similar to the one shown in figure A1.1 is probably present as only a fraction of the channels inactivate when calcium is buffered with 10mM BAPTA or when barium is used as the extracellular divalent charge carrier with this stimulus. This will be missing in the traces due to the slow sampling rate used to record an 800ms depolarisation, (1 point every 2ms).

A1.3 Calcium-dependency of the tail current
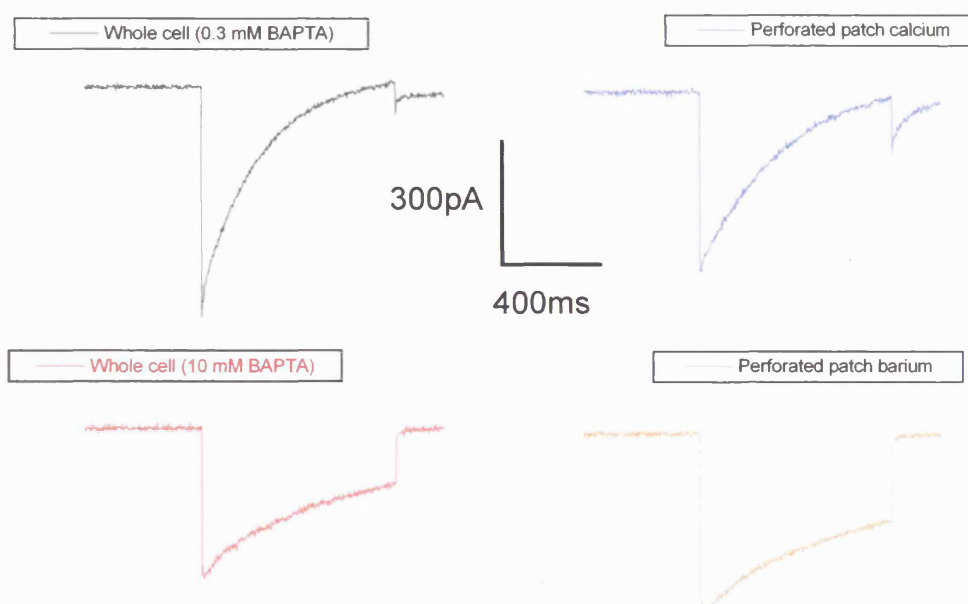
Sample 800ms traces recorded on the left in the whole cell configuration with the intracellular [BAPTA] either 0.3mM (black) or 10mM (red). On the right are perforated patch recordings with either calcium (blue), or barium (orange) as the extracellular divalent charge carrier.

Having discovered that the slow tail current displayed calcium-dependency, possible candidate channels mediating this current were assessed. Initially it was thought that the current would be mediated by either a calcium-dependent chloride or potassium

current. Calcium-activated chloride channels looked a promising candidate, as isolated calcium-activated chloride currents display a slowly inactivating tail current (Evans and Marty 1986). The slow chloride tail current is thought to arise from a change in channel open probability (P_O) with voltage. Depolarisations to positive potentials evoke an outward current that slowly increases in amplitude until a steady-state level is reached, indicative that P_O increases at positive membrane voltages. After repolarisation the inward current slowly declines towards a steady-state value giving rise to tail currents with a slow time course (several hundred ms), as the channels return to a lower level of P_O (Evans and Marty 1986). These channels, as their name suggests are activated by raised intracellular calcium, and it has been reported that the amplitude of a chloride mediated tail current can be related to the amount of inward charge carried by calcium flow through voltage-gated calcium channels (Currie et al. 1995). Alternatively the current could be mediated by a calcium-activated potassium channel. Three types of calcium-activated potassium channels have been identified based on biophysical and pharmacological criteria, large conductance (BK), small conductance (SK) and intermediate conductance (IK). BK and SK channels are widely expressed in the nervous system whereas IK expression is limited mainly to epithelia cells (Sah and Faber 2002). Both BK (Marty and Neher 1985; Lovell et al. 2000) and SK (Artalejo et al. 1993) are expressed in cultured bovine adrenal chromaffin cells. Before commencing pharmacological studies a current voltage relationship was undertaken to discover the tail currents reversal potential and hopefully give an indication of the channels molecular identity. To do this an 800ms depolarisation to +20mV was applied, immediately followed by a 100ms step to a membrane voltage ranging from-120mV to +100mV (figure A1.4). These experiments were performed in both the whole cell and perforated patch configuration and lead to a current that was outward rectifying and reversed just positive of +20mV.

A1.4 Current-voltage relationship of the tail current.

A.

+20mV   800ms

-80mV

100ms
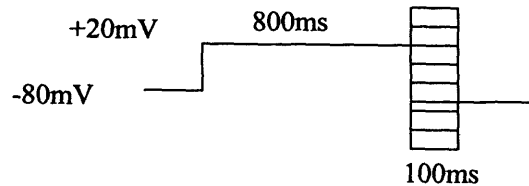
B.

Whole cell recording tail potential -120mV.   Perforated recording Tail potential -120mV.
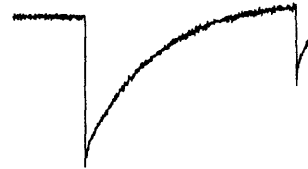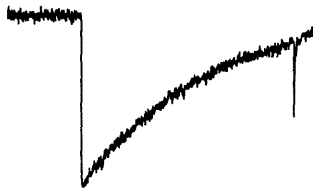
Whole cell recording Tail potential +40mV   Perforated recording Tail potential +40mV
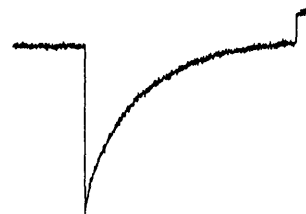
C.
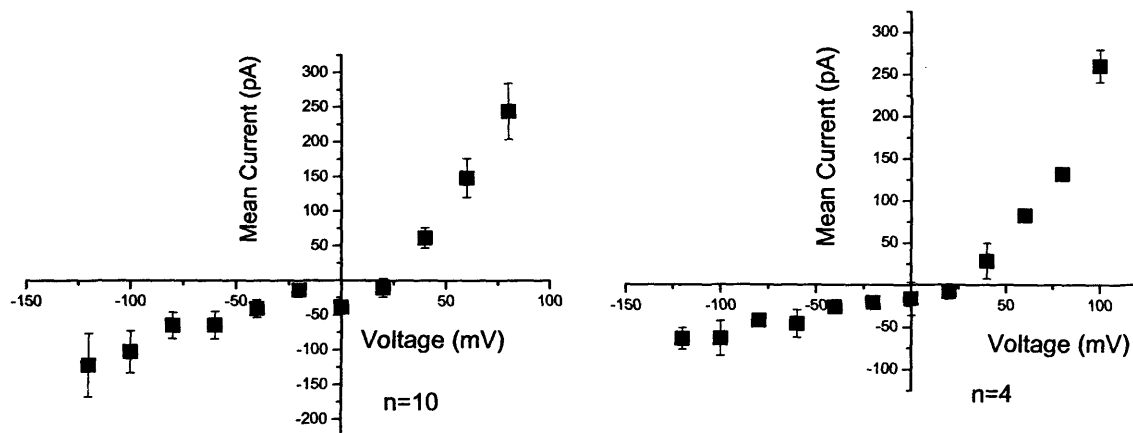
A. An 800ms prepulse to +20mV was delivered immediately followed by a 100ms test pulse to a new membrane potential, ranging from -120mV to +100mV.

B. Sample current traces recorded in either the whole cell or perforated patch configuration in response to test pulses of either -120mV or +40mV.

C. I/V plots, the peak amplitude of the test pulse is plotted against membrane voltage. Points represent the mean current size ± s.e.m. Perforated patch recordings are shown on the left, (n = 10), whole cell configuration recordings on the right, (n=4).

259

The reversal potential (E_{Rev}) of around +25mV was surprising, suggesting that the current was not mediated by a calcium-activated chloride or potassium channel. Using the Nersnt equation, the E_{Rev} for chloride ions with the standard intracellular and extracellular solutions in the whole cell configuration is calculated to be ~ - 70mV. E_{Rev} Cl⁻ (E_{Cl}) is more difficult to assess in the perforated patch configuration, as in these experiments I used gramicidin A as the perforant, which produces channels impermeable to chloride ions (Busath 1993). This means that by using gramicidin (to gain electrical access) and my standard extracellular solution, a physiological E_{Cl} will be maintained. The I/V relationship for whole cell recordings was the same as that recorded in the perforated patch configuration (figure A1.4). In these studies it is not possible to directly calculate the E_{Rev} for potassium channels using the Nersnt equation as the intracellular solution contains cesium instead of potassium. However one would expect the E_{Rev} to have a highly hyperpolarized membrane potential, so given the reversal potential of the measured tail current (~ +25mV, figure A1.4), I do not believe that it is mediated by activation of a calcium-activated potassium channel. Also calcium-activated potassium channels in bovine adrenal chromaffin cells have been shown to activate at potentials more positive than -30mV with an outward current that increases with amplitude as the membrane voltage becomes more polarized (Marty and Neher 1985), with no inward current recorded through these channels.

As an additional check to see whether the current was supported by chloride ions I changed E_{Cl} so that it was close to the step potential of +20mV. This was achieved by using a cesium-chloride based internal instead of the standard cesium-glutamate one. In this case the calculated E_{Cl} would be ~ +2mV. It would therefore be possible to observe whether there is a difference in inactivation during the standard 800ms long pulse indicative of a contaminating outward current (if this was the case one would expect less inactivation as E_{Cl} is now close to the step potential reducing the driving force for current flow). Also if the tail current is mediated by chloride ions then the tail current should be larger in amplitude due to a larger electrochemical driving force at -80mV. Similarly the tail current should be smaller in amplitude at

positive membrane potentials when recording with the cesium-chloride based internal.

Electrochemical driving force (Edf) = Voltage – ECl

$$-10mV = -80mV - (\sim -70mV)$$
$$-82mV = -80mV - (\sim +2mV)$$

The % inactivation over the 800ms prepulse was unchanged for the two recording solutions, 91.0 ± 1.5 % n = 4 for cesium-glutamate based internal and 88.7 ± 2.4 % n = 3 for cesium-chloride based internal. A similar I/V relationship was observed with both recording conditions (figure A1.5) and the amplitude of the inward tail current recorded with a test pulse potential of -120mV was -63.7 ± 12.6 pA n = 4 for cesium-glutamate and -40.0 ± 5.3 pA n = 3 for cesium-chloride based internal respectively. With a test pulse potential of +40mV the mean amplitude was $+28.3 \pm 21$ and $+45.0 \pm 20$pA respectively. If you normalise the amplitude of the test pulse to the peak of the prepulse then you obtain a fractional ratio of 0.27 and 0.24 with a test pulse of -120mV and 0.12 and 0.26 with a test pulse to +40mV for cesium-glutamate and cesium-chloride solutions respectively. Therefore an 800ms depolarisation does not show a significant decrease in measured inactivation and the I/V is not shifted in the manner predicted from a current carried by chloride ions. There is an absence of highly specific blockers for calcium-activated chloride currents (Frings et al. 2000). General chloride channel blockers such as the fenamtes, nifluric and flufenamic acid or the disufonic stilbene derivatives DIDS and SITS have been used, although their reported potency is variable depending on the cell type being examined (Frings et al. 2000). Application of 10μM DIDS, a concentration shown to block chloride channels in bovine adrenal chromaffin cells (Doroshenko et al. 1991) did not affect current amplitude or the I/V relationship (figure A1.5). Therefore I concluded that the current was unlikely to be mediated by a calcium-activated chloride current.

A1.5 Cesium-glutamate verses cesium-chloride based internal solution.

A.

Cs-Glutamate based.

Cs-Cl based.

-80mV

-70mv

2mV +20mV

B.
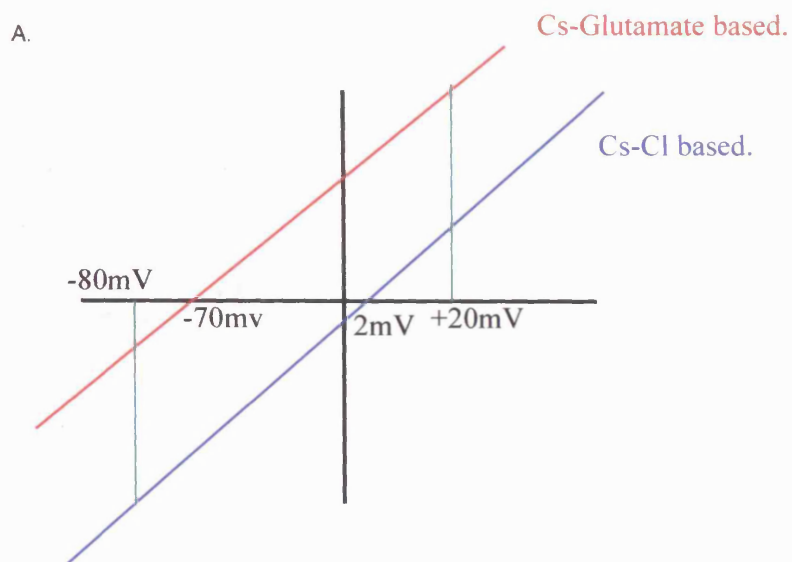
EСl ~ -70mV

(Cs-Glutamate)

EСl ~ +2mV

(CsCl)

Whole cell recording tail potential -120mV.
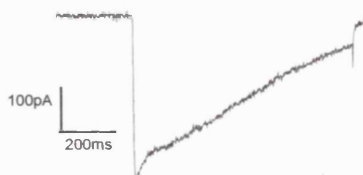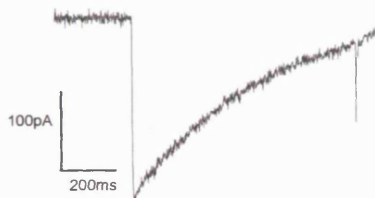
100pA

200ms

Whole cell recording Tail potential -120mV.

100pA

200ms

Whole cell recording Tail potential +40mV

100pA

200ms

Whole cell recording Tail potential +40mV.

100pA

200ms
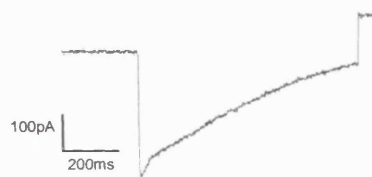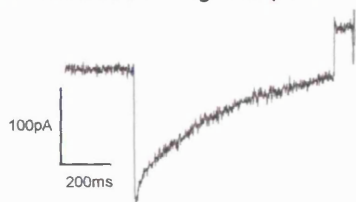
A. Scheme showing how the calculated driving force for chloride changes with membrane voltage for internal solutions containing either cesium-glutamate or cesium-chloride.
B. Sample traces from whole cell experiments when the test potential is either -120mV or +40mV from cesium-glutamate or cesium-chloride based internal solutions.

C.
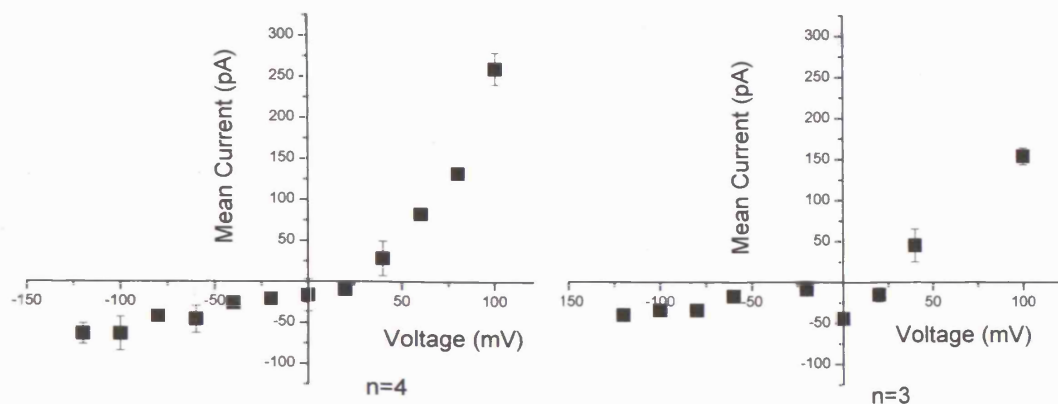
D.
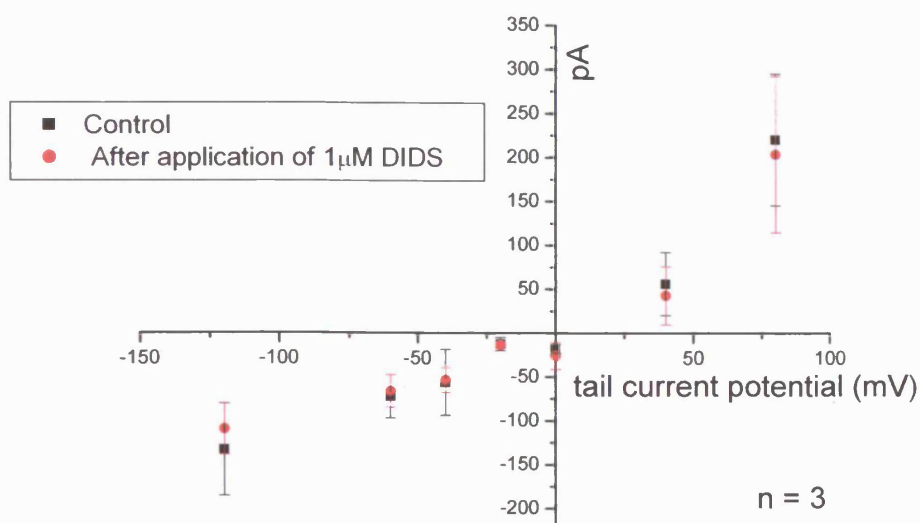
C. I/V curves, data points are the mean ± s.e.m peak amplitude of the test pulse following an 800ms prepulse. On the left for cesium-glutamate based internal (n = 4), and on the right for cesium-chloride based internal (n = 3).

D. I/V before and after 10μM DIDS using cesium-glutamate based internal (1 cell perforated patch others whole cell).Limited data points were recorded to ensure currents were recorded before calcium current rundown was appreciable. Data is mean ± s.e.m peak amplitude of the test pulse following an 800ms prepulse, n = 3. There was no significant change in I/V relationship or current amplitude following DIDS application.

A search of the literature revealed a study in which calcium currents were measured in pancreatic α-cells using similar recording solutions to the ones used in this thesis (Gromada et al. 2001). In this study they state that they apply 20mM TEA-Cl to their

external solution in order to block an outward current that persists after replacement of intracellular potassium with cesium. They presumed that this outward current was a potassium conductance but they did not directly investigate this. Therefore I next examined whether TEA-Cl could inhibit the calcium-dependent outward current observed in my studies. This would act as an additional check to investigate whether this current was in fact due to activation of a calcium-activated potassium channel. BK channels can be blocked by TEA in the low millimolar range (Blatz and Magleby 1987). A previous study examining calcium-dependent potassium channels in bovine adrenal chromaffin cells reports an 87% reduction in current after application of 1mM TEA (Marty and Neher 1985). To investigate this possibility, in addition to the standard 145mM intracellular cesium, 10mM TEA-Cl was substituted with 10mM NaCl of the standard extracellular solution. This substitution reduced the amount of inactivation observed in response to an 800ms depolarisation and prevented the current from ever going outward. The degree of inactivation was 96 ± 3 % reduced to 87 ± 2 % n = 4, p = 0.001 when standard extracellular solution was replaced with one containing 10mM TEA-Cl (figure A1.6). The peak amplitude of the current was not significantly different, control value of 326 ± 75 pA verses 350 ± 74 pA n = 4 after addition of TEA-Cl. However the amount of calcium entering during the pulse was increased from 253 ± 68 x 10^6 Ca^{2+} ions to 334 ± 65 x 10^6 Ca^{2+} ions n = 4 p = 0.009, and the peak amplitude of the tail current observed at the end of the pulse was reduced from 99 ± 28 pA to 59 ± 6 pA n =4. The remaining tail current may be due to calcium flow through channels that are not inactivated by the end of the pulse or through the unidentified channel. The latter explanation is more likely as the tail current retains its slow kinetics. The tail in both cases could be fit by a double exponential with mean τ_1 = 13ms and τ_2 = 82ms for control and τ_1 = 7 ms and τ_2 = 68ms after application of 10mM TEA-Cl. As 10mM TEA is only partially reducing the amplitude of the tail current (41%), it is possible that a TEA insensitive SK channel carries the remaining current. Direct testing of this hypothesis by application of apamin was not conducted, but would have been useful in investigating this scenario.

The amount of inactivation observed during a robust train of depolarisations was also reduced upon application of 10mM TEA-Cl. Fractional inactivation after a train of 50, 10ms pulses at 20Hz was 0.39 ± 0.08 in control, reduced to 0.51 ± 0.02 ($n = 3$) after exchange of recording solutions. This difference was not considered significant in a paired t-test, $p = 0.25$. Similarly when unpaired cells were analysed, fractional inactivation was 0.38 ± 0.03 $n = 17$ in standard solution reduced to 0.45 ± 0.02 $n = 20$ when the extracellular solution contained 10mM TEA-Cl. Again this difference was not found to be statistically significant, $p = 0.11$ (figure A1.7). This may reflect the amount and temporal properties of calcium entry, suggesting that the current sensitive to TEA-Cl is only switched on when the cell experiences very high calcium levels. Mean calcium entry during an 800ms depolarisation is 489 ± 38 x 10^6 Ca^{2+} ions whereas the total calcium entry during the train of depolarisations is 226 ± 22 x 10^6 Ca^{2+} ions $n = 20$ over a time period of 3 seconds.

A1.6 10mM TEA-Cl prevents the recorded current from going outward during a long pulse and reduces the peak amplitude of the resultant tail current.
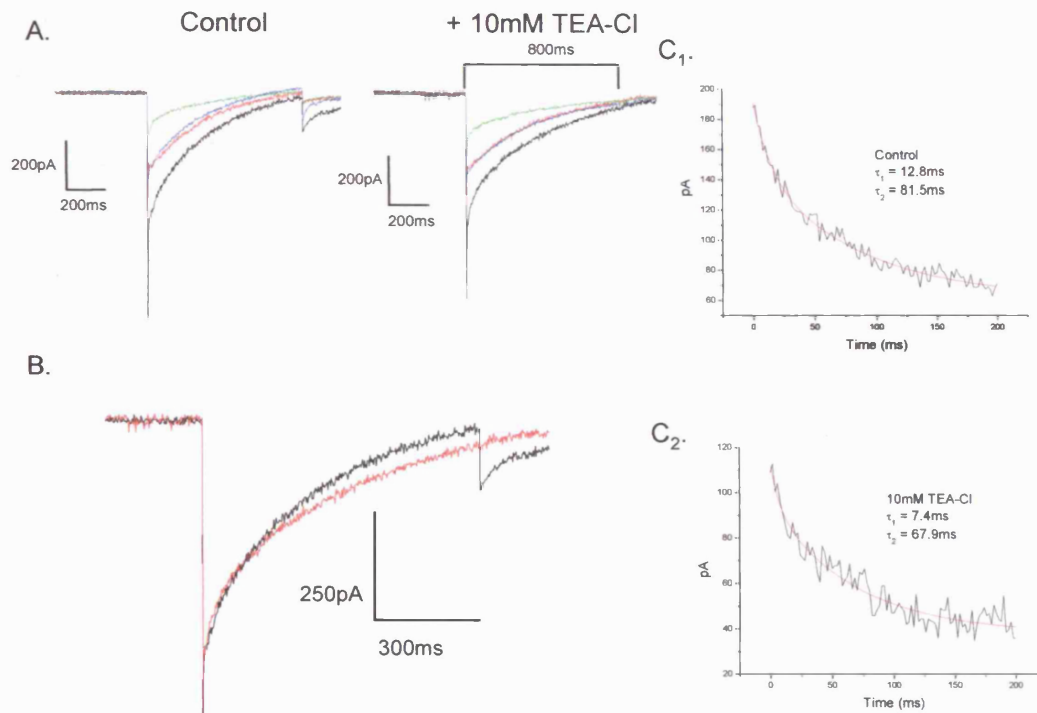
A. Current traces from 4 cells in control (left) and after change of external solution to one in which 10mM [NaCl] was substituted with 10mM TEA-Cl (right). Depolarisations were evoked in response to a long (800ms) depolarisation. Current inactivation was reduced from 96 ± 3 % to 87 ± 2 % n = 4 after application of external solution containing 10mM TEA-Cl.

B. Overlapping trace from an 800ms depolarisation before (black) and after application of 10mM TEA-Cl (red).

C. Tail currents were averaged together and the mean trace fitted by a double exponential, $y = y_0 + A_1e^{-x/t1} + A_2e^{-x/t2}$. The time course for current decay was similar for each condition. $\tau_1 = 13$ and 7ms, and $\tau_2 = 82$ and 68ms for control and 10mM TEA-Cl respectively.

A1.7 10mM TEA-Cl does not significantly reduce current inactivation following a train of short depolarisations.
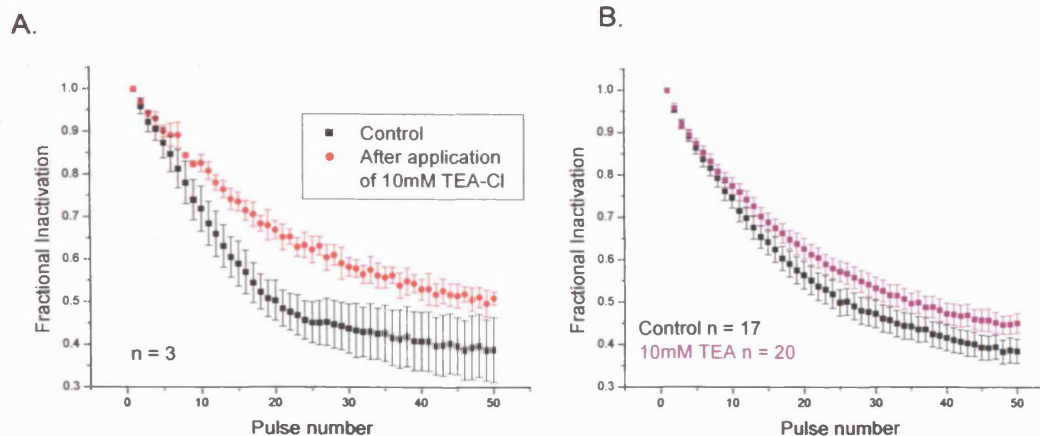
A. Fractional inactivation was determined by dividing the peak current (after 3ms to exclude contributions from sodium currents) of each pulse in the train by the peak current of the first pulse. % inactivation is a measure of how much the current inactivates during the course of the train. Each point is the mean ± s.e.m. Fractional inactivation at pulse 20 was 0.50 ± 0.05 reduced to 0.67 ± 0.02 (n = 3), after application of external solution containing 10mM TEA-Cl this was considered significant in a paired t-test, p = 0.03. However by pulse 50 fractional inactivation was 0.39 ± 0.08 reduced to 0.51 ± 0.02 (n = 3). This reduction was not found to be significant in a paired t-test, (p = 0.25).
B. Results from all cells were then analysed. Fraction inactivation at pulse 50 is reduced from 0.38 ± 0.03 n = 17 in standard solution to 0.45 ± 0.02 n = 20, in an unpaired t-test this reduction was not found to be significant (p = 0.11). In this case no significant difference at earlier pulse intervals was detected.

These results show that TEA can inhibit the calcium-dependent outward current, but the molecular identity of the channel is still unresolved. As mentioned earlier the reversal potential of the measured tail current (~ +25mV, figure A1.4) is at odds with the current being mediated by a calcium-activated potassium channel. Therefore the effects of TEA shown here may be due to block of some other channel. A possible candidate is a TRP (Transient Receptor Potential) channel (Clapham 2003). During long pulses or robust trains of depolarisations cytoplasmic calcium concentrations will rise substantially. High $[Ca^{2+}]i$ has been reported to activate PLC (Allen et al. 1997; Ellis et al. 1998). Recent characterization of some TRP family members, particularly from the sub-group TRPC, shows regulation by PLC (Clapham et al. 2001). These TRP channels are usually non-selective channels, which have a reversal

267

potential close to zero. It is possible that by stimulating the cell with a long (800ms) depolarisation or by a robust train of depolarisations, cytoplasmic calcium concentrations rise sufficiently to activate PLC and switch on a TRP channel. Although I can find no evidence from the literature to support a role of TEA-Cl in blocking TRP channels, if the tail current conductance is mediated by ion flow through a TRP channel then TEA-Cl at 10mM could be considered a partial blocker. It was beyond the scope of my PhD to thoroughly characterize this current. As addition of 10mM TEA-Cl reduced the measured inactivation and the amplitude of the tail current presumably by inhibiting a calcium-dependent outward current, it became routine in my studies to switch to a solution containing 10mM TEA-Cl after obtaining voltage clamp, therefore reducing the error in evaluating channel inactivation in response to long pulses. The remaining error is presumed to be slight due to a low driving force for the current as its reversal potential is close to the standard depolarisation of +20mV.

A slow tail current is not often seen when inspecting published calcium currents in chromaffin cells. This probably results from differences in recording conditions. Barium is often used as the charge carrier (preventing calcium-dependent activation of the slow tail), short depolarisations are more typically shown, (the slow tail is only apparent after long depolarisations), and TEA is often used either as a substitute for extracellular sodium or as an additional potassium channel blocker in the extracellular solution. Groups using recording solutions similar to ours have published calcium currents, which contain a slow tail current in response to long depolarisations (Engisch and Nowycky 1996). They do not try to block this current, but they mention in their materials and methods that they simply exclude tail currents from analysis, as 'they are composed of at least one calcium-activated conductance of unknown origin'.

In summary, following a long depolarisation (800ms), tail current kinetics become slower suggesting the activation of a calcium-dependent conductance of unknown identity. This undetermined current can be significantly reduced by external application of 10mM TEA-Cl.

Appendix 2 Production of a virus

Gene delivery to primary cultures of chromaffin cells has proven very demanding. Transfection methods developed for use in stable cell lines have usually proved inefficient in transducing neuronal primary cells or slice preparations. I have tried transient transfections with fugene 6, lipofectamine 2000, or by electroporation with poor transfection efficiency. However viral vectors have been shown to infect these cell types with high efficiency. Initially an adenovirus carrying DNA for phogrin (a vesicle associated protein) tagged with EGFP (kind gift from Dr Guy Rutter, University of Bristol) was applied directly to the cell feeding media and fluorescence observed 24 hours later. This experiment proved adenoviral delivery of DNA to be extremely effective in primary chromaffin cell cultures and acute slices of chromaffin cells. Other viruses like Semliki Forest Virus (SFV) have been used to successfully infect chromaffin cells (Ashery et al. 1999; Duncan et al. 1999). SFV's had the advantage until recently of being far less labour-intensive and time-consuming to produce compared to adenovirus. However they appear to be more toxic, resulting in a narrow window after infection for conducting experiments. During the course of my PhD I attempted to make several adenoviruses and SFV's. This appendix describes the methods used to make each type of virus and my results.

A2.1 Adenovirus

Adenovirus are encapsidated double stranded linear DNA viruses, they are very stable and very infectious. Adenoviruses can attach to two receptors found on the surface of mammalian cells; the car protein is a receptor for the adenovirus fiber (Bergelson et al. 1997) and surface integrins $\alpha_v\beta_3$ or $\alpha_v\beta_5$ can serve as receptors for the adenovirus penton (Wickham et al. 1993). Binding to these receptors leads to phagocytosis of the entire virus. Once inside the cell the virus travels to the nucleus where it forms a virus DNA-cell histone complex and recombines with the host DNA. Wild type adenovirus then highjacks the cell protein synthesis machinery, effectively

269

shutting down host cell protein synthesis and inducing synthesis of proteins needed to make new virions. Eventually lysis of the host cell occurs and the new viral particles infect other cells. By manipulating the genome of the adenovirus it is possible to take advantage of its efficient cell entry mechanism and eliminate its capacity to replicate and lyse the cell. This is achieved by deleting the E1 region of the virus and inserting in its place your gene of interest. This adaptation essentially allows you to easily insert a functional gene into the host cell in a well tolerated way. The low cytotoxicity of adenoviral gene delivery means that a high number of cells survive the infection procedure and express the gene of interest.

I attempted to make three adenoviruses, one containing wild type calmodulin, one containing a mutant calmodulin in which all 4 EF hands were rendered incapable of binding calcium (DNA kind gift from Dr Aldeman, The Vollum Institute, Portland) and the third was NPY-EGFP. NPY is a peptide localised to secretory granules in chromaffin cells (DNA kind gift from Dr Almers, The Vollum Institute, Portland). Figure A2.1.1 is a schematic overview of the technique used to make a recombinant adenovirus using the AdEasy (Quantumbiotech) kit. Briefly, the DNA of interest is sub-cloned into a pShuttle transfer vector (Step 1) which is co-transformed with the pAdEasy plasmid (Step 2). This recombinant plasmid is transfected into a specialised human embryonic kidney (HEK) cell line, which permits viral replication (Step3). The recombinant adenovirus is then amplified and purified.

A2.1.1 Overview of the technique.

Generation of a Recombinant Adenovirus Using AdEasy™
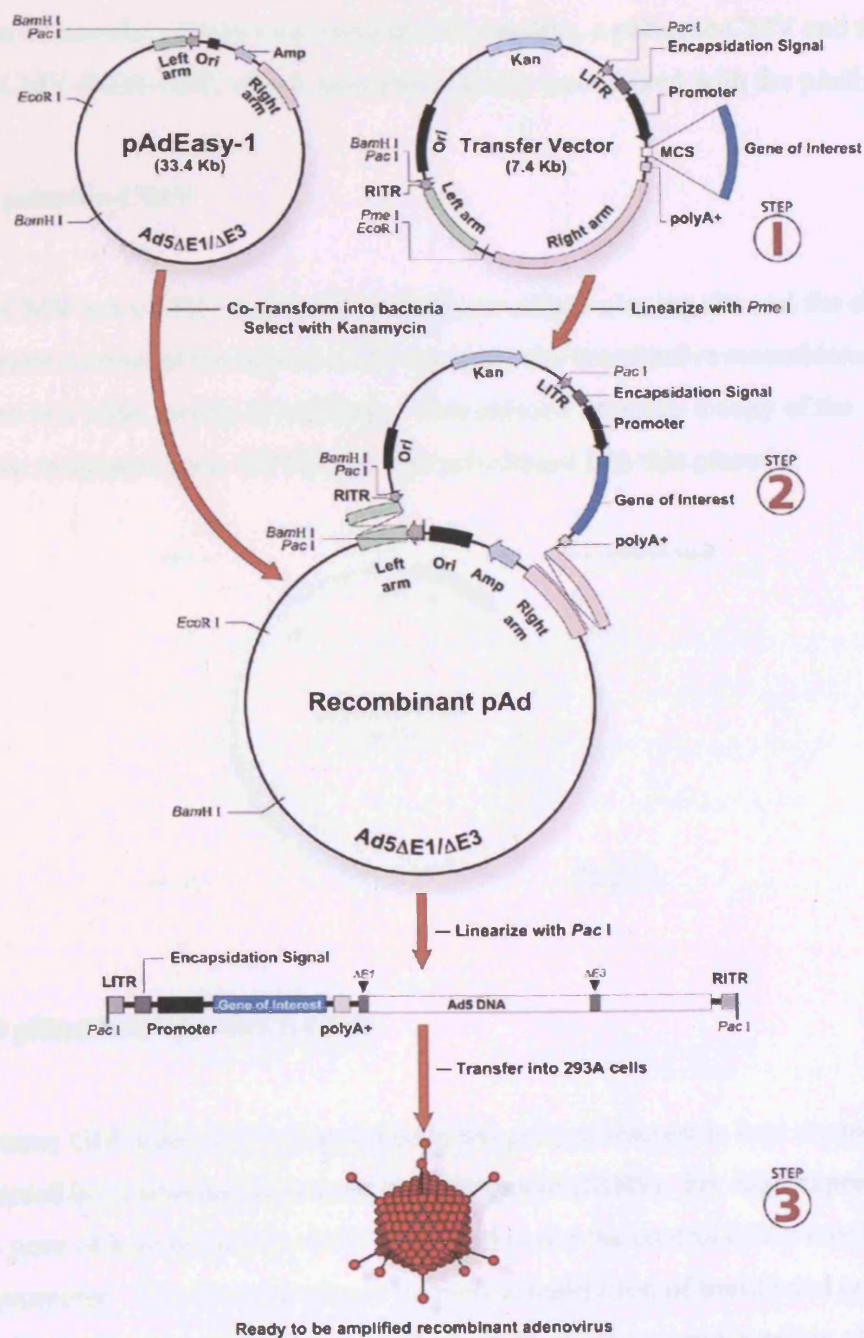
Diagram taken from the AdEasy web site: www.quantumbiotech.com

271

A2.1.2 Plasmids.

Two types of transfer vectors were used in these studies, a pShuttle-CMV and a
pShuttle-CMV-IRES-GFP, which were individually recombined with the pAdEasy-1
plasmid.

A2.1.2.1 pshuttle-CMV

pShuttle-CMV is a useful vector as it contains a multiple cloning site and the cloned
gene is under control of the human CMV promoter for constitutive recombinant
expression in a wide variety of cell lines. This plasmid contains a copy of the
kanamycin resistance gene. NPYEGFP was sub-cloned into this plasmid.
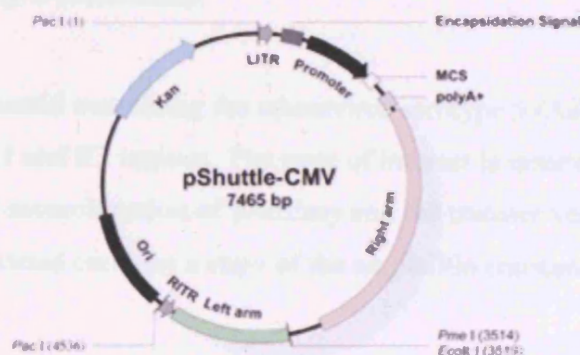
A2.1.2.2 pShuttle-CMV-IRES-GFP.

In this vector GFP instead of being linked to the gene of interest is kept separate and
co-expressed in an Internal Ribosome Entry Segment (IRES). For high expression
both the gene of interest and the GFP are placed under the control of the modified
CMV5 promoter. This plasmid allows for easy visualisation of transfected cells
without the need to have GFP ligated to the protein of interest and possibly affecting
its function. As calmodulin is thought to bind to calcium channels and undergo a

large conformational change upon binding calcium it is preferable not to dramatically extend the length of the molecule by adding GFP.
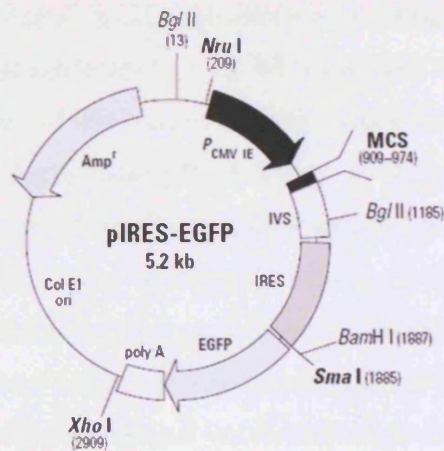
A2.1.2.2 pAdEasy-1 (AES1010).

This is a large plasmid containing the adenovirus serotype 5 (Ad5) genome, with deletions in the E1 and E3 regions. The gene of interest is inserted into the E1 region after homologous recombination of pAdEasy and the transfer vector in BJ5183 bacteria. This plasmid contains a copy of the ampicillin resistance gene.

273
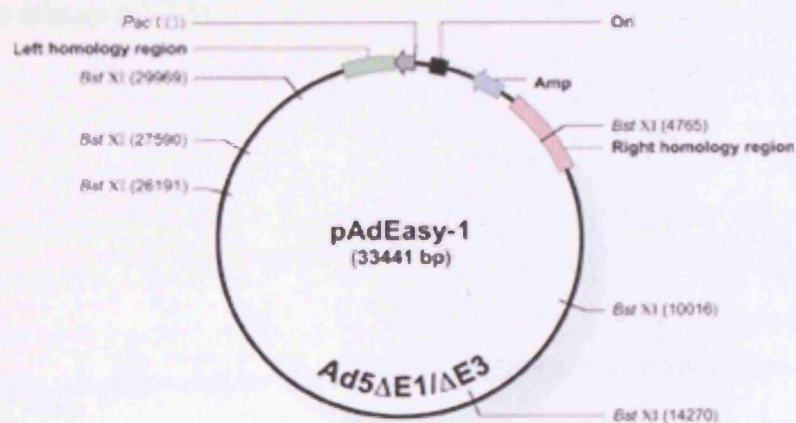
A2.2 Full details of technique.

The gene of interest is cut out of its original vector with restriction enzymes (RE's); the pShuttle vectors are also cut with the same RE's and then dephosphorylated to prevent resealing. The piece of DNA containing the gene of interest and the linearised plasmid are then ligated using DNA ligase. Using a heat shock technique (protocol 1, section 2.4.1), which briefly loosens the plasma membrane allowing the insertion of the plasmid, the success of the ligation can be assessed. Only colonies containing the plasmid will grow on kanamycin loaded agar plates and these are then screened for the presence and correct insertion of the gene of interest by restriction analysis. The calmodulin inserts were cut out of their original vector with BglII, therefore creating the possibility that when ligated with the pShuttle-CMV the gene could run in either direction. To check the orientation of the insert, colonies were picked and grown overnight; the plasmids were then recovered using a miniprep kit (Amersham Pharmacia Biotech, GFX Micro Plasmid Kit). The purified plasmid DNA was then digested with HindIII. If the insert is in the correct orientation there will be one very large fragment and two smaller fragments, one at 347bp and the other at 313bp. If the insert is in the wrong orientation there will be one very large fragment, one at 347bp and one at 663bp. Therefore by running the digested DNA on an agarose gel it is possible to detect which colonies contain the insert in the correct orientation (figure A2.2.1).

A2.2.1. Checking that the insert is correctly orientated into the plasmid

A photograph of a restriction digest to check for the correct orientation of the DNA sequence in the plasmid. If it has ligated in the wrong direction then a HindIII digest will cut a unique fragment of 663bp. From 7 colonies 3 were found to contain the DNA sequence in the correct orientation.

Successful colonies were then amplified using a maxiprep kit (Clontech, Nucleobond Plasmid Maxi Kit). To check the integrity of the DNA and that no mutations had occurred restriction analysis was performed as before and some of the purified plasmid was sent off for sequencing. At this stage transient transfections into cell lines, like PC12 is possible and useful way to test the construct. To create the adenovirus the next step is to recombine the pShuttle plasmid with the pAdEasy plasmid (see protocol 2, section 2.4.2). Potential colonies containing the recombinant plasmid were grown and the plasmids extracted using a miniprep kit. Restriction digestion was then performed to verify recombination. A BstXI restriction pattern is a good way to check recombination as pAdEasy contains six sites for this enzyme yielding restriction fragments of different size (1 – 11921 bp, 2 – 8237 bp, 3 – 5251 bp, 4 – 4254 bp, 5 – 2379 bp, 6 – 1399 bp). Fragment number two is the only one that will vary with the size of the insert and from one insert to the other. Using either pShuttles or NPYEGFP/Calmodulin the second band will shift to around 11-12kb (roughly the same size as band 1) if the plasmids have successfully recombined. Figure A2.2.2 is a gel showing successful recombination of pAdEasy and pShuttle-CMV-NPYEGFP.

275

A2.2.2 DNA gel of successful recombinants

PAdEasy plasmid digested with BstXI. Note the 2nd band @ 8237bp which is absent in the successful recombinants. (The bottom two bands are very faint in this photo of the gel).

Resealed pShuttle-CMV-NPYEGFP.

Sucessful recombinants, the 2nd band has merged with the 1st.
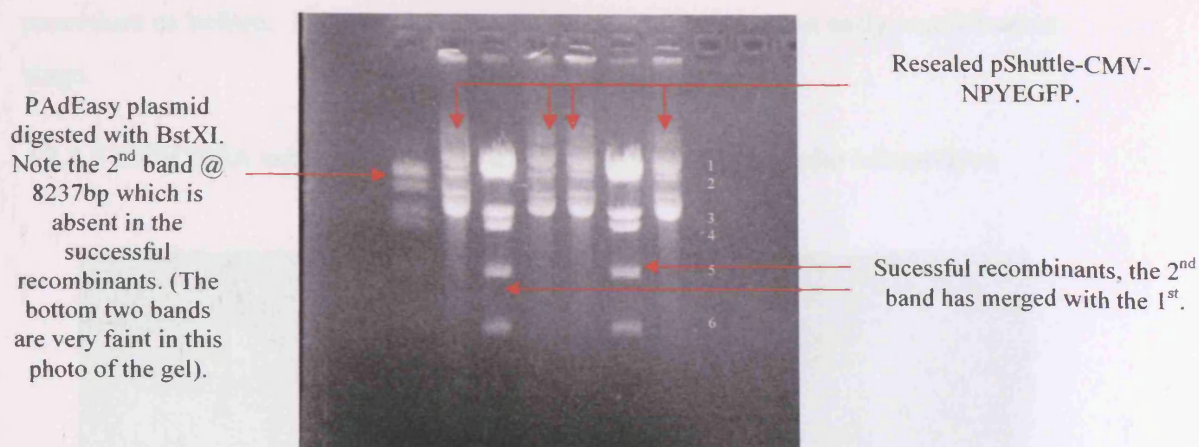
DNA from successful colonies was then amplified by transfection of the plasmid into DH5α cells using the heat shock technique. I then checked again the integrity of the construct and performed a maxiprep of the plasmid taking the necessary precautions needed as the plasmid size is now very large >40kb. 5-10 μg of DNA was then digested with PacI and ethanol extracted. Viral particles were produced when this DNA was transfected into HEK 293A cells. These cells allow the replication of the viral particles as they contain the E1 region, which is deleted in the pAdEasy plasmid. I transfected a small (T25) flask ~30-40% confluent, with fugene 6, other reagents like lipofectamine or techniques such as calcium-phosphate transfer have also been reported to work well (personal communication E.Ainscow & H. Witrow). After 11 days a streak of bright green cells was observed under a fluorescent microscope. I then amplified the number of viral particles by spinning down the cells, adding a small amount of PBS and undergoing 3-4 freeze-thaw cycles to rupture the plasma membrane and release the virus into the supernatant. This supernatant was used to infect larger flasks of HEK 293A cells. Unfortunately, during amplification I had two misfortunes, the first was flask infection, and the second was cell death due to a faulty incubator, which maintained a temperature of 42°C and not 37°C. After these set backs the project was paused to focus my time on electrophysiology. In the interim, discussions with Dr David Yue (John Hopkins Medical School, Baltimore) lead to him sending us a small quantity of his calmodulin WT and mutant virus to test

on our cells. This virus worked well and was subsequently amplified using the same procedure as before. Figure A2.2.3 shows viral production at an early amplification stage.

A2.2.3 HEK293A cells successfully making mutant calmodulin adenovirus
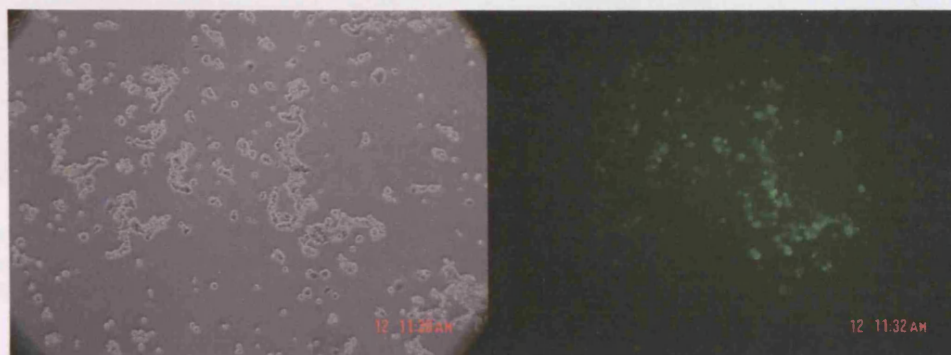
HEK293A cells were used to amplify the virus. Above (left), is a bright field image and (right), successfully infected cells are shown by fluorescent microscopy.

Once 10 T75 flasks were infected and ready, the flasks are combined, the cells pelleted and the virus released by 4 cycles of freeze-thaw to produce 4mls of crude viral lysate. To purify the virus the AdEasy protocol suggests that the lysate is CsCl density centrifuged at 32,000 rpm at 10°C for 18-24 hours. The department did not have a suitable rotor for this centrifugation, however discussion with Dr Terry Herbet (University of Leicester), who has made and used several adenoviruses reported that he does not require this purification step for successful infection of the cells he uses (primary pancreatic β cells). Therefore the crude lysate was used to infect our chromaffin cells. As can be seen in A2.2.4, infection with this adenovirus resulted in a high level of infection in bovine adrenal chromaffin cells.

A2.2.4. Adenoviral infection of bovine adrenal chromaffin cells.
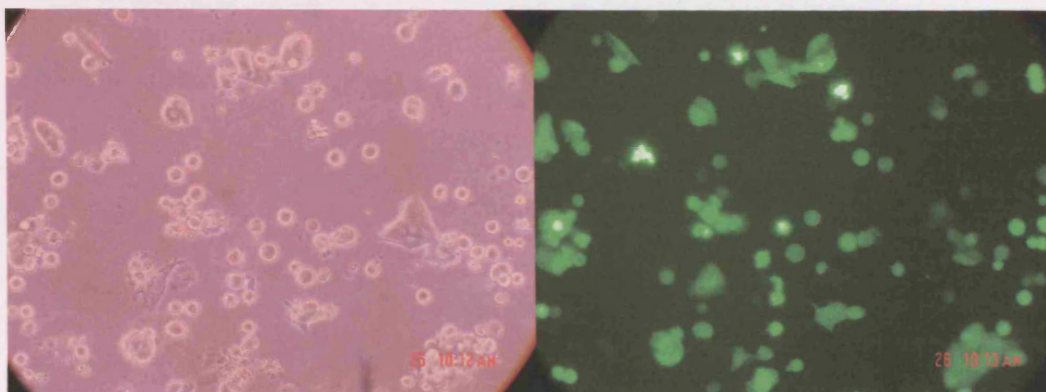
On the left is a bright field image from a coverslip of bovine chromaffin cells and successfully infected cells are shown by fluorescent imaging on the right. Images were taken 48hrs after infection with 3μl of WT calmodulin adenovirus.

In fact these adenoviruses have successfully infected every other cell type tested. This includes PC12 cells, HEK cells, BHK cells and an astrocyte cell line (supplied by Ken Harden University of Leicester), (figure A2.2.5).

A2.2.5 Adenoviral infection of an astrocyte cell line.
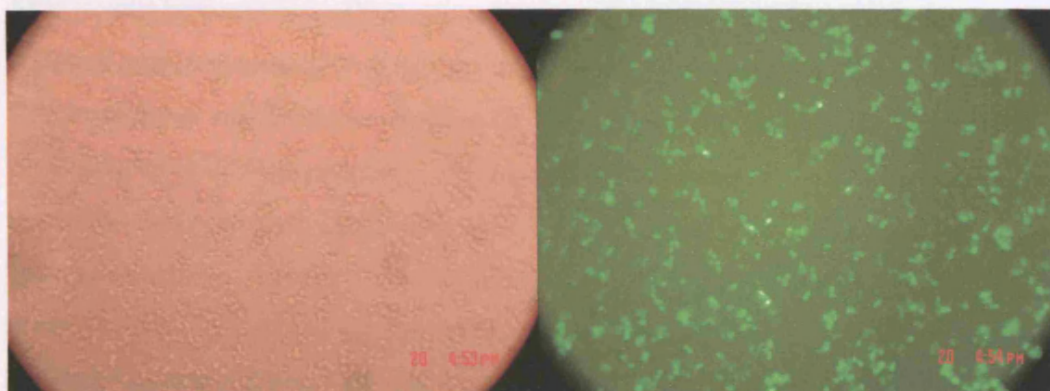
A bright field image of astrocytes is shown on the left with successfully infected cells shown by fluorescent imaging on the right. Images were taken 24hrs after infection with 3μl of mutant calmodulin adenovirus.

Western Blot analysis was used as a functional assay to test for protein expressed by the virus (Protocol 3, section A2.4.3). Figure A2.2.6 is a western blot showing that

278

virally infected cells greatly over-express calmodulin compared to the expression level of endogenous calmodulin shown in the control (C) uninfected lane.

A2.2.6. Western blot of virally infected cells
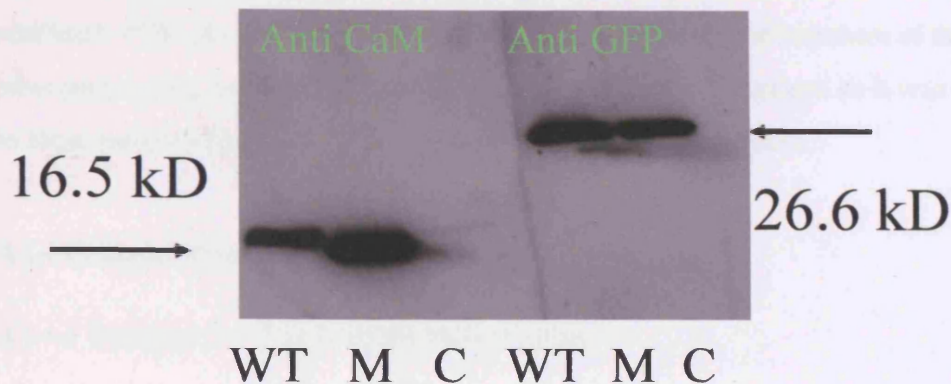
A western blot of WT, mutant and uninfected control cells. Cells were infected for 48hrs with adenovirus and blotted with anti-CaM and anti-GFP antibodies.

A2.3 Semliki Forest Virus.

SFV is an enveloped virus with a single stranded RNA genome. The genome of the SFV is split between two cDNA plasmids, one of which is the cloning vector and contains non-structural SFV genes, the other is a helper vector which does contain structural genes and therefore encodes for the capsid and other proteins required for packaging of infectious particles. The helper plasmid we used, contained three point mutations that produce a virus, which needs to be treated by α-chymotypsin to become infectious. *In vitro* transcription of both cloning and helper plasmids produces RNA, which is electroporated into baby hamster kidney (BHK-21) cells for *in vivo* production of recombinant SFV particles. 24-48 hrs post-transfection a high-titre of mature virus can be collected from the supernatant and used to infect your cells of choice, in our case chromaffin cells. No further purification is necessary. This virus has been used successfully to transfect chromaffin cells, hipocampal slice cultures, cortical neurones and superior cervical and dorsal root ganglia neurones with high efficiency (reviewed in Lundstrom et al. 2001a; Lundstrom et al. 2001b). I attempted to create an SFV encoding NPY-EGFP (full details of the method are in

279

protocol 4, section A2.4.4). However despite the integrity of the DNA being checked and found to be good and RNA successfully transcribed, the supernatant collected from electroporated BHK cells did not infect primary cultures of adrenal chromaffin cells. This may have been due to RNA degradation during electroporation, or problems with activating the virus with α-chymatrypsin. Other members of the laboratory trying to create SFV's encountered similar problems and so it was decided to focus on the adenoviral system to create future viral constructs.

A2.4 Protocol details

A2.4.1 Protocol 1 – The heat shock technique.

50μl of DH5α bacteria are incubated on ice for 30 minutes with 10μl of ligation mixture. The cells are then heat shocked by placing them in a waterbath at 42°C for 45-60 seconds. The tube is then immediately plunged back into ice for a couple of minutes before 0.5 ml of Luria-Bertani medium is added. The cells are left to grow in a shaker-incubator at 37°C for one hour before ~200μl of mixture is plated out onto agar containing a suitable antibiotic for selection; in our case this was kanamycin (1:1000). The plates are left in the incubator (37°C) overnight and colonies are subsequently screened.

A2.4.2 Protcol 2 – Co-transformation of pShuttle and pAdEasy plasmids.

I linearised the pShuttle with PmeI, and gel extracted a band ~9kb. Then 20μl of electrocompetant BJ5183 cells were placed into a pre-cooled electroporation chamber with the digested shuttle DNA and ~ 300ng of pAdEasy DNA. This mixture was electroporated using a BIORADGene Pulser at 2,500V, 200 Ohms, and 25 mFD, with a time constant of around 4.5-4.8 seconds. The chamber was then left on ice for a couple of minutes before 0.5ml of LB (room temp) was added. Then as much of the mixture as possible was transferred to an eppendorf tube and incubated for 40 minutes in a shaking incubator. Cells were plated onto kanamycin-loaded plates and

incubated overnight. The next step was the most critical, 24hrs later there will many colonies of different sizes, most will contain just the resealed pShuttle plasmid and a few will contain the recombinants. As the recombinants will grow more slowly, the very small translucent colonies are most likely to contain a recombined plasmid.

A2.4.3. Protocol 3 – Western Blotting.

Cells were plated at 500,000 cells per well and infected with adenovirus for 48hrs. The cells were then washed twice with PBS and then 250µl of lysis buffer (RIPA) was added for 15 mins at 4°C. 200µl from each well was collected and spun at 13,000rpm for 1 minute. The supernatant was mixed 50:50 with loading buffer and heated at 80°C for 5 mins. 25µl was then loaded per lane to a 15% gel and run for 1hr at 180V. This was then overlayed with a nitrocellulose membrane and transferred for 1hr at 60mA and 5V. The membrane was then incubated with 0.5µg/ml, 10ml final volume anti-CaM (Research Diagnostics) in 5% milk solution, or a 1:5000 dilution of anti-GFP (kind gift from Dr Dickins, University of Leicester). The antibodies were incubated at 4°C overnight with gentle rocking, washed 4 times with Tris-buffered saline with tween (TBST) for around 40mins before application of the secondary antibody. Goat anti-mouse horseradish peroxidase was used against CaM and goat anti-rabbit against GFP. The secondary was applied for 90 mins at room temperature, and then washed 4 times with TBST. Chemiluminance solutions A and B (Amersham) were mixed at a ratio of 1:40, and poured onto cleaned sheets of glass. The nitrocellulose membrane was laid face down on the glass for 5 mins at room temperature and excess solution removed. The membrane was then mounted and exposed to film.

A2.4.4. Protocol 4. Details of the protocol used to generate a SFV and its subsequent infection into chromaffin cells.

Vectors and sub-cloning. The vector used for insert ligation was the pSFV2gen, which is a low cytotoxic (PD) version (originally supplied by Ken Lundstrom, Roche), which contains a Multi-Cloning Site (MCS) for BamHI, RsrII, BssHII, SciI, XhoI, SpeI, NotI, AvrII and ApaI. It is essential that potential inserts lack either NruI or SapI sites as one of these is necessary later to linearise the plasmid. Fortunately NPY-EGFP is not cut by either of these enzymes. The helper plasmid was pSFV2 (Life Sciences, Inc), which contains three point mutations from the original, so that the virus needs to be treated with α-chymotypsin to become infectious. This plasmid was linearised with SpeI.

In vitro **transcription.** 5μg of pSFV2gen (containing NPY-EGFP) and pSFV2 Helper plasmid were linearised, and the DNA phenol extracted and ethanol precipitated. The DNA was then washed and the pellet resuspended in DPEC treated water at a concentration of ~0.6μg/μl. DNA was transcribed *in vitro* for 1-2 hrs at 37°C using an SP6 RNA polymerase based reaction (Protocol 5, section A2.4.5 contains full details of mRNA preparation).

BHK transfection with RNA. BHK-21 cells (cultured in Glasgow Modified Eagle's medium supplemented with 10% (v/v) tryptose phosphate broth, 10% foetal bovine serum, 2mM L-glutamine and 100 units/ml penicillin/streptomycin (all Gibco) at 37°C in 95% (v/v) air, 5% (v/v) CO_2), were grown to confluency in a 163cm^2 flask. The cells were washed with 5mls of Versene, followed by 3ml of typsin/EDTA to remove the cells from the flask. 10ml of complete medium (Glasgow MEM/10% (v/v) NBCS/10% (v/v) tryptose-phosphate broth, and 2mM L-glutamine) was then added, before centrifugation at 400xg for 5 mins. The cells were wash 10 mls without serum, and then again in 10ml of sterile 1 x Hanks Balanced Salt Solution (HBSS) (w/o Ca^{2+}). Cells were then pelleted as before, and then re-suspended in 1600μl of 1 x HBSS. 10-35μl of *in vitro* transcribed pSFV2gen RNA along with 10-35μl of pSFV2 helper RNA was electroporated (using a BIORAD genepulser) into 800μl of cells. The cells were shocked as soon as possible after adding the RNA with

282

two pulses at 850 V, and 25μF. The cells were allowed to stand for 5 minutes before addition of 8.5mls of complete medium, plating and overnight incubation.

Virus harvest. The virus was harvested from the BHK medium in batches between 16 and 36hrs post transfection. The medium was filtered through a 0.25 mm-pore filter and then frozen into aliquots at –20°c for short-term storage.

Infection of chromaffin cells. For infection of ~ 1 x 10^5 – 1 x 10^6 plated cells, viral particles were activated by adding 10μl of chymotrysin A4 (5mg/ml) to 200μl of virus stock and incubated on ice for 10mins. 5ml of aprotinin (1mg/ml) was added to inactivate the protease. The activated stock was diluted 1:10 with conditioned chromaffin cell media before overlaying the cells to be infected and incubation at 37°C. This protocol was obtained from Drs Duncan & Shipston at the University of Edinburgh.

A2.4.5 Protocol 5. Preparation of mRNA *in vitro*.

This is the protocol (written by Dr Mike Shipston, Univeristy of Edinburgh), which I followed to prepare mRNA.

1. Add DEPC water to each of the digested pSFV1 and pSFV2 to make 100μl final volume.
2. Add 100ml phenol, vortex, spin at 13,000rpm for 2 minutes.
3. Aliquot 100 ml chloroform to two new RNAse safe eppendorfs. Using RNAse-free tips, pipette the upper phase from the phenol extractions into the chloroform.
4. Vortex and spin again.
5. Pipette upper phase into 2 new RNAse sfare eppendorfs.
6. Add 10ml NaAcetate (3M, pH 5.5).
7. Add 2.5 x volume of absolute ethanol (stored at –20°C) i.e 250μl to each tube, then put in –20°C freezer for 10 minutes.
8. Meanwhile, make up NTPs in an RNAse safe eppendoff as follows   10μl 100mM ATP, 10μl 100mM CTP, 10μl 100mM UTP, 5μl 100mM GTP, 65μl DEPC water
9. Put NTPs, 5x Buffer, RNA Capping Analogue, Rnasin and DTT (10mM) on ice to thaw.
10. Take DNA out of the freezer and spin for 30 minutes.
11. Aspirate off ethanol taking care not to dislodge DNA pellet. Add 100μl of 70% (v/v) ethanol and briefly spin again.
12. Heat a glass Pasteur pipette in a Bunsen flame until almost melted, remove, pull it apart to give a very fine sterile pipette and use this to remove the ethanol.

13. Resuspend each pellet in DEPC water to give ~ 0.6µg/µl., (started with 5mg, assume lost 1/5th in phenol extraction, so resuspend in 6.66ml, 2nd DNA pellet may be smaller, so adjust accordingly).

14. Place 2 new RNAse safe eppendorfs on ice and add to each in this order: 20µl NTP, 10µl 5x Buffer, 5µl Cap analogue, 5µl of DTT (10mM), 5µl Rnasin (Human placenta - sinks so mix immediately), 2.5µl pSFV1/pSFV2 DNA, 2.5µl SP6

15. Mix thoroughly and spin if there are any drops on the side.

16. Place at 37°C for 1-2 hrs.

When preparing RNA it is important to use RNAse-free eppendorfs and tips, fresh DEPC water, and to change your gloves every 5 minutes.

Bibliography

Akita, T. and Kuba, K. (2000). Functional triads consisting of ryanodine receptors, Ca2+ channels, and Ca2+-activated K+ channels in bullfrog sympathetic neurons - Plastic modulation of action potential. *Journal of General Physiology* **116**, 697-720.

Albillos, A., Neher, E. and Moser, T. (2000). R-type Ca2+ channels are coupled to the rapid component of secretion in mouse adrenal slice chromaffin cells. *Journal of Neuroscience* **20**, 8323-8330.

Aldea, M., Jun, K., Shin, H. S., Andres-Mateos, E., Solis-Garrido, L. M., Montiel, C., Garcia, A. G. and Albillos, A. (2002). A perforated patch-clamp study of calcium currents and exocytosis in chromaffin cells of wild-type and alpha(1A) knockout mice. *Journal of Neurochemistry* **81**, 911-921.

Alexander, K. A., Cimler, B. M., Meier, K. E. and Storm, D. R. (1987). Regulation of Calmodulin Binding to P-57 - a Neurospecific Calmodulin Binding-Protein. *Journal of Biological Chemistry* **262**, 6108-6113.

Allen, V., Swigart, P., Cheung, R., Cockcroft, S. and Katan, M. (1997). Regulation of inositol lipid-specific phospholipase C delta by changes in Ca2+ ion concentrations. *Biochemical Journal* **327**, 545-552.

Almers, W. and McCleskey, E. W. (1984). Non-Selective Conductance in Calcium Channels of Frog-Muscle - Calcium Selectivity in a Single-File Pore. *Journal of Physiology-London* **353**, 585-608.

Andreasen, T. J., Luetje, C. W., Heideman, W. and Storm, D. R. (1983). Purification of a Novel Calmodulin Binding-Protein from Bovine Cerebral-Cortex Membranes. *Biochemistry* **22**, 4615-4618.

Aravamudan, B. and Broadie, K. (2003). Synaptic Drosophila UNC-13 is regulated by antagonistic G- protein pathways via a proteasome-dependent degradation mechanism. *Journal of Neurobiology* **54**, 417-438.

Aravanis, A. M., Pyle, J. L. and Tsien, R. W. (2003). Single synaptic vesicles fusing transiently and successively without loss of identity. *Nature* **423**, 643-647.

Archer, D. A., Graham, M. E. and Burgoyne, R. D. (2002). Complexin regulates the closure of the fusion pore during regulated vesicle exocytosis. *Journal of Biological Chemistry* 277, 18249-18252.

Arikkath, J. and Campbell, K. P. (2003). Auxiliary subunits: essential components of the voltage-gated calcium channel complex. *Current Opinion in Neurobiology* 13, 298-307.

Artalejo, A. R., Garcia, A. G. and Neher, E. (1993). Small-Conductance Ca-2(+)-Activated K+ Channels in Bovine Chromaffin Cells. *Pflugers Archiv-European Journal of Physiology* 423, 97-103.

Artalejo, C. R., Adams, M. E. and Fox, A. P. (1994). 3 Types of Ca2+ Channel Trigger Secretion with Different Efficacies in Chromaffin Cells. *Nature* 367, 72-76.

Artalejo, C. R., Elhamdani, A. and Palfrey, H. C. (1996). Calmodulin is the divalent cation receptor for rapid endocytosis, but not exocytosis, in adrenal chromaffin cells. *Neuron* 16, 195-205.

Artalejo, C. R., Elhamdani, A. and Palfrey, H. C. (2002). Sustained stimulation shifts the mechanism of endocytosis from dynamin-1-dependent rapid endocytosis to clathrin- and dynamin- 2-mediated slow endocytosis in chromaffin cells (vol 99, pg 6358, 2002). *Proceedings of the National Academy of Sciences of the United States of America* 99, 9082-9082.

Ashery, U., Betz, A., Xu, T., Brose, N. and Rettig, J. (1999). An efficient method for infection of adrenal chromaffin cells using the Semliki Forest virus gene expression system. *European Journal of Cell Biology* 78, 525-532.

Ashery, U., Varoqueaux, F., Voets, T., Betz, A., Thakur, P., Koch, H., Neher, E., Brose, N. and Rettig, J. (2000). Munc13-1 acts as a priming factor for large dense-core vesicles in bovine chromaffin cells. *Embo Journal* 19, 3586-96.

Augustin, I., Rosenmund, C., Sudhof, T. C. and Brose, N. (1999). Munc13-1 is essential for fusion competence of glutamatergic synaptic vesicles. *Nature* 400, 457-61.

Bai, J. H. and Chapman, E. R. (2004). The C2 domains of synaptotagmin - partners in exocytosis. *Trends in Biochemical Sciences* 29, 143-151.

Bai, J. H., Tucker, W. C. and Chapman, E. R. (2004a). PIP2 increases the speed of response of synaptotagmin and steers its membrane-penetration activity toward the plasma membrane. *Nature Structural & Molecular Biology* **11**, 36-44.

Bai, J. H., Wang, C. T., Richards, D. A., Jackson, M. B. and Chapman, E. R. (2004b). Fusion pore dynamics are regulated by synaptotagmin center dot t-SNARE interactions. *Neuron* **41**, 929-942.

Bajjalieh, S. M. (1999). Synaptic vesicle docking and fusion. *Current Opinion in Neurobiology* **9**, 321-8.

Barry, P. H. and Lynch, J. W. (1991). Liquid Junction Potentials and Small-Cell Effects in Patch- Clamp Analysis. *Journal of Membrane Biology* **121**, 101-117.

Becherer, U., Moser, T., Stuhmer, W. and Oheim, M. (2003). Calcium regulates exocytosis at the level of single vesicles. *Nature Neuroscience* **6**, 846-853.

Benfenati, F., Onofri, F. and Giovedi, S. (1999). Protein-protein interactions and protein modules in the control of neurotransmitter release. *Philosophical Transactions of the Royal Society of London - Series B: Biological Sciences* **354**, 243-57.

Bennett, M. K. (1997). Ca2+ and the regulation of neurotransmitter secretion. *Current Opinion in Neurobiology* **7**, 316-22.

Bergelson, J. M., Cunningham, J. A., Droguett, G., KurtJones, E. A., Krithivas, A., Hong, J. S., Horwitz, M. S., Crowell, R. L. and Finberg, R. W. (1997). Isolation of a common receptor for coxsackie B viruses and adenoviruses 2 and 5. *Science* **275**, 1320-1323.

Berridge, M. J. (1998). Neuronal calcium signaling. *Neuron* **21**, 13-26.

Berrow, N. S., Campbell, V., Fitzgerald, E. M., Brickley, K. and Dolphin, A. C. (1995). Antisense Depletion of Beta-Subunits Modulates the Biophysical and Pharmacological Properties of Neuronal Calcium Channels. *Journal of Physiology-London* **482**, 481-491.

Betz, A., Ashery, U., Rickmann, M., Augustin, I., Neher, E., Sudhof, T. C., Rettig, J. and Brose, N. (1998). Munc13-1 is a presynaptic phorbol ester receptor that enhances neurotransmitter release. *Neuron* **21**, 123-36.

Betz, A., Okamoto, M., Benseler, F. and Brose, N. (1997). Direct interaction of the rat unc-13 homologue Munc13-1 with the N terminus of syntaxin. *Journal of Biological Chemistry* **272**, 2520-6.

Bezprozvanny, I., Scheller, R. H. and Tsien, R. W. (1995). Functional Impact of Syntaxin on Gating of N-Type and Q-Type Calcium Channels. *Nature* **378**, 623-626.

Bezprozvanny, I., Zhong, P. Y., Scheller, R. H. and Tsien, R. W. (2000). Molecular determinants of the functional interaction between syntaxin and N-type Ca2+ channel gating. *Proceedings of the National Academy of Sciences of the United States of America* **97**, 13943-13948.

Billups, B. and Forsythe, I. D. (2002). Presynaptic mitochondrial calcium sequestration influences transmission at mammalian central Synapses. *Journal of Neuroscience* **22**, 5840-5847.

Birch, K. A., Pober, J. S., Zavoico, G. B., Means, A. R. and Ewenstein, B. M. (1992). Calcium Calmodulin Transduces Thrombin-Stimulated Secretion - Studies in Intact and Minimally Permeabilized Human Umbilical Vein Endothelial-Cells. *Journal of Cell Biology* **118**, 1501-1510.

Blasi, J., Chapman, E. R., Yamasaki, S., Binz, T., Niemann, H. and Jahn, R. (1993). Botulinum Neurotoxin-C1 Blocks Neurotransmitter Release by Means of Cleaving Hpc-1/Syntaxin. *Embo Journal* **12**, 4821-4828.

Blatz, A. L. and Magleby, K. L. (1987). Calcium-Activated Potassium Channels. *Trends in Neurosciences* **10**, 463-467.

Bourinet, E., Soong, T. W., Sutton, K., Slaymaker, S., Mathews, E., Monteil, A., Zamponi, G. W., Nargeot, J. and Snutch, T. P. (1999). Splicing of alpha(1A) subunit gene generates phenotypic variants of P- and Q-type calcium channels. *Nature Neuroscience* **2**, 407-415.

Bracher, A., Kadlec, J., Betz, H. and Weissenhorn, W. (2002). X-ray structure of a neuronal complexin-SNARE complex from squid. *Journal of Biological Chemistry* **277**, 26517-26523.

Brailoiu, E., Miyamoto, M. D. and Dun, N. J. (2002). Calmodulin increases transmitter release by mobilizing quanta at the frog motor nerve terminal. *British Journal of Pharmacology* **137**, 719-727.

Brehm, P. and Erkert, R. (1978). Calcium entry leads to inactivation of calcium channels in Paramecium. *Science* **202**, 1203-1206.

Broadie, K., Prokop, A., Bellen, H. J., Okane, C. J., Schulze, K. L. and Sweeney, S. T. (1995). Syntaxin and Synaptobrevin Function Downstream of Vesicle Docking in Drosophila. *Neuron* **15**, 663-673.

Brose, N., Rosenmund, C. and Rettig, J. (2000). Regulation of transmitter release by Unc-13 and its homologues. *Current Opinion in Neurobiology* **10**, 303-11.

Brosenitsch, T. A. and Katz, D. M. (2001). Physiological patterns of electrical stimulation can induce neuronal gene expression by activating N-type calcium channels. *Journal of Neuroscience* **21**, 2571-2579.

Brunger, A. T. (2000). Structural insights into the molecular mechanism of Ca(2+)-dependent exocytosis. *Current Opinion in Neurobiology* **10**, 293-302.

Budde, T., Meuth, S. and Pape, H. C. (2002). Calcium-dependent inactivation of neuronal calcium channels. *Nature Reviews Neuroscience* **3**, 873-883.

Burgess, D. L. and Noebels, J. L. (1999). Voltage-dependent calcium channel mutations in neurological disease. In *Molecular and Functional Diversity of Ion Channels and Receptors*, vol. 868, pp. 199-212.

Burgoyne, R. D. and Clague, M. J. (2003). Calcium and calmodulin in membrane fusion. *Biochimica Et Biophysica Acta-Molecular Cell Research* **1641**, 137-143.

Burgoyne, R. D. and Geisow, M. J. (1982). Evidence for the Involvement of Calmodulin in Secretion by the Chromaffin Cell of the Adrenal-Medulla. *Biology of the Cell* **45**, 281-281.

Burgoyne, R. D., O'Callaghan, D. W., Hasdemir, B., Haynes, L. P. and Tepikin, A. V. (2004). Neuronal Ca2(+)-sensor proteins: multitalented regulators of neuronal function. *Trends in Neurosciences* **27**, 203-209.

Burgoyne, R. D. and Weiss, J. L. (2001). The neuronal calcium sensor family of Ca2+-binding proteins. *Biochemical Journal* **353**, 1-12.

Burley, J. R. and Sihra, T. S. (2000). A modulatory role for protein phosphatase 2B (calcineurin) in the regulation of Ca2+ entry. *European Journal of Neuroscience* **12**, 2881-2891.

Busath, D. D. (1993). The Use of Physical Methods in Determining Gramicidin Channel Structure and Function. *Annual Review of Physiology* **55**, 473-501.

Cahill, A. L., Hurley, J. H. and Fox, A. P. (2000). Coexpression of cloned alpha(1B), beta(2a), and alpha(2)/delta subunits produces non-inactivating calcium currents similar to those found in bovine chromaffin cells. *Journal of Neuroscience* **20**, 1685-1693.

Calakos, N. and Scheller, R. H. (1996). Synaptic vesicle biogenesis, docking, and fusion: A molecular description. *Physiological Reviews* **76**, 1-29.

Canti, C., Davies, A., Berrow, N. S., Butcher, A. J., Page, K. M. and Dolphin, A. C. (2001). Evidence for two concentration-dependent processes for beta- subunit effects on alpha 1B calcium channels. *Biophysical Journal* **81**, 1439-1451.

Canti, C., Page, K. M., Stephens, G. J. and Dolphin, A. C. (1999). Identification of residues in the N terminus of alpha 1B critical for inhibition of the voltage-dependent calcium channel by G beta gamma. *Journal of Neuroscience* **19**, 6855-6864.

Carabelli, V., Carra, I. and Carbone, E. (1998). Localized secretion of ATP and opioids revealed through single Ca2+ channel modulation in bovine chromaffin cells. *Neuron* **20**, 1255-1268.

Catterall, W. A. (1993). Structure and Function of Voltage-Gated Ion Channels. *Trends in Neurosciences* **16**, 500-506.

Catterall, W. A. (1998). Structure and function of neuronal Ca2+ channels and their role in neurotransmitter release. *Cell Calcium* **24**, 307-323.

Catterall, W. A. (1999). Interactions of presynaptic Ca2+ channels and snare proteins in neurotransmitter release. In *Molecular and Functional Diversity of Ion Channels and Receptors*, vol. 868, pp. 144-159.

Catterall, W. A. (2000). Structure and regulation of voltage-gated Ca2+ channels. *Annual Review of Cell and Developmental Biology* **16**, 521-555.

Cens, T., Restituito, S., Galas, S. and Charnet, P. (1999). Voltage and calcium use the same molecular determinants to inactivate calcium channels. *Journal of Biological Chemistry* **274**, 5483-5490.

Chamberlain, L. H., Burgoyne, R. D. and Gould, G. W. (2001). SNARE proteins are highly enriched in lipid rafts in PC12 cells: Implications for the spatial control of

exocytosis. *Proceedings of the National Academy of Sciences of the United States of America* **98**, 5619-5624.

Chamberlain, L. H., Roth, D., Morgan, A. and Burgoyne, R. D. (1995). Distinct Effects of Alpha-Snap, 14-3-3-Proteins, and Calmodulin on Priming and Triggering of Regulated Exocytosis. *Journal of Cell Biology* **130**, 1063-1070.

Chan, S. A. and Smith, C. (2001). Physiological stimuli evoke two forms of endocytosis in bovine chromaffin cells. *Journal of Physiology-London* **537**, 871-885.

Chan, S. A. and Smith, C. (2003). Low frequency stimulation of mouse adrenal slices reveals a clathrin-independent, protein kinase C-mediated endocytic mechanism. *Journal of Physiology-London* **553**, 707-717.

Chapman, E. R. (2002). Synaptotagmin: A Ca2+ sensor that triggers exocytosis? *Nature Reviews Molecular Cell Biology* **3**, 498-508.

Chaudhuri, D., Chang, S. Y., DeMaria, C. D., Alvania, R. S., Soong, T. W. and Yue, D. T. (2004). Alternative splicing as a molecular switch for Ca2+/calmodulin-dependent facilitation of P/Q-type Ca2+ channels. *Journal of Neuroscience* **24**, 6334-6342.

Chen, L., Bao, S. W., Qiao, X. X. and Thompson, R. F. (1999). Impaired cerebellar synapse maturation in waggler, a mutant mouse with a disrupted neuronal calcium channel gamma subunit. *Proceedings of the National Academy of Sciences of the United States of America* **96**, 12132-12137.

Chen, X. C., Tomchick, D. R., Kovrigin, E., Arac, D., Machius, M., Sudhof, T. C. and Rizo, J. (2002). Three-dimensional structure of the complexin/SNARE complex. *Neuron* **33**, 397-409.

Chen, Y., Deng, L. B., Maeno-Hikichi, Y., Lai, M. Z., Chang, S. H., Chen, G. and Zhang, J. F. (2003). Formation of an endophilin-Ca2+ channel complex is critical for clathrin-mediated synaptic vesicle endocytosis. *Cell* **115**, 37-48.

Chen, Y. A., Duvvuri, V., Schulman, H. and Scheller, R. H. (1999). Calmodulin and protein kinase C increase Ca2+-stimulated secretion by modulating membrane-attached exocytic machinery. *Journal of Biological Chemistry* **274**, 26469-26476.

291

Chen, Y. A., Scales, S. J., Duvvuri, V., Murthy, M., Patel, S. M., Schulman, H. and Scheller, R. H. (2001a). Calcium regulation of exocytosis in PC12 cells. *Journal of Biological Chemistry* **276**, 26680-26687.

Chen, Y. A., Scales, S. J. and Scheller, R. H. (2001b). Sequential SNARE assembly underlies priming and triggering of exocytosis. *Neuron* **30**, 161-170.

Chin, D. and Means, A. R. (2000). Calmodulin: a prototypical calcium sensor. *Trends in Cell Biology* **10**, 322-328.

Chow, R. (1995). Electrochemical detection of secretion from single cells: Plenum press.

Chow, R. H., Vonruden, L. and Neher, E. (1992). Delay in Vesicle Fusion Revealed by Electrochemical Monitoring of Single Secretory Events in Adrenal Chromaffin Cells. *Nature* **356**, 60-63.

Clapham, D. E. (2003). TRP channels as cellular sensors. *Nature* **426**, 517-524.

Clapham, D. E., Runnels, L. W. and Strubing, C. (2001). The TRP ion channel family. *Nature Reviews Neuroscience* **2**, 387-396.

Cloues, R. K., Cibulsky, S. M. and Sather, W. A. (2000). Ion interactions in the high-affinity binding locus of a voltage-gated Ca2+ channel. *Journal of General Physiology* **116**, 569-586.

Cochilla, A. J., Angleson, J. K. and Betz, W. J. (1999). Monitoring secretory membrane with FM1-43 fluorescence. *Annual Review of Neuroscience* **22**, 1-10.

Colecraft, H. M., Patil, P. G. and Yue, D. T. (2000). Differential occurrence of reluctant openings in G-protein- inhibited N- and P/Q-type calcium channels. *Journal of General Physiology* **115**, 175-192.

Cooper, C. B., Arnot, M. I., Feng, Z. P., Jarvis, S. E., Hamid, J. and Zamponi, G. W. (2000). Cross-talk between G-protein and protein kinase C modulation of N-type calcium channels is dependent on the G-protein beta subunit isoform. *Journal of Biological Chemistry* **275**, 40777-40781.

Coppola, T., Perret-Menoud, V., Luthi, S., Farnsworth, C. C., Glomset, J. A. and Regazzi, R. (1999). Disruption of Rab3-calmodulin interaction, but not other effector interactions, prevents Rab3 inhibition of exocytosis. *Embo Journal* **18**, 5885-5891.

Costa, M. C. R., Mani, F., Santoro, W., Espreafico, E. M. and Larson, R. E. (1999). Brain myosin-V, a calmodulin-carrying myosin, binds to calmodulin-dependent protein kinase II and activates its kinase activity. *Journal of Biological Chemistry* **274**, 15811-15819.

Cousin, M. A. (2000). Synaptic vesicle endocytosis - Calcium works overtime in the nerve terminal. *Molecular Neurobiology* **22**, 115-128.

Cousin, M. A. and Nicholls, D. G. (1997). Synaptic vesicle recycling in cultured cerebellar granule cells: role of vesicular acidification and refilling. *Journal of Neurochemistry* **69**, 1927-35.

Cousin, M. A. and Robinson, P. J. (2001). The dephosphins: dephosphorylation by calcineurin triggers synaptic vesicle endocytosis. *Trends in Neurosciences* **24**, 659-665.

Cox, D. H. and Dunlap, K. (1994). Inactivation of N-Type Calcium Current in Chick Sensory Neurons - Calcium and Voltage-Dependence. *Journal of General Physiology* **104**, 311-336.

Cruz, L. J. and Olivera, B. M. (1986). Calcium-Channel Antagonists - Omega-Conotoxin Defines a New High-Affinity Site. *Journal of Biological Chemistry* **261**, 6230-6233.

Currie, K. P. and Fox, A. P. (2000). Voltage-dependent, pertussis toxin insensitive inhibition of calcium currents by histamine in bovine adrenal chromaffin cells. *Journal of Neurophysiology* **83**, 1435-42.

Currie, K. P. M. and Fox, A. P. (1996). ATP serves as a negative feedback inhibitor of voltage-gated Ca2+ channel currents in cultured bovine adrenal chromaffin cells. *Neuron* **16**, 1027-1036.

Currie, K. P. M. and Fox, A. P. (1997). Comparison of N- and P/Q-type voltage-gated calcium channel current inhibition. *Journal of Neuroscience* **17**, 4570-4579.

Currie, K. P. M. and Fox, A. P. (2002). Differential facilitation of N- and P/Q-type calcium channels during trains of action potential-like waveforms. *Journal of Physiology-London* **539**, 419-431.

Currie, K. P. M., Wootton, J. F. and Scott, R. H. (1995). Activation of Ca2+-Dependent Cl- Currents in Cultured Rat Sensory Neurons by Flash-Photolysis of Dm-Nitrophen. *Journal of Physiology-London* **482**, 291-307.

Cuttle, M. F., Tsujimoto, T., Forsythe, I. D. and Takahashi, T. (1998). Facilitation of the presynaptic calcium current at an auditory synapse in rat brainstem. *Journal of Physiology 1998 Nov 1;512 (Pt 3):723-9.*

Davila, H. M. (1999). Molecular and functional diversity of voltage-gated calcium channels. In *Molecular and Functional Diversity of Ion Channels and Receptors*, vol. 868, pp. 102-117.

de Haro, L., Ferracci, G., Opi, S., Iborra, C., Quetglas, S., Miquelis, R., Leveque, C. and Seagar, M. (2004). Ca2+/calmodulin transfers the membrane-proximal lipid-binding domain of the v-SNARE synaptobrevin from cis to trans bilayers. *Proceedings of the National Academy of Sciences of the United States of America* **101**, 1578-1583.

de Vries, K. J., Geijtenbeek, A., Brian, E. C., de Graan, P. N. E., Ghijsen, W. and Verhage, M. (2000). Dynamics of munc18-1 phosphorylation/dephosphorylation in rat brain nerve terminals. *European Journal of Neuroscience* **12**, 385-390.

Degtiar, V. E., Scheller, R. H. and Tsien, R. W. (2000). Syntaxin modulation of slow inactivation of N-type calcium channels. *Journal of Neuroscience* **20**, 4355-67.

Deisseroth, K., Mermelstein, P. G., Xia, H. H. and Tsien, R. W. (2003). Signaling from synapse to nucleus: the logic behind the mechanisms. *Current Opinion in Neurobiology* **13**, 354-365.

DeMaria, C. D., Soong, T. W., Alseikhan, B. A., Alvania, R. S. and Yue, D. T. (2001). Calmodulin bifurcates the local Ca2+ signal that modulates P/Q- type Ca2+ channels. *Nature* **411**, 484-489.

DeWaard, M., Liu, H. Y., Walker, D., Scott, V. E. S., Gurnett, C. A. and Campbell, K. P. (1997). Direct binding of G-protein beta gamma complex to voltage- dependent calcium channels. *Nature* **385**, 446-450.

Dodge, F. A. J. and Rahamimoff, R. (1967). Co-operative action of calcium ions in transmitter release at the neuromuscular junction. *Journal of Physiology-London* **193**, 419-432.

Doering, C. J. and Zamponi, G. W. (2003). Molecular pharmacology of high voltage-activated calcium channels. *Journal of Bioenergetics and Biomembranes* **35**, 491-505.

Dolmetsch, R. E., Pajvani, U., Fife, K., Spotts, J. M. and Greenberg, M. E. (2001). Signaling to the nucleus by an L-type calcium channel - Calmodulin complex through the MAP kinase pathway. *Science* **294**, 333-339.

Dolphin, A. C. (2003a). beta subunits of voltage-gated calcium channels. *Journal of Bioenergetics and Biomembranes* **35**, 599-620.

Dolphin, A. C. (2003b). G protein modulation of voltage-gated calcium channels. *Pharmacological Reviews* **55**, 607-627.

Dolphin, A. C., Page, K. M., Berrow, N. S., Stephens, G. J. and Canti, C. (1999). Dissection of the calcium channel domains responsible for modulation of neuronal voltage-dependent calcium channels by G proteins. In *Molecular and Functional Diversity of Ion Channels and Receptors*, vol. 868, pp. 160-174.

Dolphin, A. C., Scott, R. H., Trentham, D. R. and Wootton, J. F. (1987). Photoactivation of a Gtp Analog Differentially Inhibits the Transient Component of the Calcium-Channel Current in Rat Sensory Neurons. *Journal of Physiology-London* **390**, P89-P89.

Dolphin, A. C., Wootton, J. F., Scott, R. H. and Trentham, D. R. (1988). Photoactivation of Intracellular Guanosine Triphosphate Analogs Reduces the Amplitude and Slows the Kinetics of Voltage- Activated Calcium-Channel Currents in Sensory Neurons. *Pflugers Archiv-European Journal of Physiology* **411**, 628-636.

Doroshenko, P., Penner, R. and Neher, E. (1991). Novel Chloride Conductance in the Membrane of Bovine Chromaffin Cells Activated By Intracellular Gtp-Gamma-S. *Journal of Physiology-London* **436**, 711-724.

Douglas, W. W. and Poisner, A. M. (1967). On the relation between ATP splitting and secretion in the adrenal chromaffin cell: extrusion of ATP (unhydrolysed) during release of catecholamines. *Journal of Physiology-London* **183**, 249-256.

Doussau, F. and Augustine, G. J. (2000). The actin cytoskeleton and neurotransmitter release: an overview. *Biochimie* **82**, 353-63.

Duan, K., Yu, X., Zhang, C. and Zhou, Z. (2003). Control of secretion by temporal patterns of action potentials in adrenal chromaffin cells. *The Journal of Neuroscience* **23**, 11235-11243.

Dulubova, I., Sugita, S., Hill, S., Hosaka, M., Fernandez, I., Sudhof, T. C. and Rizo, J. (1999). A conformational switch in syntaxin during exocytosis: role of munc18. *Embo Journal* **18**, 4372-4382.

Duncan, R. R., Don-Wauchope, A. C., Tapechum, S., Shipston, M. J., Chow, R. H. and Estibeiro, P. (1999). High-efficiency Semliki Forest virus-mediated transduction in bovine adrenal chromaffin cells. *Biochemical Journal* **342**, 497-501.

Duncan, R. R., Greaves, J., Wiegand, U. K., Matskovich, I., Bodammer, G., Apps, D. K., Shipston, M. J. and Chow, R. H. (2003). Functional and spatial segregation of secretory vesicle pools according to vesicle age. *Nature* **422**, 176-180.

Duncan, R. R., Shipston, M. J. and Chow, R. H. (2000). Double C2 protein. A review. *Biochimie* **82**, 421-6.

Dzhura, I., Wu, Y. J., Colbran, R. J., Balser, J. R. and Anderson, M. E. (2000). Calmodulin kinase determines calcium-dependent facilitation of L-type calcium channels. *Nature Cell Biology* **2**, 173-177.

Earles, C. A., Bai, J. H., Wang, P. and Chapman, E. R. (2001). The tandem C2 domains of synaptotagmin contain redundant Ca2+ binding sites that cooperate to engage t-SNAREs and trigger exocytosis. *Journal of Cell Biology* **154**, 1117-1123.

Eckert, R. and Chad, J. E. (1984). Inactivation of Ca Channels. *Progress in Biophysics & Molecular Biology* **44**, 215-267.

Eller, P., Berjukov, S., Wanner, S., Huber, I., Hering, S., Knaus, H. G., Toth, G., Kimball, S. D. and Striessnig, J. (2000). High affinity interaction of mibefradil with voltage-gated calcium and sodium channels. *British Journal of Pharmacology* **130**, 669-677.

Ellinor, P. T., Zhang, J. F., Horne, W. A. and Tsien, R. W. (1994). Structural Determinants of the Blockade of N-Type Calcium Channels by a Peptide Neurotoxin. *Nature* **372**, 272-275.

Ellis, M. V., James, S. R., Perisic, O., Downes, C. P., Williams, R. L. and Katan, M. (1998). Catalytic domain of phosphoinositide-specific phospholipase C (PLC) - Mutational analysis of residues within the active site and hydrophobic ridge of PLC delta 1. *Journal of Biological Chemistry* **273**, 11650-11659.

Engisch, K. L., Chernevskaya, N. I. and Nowycky, M. C. (1997). Short-term changes in the Ca2+-exocytosis relationship during repetitive pulse protocols in bovine adrenal chromaffin cells. *Journal of Neuroscience* **17**, 9010-9025.

Engisch, K. L. and Nowycky, M. C. (1996). Calcium dependence of large dense-cored vesicle exocytosis evoked by calcium influx in bovine adrenal chromaffin cells. *Journal of Neuroscience* **16**, 1359-1369.

Engisch, K. L. and Nowycky, M. C. (1998). Compensatory and excess retrieval: two types of endocytosis following single step depolarizations in bovine adrenal chromaffin cells. *Journal of Physiology-London* **506**, 591-608.

Erickson, M. G., Liang, H. Y., Mori, M. X. and Yue, D. T. (2003). FRET two-hybrid mapping reveals function and location of L-type Ca2+ channel CaM preassociation. *Neuron* **39**, 97-107.

Evans, G. J. O., Wilkinson, M. C., Graham, M. E., Turner, K. M., Chamberlain, L. H., Burgoyne, R. D. and Morgan, A. (2001). Phosphorylation of cysteine string protein by protein kinase A. Implications for the modulation of exocytosis. *Journal of Biological Chemistry* **276**, 47877-47885.

Evans, M. G. and Marty, A. (1986). Calcium-dependent chloride currents in isolated cells from rat lacrimal glands. *The Journal of Physiology* **378**, 437-460.

Fasshauer, D., Sutton, R. B., Brunger, A. T. and Jahn, R. (1998). Conserved structural features of the synaptic fusion complex: SNARE proteins reclassified as Q- and R-SNAREs. *Proceedings of the National Academy of Sciences of the United States of America* **95**, 15781-15786.

Feng, Z. P., Hamid, J., Doering, C., Bosey, G. M., Snutch, T. P. and Zamponi, G. W. (2001). Residue Gly(1326) of the N-type calcium channel alpha(1B) subunit controls reversibility of omega-conotoxin GVIA and MVIIA block. *Journal of Biological Chemistry* **276**, 15728-15735.

297

Fenwick, E. M., Marty, A. and Neher, E. (1982a). A Patch-Clamp Study of Bovine Chromaffin Cells and of Their Sensitivity to Acetylcholine. *Journal of Physiology-London* **331**, 577-597.

Fenwick, E. M., Marty, A. and Neher, E. (1982b). Sodium and Calcium Channels in Bovine Chromaffin Cells. *Journal of Physiology-London* **331**, 599-635.

Fernandez, J. M., Bezanilla, F. and Taylor, R. E. (1982). Effect of Chloroform on Charge Movement in the Nerve Membrane. *Nature* **297**, 150-152.

Fernandez-Chacon, R., Konigstorfer, A., Gerber, S. H., Garcia, J., Matos, M. F., Stevens, C. F., Brose, N., Rizo, J., Rosenmund, C. and Sudhof, T. C. (2001). Synaptotagmin I functions as a calcium regulator of release probability. *Nature* **410**, 41-49.

Filder, N. and Fernandez, J. (1989). Phase tracking: an improved phase detection technique for cell membrane capacitance measurements. *Biophysical Journal* **56**, 1153-1162.

Fili, O., Michaelevski, I., Bledi, Y., Chikvashvili, D., Singer-Lahat, D., Boshwitz, H., Linial, M. and Lotan, I. (2001). Direct interaction of a brain voltage-gated K+ channel with syntaxin 1A: Functional impact on channel gating. *Journal of Neuroscience* **21**, 1964-1974.

Fill, M. and Copello, J. A. (2002). Ryanodine receptor calcium release channels. *Physiological Reviews* **82**, 893-922.

Findlay, I. (2004). Physiological modulation of inactivation in L-type Ca2+ channels: one switch. *Journal of Physiology-London* **554**, 275-283.

Firestone, J. A. and Browning, M. D. (1992). Synapsin-Ii Phosphorylation and Catecholamine Release in Bovine Adrenal Chromaffin Cells - Additive Effects of Histamine and Nicotine. *Journal of Neurochemistry* **58**, 441-447.

Fisher, R. J., Pevsner, J. and Burgoyne, R. D. (2001). Control of fusion pore dynamics during exocytosis by Munc18. *Science* **291**, 875-878.

Fletcher, A. I., Shuang, R., Giovannucci, D. R., Zhang, L., Bittner, M. A. and Stuenkel, E. L. (1999). Regulation of exocytosis by cyclin-dependent kinase 5 via phosphorylation of Munc18. *Journal of Biological Chemistry* **274**, 4027-35.

Forsythe, I. D., Tsujimoto, T., Barnes-Davies, M., Cuttle, M. F. and Takahashi, T. (1998). Inactivation of presynaptic calcium current contributes to synaptic depression at a fast central synapse. *Neuron 1998 Apr;20(4):797-807.*

Fournier, S. and Trifaro, J. M. (1988). Calmodulin-Binding Proteins in Chromaffin Cell Plasma-Membranes. *Journal of Neurochemistry* **51**, 1599-1609.

Fox, A. P., Nowycky, M. C. and Tsien, R. W. (1987). Kinetic and Pharmacological Properties Distinguishing 3 Types of Calcium Currents in Chick Sensory Neurons. *Journal of Physiology-London* **394**, 149-172.

Frings, S., Reuter, D. and Kleene, S. J. (2000). Neuronal Ca2+-activated Cl-channels - homing in on an elusive channel species. *Progress in Neurobiology* **60**, 247-289.

Fujita, Y., Sasaki, T., Fukui, K., Kotani, H., Kimura, T., Hata, Y., Sudhof, T. C., Scheller, R. H. and Takai, Y. (1996). Phosphorylation of Munc-18/n-Sec1/rbSec1 by protein kinase C - Its implication in regulating the interaction of Munc-18/n-Sec1/rbSec1 with syntaxin. *Journal of Biological Chemistry* **271**, 7265-7268.

Fujita, Y., Shirataki, H., Sakisaka, T., Asakura, T., Ohya, T., Kotani, H., Yokoyama, S., Nishioka, H., Matsuura, Y., Mizoguchi, A. et al. (1998). Tomosyn: a syntaxin-1-binding protein that forms a novel complex in the neurotransmitter release process. *Neuron* **20**, 905-915.

Furukawa, T., Miura, R., Mori, Y., Strobeck, M., Suzuki, K., Ogihara, Y., Asano, T., Morishita, R., Hashii, M., Higashida, H. et al. (1998a). Differential interactions of the C terminus and the cytoplasmic I-II loop of neuronal Ca2+ channels with G-protein alpha and beta gamma subunits - II. Evidence for direct binding. *Journal of Biological Chemistry* **273**, 17595-17603.

Furukawa, T., Nukada, T., Mori, Y., Wakamori, M., Fujita, Y., Ishida, H., Fukuda, K., Kato, S. and Yoshii, M. (1998b). Differential interactions of the C terminus and the cytoplasmic I-II loop of neuronal Ca2+ channels with G-protein alpha and beta gamma subunits - I. Molecular determination. *Journal of Biological Chemistry* **273**, 17585-17594.

Gandhi, S. P. and Stevens, C. F. (2003). Three modes of synaptic vesicular recycling revealed by single- vesicle imaging. *Nature* **423**, 607-613.

299

Gandia, L., Mayorgas, I., Michelena, P., Cuchillo, I., de Pascual, R., Abad, F., Novalbos, J. M., Larranaga, E. and Garcia, A. G. (1998). Human adrenal chromaffin cell calcium channels: drastic current facilitation in cell clusters, but not in isolated cells. *Pflugers Archiv-European Journal of Physiology* **436**, 696-704.

Ganguly, A., Chiou, S., Fineberg, N. S. and Davis, J. S. (1992). Greater Importance of Ca-2+-Calmodulin in Maintenance of Ang Ii-and K+- Mediated Aldosterone Secretion - Lesser Role of Protein-Kinase-C. *Biochemical and Biophysical Research Communications* **182**, 254-261.

Garner, C. C., Kindler, S. and Gundelfinger, E. D. (2000). Molecular determinants of presynaptic active zones. *Current Opinion in Neurobiology* **10**, 321-7.

Geppert, M., Goda, Y., Hammer, R. E., Li, C., Rosahl, T. W., Stevens, C. F. and Sudhof, T. C. (1994). Synaptotagmin-I - a Major Ca2+ Sensor for Transmitter Release at a Central Synapse. *Cell* **79**, 717-727.

Gera, S. and Byerly, L. (1999). Measurement of calcium channel inactivation is dependent upon the test pulse potential. *Biophysical Journal* **76**, 3076-3088.

Gerst, J. E. (1999). SNAREs and SNARE regulators in membrane fusion and exocytosis. *Cellular & Molecular Life Sciences* **55**, 707-34.

Gillis, K. (1995). Techniques for membrane capacitance. In *Single channel recording*, vol. chapter 7 (ed. B. a. N. E. Sakmann), pp. 155-198.

Gillis, K. D., Mossner, R. and Neher, E. (1996). Protein kinase C enhances exocytosis from chromaffin cells by increasing the size of the readily releasable pool of secretory granules. *Neuron* **16**, 1209-1220.

Goda, Y. and Stevens, C. F. (1994). 2 Components of Transmitter Release at a Central Synapse. *Proceedings of the National Academy of Sciences of the United States of America* **91**, 12942-12946.

Graff, J. M., Young, T. N., Johnson, J. D. and Blackshear, P. J. (1989). Phosphorylation-Regulated Calmodulin Binding to a Prominent Cellular Substrate for Protein Kinase-C. *Journal of Biological Chemistry* **264**, 21818-21823.

Graham, M. E., Fisher, R. J. and Burgoyne, R. D. (2000). Measurement of exocytosis by amperometry in adrenal chromaffin cells: effects of clostridial

neurotoxins and activation of protein kinase C on fusion pore kinetics. *Biochimie* **82**, 469-79.

Graham, M. E., O'Callaghan, D. W., McMahon, H. T. and Burgoyne, R. D. (2002). Dynamin-dependent and dynamin-independent processes contribute to the regulation of single vesicle release kinetics and quantal size. *Proceedings of the National Academy of Sciences of the United States of America* **99**, 7124-7129.

Gromada, J., Hoy, M., Buschard, K., Salehi, A. and Rorsman, P. (2001). Somatostatin inhibits exocytosis in rat pancreatic alpha-cells by G(i2)-dependent activation of calcineurin and depriming of secretory granules. *Journal of Physiology-London* **535**, 519-532.

Gundelfinger, E. D., Kessels, M. M. and Qualmann, B. (2003). Temporal and spatial coordination of exocytosis and endocytosis. *Nature Reviews Molecular Cell Biology* **4**, 127-139.

Haeseleer, F., Sokal, I., Verlinde, C., Erdjument-Bromage, H., Tempst, P., Pronin, A. N., Benovic, J. L., Fariss, R. N. and Palczewski, K. (2000). Five members of a novel Ca2+-binding protein (CABP) subfamily with similarity to calmodulin. *Journal of Biological Chemistry* **275**, 1247-1260.

Halliwell, J. V., Plant, T. D. and Standen, N. B. (1994). Voltage clamp techniques. In *Microelectrode techniques*, (ed. D. Ogden). Cambridge: The Company of Biologists.

Han, X., Wang, C. T., Bai, J. H., Chapman, E. R. and Jackson, M. B. (2004). Transmembrane segments of syntaxin line the fusion pore of Ca2+-triggered exocytosis. *Science* **304**, 289-292.

Handrock, R., Rao-Schymanski, R., Klugbauer, N., Hofmann, F. and Herzig, S. (1999). Dihydropyridine enantiomers block recombinant L-type Ca2+ channels by two different mechanisms. *Journal of Physiology-London* **521**, 31-42.

Harrison, S. D., Broadie, K., Vandegoor, J. and Rubin, G. M. (1994). Mutations in the Drosophila Rop Gene Suggest a Function in General Secretion and Synaptic Transmission. *Neuron* **13**, 555-566.

Haynes, L. P., Morgan, A. and Burgoyne, R. D. (1999). nSec-1 (munc-18) interacts with both primed and unprimed syntaxin 1A and associates in a dimeric complex on adrenal chromaffin granules. *Biochemical Journal* **342**, 707-714.

Haynes, L. P., Tepikin, A. V. and Burgoyne, R. D. (2004). Calcium-binding protein 1 is an inhibitor of agonist-evoked, inositol 1,4,5-trisphosphate-mediated calcium signaling. *Journal of Biological Chemistry* **279**, 547-555.

Heinemann, C., Chow, R. H., Neher, E. and Zucker, R. S. (1994). Kinetics of the Secretory Response in Bovine Chromaffin Cells Following Flash-Photolysis of Caged Ca2+. *Biophysical Journal* **67**, 2546-2557.

Hering, S. (2002). beta-subunits: fine tuning of Ca2+ channel block. *Trends in Pharmacological Sciences* **23**, 509-513.

Hering, S., Berjukow, S., Sokolov, S., Marksteiner, R., Weiss, R. G., Kraus, R. and Timin, E. N. (2000). Molecular determinants of inactivation in voltage-gated Ca2+ channels. *Journal of Physiology-London* **528**, 237-249.

Herlitze, S., Garcia, D. E., Mackie, K., Hille, B., Scheuer, T. and Catterall, W. A. (1996). Modulation of Ca2+ channels by G-protein beta gamma subunits (vol 380, pg 258, 1996). *Nature* **381**, 172-172.

Herlitze, S., Hockerman, G. H., Scheuer, T. and Catterall, W. A. (1997). Molecular determinants of inactivation and G protein modulation in the intracellular loop connecting domains I and II of the calcium channel alpha(1A) subunit. *Proceedings of the National Academy of Sciences of the United States of America* **94**, 1512-1516.

Hernandez-Guijo, J. M., Maneu-Flores, V. E., Ruiz-Nuno, A., Villarroya, M., Garcia, A. G. and Gandia, L. (2001). Calcium-dependent inhibition of L,N, and P/Q Ca2+ channels in chromaffin cells: Role of mitochondria. *Journal of Neuroscience* **21**, 2553-2560.

Heuser, J. E. and Anderson, R. G. W. (1989). Hypertonic Media Inhibit Receptor-Mediated Endocytosis by Blocking Clathrin-Coated Pit Formation. *Journal of Cell Biology* **108**, 389-400.

Hilfiker, S. (2003). Neuronal calcium sensor-1: a multifunctional regulator of secretion. *Biochemical Society Transactions* **31**, 828-832.

302

Hilfiker, S., Pieribone, V. A., Czernik, A. J., Kao, H. T., Augustine, G. J. and Greengard, P. (1999a). Synapsins as regulators of neurotransmitter release. *Philosophical Transactions of the Royal Society of London - Series B: Biological Sciences* **354**, 269-79.

Hilfiker, S., Pieribone, V. A., Nordstedt, C., Greengard, P. and Czernik, A. J. (1999b). Regulation of synaptotagmin I phosphorylation by multiple protein kinases. *Journal of Neurochemistry* **73**, 921-932.

Hille, B. (1992). Calcium channels: Sinauer Associates Inc.

Hoeflich, K. P. and Ikura, M. (2002). Calmodulin in action: Diversity in target recognition and activation mechanisms. *Cell* **108**, 739-742.

Holz, G. G., Rane, S. G. and Dunlap, K. (1986). Gtp-Binding Proteins Mediate Transmitter Inhibition of Voltage- Dependent Calcium Channels. *Nature* **319**, 670-672.

Horn, R. and Marty, A. (1988). Muscarinic Activation of Ionic Currents Measured by a New Whole-Cell Recording Method. *Journal of General Physiology* **92**, 145-159.

Horrigan, F. T. and Bookman, R. J. (1994). Releasable Pools and the Kinetics of Exocytosis in Adrenal Chromaffin Cells. *Neuron* **13**, 1119-1129.

Hosaka, M. and Sudhof, T. C. (1998a). Synapsin III, a novel synapsin with an unusual regulation by Ca2+. *Journal of Biological Chemistry* **273**, 13371-13374.

Hosaka, M. and Sudhof, T. C. (1998b). Synapsins I and II are ATP-binding proteins with differential Ca2+ regulation. *Journal of Biological Chemistry* **273**, 1425-1429.

Hu, K., Carroll, J., Fedorovich, S., Rickman, C., Sukhodub, A. and Davletov, B. (2002). Vesicular restriction of synaptobrevin suggests a role for calcium in membrane fusion. *Nature* **415**, 646-650.

Hurley, J. F., Cahill, A. L., Currie, K. P. M. and Fox, A. P. (2000). The role of dynamic palmitoylation in Ca2+ channel inactivation. *Proceedings of the National Academy of Sciences of the United States of America* **97**, 9293-9298.

Ikeda, S. R. (1996). Voltage-dependent modulation of N-type calcium channels by G- protein beta gamma subunits. *Nature* **380**, 255-258.

Jahn, R. (2000). Sec1/Munc18 proteins: mediators of membrane fusion moving to center stage. *Neuron* **27**, 201-4.

Jahn, R., Lang, T. and Sudhof, T. C. (2003). Membrane fusion. *Cell* **112**, 519-533.

Jahn, R. and Sudhof, T. C. (1999). Membrane fusion and exocytosis. *Annual Review of Biochemistry* **68**, 863-911.

Jarvis, S. E., Magga, J. M., Beedle, A. M., Braun, J. E. A. and Zamponi, G. W. (2000). G protein modulation of N-type calcium channels is facilitated by physical interactions between syntaxin 1A and G beta gamma. *Journal of Biological Chemistry* **275**, 6388-6394.

Jarvis, S. E. and Zamponi, G. W. (2001). Distinct molecular determinants govern syntaxin 1A-mediated inactivation and G-protein inhibition of N-type calcium channels. *Journal of Neuroscience* **21**, 2939-2948.

Jones, L. P., DeMaria, C. D. and Yue, D. T. (1999). N-type calcium channel inactivation probed by gating-current analysis. *Biophysical Journal* **76**, 2530-2552.

Jones, S. W. (1999). Inactivation of N-type Ca2+ channels: Ca2+ vs. voltage. *Journal of Physiology-London* **518**, 630-630.

Jones, S. W. (2003). Calcium channels: Unanswered questions. *Journal of Bioenergetics and Biomembranes* **35**, 461-475.

Jorgensen, E. M., Hartwieg, E., Schuske, K., Nonet, M. L., Jin, Y. S. and Horvitz, H. R. (1995). Defective Recycling of Synaptic Vesicles in Synaptotagmin Mutants of Caenorhabditis-Elegans. *Nature* **378**, 196-199.

Joshi, C. and Fernandez, J. (1988). Capacitance measurements. An analysis of the phase dectector technique used to study exocytosis and endocytosis. *Biophysical Journal* **53**, 885-892.

Junge, H. J., Rhee, J. S., Jahn, O., Varoqueaux, F., Spiess, J., Waxham, M. N., Rosenmund, C. and Brose, N. (2004). Calmodulin and Munc13 form a Ca2+ sensor/effector complex that controls short-term synaptic plasticity. *Cell* **118**, 389-401.

Jurkat-Rott, K. and Lehmann-Horn, F. (2004). The impact of splice isoforms on voltage-gated calcium channel alpha(1) subunits. *Journal of Physiology-London* **554**, 609-619.

Kaneko, S., Cooper, C. B., Nishioka, N., Yamasaki, H., Suzuki, A., Jarvis, S. E., Akaike, A., Satoh, M. and Zamponi, G. W. (2002). Identification and characterization of novel human Ca(v)2.2 (alpha(1B)) calcium channel variants lacking the synaptic protein interaction site. *Journal of Neuroscience* **22**, 82-92.

Katz B. (1969). The release of neurotransmitter substances. *Liverpool University Press* .

Kenigsberg, R. L. and Trifaro, J. M. (1985). Microinjection of Calmodulin Antibodies into Cultured Chromaffin Cells Blocks Catecholamine Release in Response to Stimulation. *Neuroscience* **14**, 335-347.

Kibble, A. V. and Burgoyne, R. D. (1996). Calmodulin increases the initial rate of exocytosis in adrenal chromaffin cells. *Pflugers Archiv-European Journal of Physiology* **431**, 464-466.

Kim, J., Ghosh, S., Nunziato, D. A. and Pitt, G. S. (2004). Identification of the components controlling inactivation of voltage-gated Ca2+ channels. *Neuron* **41**, 745-754.

Kim, J. Y., Shishido, T., Jiang, X. L., Aderem, A. and McLaughlin, S. (1994). Phosphorylation, High Ionic-Strength, and Calmodulin Reverse the Binding of Marcks to Phospholipid-Vesicles. *Journal of Biological Chemistry* **269**, 28214-28219.

Kim, S. J., Lim, W. and Kim, J. (1995). Contribution of L-Type and N-Type Calcium Currents to Exocytosis in Rat Adrenal-Medullary Chromaffin Cells. *Brain Research* **675**, 289-296.

Kitamura, N., Ohta, T., Ito, S. and Nakazato, Y. (1997). Calcium channel subtypes in porcine adrenal chromaffin cells. *Pflugers Archiv-European Journal of Physiology* **434**, 179-187.

Klenchin, V. A. and Martin, T. F. (2000). Priming in exocytosis: attaining fusion-competence after vesicle docking. *Biochimie* **82**, 399-407.

Klingauf, J. and Neher, E. (1997). Modeling buffered Ca2+ diffusion near the membrane: Implications for secretion in neuroendocrine cells. *Biophysical Journal* **72**, 674-690.

Kobrinsky, E., Schwartz, E., Abernethy, D. R. and Soldatov, N. M. (2003). Voltage-gated mobility of the Ca2+ channel cytoplasmic tails and its regulatory role. *Journal of Biological Chemistry* **278**, 5021-5028.

Koh, T. W. and Bellen, H. J. (2003). Synaptotagmin I, a Ca2+ sensor for neurotransmitter release. *Trends in Neurosciences* **26**, 413-422.

Krupp, J. J., Vissel, B., Thomas, C. G., Heinemann, S. F. and Westbrook, G. L. (1999). Interactions of calmodulin and alpha-actinin with the NR1 subunit modulate Ca2+-dependent inactivation of NMDA receptors. *Journal of Neuroscience* **19**, 1165-1178.

Kumar, P. P., Stotz, S. C., Paramashivappa, R., Beedle, A. M., Zamponi, G. W. and Rao, A. S. (2002). Synthesis and evaluation of a new class of nifedipine analogs with T-type calcium channel blocking activity. *Molecular Pharmacology* **61**, 649-658.

Kurokawa, H., Osawa, M., Kurihara, H., Katayama, N., Tokumitsu, H., Swindells, M. B., Kainosho, M. and Ikura, M. (2001). Target-induced conformational adaptation of calmodulin revealed by the crystal structure of a complex with nematode Ca2+/calmodulin-dependent kinase kinase peptide. *Journal of Molecular Biology* **312**, 59-68.

Lackner, M. R., Nurrish, S. J. and Kaplan, J. M. (1999). Facilitation of synaptic transmission by EGL-30 Gqalpha and EGL-8 PLCbeta: DAG binding to UNC-13 is required to stimulate acetylcholine release [see comments]. *Neuron* **24**, 335-46.

Lara, B., Gandia, L., Martinez-Sierra, R., Torres, A. and Garcia, A. G. (1998). Q-type Ca2+ channels are located closer to secretory sites than L-type channels: functional evidence in chromaffin cells. *Pflugers Archiv-European Journal of Physiology* **435**, 472-478.

Larkin, J. M., Brown, M. S., Goldstein, J. L. and Anderson, R. G. W. (1983). Depletion of Intracellular Potassium Arrests Coated Pit Formation and Receptor-Mediated Endocytosis in Fibroblasts. *Cell* **33**, 273-285.

Lawrence, G. W., Weller, U. and Dolly, J. O. (1994). Botulinum-a and the Light-Chain of Tetanus Toxins Inhibit Distinct Stages of Mg-Center-Dot-Atp-Dependent

Catecholamine Exocytosis from Permeabilized Chromaffin Cells. *European Journal of Biochemistry* **222**, 325-333.

Lee, A., Scheuer, T. and Catterall, W. A. (2000). Ca2+/calmodulin-dependent facilitation and inactivation of P/Q- type Ca2+ channels. *Journal of Neuroscience* **20**, 6830-6838.

Lee, A., Westenbroek, R. E., Haeseleer, F., Palczewski, K., Scheuer, T. and Catterall, W. A. (2002). Differential modulation of Ca(v)2.1 channels by calmodulin and Ca2+-binding protein 1. *Nature Neuroscience* **5**, 210-217.

Lee, A., Wong, S. T., Gallagher, D., Li, B., Storm, D. R., Scheuer, T. and Catterall, W. A. (1999). Ca2+/calmodulin binds to and modulates P/Q-type calcium channels. *Nature* **399**, 155-159.

Lee, A., Zhou, H., Scheuer, T. and Catterall, W. A. (2003). Molecular determinants of Ca2+/calmodulin-dependent regulation of Ca(v)2.1 channels. *Proceedings of the National Academy of Sciences of the United States of America* **100**, 16059-16064.

Li, C., Davletov, B. A. and Sudhof, T. C. (1995). Distinct Ca2+ and Sr2+ Binding-Properties of Synaptotagmins - Definition of Candidate Ca2+ Sensors for the Fast and Slow Components of Neurotransmitter Release. *Journal of Biological Chemistry* **270**, 24898-24902.

Li, L. and Chin, L. S. (2003). The molecular machinery of synaptic vesicle exocytosis. *Cellular and Molecular Life Sciences* **60**, 942-960.

Liang, H. Y., DeMaria, C. D., Erickson, M. G., Mori, M. X., Alseikhan, B. A. and Yue, D. T. (2003). Unified mechanisms of Ca2+ regulation across the Ca2+ channel family. *Neuron* **39**, 951-960.

Lin, R. C. and Scheller, R. H. (2000). Mechanisms of synaptic vesicle exocytosis. *Annual Review of Cell and Developmental Biology* **16**, 19-49.

Lindau, M. and Neher, E. (1988). Patch-Clamp Techniques for Time-Resolved Capacitance Measurements in Single Cells. *Pflugers Archiv-European Journal of Physiology* **411**, 137-146.

Lopez, M. G., Albillos, A., Delafuente, M. T., Borges, R., Gandia, L., Carbone, E., Garcia, A. G. and Artalejo, A. R. (1994a). Localized L-Type Calcium Channels

Control Exocytosis in Cat Chromaffin Cells. *Pflugers Archiv-European Journal of Physiology* **427**, 348-354.

Lopez, M. G., Villarroya, M., Lara, B., Sierra, R. M., Albillos, A., Garcia, A. G. and Gandia, L. (1994b). Q-Type and L-Type Ca2+ Channels Dominate the Control of Secretion in Bovine Chromaffin Cells. *Febs Letters* **349**, 331-337.

Lovell, P. V., James, D. G. and McCobb, D. P. (2000). Bovine versus rat adrenal chromaffin cells: Big differences in BK potassium channel properties. *Journal of Neurophysiology* **83**, 3277-3286.

Lu, Q., AtKisson, M. S., Jarvis, S. E., Feng, Z. P., Zamponi, G. W. and Dunlap, K. (2001). Syntaxin 1A supports voltage-dependent inhibition of alpha(1B) Ca2+ channels by G beta gamma in chick sensory neurons. *Journal of Neuroscience* **21**, 2949-2957.

Lukyanetz, E. A. and Neher, E. (1999). Different types of calcium channels and secretion from bovine chromaffin cells. *European Journal of Neuroscience* **11**, 2865-73.

Lundstrom, K., Rotmann, D., Hermann, D., Schneider, E. M. and Ehrengruber, M. U. (2001a). Novel mutant Semliki Forest virus vectors: gene expression and localization studies in neuronal cells. *Histochemistry and Cell Biology* **115**, 83-91.

Lundstrom, K., Schweitzer, C., Rotmann, D., Hermann, D., Schneider, E. M. and Ehrengruber, M. U. (2001b). Semliki Forest virus vectors: efficient vehicles for in vitro and in vivo gene delivery. *Febs Letters* **504**, 99-103.

MacDermott, A. B., Role, L. W. and Siegelbaum, S. A. (1999). Presynaptic ionotropic receptors and the control of transmitter release. *Annual Review of Neuroscience* **22**, 443-85.

Magga, J. M., Jarvis, S. E., Arnot, M. I., Zamponi, G. W. and Braun, J. E. A. (2000). Cysteine string protein regulates G protein modulation of N- type calcium channels. *Neuron* **28**, 195-204.

Majewski, H., Kotsonis, P., Iannazzo, L., Murphy, T. V. and Musgrave, I. F. (1997). Protein kinase C and transmitter release. *Clinical & Experimental Pharmacology & Physiology* **24**, 619-23.

Marek, K. W. and Davis, G. W. (2002). Transgenically encoded protein photoinactivation (FIAsH-FALI): Acute inactivation of synaptotagmin I. *Neuron* **36**, 805-813.

Marengo, F. D. and Monck, J. R. (2000). Development and dissipation of Ca2+ gradients in adrenal chromaffin cells. *Biophysical Journal* **79**, 1800-1820.

Marengo, F. D. and Monck, J. R. (2003). Spatial distribution of Ca2+ signals during repetitive depolarizing stimuli in adrenal chromaffin cells. *Biophysical Journal* **85**, 3397-3417.

Marrion, N. V. and Tavalin, S. J. (1998). Selective activation of Ca2+-activated K+ channels by co- localized Ca2+ channels in hippocampal neurons. *Nature* **395**, 900-905.

Marsal, J., Ruiz-Montasell, B., Blasi, J., Moreira, J. E., Contreras, D., Sugimori, M. and Llinas, R. (1997). Block of transmitter release by botulinum C1 action on syntaxin at the squid giant synapse. *Proceedings of the National Academy of Sciences of the United States of America* **94**, 14871-14876.

Martin, T. F. J. (2003). Tuning exocytosis for speed: fast and slow modes. *Biochimica Et Biophysica Acta-Molecular Cell Research* **1641**, 157-165.

Martin, T. F. J. and Kowalchyk, J. A. (1997). Docked secretory vesicles undergo Ca2+-activated exocytosis in a cell-free system. *Journal of Biological Chemistry* **272**, 14447-14453.

Marty, A. and Neher, E. (1985). Potassium Channels in Cultured Bovine Adrenal Chromaffin Cells. *Journal of Physiology-London* **367**, 117-141.

Matos, M. F., Mukherjee, K., Chen, X. C., Rizo, J. and Sudhof, T. C. (2003). Evidence for SNARE zippering during Ca2+-triggered exocytosis in PC12 cells. *Neuropharmacology* **45**, 777-786.

Matsumura, C., Kuwashima, H. and Kimura, T. (1999). Myosin light chain kinase inhibitors and calmodulin antagonist inhibit Ca(2+)- and ATP-dependent catecholamine secretion from bovine adrenal chromaffin cells. *Journal of Autonomic Pharmacology* **19**, 115-21.

Maximov, A., Sudhof, T. C. and Bezprozvanny, I. (1999). Association of neuronal calcium channels with modular adaptor proteins. *Journal of Biological Chemistry* **274**, 24453-6.

Mayer, A. (2001). What drives membrane fusion in eukaryotes? *Trends in Biochemical Sciences* **26**, 717-723.

McCullar, J. S., Larsen, S. A., Millimaki, R. A. and Filtz, T. M. (2003). Calmodulin is a phospholipase C-beta interacting protein. *Journal of Biological Chemistry* **278**, 33708-33713.

McDonough, S. I. (2004). Peptide toxin inhibition of voltage gated calcium channels: Selectivity and mechanismsCalcium channel pharmacology. In *Calcium channel pharmacology*, (ed. S. I. McDonough). New York: Kluwer Academic.

McEnery, M. W., Vance, C. L., Begg, C. M., Lee, W. L., Choi, Y. and Dubel, S. J. (1998). Differential expression and association of calcium channel subunits in development and disease. *Journal of Bioenergetics and Biomembranes* **30**, 409-418.

McFerran, B. W., Weiss, J. L. and Burgoyne, R. D. (1999). Neuronal Ca2+ sensor 1 - Characterization of the myristoylated protein, its cellular effects in permeabilized adrenal chromaffin cells, Ca2+-independent membrane association, and interaction with binding proteins, suggesting a role in rapid Ca2+ signal transduction. *Journal of Biological Chemistry* **274**, 30258-30265.

McGee, A. W., Nunziato, D. A., Maltez, J. M., Prehoda, K. E., Pitt, G. S. and Bredt, D. S. (2004). Calcium channel function regulated by the SH3-GK module in beta subunits. *Neuron* **42**, 89-99.

McMahon, H. T., Missler, M., Li, C. and Sudhof, T. C. (1995). Complexins - Cytosolic Proteins That Regulate Snap Receptor Function. *Cell* **83**, 111-119.

Mintz, I. M., Venema, V. J., Swiderek, K. M., Lee, T. D., Bean, B. P. and Adams, M. E. (1992). P-Type Calcium Channels Blocked by the Spider Toxin Omega-Aga-Iva. *Nature* **355**, 827-829.

Missler, M., Zhang, W. Q., Rohlmann, A., Kattenstroth, G., Hammer, R. E., Gottmann, K. and Sudhof, T. C. (2003). alpha-neurexins couple Ca2+ channels to synaptic vesicle exocytosis. *Nature* **423**, 939-948.

Misura, K. M. S., Scheller, R. H. and Weis, W. I. (2000). Three-dimensional structure of the neuronal-Sec1-syntaxin 1a complex. *Nature* **404**, 355-362.

Mochida, S., Sheng, Z. H., Baker, C., Kobayashi, H. and Catterall, W. A. (1996). Inhibition of neurotransmission by peptides containing the synaptic protein interaction site of N-type Ca2+ channels. *Neuron* **17**, 781-788.

Mochida, S., Westenbroek, R. E., Yokoyama, C. T., Zhong, H. J., Myers, S. J., Scheuer, T., Itoh, K. and Catterall, W. A. (2003). Requirement for the synaptic protein interaction site for reconstitution of synaptic transmission by P/Q-type calcium channels. *Proceedings of the National Academy of Sciences of the United States of America* **100**, 2819-2824.

Morad, M., Davies, N. W., Kaplan, J. H. and Lux, H. D. (1988). Inactivation and Block of Calcium Channels by Photo-Released Ca-2+ in Dorsal-Root Ganglion Neurons. *Science* **241**, 842-844.

Morel, N. (2003). Neurotransmitter release: the dark side of the vacuolar-H(+)ATPase. *Biology of the Cell* **95**, 453-457.

Morel, N., Dunant, Y. and Israel, M. (2001). Neurotransmitter release through the V0 sector of V-ATPase. *Journal of Neurochemistry* **79**, 485-488.

Morgan, A. and Burgoyne, R. D. (1997). Common mechanisms for regulated exocytosis in the chromaffin cell and the synapse. *Seminars in Cell & Developmental Biology* **8**, 141-149.

Morgan, J. R., Augustine, G. J. and Lafer, E. M. (2002). Synaptic vesicle endocytosis - The races, places, and molecular faces. *Neuromolecular Medicine* **2**, 101-114.

Mori, M. X., Erickson, M. G. and Yue, D. T. (2004). Functional stoichiometry and local enrichment of calmodulin interacting with Ca2+ channels. *Science* **304**, 432-435.

Moser, T. and Neher, E. (1997). Estimation of mean exocytic vesicle capacitance in mouse adrenal chromaffin cells. *Proceedings of the National Academy of Sciences of the United States of America* **94**, 6735-6740.

Mouton, J., Feltz, A. and Maulet, Y. (2001). Interactions of calmodulin with two peptides derived from the C-terminal cytoplasmic domain of the Ca(v)1.2 Ca2+

channel provide evidence for a molecular switch involved in Ca2+- induced inactivation. *Journal of Biological Chemistry* **276**, 22359-22367.

Nascimento, A. A. C., Cheney, R. E., Tauhata, S. B. F., Larson, R. E. and Mooseker, M. S. (1996). Enzymatic characterization and functional domain mapping of brain myosin-V. *Journal of Biological Chemistry* **271**, 17561-17569.

Neher, E. (1998). Vesicle pools and Ca2+ microdomains: new tools for understanding their roles in neurotransmitter release. *Neuron* **20**, 389-99.

Neher, E. and Marty A. (1982). Discrete changes of cell membrane capacitance observed under conditions of enhanced secretion in bovine adrenal chromaffin cells. *Proceedings of the National Academy of Sciences of the United States of America* **79**, 6712-6716.

Neher, E. and Zucker, R. S. (1993). Multiple Calcium-Dependent Processes Related to Secretion in Bovine Chromaffin Cells. *Neuron* **10**, 21-30.

Neves, G. and Lagnado, L. (1999). The kinetics of exocytosis and endocytosis in the synaptic terminal of goldfish retinal bipolar cells. *Journal of Physiology-London* **515**, 181-202.

Neves, G., Neef, A. and Lagnado, L. (2001). The actions of barium and strontium on exocytosis and endocytosis in the synaptic terminal of goldfish bipolar cells. *Journal of Physiology-London* **535**, 809-824.

Nucifora, P. G. P. and Fox, A. P. (1998). Barium triggers rapid endocytosis in calf adrenal chromaffin cells. *Journal of Physiology-London* **508**, 483-494.

Oconnor, V., Pellegrini, L., Dresbach, T., Bommert, K., ElFar, O., Betz, H., Debello, W., Hunt, J. M., Schweizer, F., Augustine, G. et al. (1996). Protein-protein interactions in synaptic vesicle exocytosis. *Biochemical Society Transactions* **24**, 666-670.

Ogden, D. and Stanfield, P. (1994). Patch clamp techniques for single channel and whole cell recording. In *Microelectrode Techniques*, (ed. D. Ogden). Cambridge: The Company of biologists.

Oheim, M. (2001a). Imaging transmitter release. I. Peeking at the steps preceding membrane fusion. *Lasers in Medical Science* **16**, 149-158.

312

Oheim, M. (2001b). Imaging transmitter release. II. A practical guide to evanescent-wave imaging. *Lasers in Medical Science* **16**, 159-170.

Oheim, M., Loerke, D., Chow, R. H. and Stuhmer, W. (1999). Evanescent-wave microscopy: a new tool to gain insight into the control of transmitter release. *Philosophical Transactions of the Royal Society of London Series B-Biological Sciences* **354**, 307-318.

Oheim, M., Loerke, D., Stuhmer, W. and Chow, R. H. (1998). The last few milliseconds in the life of a secretory granule - Docking, dynamics and fusion visualized by total internal reflection fluorescence microscopy (TIRFM). *European Biophysics Journal with Biophysics Letters* **27**, 83-98.

Ohyama, A., Hosaka, K., Komiya, Y., Akagawa, K., Yamauchi, E., Taniguchi, H., Sasagawa, N., Kumakura, K., Mochida, S., Yamauchi, T. et al. (2002). Regulation of exocytosis through Ca2+/ATP-dependent binding of autophosphorylated Ca2+/calmodulin-activated protein kinase II to syntaxin 1A. *Journal of Neuroscience* **22**, 3342-3351.

Okabe, T., Sugimoto, N. and Matsuda, M. (1992). Calmodulin Is Involved in Catecholamine Secretion from Digitonin-Permeabilized Bovine Adrenal-Medullary Chromaffin Cells. *Biochemical and Biophysical Research Communications* **186**, 1006-1011.

Okamoto, M. and Sudhof, T. C. (1997). Mints, Munc18-interacting proteins in synaptic vesicle exocytosis. *Journal of Biological Chemistry* **272**, 31459-64.

Pabst, S., Margittai, M., Vainius, D., Langen, R., Jahn, R. and Fasshauer, D. (2002). Rapid and selective binding to the synaptic SNARE complex suggests a modulatory role of complexins in neuroexocytosis. *Journal of Biological Chemistry* **277**, 7838-7848.

Page, K. M., Canti, C., Stephens, G. J., Berrow, N. S. and Dolphin, A. C. (1998). Identification of the amino terminus of neuronal Ca2+ channel alpha 1 subunits alpha 1B and alpha 1E as an essential determinant of G-protein modulation. *Journal of Neuroscience* **18**, 4815-4824.

Pan, C. Y., Jeromin, A., Lundstrom, K., Yoo, S. H., Roder, J. and Fox, A. P. (2002). Alterations in exocytosis induced by neuronal Ca2+ sensor-1 in bovine chromaffin cells. *Journal of Neuroscience* **22**, 2427-2433.

Park, J. B., Farnsworth, C. C. and Glomset, J. A. (1997). Ca2+/calmodulin causes Rab3A to dissociate from synaptic membranes. *Journal of Biological Chemistry* **272**, 20857-20865.

Pate, P., Mochca-Morales, J., Wu, Y. J., Zhang, J. Z., Rodney, G. G., Serysheva, II, Williams, B. Y., Anderson, M. E. and Hamilton, S. L. (2000). Determinants for calmodulin binding on voltage-dependent Ca2+ channels. *Journal of Biological Chemistry* **275**, 39786-39792.

Patil, P. G., Brody, D. L. and Yue, D. T. (1998). Preferential closed-state inactivation of neuronal calcium channels. *Neuron* **20**, 1027-1038.

Perin, M. S. (1996). Mirror image motifs mediate the interaction of the COOH terminus of multiple synaptotagmins with the neurexins and calmodulin. *Biochemistry* **35**, 13808-13816.

Peters, C., Bayer, M. J., Buhler, S., Andersen, J. S., Mann, M. and Mayer, A. (2001). Trans-complex formation by proteolipid channels in the terminal phase of membrane fusion. *Nature* **409**, 581-588.

Peterson, B. Z., DeMaria, C. D., Adelman, J. P. and Yue, D. T. (1999). Calmodulin is the Ca2+ sensor for Ca2+ -dependent inactivation of L-type calcium channels [published erratum appears in Neuron 1999 Apr;22(4):following 893]. *Neuron* **22**, 549-58.

Peterson, B. Z., Lee, J. S., Mulle, J. G., Wang, Y., de Leon, M. and Yue, D. T. (2000). Critical determinants of Ca2+-dependent inactivation within an EF-hand motif of L-type Ca2+ channels. *Biophysical Journal* **78**, 1906-1920.

Pitt, G. S., Zuhlke, R. D., Hudmon, A., Schulman, H., Reuter, H. and Tsien, R. W. (2001). Molecular basis of calmodulin tethering and Ca2+-dependent inactivation of L-type Ca2+ channels. *Journal of Biological Chemistry* **276**, 30794-30802.

Poskanzer, K. E., Marek, K. W., Sweeney, S. T. and Davis, G. W. (2003). Synaptotagmin I is necessary for compensatory synaptic vesicle endocytosis in vivo. *Nature* **426**, 559-563.

Powell, A. (2000). Capacitance methods - thesis.

Powell, A. D., Teschemacher, A. G. and Seward, E. P. (2000). P2Y purinoceptors inhibit exocytosis in adrenal chromaffin cells via modulation of voltage-operated calcium channels. *Journal of Neuroscience* **20**, 606-16.

Prekeris, R. and Terrian, D. M. (1997). Brain myosin V is a synaptic vesicle-associated motor protein: Evidence for a Ca2+-dependent interaction with the synaptobrevin-synaptophysin complex. *Journal of Cell Biology* **137**, 1589-1601.

Quetglas, S., Iborra, C., Sasakawa, N., De Haro, L., Kumakura, K., Sato, K., Leveque, C. and Seagar, M. (2002). Calmodulin and lipid binding to synaptobrevin regulates calcium-dependent exocytosis. *Embo Journal* **21**, 3970-3979.

Quetglas, S., Leveque, C., Miquelis, R., Sato, K. and Seagar, M. (2000). Ca2+-dependent regulation of synaptic SNARE complex assembly via a calmodulin- and phospholipid-binding domain of synaptobrevin. *Proceedings of the National Academy of Sciences of the United States of America* **97**, 9695-700.

Rae, J., Cooper, K., Gates, P. and Watsky, M. (1991). Low Access Resistance Perforated Patch Recordings Using Amphotericin-B. *Journal of Neuroscience Methods* **37**, 15-26.

Reim, K., Mansour, M., Varoqueaux, F., McMahon, H. T., Sudhof, T. C., Brose, N. and Rosenmund, C. (2001). Complexins regulate a late step in Ca2+-dependent neurotransmitter release. *Cell* **104**, 71-81.

Restituito, S., Cens, T., Barrere, C., Geib, S., Galas, S., De Waard, M. and Charnet, P. (2000). The beta(2a) subunit is a molecular groom for the Ca2+ channel inactivation gate. *Journal of Neuroscience* **20**, 9046-9052.

Rettig, J., Sheng, Z. H., Kim, D. K., Hodson, C. D., Snutch, T. P. and Catterall, W. A. (1996). Isoform-specific interaction of the alpha(1A) subunits of brain Ca2+ channels with the presynaptic proteins syntaxin and SNAP- 25. *Proceedings of the National Academy of Sciences of the United States of America* **93**, 7363-7368.

Rhee, J. S., Betz, A., Pyott, S., Reim, K., Varoqueaux, F., Augustin, I., Hesse, D., Sudhof, T. C., Takahashi, M., Rosenmund, C. et al. (2002). beta phorbol ester- and diacylglycerol-induced augmentation of transmitter release is mediated by Munc13s and not by PKCs. *Cell* **108**, 121-133.

Rhoads, A. R. and Friedberg, F. (1997). Sequence motifs for calmodulin recognition. *Faseb Journal* **11**, 331-340.

Richman, R. W., Tombler, E., Lau, K. K., Anantharam, A., Rodriguez, J., O'Bryan, J. P. and Diverse-Pierluissi, M. A. (2004). N-type Ca2+ channels as scaffold proteins in the assembly of signaling molecules for GABA(B) receptor effects. *Journal of Biological Chemistry* **279**, 24649-24658.

Richmond, J. E. and Broadie, K. S. (2002). The synaptic vesicle cycle: exocytosis and endocytosis in Drosophila and C-elegans. *Current Opinion in Neurobiology* **12**, 499-507.

Richmond, J. E., Davis, W. S. and Jorgensen, E. M. (1999). UNC-13 is required for synaptic vesicle fusion in C-elegans. *Nature Neuroscience* **2**, 959-964.

Richmond, J. E., Weimer, R. M. and Jorgensen, E. M. (2001). An open form of syntaxin bypasses the requirement for UNC-13 in vesicle priming. *Nature* **412**, 338-341.

Rizo, J. and Sudhof, T. C. (2002). SNAREs and Munc18 in synaptic vesicle fusion. *Nature Reviews Neuroscience* **3**, 641-653.

Robinson, I. M., Finnegan, J. M., Monck, J. R., Wightman, R. M. and Fernandez, J. M. (1995). Colocalization of Calcium-Entry and Exocytotic Release Sites in Adrenal Chromaffin Cells. *Proceedings of the National Academy of Sciences of the United States of America* **92**, 2474-2478.

Robinson, P. J. and Dunkley, P. R. (1983). Depolarization-Dependent Protein-Phosphorylation in Rat Cortical Synaptosomes - Factors Determining the Magnitude of the Response. *Journal of Neurochemistry* **41**, 909-918.

Romanin, C., Gamsjaeger, R., Kahr, H., Schaufler, D., Carlson, O., Abernethy, D. R. and Soldatov, N. M. (2000). Ca2+ sensors of L-type Ca2+ channel. *Febs Letters* **487**, 301-306.

Rose, S. D., Lejen, T., Casaletti, L., Larson, R. E., Pene, T. D. and Trifaro, J. M. (2003). Myosins II and V in chromaffin cells: myosin V is a chromaffin vesicle molecular motor involved in secretion. *Journal of Neurochemistry* **85**, 287-298.

Rose, S. D., Lejen, T., Zhang, L. and Trifaro, J. M. (2001). Chromaffin cell F-actin disassembly and potentiation of catecholamine release in response to protein

kinase C activation by phorbol esters is mediated through myristoylated alanine-rich C kinase substrate phosphorylation. *Journal of Biological Chemistry* **276**, 36757-36763.

Rosenmund, C., Rettig, J. and Brose, N. (2003). Molecular mechanisms of active zone function. *Current Opinion in Neurobiology* **13**, 509-519.

Rosenmund, C. and Westbrook, G. L. (1993). Calcium-Induced Actin Depolymerization Reduces Nmda Channel Activity. *Neuron* **10**, 805-814.

Roth, D. and Burgoyne, R. D. (1994). Snap-25 Is Present in a Snare Complex in Adrenal Chromaffin Cells. *Febs Letters* **351**, 207-210.

Rothman, J. E. and Warren, G. (1994). Implications of the Snare Hypothesis for Intracellular Membrane Topology and Dynamics. *Current Biology* **4**, 220-233.

Rousset, M., Cens, T., Gavarini, S., Jeromin, A. and Charnet, P. (2003). Down-regulation of voltage-gated Ca2+ channels by neuronal calcium sensor-1 is beta subunit-specific. *Journal of Biological Chemistry* **278**, 7019-7026.

Rousset, M., Cens, T., Restituito, S., Barrere, C., Black, J. L., McEnery, M. W. and Charnet, P. (2001). Functional roles of gamma(2), gamma(3) and gamma(4), three new Ca2+ channel subunits, in P/Q-type Ca2+ channel expressed in Xenopus oocytes. *Journal of Physiology-London* **532**, 583-593.

Royle, S. J. and Lagnado, L. (2003). Endocytosis at the synaptic terminal. *Journal of Physiology-London* **553**, 345-355.

Sah, P. and Faber, E. S. L. (2002). Channels underlying neuronal calcium-activated potassium currents. *Progress in Neurobiology* **66**, 345-353.

Saimi, Y. and Kung, C. (2002). Calmodulin as an ion channel subunit. *Annual Review of Physiology* **64**, 289-311.

Sakaba, T. and Neher, E. (2001). Calmodulin mediates rapid recruitment of fast-releasing synaptic vesicles at a calyx-type synapse. *Neuron* **32**, 1119-1131.

Sakisaka, T., Baba, T., Tanaka, S., Izumi, G., Yasumi, M. and Takai, Y. (2004). Regulation of SNAREs by tomosyn and ROCK: implication in extension and retraction of neurites. *Journal of Cell Biology* **166**, 17-25.

Sakurai, T., Hell, J. W., Woppmann, A., Miljanich, G. P. and Catterall, W. A. (1995). Immunochemical Identification and Differential Phosphorylation of

317

Alternatively Spliced Forms of the Alpha(1a) Subunit of Brain Calcium Channels. *Journal of Biological Chemistry* **270**, 21234-21242.

Salaun, C., James, D. J. and Chamberlain, L. H. (2004). Lipid rafts and the regulation of exocytosis. *Traffic* **5**, 255-264.

Sankaranarayanan, S., De Angelis, D., Rothman, J. E. and Ryan, T. A. (2000). The use of pHluorins for optical measurements of presynaptic activity. *Biophysical Journal* **79**, 2199-2208.

Sather, W. A. and McCleskey, E. W. (2003). Permeation and selectivity in calcium channels. *Annual Review of Physiology* **65**, 133-159.

Scales, S. J., Hesser, B. A., Masuda, E. S. and Scheller, R. H. (2002). Amisyn, a novel syntaxin-binding protein that may regulate SNARE complex assembly. *Journal of Biological Chemistry* **277**, 28271-28279.

Schiavo, G., Benfenati, F., Poulain, B., Rossetto, O., Delaureto, P. P., Dasgupta, B. R. and Montecucco, C. (1992). Tetanus and Botulinum-B Neurotoxins Block Neurotransmitter Release by Proteolytic Cleavage of Synaptobrevin. *Nature* **359**, 832-835.

Schulte, A. and Chow, R. H. (1998). Cylindrically etched carbon-fiber microelectrodes for low-noise amperometric recording of cellular secretion. *Analytical Chemistry* **70**, 985-990.

Schumacher, M. A., Rivard, A. F., Bachinger, H. P. and Adelman, J. P. (2001). Structure of the gating domain of a Ca2+-activated K+ channel complexed with Ca2+/calmodulin. *Nature* **410**, 1120-1124.

Scott, R. H. and Dolphin, A. C. (1986). Regulation of Calcium Currents by a Gtp Analog - Potentiation of (-)-Baclofen-Mediated Inhibition. *Neuroscience Letters* **69**, 59-64.

Seagar, M., Leveque, C., Charvin, N., Marqueze, B., Martin-Moutot, N., Boudier, J. A., Boudier, J. L., Shoji-Kasai, Y., Sato, K. and Takahashi, M. (1999). Interactions between proteins implicated in exocytosis and voltage-gated calcium channels. *Philosophical Transactions of the Royal Society of London - Series B: Biological Sciences* **354**, 289-97.

Senda, T., Nishii, Y. and Fujita, H. (1991). Immunocytochemical Localization of Synapsin-I in the Adrenal- Medulla of Rats. *Histochemistry* **96**, 25-30.

Seward, E. P., Chernevskaya, N. I. and Nowycky, M. C. (1995). Exocytosis in Peptidergic Nerve-Terminals Exhibits 2 Calcium- Sensitive Phases During Pulsatile Calcium-Entry. *Journal of Neuroscience* **15**, 3390-3399.

Seward, E. P., Chernevskaya, N. I. and Nowycky, M. C. (1996). Ba2+ ions evoke two kinetically distinct patterns of exocytosis in chromaffin cells, but not in neurohypophysial nerve terminals. *Journal of Neuroscience* **16**, 1370-1379.

Seward, E. P. and Nowycky, M. C. (1996). Kinetics of stimulus-coupled secretion in dialyzed bovine chromaffin cells in response to trains of depolarizing pulses. *Journal of Neuroscience* **16**, 553-562.

Sheng, Z. H., Rettig, L., Cook, T. and Catterall, W. A. (1996). Calcium-dependent interaction of N-type calcium channels with the synaptic core complex. *Nature* **379**, 451-454.

Sheng, Z. H., Westenbroek, R. E. and Catterall, W. A. (1998). Physical link and functional coupling of presynaptic calcium channels and the synaptic vesicle docking/fusion machinery. *Journal of Bioenergetics and Biomembranes* **30**, 335-345.

Shiraishi, S., Yokoo, H., Kobayashi, H., Yanagita, T., Uezono, Y., Minami, S., Takasaki, M. and Wada, A. (2000). Post-translational reduction of cell surface expression of insulin receptors by cyclosporin A, FK506 and rapamycin in bovine adrenal chromaffin cells. *Neuroscience Letters* **293**, 211-215.

Sidach, S. S. and Mintz, I. M. (2000). Low-affinity blockade of neuronal N-type Ca channels by the spider toxin omega-agatoxin-IVA. *Journal of Neuroscience* **20**, 7174-7182.

Sihra, T. S., Bogonez, E. and Nicholls, D. G. (1992). Localized Ca2+ Entry Preferentially Effects Protein Dephosphorylation, Phosphorylation, and Glutamate Release. *Journal of Biological Chemistry* **267**, 1983-1989.

Sippy, T., Cruz-Martin, A., Jeromin, A. and Schweizer, F. E. (2003). Acute changes in short-term plasticity at synapses with elevated levels of neuronal calcium sensor-1. *Nature Neuroscience* **6**, 1031-1038.

319

Smith, C. (1999). A persistent activity-dependent facilitation in chromaffin cells is caused by Ca2+ activation of protein kinase C. *Journal of Neuroscience* **19**, 589-98.

Smith, C. and Neher, E. (1997). Multiple forms of endocytosis in bovine adrenal chromaffin cells. *Journal of Cell Biology* **139**, 885-894.

Sokolov, S., Weiss, R. G., Timin, E. N. and Hering, S. (2000). Modulation of slow inactivation in class A Ca2+ channels by beta-subunits. *Journal of Physiology-London* **527**, 445-454.

Soldatov, M. M. (2003). Ca2+ channel moving tail: link between Ca2+-induced inactivation and Ca2+-signal transduction. *Trends in Pharmacological Sciences* **24**, 167-171.

Sollner, T., Bennett, M. K., Whiteheart, S. W., Scheller, R. H. and Rothman, J. E. (1993). A Protein Assembly-Disassembly Pathway in-Vitro That May Correspond to Sequential Steps of Synaptic Vesicle Docking, Activation, and Fusion. *Cell* **75**, 409-418.

Sorensen, J. B. (2004). Formation, stabilisation and fusion of the readily releasable pool of secretory vesicles. *Pflugers Archiv-European Journal of Physiology* **448**, 347-362.

Sorensen, J. B., Matti, U., Wei, S. H., Nehring, R. B., Voets, T., Ashery, U., Binz, T., Neher, E. and Rettig, J. (2002). The SNARE protein SNAP-25 is linked to fast calcium triggering of exocytosis. *Proceedings of the National Academy of Sciences of the United States of America* **99**, 1627-1632.

Steinhardt, R. A. and Alderton, J. M. (1981). Calmodulin Antibody Inhibits Cortical Granule Exocytosis in Sea-Urchin Eggs. *Journal of Cell Biology* **91**, A180-A180.

Stephens, G. J., Canti, C., Page, K. M. and Dolphin, A. C. (1998). Role of domain I of neuronal Ca2+ channel alpha 1 subunits in G protein modulation. *Journal of Physiology-London* **509**, 163-169.

Stewart, B. A., Mohtashami, M., Trimble, W. S. and Boulianne, G. L. (2000). SNARE proteins contribute to calcium cooperativity of synaptic transmission. *Proceedings of the National Academy of Sciences of the United States of America* **97**, 13955-13960.

Steyer, J. A., Horstmann, H. and Almers, W. (1997). Transport, docking and exocytosis of single secretory granules in live chromaffin cells [see comments]. *Nature* **388**, 474-8.

Stotz, S. C., Jarvis, S. E. and Zamponi, G. W. (2004). Functional roles of cytoplasmic loops and pore lining transmembrane helices in the voltage-dependent inactivation of HVA calcium channels. *Journal of Physiology-London* **554**, 263-273.

Stotz, S. C. and Zamponi, G. W. (2001). Structural determinants of fast inactivation of high voltage- activated Ca2+ channels. *Trends in Neurosciences* **24**, 176-181.

Striessnig, J., Murphy, B. J. and Catterall, W. A. (1991). Dihydropyridine Receptor of L-Type Ca2+ Channels - Identification of Binding Domains for H-3 (+)- Pn200-110 and H-3 Azidopine within the Alpha-1 Subunit. *Proceedings of the National Academy of Sciences of the United States of America* **88**, 10769-10773.

Sudhof, T. C. (2002). Synaptotagmins: Why so many? *Journal of Biological Chemistry* **277**, 7629-7632.

Sudhof, T. C. (2004). The synaptic vesicle cycle. *Annual Review of Neuroscience* **27**, 509-547.

Sugimori, M., Tong, C. K., Fukuda, M., Moreira, J. E., Kojima, T., Mikoshiba, K. and Llinas, R. (1998). Presynaptic injection of syntaxin-specific antibodies blocks transmission in the squid giant synapse. *Neuroscience* **86**, 39-51.

Sugita, S., Han, W. P., Butz, S., Liu, X. R., Fernandez-Chacon, R., Lao, Y. and Sudhof, T. C. (2001). Synaptotagmin VII as a plasma membrane Ca2+ sensor in exocytosis. *Neuron* **30**, 459-473.

Sutton, K. G., McRory, J. E., Guthrie, H., Murphy, T. H. and Snutch, T. P. (1999). P/Q-type calcium channels mediate the activity-dependent feedback of syntaxin-1A. *Nature* **401**, 800-804.

Sutton, R. B., Fasshauer, D., Jahn, R. and Brunger, A. T. (1998). Crystal structure of a SNARE complex involved in synaptic exocytosis at 2.4 angstrom resolution. *Nature* **395**, 347-353.

Takahashi, S. X., Miriyala, J. and Colecraft, H. M. (2004). Membrane-associated ouanviate kinase-like properties of beta- subunits required for modulation of voltage-

dependent Ca2+ channels. *Proceedings of the National Academy of Sciences of the United States of America* **101**, 7193-7198.

Taverna, E., Saba, E., Rowe, J., Francolini, M., Clementi, F. and Rosa, P. (2004). Role of lipid microdomains in P/Q-type calcium channel (Ca(v)2.1) clustering and function in presynaptic membranes. *Journal of Biological Chemistry* **279**, 5127-5134.

Teschemacher, A. G. and Seward, E. P. (2000). Bidirectional modulation of exocytosis by angiotensin II involves multiple G-protein-regulated transduction pathways in chromaffin cells. *Journal of Neuroscience* **20**, 4776-85.

Thaler, C., Gray, A. C. and Lipscombe, D. (2004). Cumulative inactivation of N-type Ca(V)2.2 calcium channels modified by alternative splicing. *Proceedings of the National Academy of Sciences of the United States of America* **101**, 5675-5679.

Thiagarajan, R., Tewolde, T., Li, Y. J., Becker, P. L., Rich, M. A. and Engisch, K. L. (2004). Rab3A negatively regulates activity-dependent modulation of exocytosis in bovine adrenal chromaffin cells. *Journal of Physiology-London* **555**, 439-457.

Tokumaru, H., Umayahara, K., Pellegrini, L. L., Ishizuka, T., Saisu, H., Betz, H., Augustine, G. J. and Abe, T. (2001). SNARE complex oligomerization by synaphin/complexin is essential for synaptic vesicle exocytosis. *Cell* **104**, 421-432.

Tomizawa, K., Ohta, J., Matsushita, M., Moriwaki, A., Li, S. T., Takei, K. and Matsui, H. (2002). Cdk5/p35 regulates neurotransmitter release through phosphorylation and downregulation of P/Q-type voltage- dependent calcium channel activity. *Journal of Neuroscience* **22**, 2590-2597.

Trifaro, J., Rose, S. D., Lejen, T. and Elzagallaai, A. (2000). Two pathways control chromaffin cell cortical F-actin dynamics during exocytosis. *Biochimie* **82**, 339-52.

Trifaro, J. M., Fournier, S. and Novas, M. L. (1989). The P65 Protein Is a Calmodulin-Binding Protein Present in Several Types of Secretory Vesicles. *Neuroscience* **29**, 1-8.

Trifaro, J. M., Lejen, T., Rose, S. D., Pene, T. D., Barkar, N. D. and Seward, E. P. (2002). Pathways that control cortical F-actin dynamics during secretion. *Neurochemical Research* **27**, 1371-1385.

Triggle, D. J. (2004). Pharmacology of Cav1 (L-type) Channels. In *Calcium channel pharmacology*, (ed. S. I. McDonough). New York: Kluwer academic.

Triggle, D. J. and Rampe, D. (1989). 1,4-Dihydropyridine Activators and Antagonists - Structural and Functional Distinctions. *Trends in Pharmacological Sciences* **10**, 507-511.

Tsujimoto, T., Jeromin, A., Saitoh, N., Roder, J. C. and Takahashi, T. (2002). Neuronal calcium sensor 1 and activity-dependent facilitation of P/Q-type calcium currents at presynaptic nerve terminals. *Science* **295**, 2276-2279.

Tully, K. and Treistman, S. N. (2004). Distinct intracellular calcium profiles following influx through N-versus L-type calcium channels: Role of Ca2+-induced Ca2+ release. *Journal of Neurophysiology* **92**, 135-143.

Turner, K. M., Burgoyne, R. D. and Morgan, A. (1999). Protein phosphorylation and the regulation of synaptic membrane traffic. *Trends in Neurosciences* **22**, 459-64.

Umbach, J. A. and Gundersen, C. B. (1997). Evidence that cysteine string proteins regulate an early step in the Ca2+-dependent secretion of neurotransmitter at Drosophila neuromuscular junctions. *Journal of Neuroscience* **17**, 7203-7209.

Unsicker, K., Finotto, S. and Krieglstein, K. (1997). Generation of cell diversity in the peripheral autonomic nervous system: The sympathoadrenal cell lineage revisited. *Annals of Anatomy-Anatomischer Anzeiger* **179**, 495-500.

Valtorta, F., Meldolesi, J. and Fesce, R. (2001). Synaptic vesicles: Is kissing a matter of competence? *Trends in Cell Biology* **11**, 324-328.

Verhage, M., de Vries, K. J., Roshol, H., Burbach, J. P., Gispen, W. H. and Sudhof, T. C. (1997). DOC2 proteins in rat brain: complementary distribution and proposed function as vesicular adapter proteins in early stages of secretion. *Neuron* **18**, 453-61.

Verhage, M., Maia, A. S., Plomp, J. J., Brussaard, A. B., Heeroma, J. H., Vermeer, H., Toonen, R. F., Hammer, R. E., van den Berg, T. K., Missler, M. et al. (2000). Synaptic assembly of the brain in the absence of neurotransmitter secretion. *Science* **287**, 864-869.

Vitale, M. L., Seward, E. P. and Trifaro, J. M. (1995). Chromaffin Cell Cortical Actin Network Dynamics Control the Size of the Release-Ready Vesicle Pool and the Initial Rate of Exocytosis. *Neuron* **14**, 353-363.

Voets, T. (2000). Dissection of three Ca2+-dependent steps leading to secretion in chromaffin cells from mouse adrenal slices. *Neuron* **28**, 537-545.

Voets, T., Moser, T., Lund, P. E., Chow, R. H., Geppert, M., Sudhof, T. C. and Neher, E. (2001a). Intracellular calcium dependence of large dense-core vesicle exocytosis in the absence of synaptotagmin I. *Proceedings of the National Academy of Sciences of the United States of America* **98**, 11680-11685.

Voets, T., Neher, E. and Moser, T. (1999). Mechanisms underlying phasic and sustained secretion in chromaffin cells from mouse adrenal slices. *Neuron* **23**, 607-15.

Voets, T., Toonen, R. F., Brian, E. C., de Wit, H., Moser, T., Rettig, J., Sudhof, T. C., Neher, E. and Verhage, M. (2001b). Munc18-1 promotes large dense-core vesicle docking. *Neuron* **31**, 581-591.

Vogel, H. J. (1994). The Merck-Frosst-Award-Lecture 1994 - Calmodulin - a Versatile Calcium Mediator Protein. *Biochemistry and Cell Biology-Biochimie Et Biologie Cellulaire* **72**, 357-376.

von Gersdorff, H. and Matthews, G. (1999). Electrophysiology of synaptic vesicle cycling. *Annual Review of Physiology* **61**, 725-52.

Walker, D. and De Waard, M. (1998). Subunit interaction sites in voltage-dependent Ca2+ channels: role in channel function. *Trends in Neurosciences* **21**, 148-154.

Wang, C. and Zucker, R. S. (1998). Regulation of synaptic vesicle recycling by calcium and serotonin. *Neuron* **21**, 155-167.

Wang, C. Y., Yang, F., He, X. P., Chow, A., Du, J., Russell, J. T. and Lu, B. (2001). Ca2+ binding protein frequenin mediates GDNF-induced potentiation of Ca2+ channels and transmitter release. *Neuron* **32**, 99-112.

Weimer, R. M., Richmond, J. E., Davis, W. S., Hadwiger, G., Nonet, M. L. and Jorgensen, E. M. (2003). Defects in synaptic vesicle docking in unc-18 mutants. *Nature Neuroscience* **6**, 1023-1030.

Weiss, J. L., Archer, D. A. and Burgoyne, R. D. (2000). Neuronal Ca2+ sensor-1/frequenin autocrine pathway regulating Ca2+ bovine adrenal chromaffin cells. *Journal of Biological Chemistry* **275**, 40082-40087.

Weiss, J. L. and Burgoyne, R. D. (2001). Voltage-independent inhibition of P/Q-type Ca2+ channels in adrenal chromaffin cells via a neuronal Ca2+ sensor-1-dependent pathway involves Src family tyrosine kinase. *Journal of Biological Chemistry* **276**, 44804-44811.

Weiss, J. L. and Burgoyne, R. D. (2002). Sense and sensibility in the regulation of voltage-gated Ca2+ channels. *Trends in Neurosciences* **25**, 489-491.

West, A. E., Griffith, E. C. and Greenberg, M. E. (2002). Regulation of transcription factors by neuronal activity. *Nature Reviews Neuroscience* **3**, 921-931.

Wickham, T. J., Mathias, P., Cheresh, D. A. and Nemerow, G. R. (1993). Integrin-Alpha-V-Beta-3 and Integrin-Alpha-V-Beta-5 Promote Adenovirus Internalization but Not Virus Attachment. *Cell* **73**, 309-319.

Wiser, O., Bennett, M. K. and Atlas, D. (1996). Functional interaction of syntaxin and SNAP-25 with voltage- sensitive L- and N-type Ca2+ channels. *Embo Journal* **15**, 4100-4110.

Wu, X. F., Zhao, X. H., Baylor, L., Kaushal, S., Eisenberg, E. and Greene, L. E. (2001). Clathrin exchange during clathrin-mediated endocytosis. *Journal of Cell Biology* **155**, 291-300.

Xia, X. M., Fakler, B., Rivard, A., Wayman, G., Johnson-Pais, T., Keen, J. E., Ishii, T., Hirschberg, B., Bond, C. T., Lutsenko, S. et al. (1998). Mechanism of calcium gating in small-conductance calcium- activated potassium channels. *Nature* **395**, 503-507.

Xu, T., Binz, T., Niemann, H. and Neher, E. (1998a). Multiple kinetic components of exocytosis distinguished by neurotoxin sensitivity. *Nature Neuroscience* **1**, 192-200.

Xu, T., Rammner, B., Margittai, M., Artalejo, A. R., Neher, E. and Jahn, R. (1999). Inhibition of SNARE complex assembly differentially affects kinetic components of exocytosis. *Cell* **99**, 713-22.

Xu, X. Z. S., Wes, P. D., Chen, H., Li, H. S., Yu, M. J., Morgen, S., Liu, Y. and Montell, C. (1998b). Retinal targets for calmodulin include proteins implicated in synaptic transmission. *Journal of Biological Chemistry* **273**, 31297-31307.

Yakel, J. L. (1997). Calcineurin regulation of synaptic function: From ion channels to transmitter release and gene transcription. *Trends in Pharmacological Sciences* **18**, 124-134.

Yang, Y., Udayasankar, S., Dunning, J., Chen, P. and Gillis, K. D. (2002). A highly Ca2+-sensitive pool of vesicles is regulated by protein kinase C in adrenal chromaffin cells. *Proceedings of the National Academy of Sciences of the United States of America* **99**, 17060-17065.

Yizhar, O., Matti, U., Melamed, R., Hagalili, Y., Bruns, D., Rettig, J. and Ashery, U. (2004). Tomosyn inhibits priming of large dense-core vesicles in a calcium-dependent manner. *Proceedings of the National Academy of Sciences of the United States of America* **101**, 2578-2583.

Yoshihara, M., Adolfsen, B. and Littleton, J. T. (2003). Is synaptotagmin the calcium sensor? *Current Opinion in Neurobiology* **13**, 315-323.

Zamponi, G. W. (2003). Calmodulin lobotomized: Novel insights into calcium regulation of voltage-gated calcium channels. *Neuron* **39**, 879-881.

Zamponi, G. W., Bourinet, E., Nelson, D., Nargeot, J. and Snutch, T. P. (1997). Crosstalk between G proteins and protein kinase C mediated by the calcium channel alpha(1) subunit. *Nature* **385**, 442-446.

Zamponi, G. W. and Snutch, T. P. (1998a). Decay of prepulse facilitation of N type calcium channels during G protein inhibition is consistent with binding of a single G(beta gamma) subunit. *Proceedings of the National Academy of Sciences of the United States of America* **95**, 4035-4039.

Zamponi, G. W. and Snutch, T. P. (1998b). Modulation of voltage-dependent calcium channels by G proteins. *Current Opinion in Neurobiology* **8**, 351-356.

Zeilhofer, H. U., Blank, N. M., Neuhuber, W. L. and Swandulla, D. (2000). Calcium-dependent inactivation of neuronal calcium channel currents is independent of calcineurin. *Neuroscience* **95**, 235-241.

Zerial, M. and McBride, H. (2001). Rab proteins as membrane organizers. *Nature Reviews Molecular Cell Biology* 2, 107-117.

Zhang, J. F., Randall, A. D., Ellinor, P. T., Horne, W. A., Sather, W. A., Tanabe, T., Schwarz, T. L. and Tsien, R. W. (1993). Distinctive Pharmacology and Kinetics of Cloned Neuronal Ca2+ Channels and Their Possible Counterparts in Mammalian Cns Neurons. *Neuropharmacology* 32, 1075-1088.

Zhang, S., Ehlers, M. D., Bernhardt, J. P., Su, C. T. and Huganir, R. L. (1998). Calmodulin mediates calcium-dependent inactivation of N-methyl- D-aspartate receptors. *Neuron* 21, 443-453.

Zheng, X. and Bobich, J. A. (1998). A sequential view of neurotransmitter release. *Brain Research Bulletin* 47, 117-28.

Zhou, H., Kim, S. A., Kirk, E. A., Tippens, A. L., Sun, H., Haeseleer, F. and Lee, A. (2004). Ca2+-binding protein-1 facilitates and forms a postsynaptic complex with Ca(v)1.2 (L-Type) Ca2+ channels. *Journal of Neuroscience* 24, 4698-4708.

Zinsmaier, K. E., Eberle, K. K., Buchner, E., Walter, N. and Benzer, S. (1994). Paralysis and Early Death in Cysteine String Protein Mutants of Drosophila. *Science* 263, 977-980.

Zuhlke, R. D., Pitt, G. S., Deisseroth, K., Tsien, R. W. and Reuter, H. (1999). Calmodulin supports both inactivation and facilitation of L-type calcium channels [see comments]. *Nature* 399, 159-62.